# Elucidating the Molecular Mechanisms of Selective Autophagy in *Drosophila melanogaster*

A thesis submitted in fulfilment of the requirements for the degree of Doctor of Philosophy in Life Sciences

ASHRAFUR RAHMAN

School of Life Sciences, University of Warwick
Submitted September 2021

# Table of contents

# List of Figures

## Chapter 1 Introduction



## Chapter 3 Characterisation of ATG8a K48A/Y49A Mutant *Drosophila Melanogaster*

## Chapter 4 Quantitative proteomics analysis of ATG8a and ATG8a K48A/Y49A mutant flies compared to wild type flies

## Chapter 5 *Drosophila* GMAP is a LIR motif containing golgin



## Chapter 6 dGMAP is a golgiphagy receptor

### Chapter 7 dGMAP is a potential regulator of autophagy



# List of tables

### Chapter 2 Materials and Methods

# Acknowledgements

I would like to thank my supervisor Professor Ioannis Nezis, for giving me the opportunity to complete my PhD project in his lab and guiding me throughout the process. I would also specifically like to thank Dr Anne-Claire Jacomin, Dr Stavroula Petridi and Panos from the Nezis Lab who has provided me with invaluable knowledge through their teachings. Finally, I would like to thank my mum, dad and particularly my wife Neelam, who have all supported and encouraged me throughout my 4-year PhD.

# COVID-19 impact Statement

Due to lockdown restrictions, I was unable access to the lab for a period of 6 months (March 2020- August 2020). Following this period, there was reduced access to the fly lab and microscopy suite, which fluctuated based on government guidelines. Consequently, this impacted my ability to carry out many of my planned experiments. For example, the data in this thesis would have been supported with additional *in-vitro* cell culture experiments. Some of these planned experiments are mentioned in the future work paragraphs of the discussion. Nonetheless, I have prioritised the most important experiments to get the data to a publishable level.

# Declarations

DECLARATION This thesis is submitted to the University of Warwick in support of my application for the degree of Doctor of Philosophy. It has been composed by the author (Ashrafur Rahman) and has not been submitted in any previous application for any degree.

Parts of this thesis have been published by the author:

“GMAP is a Golgiphagy Receptor in Drosophila.” – submitted for review, attached at the end in appendix.

Contributions: All work presented here (including data generated and data analysis) was carried out by the author except in the cases outlined below:

Dr. Anne-Claire Jacomin

- Creation of FLPout-mCherry-Atg8a flies

# List of abbreviations

| | |
|---|---|
| aa | Amino acid |
| AIM | ATG8 interaction motif |
| AMPK | AMP-activated protein kinase |
| Arl1 | Arf-like GTPase |
| ATF6 | Activating transcription factor 6 |
| Atg/ATG | Autophagy-related protein |
| Atg8a | Autophagy-related protein 8a |
| Atg8a-LDS | Atg8a LIR Docking Site |
| BNIP3 | Bcl-2 adenovirus E1a nineteen kDa interacting protein 3 |
| BNIP3L | BNIP-like |
| BSA | Bovine Serum Albumin |
| CALCOCO2 | Calcium-binding and coiled-coil domain-containing protein 2 |
| CaMKK β | Ca2+ activated calmodulin dependent kinase-β |
| CGN/TGN | Cis/trans Golgi network |
| CHOP | CEBP homologous protein |
| CID | Collision-induced dissociation |
| CKA | Connector of kinase to AP1 |
| CLEAR motif | Coordinated lysosomal expression and regulation motif |
| CMA | Chaperone-Mediated Autophagy |
| COPI/II | Coat protein complex 1/2 |
| Cvt | Cytoplasm to vacuole targeting pathway |
| DAPk | Death-associated protein kinase |
| DDR | DNA damage response |
| dGMAP | *Drosophila* GMAP |
| Dpp | Decapentaplegic |
| *Drosophila* | *Drosophila melanogaster* |
| DSK2 | Dominant suppressor of KAR 2 |
| *E. coli* | *Escherichia Coli* |
| EGF | Epidermal growth factor |
| eIF2α | Eukaryotic initiation factor-2α |
| ER | Endoplasmic reticulum |
| ERES | ER exit sites |
| ERGIC | ER to Golgi intermediary compartment |

| | |
|---|---|
| ERK1/2 | Extracellular signal-regulated kinase 1/2 |
| ESCRT | Endosomal sorting complexes required for transport |
| FASP | Filter Aided Sample Preparation |
| FIP200 | Focal adhesion kinase family-interacting protein 200 kDa |
| FOXO | Class O forkhead box transcription factors |
| FRT | FLP recognition site |
| FUNDC1 | FUN14 domain containing protein 1 |
| GABARAP | Gamma-Aminobutyric Acid Receptor-Associated Protein |
| GAL4 | Galactose-induced 4 transcription factor |
| GAP | GTPase activator proteins |
| GAPDH | Glyceraldehyde-3-phosphate dehydrogenase |
| GATE-16 | Golgi-associated ATPase enhancer of 16 kDa |
| GEF | Guanine nucleotide exchange factor |
| GIM | GABRAP interaction motif |
| GMAP | Golgi microtubule associated protein |
| GOLPH3 | Golgi phosphoprotein 3 |
| GPI | Glycosylphosphatidylinositol |
| GRAB domain | GRIP-related Arf-binding |
| GRP78 | Glucose-regulated protein 78 |
| GSK3β | glycogen synthase kinase 3β |
| GST | Glutathione S-Transferase |
| HAT | Histone acetyl transferase |
| HDAC | Histone deacetylase |
| Hg | Hedgehog |
| HIF-1 | hypoxia-inducible factor 1 |
| HOPS | Homotypic vacuole fusion and protein sorting |
| HSC70 | Heat shock cognate protein of 70 KDa |
| HSPG | Heparan sulfate proteoglycan |
| hVps34 | Human Vacuolar Protein Sorting 34 |
| IDPR | Intrinsically disordered protein regions |
| IF | Immuno-Fluorescence |
| IKKγ | Inhibitor of nuclear factor kappa-B kinase subunit gamma |
| IKKβ | Inhibitor of NF-kB kinase subunit beta (β) |
| iLIR | Interactive LIR Software |
| Imd/IMD | Immune Deficiency |
| IP3 | Inositol trisphosphate |
| Ird5 | Immune Response Deficient 5 |
| IRE1α | Inositol requiring kinase 1 |

| | |
|---|---|
| JAK-STAT | Janus kinase- signal transducer and activator of transcription |
| Kenny | Inhibitor of NFkB kinase subunit gamma/IKKgamma (γ) |
| LAMP-2A | Lysosome-associated membrane protein type 2A |
| LB | Lennox Broth |
| LC-MS | Liquid chromatography-mass spectrometry |
| LDS | LIR-Docking Site |
| LFQ | label free quantification |
| LIR | LC3-Interacting Region |
| LPS | lipopolysaccharide |
| m/z | Mass to charge ratio |
| MAP1LC3 (also LC3) | Microtubule-Associated Protein 1 Light Chain 3 |
| MAPK | Mitogen activated protein kinase |
| mCherry | Mammalian Cherry |
| MiTF | Microphthalmia-associated transcription factor |
| mRNA | Messenger RNA |
| MVB | Multi vesicular bodies |
| NBR1 | Neighbour Of BRCA1 Gene 1 |
| NDP52 | Nuclear Domain 10 Protein 52 |
| NEMO | Nfkb Essential Modulator |
| NF-κB | Nuclear Factor Kappa (K) Beta |
| Nix | NIP3-like protein X |
| NSAF | Normalised spectral abundance factor |
| OPTN | Optineurin |
| PAGE | Polyacrylamide Gel Electrophoresis |
| PARP1 | poly-ADP-ribose polymerase 1 |
| PAS | Pre-autophagosomal structure |
| PB1 | Phox and Bem1p domain |
| PBac | *PiggyBac* |
| PCA | Principal component analysis |
| PCR | Polymerase chain reaction |
| PE | Phosphatidylethanolamine |
| PERK | RNA-dependant protein kinase-like ER kinase |
| PI3K | Phosphoinositide 3-Kinase |
| PI3KC3-C | Class III PI 3-kinase complex |
| PI3P | Phosphatidylinositol 3-Phosphate |
| PIK3C3 | Phosphoinositide 3-kinase class III |
| $PIP_3$ | Phosphatidylinositol trisphosphate |
| PLEKHM1 | Plekstrin homology domain-containing family M member 1 |

| | |
|---|---|
| PMN | Piecemeal micronucleophagy |
| PSSM | Position Specific Scoring Matrix |
| Ref(2)P | Refractory to sigma P |
| RheB | Ras homologue enriched in brain |
| ROCK | Rho kinase |
| ROS | Reactive oxygen species |
| RUFY4 | RUN and FYVE domain-containing Protein 4 |
| SDS | Sodium Dodecyl Sulfate |
| SH3PX1 | Src Homology 3 And Phox Domain-Containing 1 |
| SNX | Sorting Nexin |
| SYN17 | Syntaxin 17 |
| TBK1 | TANK-binding kinase 1 |
| TCA cycle | Tricarboxylic acid cycle |
| TFEB | Transcription factor EB |
| TLR | Toll-like receptors |
| TOR | Target of rapamycin |
| TRAPP | Transport protein particle |
| TRIFF | TIR-domain-containing adapter-inducing interferon-β |
| TSC1/2 | Tuberous sclerosis complex 1/2 |
| UAS | Upstream Activating Sequence |
| Ub | Ubiquitin |
| UBA | ubiquitin associated |
| UBA5 | Ubiquitin like modifier activating enzyme 5 |
| UBD | Ubiquitin Binding Domain |
| Ubl | Ubiquitin-like |
| UDS | UIM-docking site |
| UIM | Ubiquitin interacting motif |
| ULK1 | Unc-51-like kinase 1 |
| UPR | Unfolded protein response |
| UVRAG | UV Radiation Resistance-Associated Gene Protein |
| WB | Western Blot |
| Wg | Wingless |
| WT | Wild Type |
| XBP1 | X-box binding protein 1 |
| Y2H | Yeast-2-Hybrid |

# Abstract

Autophagy is an evolutionary conserved process of cellular self-degradation. It involves the lysosomal degradation of cellular materials, via an intermediate double membrane vesicle, where the degradation products can be reused by the cell. It is known that as well as bulk degradation autophagy can happen in a highly selective manner through receptors and adapters. One of the key players in this is the LC3 protein. This project investigates selective autophagy using *Drosophila Melanogaster* as a genetically modifiable organism. The *Drosophila* homologue of the mammalian LC3 proteins is ATG8a. ATG8a has a hydrophobic binding pocket (LDS) which binds autophagy substrates that contain a LC3 interacting region (LIR). Quantitative proteomics on *Drosophila* with a mutated LDS hydrophobic binding pocket was used to identify a panel of ATG8a interacting proteins. From this analysis, *Drosophila* GMAP (Golgi microtubule-associated protein) was discovered as a novel autophagy receptor. This study has shown that *Drosophila* GMAP has a role in golgiphagy, the selective degradation of the Golgi complex.

# Chapter 1 Introduction

## 1.1 Overview of Autophagy

### 1.1.1 Summary of the Three Main Types of Autophagy

Intracellular degradation happens in two main ways, the proteasome system and autophagy. The proteasome system is involved in the degradation of individual ubiquitinated proteins (Bochtler *et al.*, 1999), whereas autophagy is more commonly associated with bulk degradation (Glick, Barth and Macleod, 2010). The degradation products of both autophagy and the proteasome can be re-used by the cell. Autophagy is typically triggered through nutrient stress or starvation, although there is a basal level of autophagy which is involved in cell homeostasis. Basal autophagy tends to happen in a very selective manner through specific receptors and adapters (Sharma *et al.*, 2018). During autophagy, misfolded proteins, damaged organelles, and pathogens are all degraded through the lysosome and recycled to produce new cellular materials. The three main types of autophagy comprise microautophagy, macroautophagy and chaperone mediated autophagy of which macroautophagy is the most well characterised.

Microautophagy is the direct uptake of cytosolic components by lysosomes (Figure 1-1). The two main ways in which this can occur is through lysosomal invagination or lysosomal protrusions. Microautophagy can also happen through endosomal-microautophagy whereby sequestration of cargo into multivesicular bodies (MVB) on late endosomes in a process dependent on the ESCRT family of proteins. Chaperone proteins would then deliver these MVB to the lysosome (Tekirdag and Cuervo, 2018). The most characterised form of microautophagy is lysosomal invagination which has been studied mostly in yeast. Initially, there is an invagination of the lysosomal membrane, forming a tube like structure known as an autophagic tube, on the end of which a lipid rich vesicle forms and grows (Muller *et al.*, 2000). The subsequent fission of vesicles into the lysosomal lumen is a process that is not fully

understood but it does not seem to involve the t-SNARES and v-SNARES that are required for homotypic fission. The vesicles and its cytoplasmic contents are then degraded by lysosomal hydrolases (Epple *et al.*, 2001), and then permeases export the degradation products into the cytoplasm for reuse (Yang and Klionsky, 2007). Microautophagy can also happen in a selective manner, mainly for the degradation of organelles. For example, micropexophagy is the degradation of peroxisomes (Bellu *et al.*, 2001), piecemeal microautophagy degrades non-essential parts of the nucleus (Dawaliby and Mayer, 2010) and micromitophagy degrades mitochondria (Kissova *et al.*, 2007).

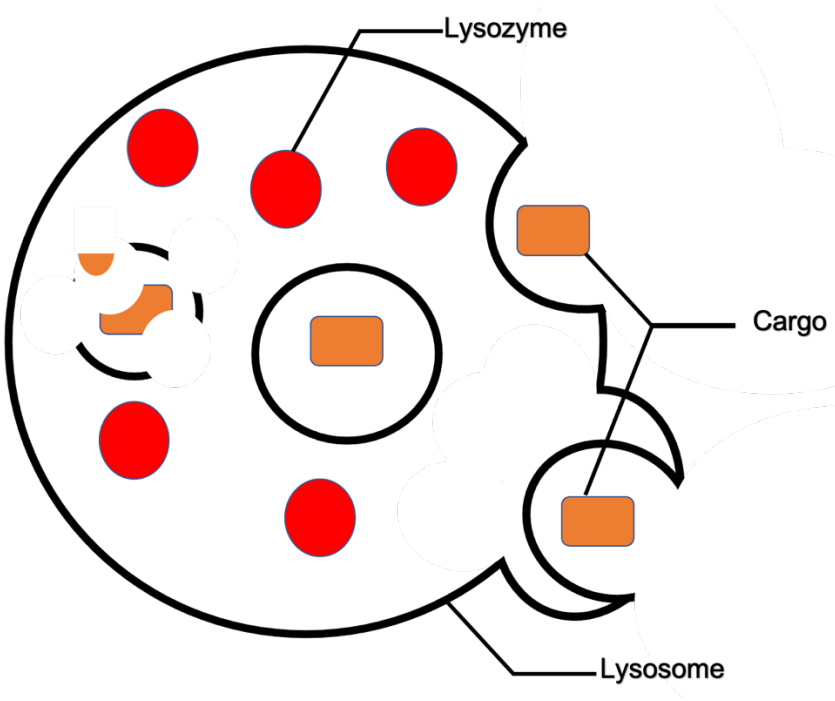


Figure 1-1 **Overview of microautophagy.** Cargo is directly taken up into lysosomes and captured into vesicles. Vesicles are lysed so cargo is now exposed to lysosomal hydrolases and degraded. The breakdown products can then be exported from the lysosome for reuse.

Chaperone-mediated autophagy (CMA) is more selective by nature and is specifically involved in the degradation of cytosolic proteins (Figure 1-2). Specific proteins are transported into the lysosome with the help of chaperone proteins, the

main chaperone being heat shock cognate protein of 70 kDa (HSC70) (Sahu *et al.*, 2011). Specific proteins to be degraded by CMA contain a pentapeptide motif, KFERQ (Dice *et al.*, 1986), which is recognised by and directly binds to the chaperone HSC70. The motif needs to have a glutamine on one end and contain a positive residue (K or R), a hydrophobic residue (F, L, I, or V) and a negatively charged residue (E or D). However, the amount of CMA substrates is not limited to proteins that contain this specific motif, as post-translational modifications allow similar motifs to become functional. For example, the phosphorylation of residue S, T, or Y within the motif can compensate for the lack of a full KFERQ motif (Park, Suh and Cuervo, 2015; Zhou *et al.*, 2016). Other modifications include ubiquitination and acetylation which produce similar effects (Li *et al.*, 2016a). Once a CMA substrate has bound HSC70, the protein can enter the lysosome through a translocation protein called lysosome-associated membrane protein type 2A (LAMP2A) (Cuervo and Dice, 1996). Lysosomal membrane bound HSC70 in a complex with other chaperones is involved in the unfolding of proteins, which is then translocated into the lysosomal lumen (Agarraberes and Dice, 2001). Luminal HSC70 is also required to complete this translocation step (Bandyopadhyay *et al.*, 2008). Thus, proteins entering the lysosomal lumen this way enter one by one. So far, LAMP2A has only been found in mammals and birds (Tekirdag and Cuervo, 2018). CMA is usually activated in response to nutrient stress and hypoxia as well as being part of protein quality control (Dohi *et al.*, 2012; Cuervo *et al.*, 1995; Arias and Cuervo, 2011). CMA usually degrades damaged or misfolded proteins before they get a chance to become aggregates (Cuervo *et al.*, 2004). Once the aggregated proteins are formed, macroautophagy is required for its removal.

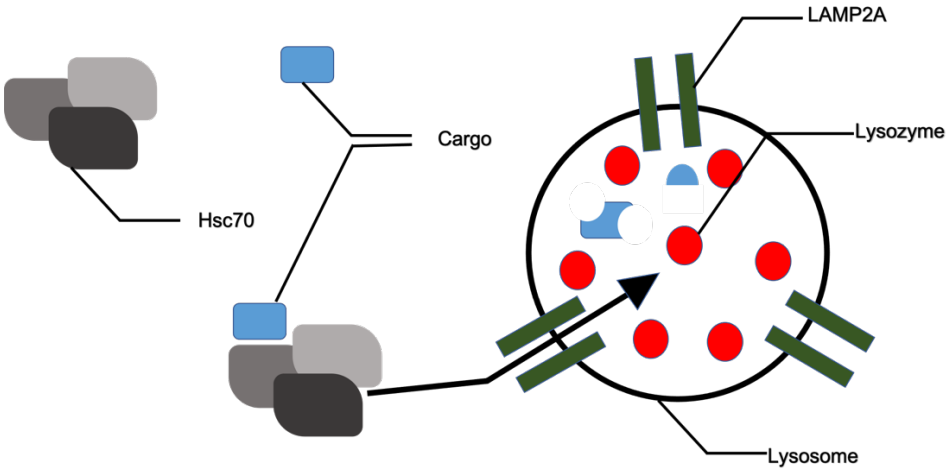


Figure 1-2 **Overview of chaperone mediated autophagy.** Cargo is directed into the lysosome with the help of chaperone proteins such as HSC70. The cargo-chaperone complex then enters the lysosome through the translocation protein LAMP2A. Cargo is then degraded through lysosomal hydrolases and degradation products exported for reuse.

Macroautophagy involves the sequestration of autophagic substrate in a double membrane phagophore forming an autophagosome (Figure 1-3). The autophagosome then fuses with a lysosome, forming an autolysosome where the cargo is then degraded. The degradation products are recycled and reused by the cell (Parzych and Klionsky, 2014). Macroautophagy is responsible for the breakdown of damaged or aggregated proteins, damaged organelles, and foreign bodies, and is usually upregulated in response to nutrient or energy stress. Much of what we know about macroautophagy has been gained from studying yeast, and eventual mammalian studies (Parzych and Klionsky, 2014). This thesis will focus on macroautophagy and our current understanding of this process. The main stages of macroautophagy are the following: initiation of autophagy and the molecular switches which trigger its activation, LC3 processing, selection of cargo, and the fusion of autophagosome with lysosome.

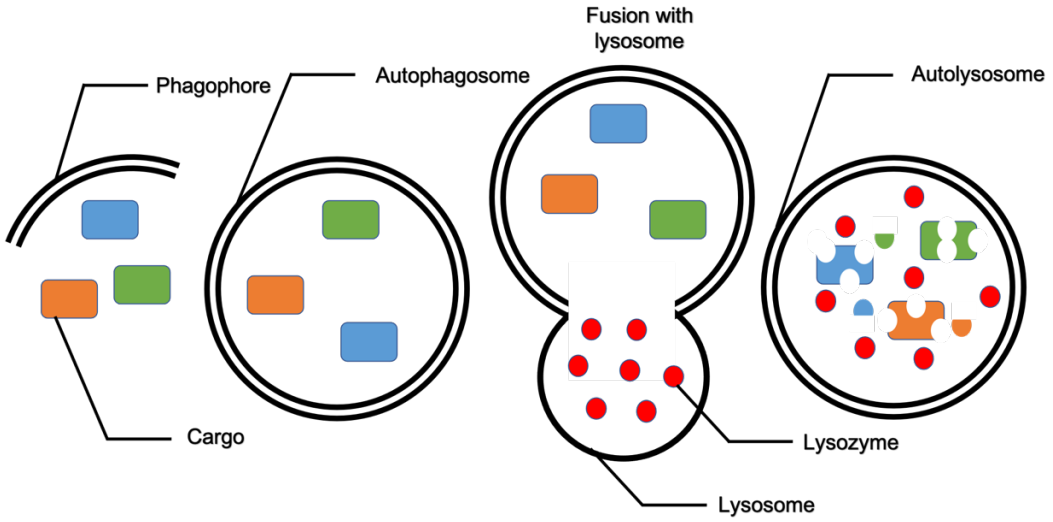


Figure 1-3 **Overview of macroautophagy.** Cargo is sequestered into a growing phagophore double membrane which eventually closes and forms and autophagosome. The cargo containing autophagosome then fuses with a lysosome to form an autolysosome. The lysosomal hydrolases break down the cargo and the degradation products are exported out of the cell for reuse.

### 1.1.2 Overview of Macroautophagy

The mechanism of macroautophagy, which from now on will be referred to as autophagy, was primarily discovered in yeast. The initiation of autophagy begins with the formation of a phagophore membrane, where in yeast this originates at a cytosolic component called the pre-autophagosomal structure (PAS) (Kawamata *et al.*, 2008). There is no evidence for a PAS in mammals. Instead, the phagophore formation appears to initiate at the ER with help from other membrane bound organelles such as the trans-Golgi, late endosome, and nuclear envelope. The ER membrane used to form the phagophore is usually enriched for phosphatidylinositol 3-phosphate (PI(3)P) forming what is called an omegasome (Axe *et al.*, 2008). The two major complexes involved with phagophore initiation is the Unc-51-like kinase 1 (ULK1) complex (Zachari and Ganley, 2017) and the class III PI 3-kinase complex I (PI3KC3-C1) (Burman and Ktistakis, 2010). Following this, the elongation of the phagophore membrane

involves the ATG8 family of proteins (ATG8 in yeast/flies and LC3s and GABARAPs in mammals), the ATG5-ATG12 conjugation system as well as other ATG proteins (autophagy related proteins). A common marker of autophagosomes is the presence of ATG8a/LC3 in the phagophore membrane, which is a result of LC3 processing and lipidation via a ubiquitin-like conjugation system (Abounit, Scarabelli and McCauley, 2012). There are also many other factors necessary for autophagy for example membrane budding and fusion proteins such as COPI/COPII, Rab GTPases and SNAREs (Soreng, Neufeld and Simonsen, 2018). Finally, a group of selective autophagy adapters are required for the selection of cargo which is targeted for degradation (Johansen and Lamark, 2011; Nezis, 2012). This process is discussed in more detail in the following sections.

## 1.2 Regulation of Autophagy

### 1.2.1 Nutrient sensing

As alluded to previously, one of the main functions of autophagy is to provide resources and energy for a cell during a state of nutrient depravation (Figure 1-4). Therefore, it makes sense that there are various nutrient sensing pathways that can trigger the initiation of autophagy. These pathways usually converge onto the protein kinase TOR (target of rapamycin), which has a central role balancing between cell growth and autophagy (Jung et al., 2010). mTOR (mammalian TOR) activation leads to the phosphorylation of various autophagy proteins (ATG proteins), that are part of the ULK/ATG1 complex, which leads to the inhibition of autophagy (Laplante and Sabatini, 2009). The other pathway that is negatively regulated during nutrient depravation is the Ras-cAMP-PKA pathway, which has a role in glucose sensing (Caza and Kronstad, 2019). mTOR acts to inhibit autophagy and is activated by the presence of nutrients such as amino acids and glucose (Hara et al., 1998). Conflicting literature reports on the exact mechanism of mTOR nutrient sensing include: direct sensing and

phosphorylation in response to nutrients (Long *et al.*, 2005b), indirect activation through Ras-related small GTPases (Rag GTPases) (Kim et al., 2008) and also indirectly though hVps34 (Human vacuolar sorting protein 34, also known as PIK3C3 (phosphoinositide 3-kinase class III)) (Nobukuni et al., 2005). Amino acid sensing and mTOR activation also occurs through vacuolar V-ATPase in the lysosomal membrane (Zoncu *et al.*, 2011). A reduction of glucose in the cell can trigger autophagy through AMP-activated protein kinase (AMPK). When glucose levels are low, the ATP:AMP ratio is also low which leads to the phosphorylation and activation of AMPK by Liver Kinase B1 (LKB1 also known as STK11) (Shaw *et al.*, 2004). AMPK inhibits autophagy through the phosphorylation of members of the mTOR complex or through phosphorylation and activation of tuberous sclerosis complex 1/2 (TSC1/2), which in turn inhibits an activator of mTOR, RheB (Ras homologue enriched in brain) (Long *et al.*, 2005a). Other glucose sensing mechanisms exist such as glyceraldehyde-3-phosphate dehydrogenase (GAPDH) which acts through the RheB-mTOR pathway independent of TSC1/2 (Lee *et al.*, 2009). When GAPDH is active in the glycolytic pathway, it is no longer able to sequester Rheb which leads to autophagy inhibition. The Ras/protein kinase A (PKA) is also involved in glucose sensing. Ras 1/2 lead to the increased production of cAMP through adenylyl cyclase. Although not particularly well studied, elevation of cAMP levels leads to the inhibition of PKA which appears to suppress TOR inhibition dependent autophagy (Budovskaya *et al.*, 2004). Due to these nutrient sensing pathways, it is common practice in labs to induce autophagy through starvation.

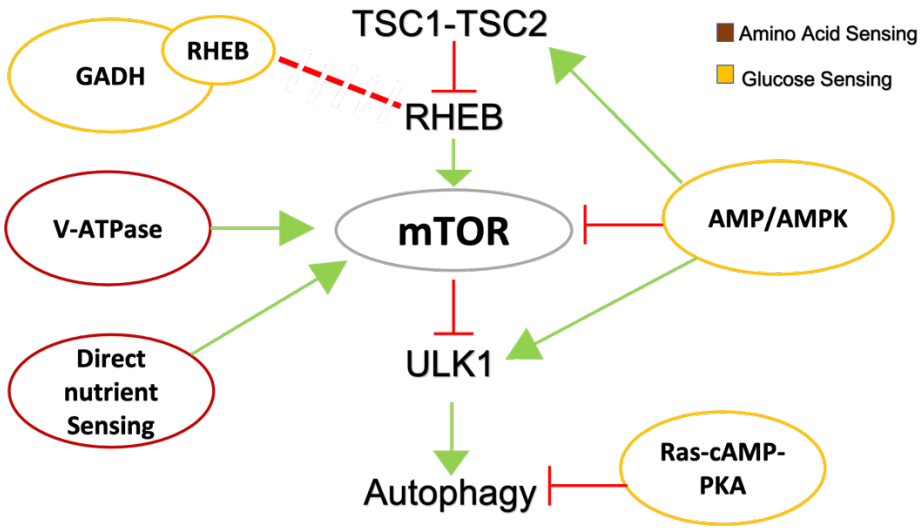


Figure 1-4 **Regulation of autophagy through nutrient sensing.** Various nutrient (glucose and amino acid) sensing pathways are involved with the induction of autophagy. mTOR is a negative regulator of autophagy and found central in the autophagy initiation signalling pathway. Autophagy is regulated through different nutrient sensing pathways, as a lack of nutrient availability/starvation will trigger autophagic degradation of cytosolic material for recycling. Different nutrient sending pathways include glucose sensing pathways such as Ras-cAMP-PKA, AMP/AMPK, GADH/RHEB, as well as amino acid sensing pathways such as V-ATPase or direct mTOR sensing.

### 1.2.2 Insulin and growth factors

Insulin and growth factor signalling can also regulate autophagy through the activation of membrane tyrosine kinase receptors (Lum *et al.*, 2005) (Figure 1-5). Autophosphorylation of these receptors recruit insulin receptor substrates 1/2, which in turn leads to the activation of class I PI3K. Production of phosphatidylinositol trisphosphate ($PIP_3$) leads to protein kinase B (PKB)/Akt signalling which ultimately activates mTOR through inactivation of TSC1/2. Conversely, when there is a loss in insulin and growth factor signalling, autophagy is activated (Stokoe *et al.*, 1997; Vander Haar *et al.*, 2007). This is because there is a loss in Akt activity which normally acts to inhibit glycogen synthase kinase 3β (GSK3β). GSK3β activates both TSC1/2 and ULK1 which is one of the main initiators of autophagy (Inoki *et al.*, 2006). Growth factor signalling can also regulate autophagy through a TOR independent way. The Ras

signalling/Raf1-MAPK (mitogen activated protein kinase) pathway can be activated by growth factors which activate extracellular signal-regulated kinase 1/2 (ERK1/2). ERK1 activity leads to the induction of autophagy which can be reversed through the binding of amino acids to the Raf1 kinase (Furuta *et al.*, 2004).

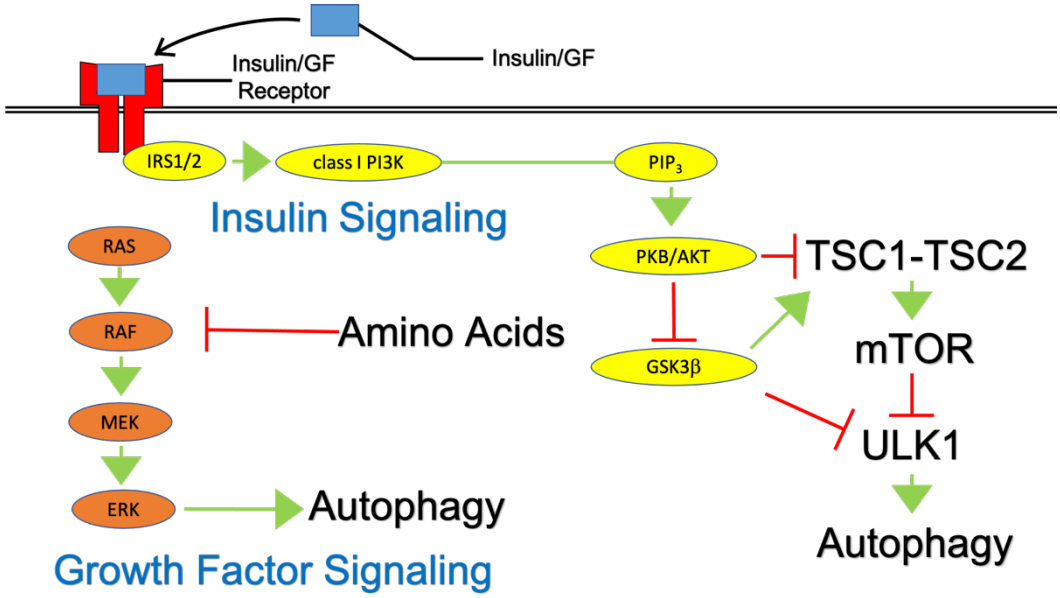


Figure 1-5 **Regulation of autophagy through insulin and growth factors.** Insulin is an indication of nutrient availability and so can inhibit autophagy. Insulin binding to its tyrosine kinase receptor leads to activation of class I PI3K and production of $PIP_3$. This in turn activates the PKB/AKT signalling which activates mTOR through inhibition of TSC1/2. Growth factors cause the activation of autophagy as there is more of a need for nutrient availability. Growth factor signalling which activates the Ras-RAF-MEK-ERK pathway can lead to autophagy activation through ERK1.

### 1.2.3 ER-stress

Endoplasmic reticulum (ER) stress can also lead to the induction of autophagy (Figure 1-6). The role of the ER normally is to correctly fold proteins and ready them to be sent to other organelles. As well as this the ER in mammalian cells acts as a $Ca^{2+}$ reserve. ER stress is when there is an excessive amount of misfolded and unfolded proteins due to low energy levels, production of aggregate-prone proteins, and

oxidative stress. In this situation both yeast and mammalian cells trigger the unfolded protein response (UPR) (Chakrabarti, Chen and Varner, 2011), which can in turn lead to autophagy activation. There are three main pathways associated with the UPR including: ATF6 (activating transcription factor 6), IRE1α (inositol requiring kinase 1), and PERK (RNA-dependant protein kinase-like ER kinase), where GRP78 (glucose-regulated protein 78) plays an important role in the ATF6 pathway. GRP78 appears to be necessary for ER stress activated autophagy but evidence suggests it acts on the phagophore elongation step rather than initiation (Li *et al.*, 2008). The IRE1-JNK and PERK-eIF2α pathway has a role in LC3 lipidation and targeted degradation of mutated proteins (Kouroku *et al.*, 2007; Yan *et al.*, 2019). The ATF6 pathway leads to the expression of CHOP (CEBP homologous protein), XBP1 (X-box binding protein 1) and GRP78 which all act to activate autophagy (Yung, Charnock-Jones and Burton, 2011). During a period of ER stress $Ca^{2+}$ is released into the cytoplasm through various channels such as the IP3 receptors (inositol trisphosphate receptor). $Ca^{2+}$ in the cytoplasm activates $Ca^{2+}$ activated calmodulin dependent kinase-β (CaMKK-β) which can activate autophagy through AMPK. $Ca^{2+}$ efflux also induces phosphorylation and activation of protein kinase Cθ (PKCθ) which again can activate autophagy (Sakaki, Wu and Kaufman, 2008). Finally, calmodulin regulates death-associated protein kinase (DAPk) activity which can phosphorylate and inhibit beclin1 promoting autophagy (Gozuacik *et al.*, 2008).

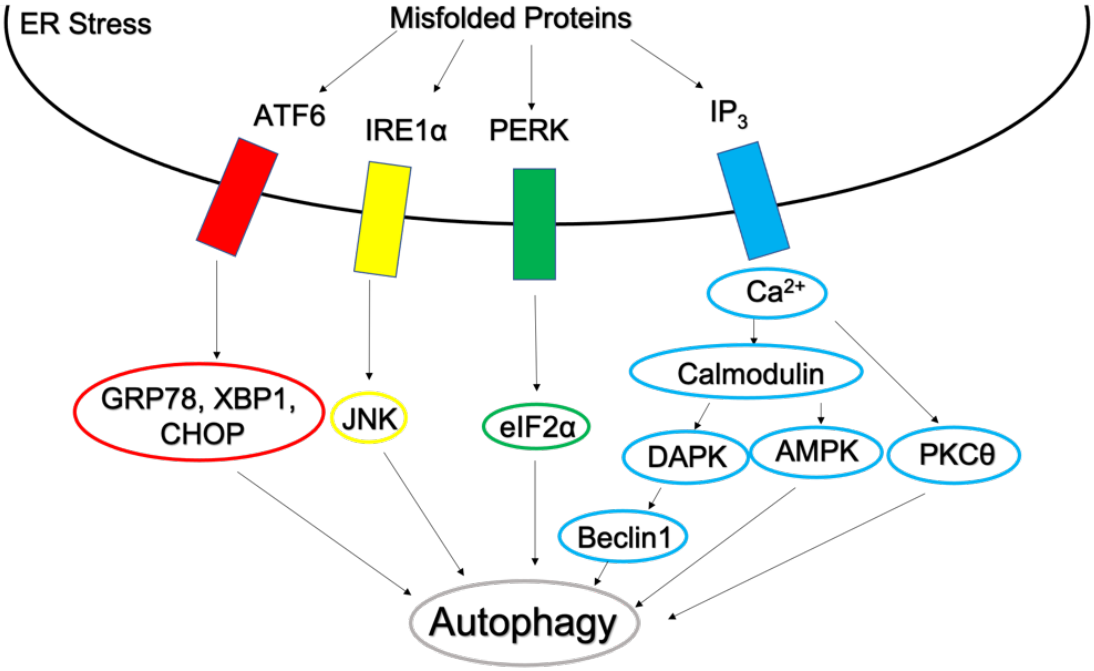


Figure 1-6 **Regulation of autophagy through ER-stress.** Er stress can be triggered upon accumulation of misfolded proteins. This leads to the unfolded protein response which can happen through the ATF6, IRE1α, and PERK pathways. All three pathways can induce autophagy. ER stress can also lead to the release of $Ca^{2+}$ through $IP_3$ receptors which can activate autophagy through calmodulin.

### 1.2.4 Oxidative stress and hypoxia

Another trigger of autophagy is oxidative stress (Figure 1-7). Reactive oxygen species (ROS) can cause damage to cells as they are highly reactive and can disrupt the function of DNA, proteins, and lipids. One of the main sources of these ROS is damaged mitochondria (Murphy, 2009). If the enzymatic removal of these ROS using superoxide dismutase is not enough, then the damaged mitochondria can be degraded through autophagy (a process called mitophagy, discussed in Chapter 6) as a last resort (Shefa *et al.*, 2019). ROS themselves can trigger autophagy by oxidising the residue Cys81 on ATG4 (Scherz-Shouval *et al.*, 2007). ATG4 is an autophagy protein that is a cysteine protease and usually has a role in cleaving ATG8/LC3 from the membrane after lysosomal fusion. Once the Cys81 residue is oxidised, the LC3

cleavage activity of ATG4 is inhibited, therefore promoting LC3 lipidation. Although LC3 lipidation is required early on to start autophagy, ATG4's cleavage activity post lysosomal fusion is still required. The balance of ATG4 activity and inactivation is not very well studied. The presence of hydrogen peroxide in the cell can also initiate autophagy through the AMPK pathway by activating poly-ADP-ribose polymerase 1 (PARP1) (He and Klionsky, 2009). ROS, when it leads to DNA damage, also activates the DNA damage response (DDR). There are various proteins that are involved in both the DDR and autophagy, one of which is PARP1. PARP1 is a single strand break repair enzyme as well as an autophagy inducer (Munoz-Gamez *et al.*, 2009). One of the main regulators of the DDR is p53 which has targets that are upstream of autophagy (such as AMPK/TSC2) as well as those directly involved with autophagy (such as ULK1) (Eliopoulos, Havaki and Gorgoulis, 2016). Similarly, reactive nitrogen species can also activate autophagy through the ATM (ataxia-telangiectasia mutated) protein. This protein is involved in cell cycle checkpoints as well as being able to activate the AMPK/TSC2 pathway (Tripathi *et al.*, 2013).

Hypoxia can lead to the production of ROS and activate autophagy through the previously mentioned mechanism, but it can also activate autophagy directly (Figure 1-7). One of the ways is through TOR inhibition where the AMPK pathway can act as a sensor for hypoxia (Papandreou *et al.*, 2008). The other method is through hypoxia-inducible factor 1 (HIF-1) which is a transcription factor that is activated upon local oxygen depletion (Schofield and Ratcliffe, 2004). HIF-1 activation leads to the expression of BNIP3 (Bcl-2 adenovirus E1a nineteen kDa interacting protein 3) and BNIP3L (BNIP-like protein also known as NIX) which belong to the Bcl2 family of proteins involved in cell death. BNIP3 and BNIP3L are involved in activating mitochondrial degradation through mitophagy (Bellot *et al.*, 2009). Whereby BNIP3L interacts with GABARAP (one of the mammalian homologues of ATG8) as well as Rheb (upstream of mTOR) (Li *et al.*, 2007; Schwarten *et al.*, 2009). BNIP3L can interact with other survival factors and release Beclin1 which can induce autophagy.

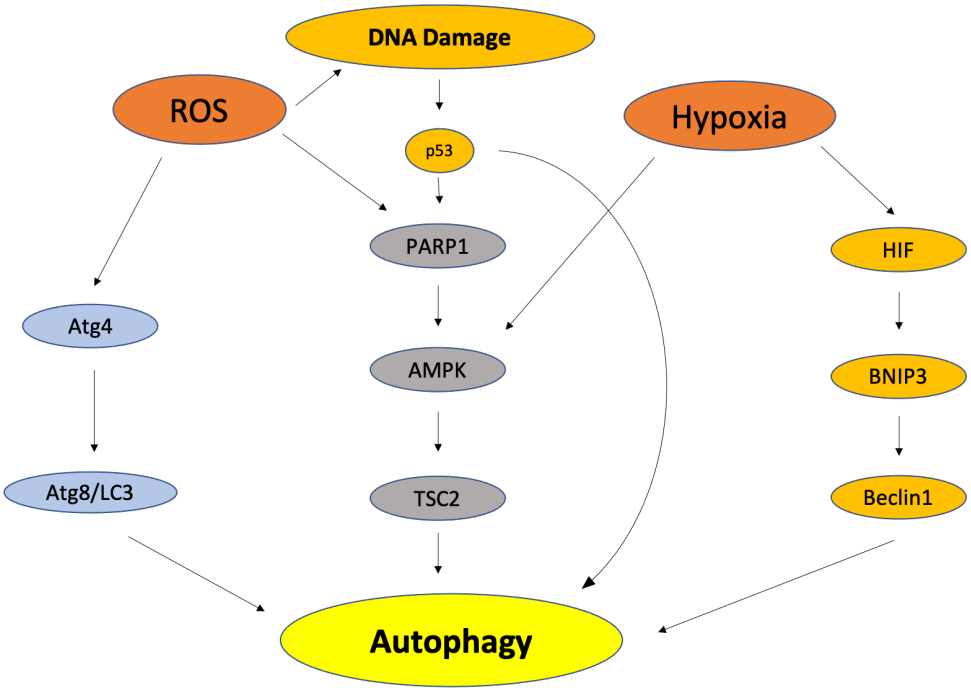


Figure 1-7 **Activation of autophagy through reactive oxygen species and hypoxia.** Reactive oxygen species can oxidise residues on the cysteine protease ATG4, which would normally cleave ATG8/LC3 from the autophagosome, promoting ATG8/LC3 lipidation and autophagy. Hydrogen peroxide can also activate autophagy though the PARP1/AMPK pathway. Reactive oxygen species can damage DNA which can lead to the DNA damage response activating p53 and eventually autophagy. Hypoxia can lead to autophagy activation either through the AMPK pathway or through activation of the HIF transcription factor and the BNIP3/Beclin1 pathway.

### 1.2.5 Pathogens

Autophagy is also activated in response to pathogens (Figure 1-8) and many pathogens have evolved methods of evading phagocytic degradation. For example, some pathogens can puncture the phagosome membrane and escape into the cytoplasm where they can grow and divide (Colombo, 2007). Autophagic degradation through autophagosomes is a key method of eliminating and limiting the growth of many pathogens such as *Salmonella typhimurium* and *Burkholderia pseudomallei* (Birmingham et al., 2006; Cullinane et al., 2008). Not only the bacteria itself, but autophagy can be an effective way of dealing with bacterial toxins such as those produced by *Vibrio cholerae* (Gutierrez et al., 2007). The autophagic degradation of

foreign molecules is called xenophagy, which is discussed in more detail later in this chapter. The signal to start autophagy manifest through various receptors which are stimulated by pathogens. Toll-like receptors (TLR) are a key player in mammalian innate and adaptive immunity, and act as a method of autophagy activation. Different TLRs respond to different bacterial components and activate the immune system primarily through T-cell activation. TLR7 detects ssRNA, TLR2 detects zymosan and TLR4 binds lipopolysaccharide (LPS) (Delgado *et al.*, 2008; Sanjuan *et al.*, 2007). Majority of TLRs signal through downstream adapter proteins, the main two being MyD88 and TRIF. These adapters that mediate the crosstalk between immunity and autophagy. MyD88 and TRIF can prime innate and adaptive immune cells through the NF-κB pathway but can also act to upregulate pathogen clearance through autophagy. It has been suggested that the two adapters are able to work together in the presence of bacterial components such as LPS to activate autophagy through reducing the interaction of Beclin1 with Bcl-2 (Shi and Kehrl, 2008). Moreover, cytokines such as interferon-γ can activate autophagy and is the signalling molecule most important in dealing with intracellular *Mycobacterium tuberculosis*. Interferon-γ promotes the fusion of *Mycobacterium tuberculosis* containing autophagosomes with late endosomes and lysosomes (Gutierrez *et al.*, 2004). Viral infections and viral genetic material lead to the protein kinase R (PKR)/eIF2α pathway which activates autophagy and has been shown to involved in the degradation of Herpes simplex virus type 1 (HSV-1)(Talloczy, Virgin and Levine, 2006).

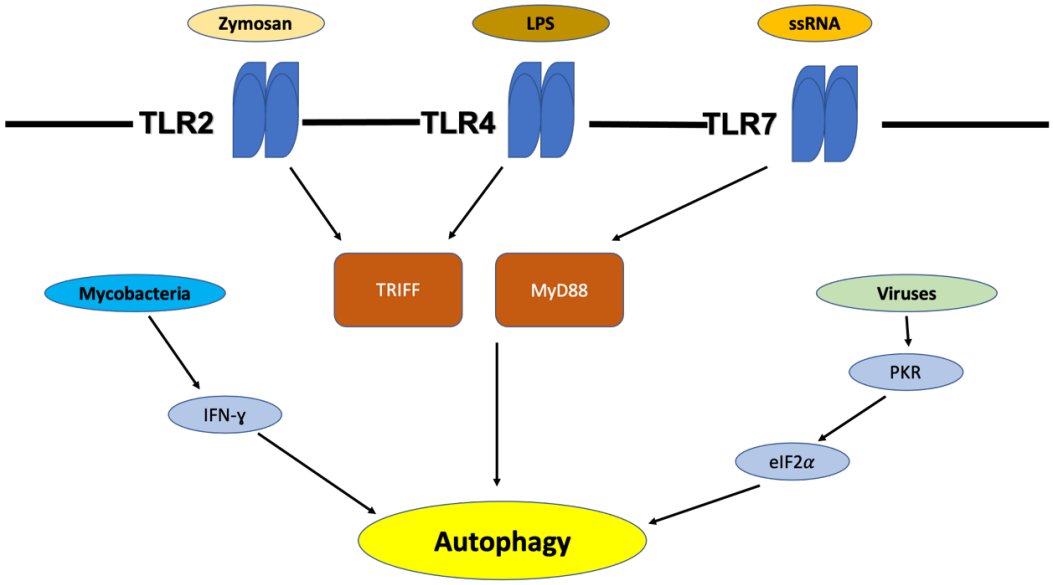


Figure 1-8 **Autophagy activation through pathogens.** Toll-like receptors 2, 4, and 7, detect zymosan, LPS and ssRNA respectively and can activate autophagy through the adapter molecules TRIFF and MyD88. Cytokines such as interferon-γ are very important triggering the fusion of *Mycobacterium* containing autophagosomes with lysosomes. Viruses such as herpes simplex 1 virus leads to autophagy activation through the protein kinase R/eIF2α pathway.

### 1.2.6 Transcriptional Regulation

Upon autophagy activation, for example through starvation, not only is there activation and mobilisation of the autophagic machinery but the transcription of many autophagy proteins like LC3/ATG8 are upregulated (Figure 1-9). Transcription factor EB (TFEB) is part of the microphthalmia-associated transcription factor (MiTF) family of transcription factors and plays an important role in the activation of autophagy (Settembre *et al.*, 2011). TFEB is usually sequestered in the cytoplasm through its phosphorylation by many different kinases including the mTOR complex. Once dephosphorylated, through phosphatases such as PP2a, it can translocate into the nucleus where it is able to activate a plethora of autophagy related genes including GABARAP, ATG9B and ATG5. (Martina *et al.*, 2012). TFEB, like other basic-loop-helix leucine zipper transcription factors, binds to DNA at the CANNTG motif which must be

flanked by the CLEAR motif (coordinated lysosomal expression and regulation motif). Many of these CLEAR motifs are found upstream of lysosomal genes such as protein channels and hydrolytic enzymes (Sardiello *et al.*, 2009). TFEB also upregulates the expression of genes involved throughout the autophagy process including initiation, phagophore elongation and lysosomal fusion. Similarly, class O forkhead box transcription factors (FOXO) family, control the transcription many autophagy related genes (ULK1, ULK2, ATG12 and LC3). Growth factor signalling leads to activation of AKT which phosphorylates FOXO family members and retains them in the cytoplasm. P53, a major tumour suppressor protein, is also thought to be involved in the transcriptional regulation of autophagy. Although our understanding is limited, P53 can activate the transcription of many autophagy genes, as well as control the transcription of TFEB and FOXO family genes (Di Malta, Cinque and Settembre, 2019). When P53 is not in the nucleus it acts as a negative regulator of autophagy through an unknown mechanism (Di Malta, Cinque and Settembre, 2019). E2F1 and NF-kB are transcription factors that work antagonistically to control transcription of BNIP3, the hypoxia related autophagy protein, as well as other autophagy genes. During a hypoxic state NF-kB, the negative regulator of BNIP transcription is released from the promotor of BNIP3 so that E2F1 can upregulate its transcription (Shaw *et al.*, 2008).

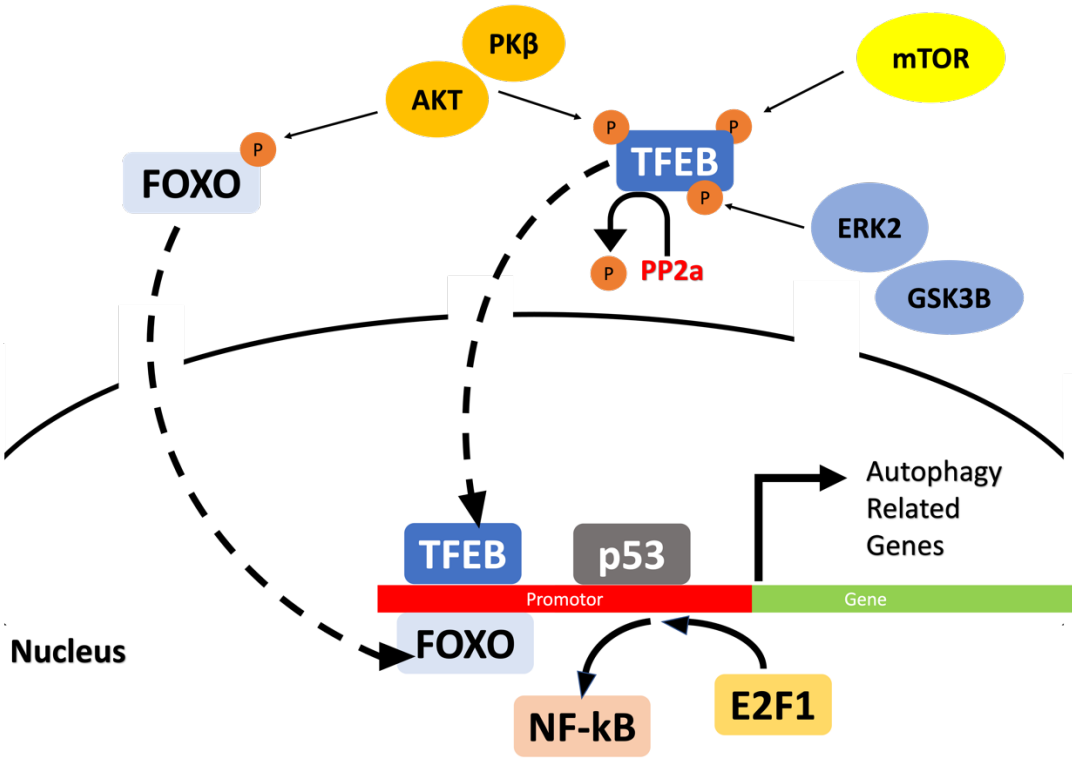


Figure 1-9 **Regulation of autophagy through transcription.** Transcription factors such as the FOXO family of proteins and TFEB are sequestered in the cytoplasm through phosphorylation by kinases such as mTOR and AKT. Upon dephosphorylation through phosphatases like PP2a they can enter the cytoplasm and switch on the transcription of autophagy related genes. P53 and E2F1/NF-kB are also transcription factors involved in this.

### 1.2.7 Epigenetic regulation

As well as at the level of transcription, autophagy is epigenetically regulated through DNA methylation, histone modifications (methylation and acetylation), and micro-RNAs. There is evidence to show DNA methylation on the promotor region of autophagy genes including, ULK2, beclin1, LC3, LAMP2, DAPK and others (Hu, 2019). Methylation of CpG islands in the promotor regions of genes usually results in transcriptional inhibition. However, this process is reversible, and demethylation can restart transcription of such genes. Histone acetylation also has a role in autophagy regulation. SIRT1 histone deacetylase (HDAC), removes acetylation from histone H4K16ac and inhibits basal autophagy levels, whereas hMOF a histone acetyl

transferase (HAT) counteracts this effect. hMOF itself is an autophagy substrate which leads to a reduction in histone acetylation and acts as a negative feedback loop (Hargarten and Williamson, 2018). Interestingly, many of the HATs and HDACs that acetylate and deacetylate histones post-translationally modify non-histone proteins including autophagy proteins. Therefore, when analysing experiments involving up and down regulation of these enzymes, it can be hard to determine whether the primary driver of autophagy induction/inhibition is the histone modification or cytosolic protein modification. Histones can also be methylated, however, this can both activate and supress transcription depending on the histone as well as the methylated residue (lysine or arginine). For example, methylation of histone H3R17me2 leads to the transcription of TFEB, one of the key transcription factors that activate autophagy. While histone H3K9 methylation leads to the silencing of many autophagy linked genes such as LC3B and WIPI1 (WD-repeat protein Interacting with PhosphoInositide 1) (Hu, 2019). Micro-RNAs are small single stranded RNA molecules that are complementary to certain mRNAs and promote their degradation before translation can happen. Evidence suggests that miRNAs play a role in autophagy regulation. MIR34 has been shown to target Bcl-2 and the HDAC SIRT1 which both play a role in autophagy. Other microRNAs have been shown to interact with BENC1, ATG4, Rheb1, TFEB and many other transcripts (Lapierre *et al.*, 2015).

### 1.2.8 Post-translational modification

Post-translational modifications of proteins play an important role in the regulation of autophagy. Phosphorylation of proteins is one of the key methods to activating or sequestering proteins in the cell. Some examples of post-translational modification have already been mentioned (Section 1.2.6). mTOR inhibits autophagy mainly through phosphorylating autophagy proteins. AMPK is activated in nutrient starved conditions through its phosphorylation and, being a kinase itself, acts on downstream proteins through phosphorylation. The activity of TFEB and PKCθ are both controlled through their phosphorylation. Another example of where

phosphorylation regulates autophagy is the phosphorylation of beclin1 by JNK and DAPk which activate autophagy (Wei *et al.*, 2008; Zalckvar *et al.*, 2009). Other important post-translational modifications include glycosylation, acetylation, and ubiquitination (Xie *et al.*, 2015). Glycosylation is an important modification in membrane trafficking and the secretory pathway. ATG9 is a membrane protein that is glycosylated and has a key role in growing the phagophore membrane through coordinating membrane transport. SIRT1 the histone deacetylase mentioned previously (Section 1.2.7) also has a dual effect of removing acetylation from histones as well as autophagy related proteins. One target of SIRT1 is the FOXO3 transcription factor which can activate autophagy. Ubiquitination also plays a role in autophagy regulation. Two autophagy proteins that are ubiquitinated include BENC1 and ULK1. Ubiquitination of BENC1 can regulate its interaction with BCL2, whereas ubiquitination of ULK1 can stabilise and activate it (Xie *et al.*, 2015). As well as activation of autophagy, ubiquitination plays an important role in the selection of cargo which is discussed in more detail later in the chapter.

## 1.3 Initiation of Autophagy

Two key components of autophagy are the initiation and nucleation of the phagophore membrane are the ULK1 (Unc51-like kinase 1)/ATG1 complex and the class III phosphatidylinositol 3-kinase (PI3KCIII).

### 1.3.1 ULK1/ATG1 Complex

The signals for the initiation of autophagy usually converge on the downstream ULK1 (mammals)/ATG1 (yeast/*Drosophila*) complex. The yeast and *Drosophila* ATG1 complex comprise of ATG1, ATG11, ATG13, and ATG17-ATG29-ATG31. The mammalian ULK1 complex consists of ULK1, FIP200 (Focal adhesion kinase family-interacting protein 200 kDa), ATG13, and ATG101 (Hurley and Young, 2017). Under

normal fed conditions, the mTOR1 complex would hyperphosphorylate ATG13 and ULK1/ATG1 preventing the formation of the ULK1/ATG1 complex. However, once autophagy has been triggered, for example through starvation, there is inhibition of mTOR which inactivates its kinase activity on ULK1/ATG1. This alone is not enough and widespread dephosphorylation of the ULK1/ATG1 complex through currently unknown phosphatases is also necessary (Wong *et al.*, 2013). In addition, there is dimerization of ULK1/ATG1 followed by the specific autophosphorylation of Thr 180 in ULK1 and Thr 226 in ATG1 which activates ULK1/ATG1 (Li and Zhang, 2019). This then encourages the formation of the ULK1/ATG1 complex and enables its kinase activity. Therefore, are careful balance between autophosphorylation and hyperphosphorylation through mTOR and other means controls whether the ULK1/ATG1 complex forms or not. Although not as well studied, the acetylation and ubiquitination state of ULK1 also seems to play a role in its activation. TIP60, which is downstream of AKT/GSK3B pathway, in mammals has been shown to acetylate and activate the ULK1 complex (Lin *et al.*, 2012). Lysine ubiquitination of ULK1 by Cul3-KLHL20 ligase complex leads to its degradation (Liu *et al.*, 2016). It is thought that this degradation acts as a negative feedback loop to prevent excessive autophagy.

Once the ULK1/ATG1 complex has been activated, it needs to be recruited to the phagophore initiation site. In yeast, autophagy is initiated at the pre-autophagosome structure (PAS). In mammals, the membrane for the phagophore can come from many different membrane bound organelles and forms around the PI(3)P rich omegasome. In both mammals and yeast, assembly at the autophagy initiation site is regulated through ATG13 phosphorylation (Suzuki *et al.*, 2007). In yeast, ATG17 is the first to arrive at the PAS along with its accessory proteins ATG29 and ATG31, which is then able to act as a scaffold to recruit ATG1 and ATG13. It is thought that mammalian recruitment of ULK1 transpires in a similar way (Cheong and Klionsky, 2008). As mentioned previously, the ULK1 complex has kinase activity, the targets of which include other members of the ULK1 complex, the PI3KC3-C1 complex and ATG9 (Papinski and Kraft, 2016).

### 1.3.2 PI3KC Complex

Phosphatidylinositol 3-kinase (PI3K) phosphorylates phosphatidylinositol which produces phosphatidylinositol 3-phosphate (PI(3)P), a key player in autophagy initiation (Dikic and Elazar, 2018). PI3Ks form three complexes class I, class II and class III PI3KC. Each plays a role in autophagy, however, the class II PI3KC is particularly important in autophagy initiation. In yeast and *Drosophila*, the class III PI3KC complex is the VPS34 (vacuolar protein sorting 34) complex which forms a complex with Vsp15 (P150 in mammals), ATG6 (beclin1 in mammals) and ATG14L (ATG14 in mammals) (Juhasz *et al.*, 2008). Class III PI3Ks forms two complexes PI3KC3-C1 and PI3KC3-C2 (Kihara *et al.*, 2001; Itakura *et al.*, 2008). PI3KC3-C1 is involved in phagophore membrane elongation while PI3KC3-C2 with the help of UVRAG (UV radiation resistance-associated gene protein) is involved in autophagosome/endosome maturation. The interaction of PI3KC3 with beclin1 is necessary to increase the levels of PI(3)P. It is the sequestering of beclin1 through its binding to Bcl-2 that prevents the interaction with PI3KC3 from occurring (Dikic and Elazar, 2018). The sequestration of beclin1 is inhibited through methods such as toll-like receptors signalling or the ubiquitination of beclin1. PI(3)P is involved in the targeting of autophagy protein to the phagophore membrane. Some of these autophagy proteins include: Atg18, Atg20, Atg21, and Atg24 (He and Klionsky, 2009). ATG14L/ATG14 is necessary to target PI3KC to the PAS of yeast and the autophagy initiation site in mammals (Li and Zhang, 2019). Two other important proteins part of the complex are ATG38 (NRBF2-nuclear receptor binding factor 2 in mammals) and AMBRA1 (activating molecule in BENC1-regulated autophagy protein 1). NRBF2/ATG38 helps with the kinase activity of PI3KC3-C1. AMBRA1 is a phosphorylation target for the ULK1 complex, which then goes on to activate PI3KC3-C1. Although extensive work has not been carried out on this protein, it is thought that AMBRA1 helps with the PI3KC3 complex assembly (Li and Zhang, 2019). The primary role of PI3KC-C1, along with the other recruited ATG proteins, is to recruit the ubiquitin-like conjugation system ATG12-ATG5-ATG16 and ATG8-phosphatidylethanolamine (PE) which is discussed later.

### 1.3.4 ATG9/COPII Vesicles

ATG9 is a six-transmembrane protein that is phosphorylated by ULK1 and is important in autophagosome formation. Both ATG9 containing vesicles and COPII vesicles are necessary components (Hurley and Young, 2017). Trafficking between the ER and Golgi happens through specialised ER regions called ER exit sites (ERES), it is here that COP II vesicles are found. ATG9 vesicles, which are very small and referred to as micro-vesicles, are derived from the Golgi. Upon autophagy activation, the protein Sec24 on the COPII vesicle membrane is phosphorylated (T324, T325, T328) by the Hrr25 kinase, and a number of these vesicles are redirected to the PAS or autophagy initiation site (Wang *et al.*, 2017). Therefore, COPII vesicles provide a mechanism whereby membrane can be exchanged form the ER to the growing phagophore. Similarly, ATG9 containing vesicle relocate to the autophagy initiation site from a vesicle reservoir which is found close to the Golgi. The activation of ATG9 as well as its cycling between the PAS/autophagosome and the vesicular pools are necessary for autophagosome formation (Reggiori and Tooze, 2012; Reggiori *et al.*, 2004). Therefore, ATG9 can also be seen as a delivery mechanism to donate membrane to the growing phagophore membrane. However, it should be noted that ATG9 vesicles are small and do not provide anywhere near enough membrane to form an autophagosome and the membrane donated is likely just a requirement of the initial phagophore membrane growth (Yamamoto *et al.*, 2012). Mammalian ATG9 is not found on closed autophagosomes therefore, it is likely removed before this process is completed.

### 1.3.5 ATG5-ATG12 Conjugation

Phagophore extension and formation of the autophagosome requires two ubiquitin-like (Ubl) systems. One of these is the ATG5-ATG12 conjugation system. The E1 activating enzyme equivalent, ATG7, uses a molecule of ATP and forms a thioester bond with ATG12. The ATG12 is then transferred to ATG10, the E2 conjugating enzyme

equivalent, and then finally attached to lysine 130 on the substrate ATG5, forming an isometric peptide. There does not appear to be an equivalent E3 ligase enzyme and the conjugation works without it. This is because the E2 conjugation like enzyme ATG10 directly recognises the substrate ATG5 and transfers the ATG12 (Geng and Klionsky, 2008). A pair of ATG12-ATG5 then forms a complex with ATG16 (ATG16L in mammals) and dimerises. The ATG12-ATG5-ATG16 complex then attaches to the growing phagophore membrane (Mizushima, Noda and Ohsumi, 1999). One of the roles of the ATG12-ATG5-ATG16 complex it to promote curvature of the phagophore membrane and to form/recruit LC3B-II/ATG8-PE which is discussed next. This complex forms even without the induction of autophagy, and similar to ATG9, it is not found on a completed autophagosome so is removed through some mechanism (Barth, Glick and Macleod, 2010). It is worth noting here that there is a lot of interplay between the two conjugation systems (ATG5-ATG12 and ATG8-PE), which will be discussed in more detail later.

### 1.3.6 LC3 Processing

LC3 (microtubule associated protein 1 light chain 3) is the mammalian homologue of the yeast ATG8 protein (ATG8a in *Drosophila*), which is part of the second Ubl conjugation systems in autophagy. In fact, mammals contain a family of ATG8 proteins which fall into two sub-families known as the microtubule-binding protein-1 light-chain-3 (MAP1LC3, also known as LC3), and GABARAP (GABA type A receptor associated protein)/Golgi-associated ATPase enhancer of 16 kDa (GATE-16). (Weidberg *et al.*, 2010). LC3A, LC3B, LC3C is part of the LC3 family, while GABARAP, GABARAPL1 (GEC1), GABARAPL2 (GATE-16), GABARAPL3 is part of the GABARAP/GATE-16 family. *Drosophilas* have two ATG8 proteins; ATG8a and ATG8b. ATG8a is the only one which has ubiquitous expression and is known to be vital for autophagy. LC3 processing (Figure 1-10) refers to the proteolytic cleavage of LC3 followed by the Ubl conjugation of the lipid phosphatidylethanolamine (PE) to LC3. LC3 is expressed as a full-length protein and when autophagy is induced, it is cleaved

into LC3-I by the cysteine protease ATG4. Parallel to the ATG5-ATG12 conjugation, LC3-I is activated by the E1 activating enzyme equivalent, ATG7, and then transferred onto PE by ATG3. The membrane bound form of LC3-I is known as LC3-II-PE (or ATG8-II-PE in yeast). The process of LC3B attaching to a membrane is sometimes referred to as LC3 lipidation. ATG3 is the E2 conjugating enzyme equivalent(Geng and Klionsky, 2008). GABARAP is processed in a very similar way. Since autophagy induction leads to a conversion of LC3-I to LC3-II, the conversion of LC3 to a lipidated molecule is a commonly used marker for autophagy induction (Kirkin *et al.*, 2009). LC3II is found on both the outside and inside of the phagophore membrane and has various effects. For one, it has been shown to promote hemi-fusion of membranes in liposomes (where only the outer layer of two membranes fuse together), leading to liposome aggregation. Considering that the lack of ATG8 in cells leads to much smaller autophagosomes, it is thought that this hemi-fusion process can be involved in the growing of the phagophore membrane. Interestingly, upon ATG4 binding to LC3B, it blocks the binding to PE (Li and Zhang, 2019). Therefore, ATG4 also acts to dissociate LC3 from the autophagosome membrane. ATG8/LC3B is also critical to the selection of cargo through a very specific motif, this is discussed at length in a later chapter.

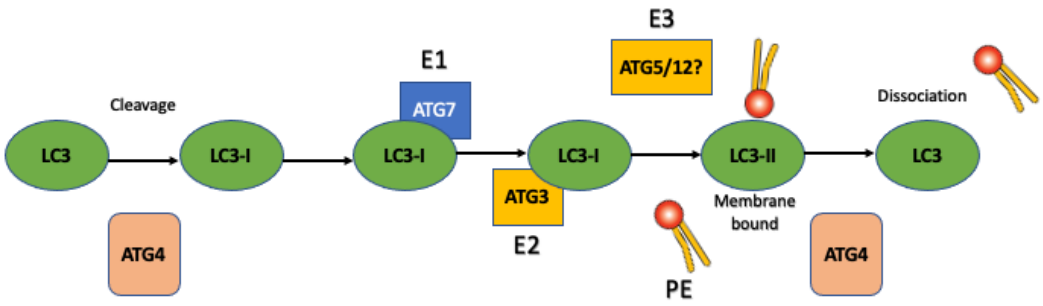


Figure 1-10 **LC3 processing.** This includes cleavage of LC3 into LC3-I followed by the ubiquitin-like conjugation system. This results in the formation of LC3-PE (LC3 conjugated to phosphatidylethanolamine (PE)). As well as being involved in the initial cleavage process, ATG4 is also involved in dissociation of LC3 from PE once the autophagosome is fully matured. There is also evidence that ATG12-ATG5 complex (described below) is the E3 ligase in this process.

The ATG12-ATG5 conjugation system interacts with the ATG8-PE conjugation system. As well as being part of the ATG12-ATG5-ATG16 complex which binds to the phagophore membrane, ATG16 appears to be very important in the formation of both ATG12-ATG5 and ATG8-PE. In an in-vitro system, it was shown that ATG12-ATG5 itself was able to promote the formation of ATG8-PE (Walczak and Martens, 2013; Zens, Sawa-Makarska and Martens, 2015). There is also evidence that ATG12-ATG5 can act as an E3 ligase enzyme for ATG8-PE. ATG12-ATG5 interacted with ATG3, the E2 conjugating enzyme equivalent for the ATG8-PE conjugation system, and promoted the transfer of ATG8 to PE (Li and Zhang, 2019).

## 1.4 The autophagosome

### 1.4.1 Cargo Selection

Autophagic degradation of cellular material was largely thought to be a non-specific bulk process. This is because when looking at the contents of autophagosomes, there was usually a variety of contents for example, mitochondria, ER, Golgi, and aggregated proteins. However, it is now known that autophagy can happen in a very selective manner through receptors and adapters. The exact mechanism of selective autophagy in different species is discussed in detail later in the chapter. Both bulk and selective autophagy can happen alongside each other and there is usually a basal level of autophagy continuously occurring in cells.

Whether the phagophore membrane comes first and then cargo is recruited to the site or the phagophore membrane forms around already present cargo is dependent on the cause of autophagy (Zaffagnini and Martens, 2016). Starvation induced autophagy seems to involve the formation of a phagophore membrane upstream of cargo selection. However, when autophagy is occurring independent of starvation, for example basal autophagy, the autophagic membrane appears to form around the cargo to be degraded. In this scenario, cargo accumulates in one location

and recruits various autophagy adapters and scaffold proteins. This in turn will activate the autophagic machinery and trigger the formation of an isolation membrane around the cargo. The Cvt pathway (Cytoplasm to vacuole targeting pathway) is a commonly used model of selective autophagy in yeast and provides evidence of cargo selection being upstream of phagophore nucleation (Lynch-Day and Klionsky, 2010). The Cvt pathway involves the use of the autophagic machinery to sequester hydrolases in autophagosomes and deliver them to the vacuole (yeast lysosome). When the protein preApe1, a cargo for the Cvt pathway, was deleted in yeast, it reduced basal autophagy through preventing the recruitment of autophagy proteins to the PAS (Shintani and Klionsky, 2004). However, starvation induced autophagy in the same yeast was unaffected. Another piece of evidence for this model is during the selective degradation of mitochondria (Mitophagy). Cargo receptors binding to damaged mitochondria recruit autophagy proteins and trigger the formation of an autophagosome around the mitochondria (Lazarou *et al.*, 2015). Thus, it seems to be that when there is the selective autophagy of specific proteins or organelles, the cargo is what triggers the formation of the autophagosome. Whereas for starvation induced autophagy, the phagophore membrane nucleation occurs upstream of cargo selection. This is likely how most bulk degradation pathways occur.

### 1.4.2 Autophagosome maturation and fusion

The phagophore elongates and eventually closes off to form an autophagosome. Once the autophagosome has been sealed, it undergoes maturation which includes the removal of various autophagy proteins (Reggiori and Ungermann, 2017). The main one being ATG8/LC3 which in turn may destabilise other autophagy proteins and lead to their dissociation. In yeast, when cells were expressing post cleavage ATG8 and had ATG4 knocked down, they were able to form autophagosomes but unable to fuse with the vacuole (Yu *et al.*, 2012). This highlights the importance of ATG4 action to dissociate ATG8 form the autophagosome. Similarly, PI3P phosphatases (such as Ymr1 and Sjl2/Sjl3), which remove PI2P from the

autophagosome are also necessary for the fusion step to happen (Parrish, Stefan and Emr, 2004). In mammalian cells, the importance of ATG4 and PIP3 phosphatases in LC3/PIP3 removal is less characterised but various PIP3 phosphatases being involved in autophagy initiation have been identified. As well as the removal of ATG proteins, the recruitment of the fusion machinery, and the cellular localisation of the autophagosome and vacuole/lysosome, is also a part of autophagosome maturation (Nakamura and Yoshimori, 2017). This process occurs differently in yeast compared to metazoan cells.

In yeast, fusion of the autophagosome with the vacuole requires various factors including the HOPS (homotypic vacuole fusion and protein sorting) tethering complex, SNAREs, and Rab7-like Ypt7 protein. The RAB GTPase Ypt7 requires the guanine nucleotide exchange factor (GEF) Mon1-Ccz1 (Nordmann *et al.*, 2010). The HOPS complex is able to bind both Ypy7 and SNAREs, therefore able to connect the two on different membranes (Stroupe *et al.*, 2006). There are various SNARE proteins found to be involved in autophagosome fusion including: Vam3, Vti1, Vam7, and Ykt6. Vam7 appears to be particularly important as it interacts with ATG17, which is part of the ATG17-ATG31-ATG29 complex. Without this interaction, there is a significant reduction in autophagosome fusion (Reggiori and Ungermann, 2017). Unlike yeast, the fusion of the autophagosome happens with both the late endosome (amphisomes) and the lysosome. In metazoan cells RAB7 is required for autophagosome fusion with late endosomes and lysosomes, and it was found that in *Drosophila,* the GEF is also Mon1-Ccz1 (Hegedus *et al.*, 2016). The recruitment of HOPS to the autophagosome was suggested to be mediated by UVRAG (VPS38 in yeast) which itself is regulated by mTORC1, making this another point of autophagy control (Kim *et al.*, 2015). HOPS in metazoan cells binds indirectly to RAB7 through the GTPases ARL8, RAB2 and RAB7-interacting lysosomal protein. Additionally, other proteins have been found to be very important in the autophagosome fusion process such as PLEKHM1 (Plekstrin homology domain-containing family M member 1), TECPR1 (Tectonin beta-propeller repeat-containing protein 1), and RUFY4 (RUN and FYVE domain-containing Protein 4). PLEKHM1 promotes fusion by being able to interact with both LC3 and HOPS (McEwan *et al.*, 2015). TECPR1 seems to modulate

its fusion effect through its interaction with the ATG12-ATG5 conjugate and PI3P (Chen *et al.*, 2012). RUFY4 promotes tethering of autophagosomes with lysosomes as it contains both a RUN domain and an FYVE domain which allows it to interact with small GTPases and PI3P respectively (Terawaki *et al.*, 2015). The need for fusion proteins to be binding both LC3 and PI3P seems contradictory to the previously mentioned removal of these components during the maturation of autophagosomes. An explanation for this may stem from incomplete removal of ATG8/LC3 and PI3P, resulting in small clusters of these proteins remaining in position for fusion. Alternatively, maturation and fusion can happen simultaneously, where fusion can take place while the last few molecules of LC3 and PI3P are being cleaved off the autophagosome. The SNAREs involved in metazoan autophagosome fusion include SYN17 (Syntaxin 17), SNAP29, and VAMP7/8 (Itakura, Kishi-Itakura and Mizushima, 2012). There is also some evidence that ATG14L, which forms part of the PI3P kinase complex, supports the assembly of these SNAREs (Diao *et al.*, 2015).

### 1.4.3 Degradation and release of products

Once the autophagosome has fused with the lysosome, the lysosomal hydrolases will have access to the autophagosome cargo and can degrade it. An important hydrolase found in yeast vacuole is the Atg15/Aut5/Cvt17, a lipase which has a role in the degradation of autophagic bodies in the vacuole (Epple *et al.*, 2001). Lysosomes in metazoan cells will receive both intracellular material from the autophagosome as well as extracellular material from the endocytic pathway. The primary role for the degradation of these molecules, is to reuse the material for the synthesis of new macromolecules. To get the breakdown products back into the cytoplasm, transporters and permeases are needed. In yeast this includes, Atg22, Avt3 (SLC36A1/LYAAT-1in mammals) and Avt4 (SLC36A4/LYAAT-2 in mammals) (Sagne *et al.*, 2001). However, much is unknown about this process. Another use for the degradation products includes regeneration of storage molecules like glucose, where processes like gluconeogenesis in the liver rely on these materials. Similar to this, the

degradation products can be used directly as a source of energy through the tricarboxylic acid cycle (TCA cycle) (Mizushima, 2007).

## 1.5 Selective Autophagy

### 1.5.1 The Cvt Pathway in yeast as a model for selective autophagy

The Cvt pathway is commonly used as a way of modelling selective autophagy (Lynch-Day and Klionsky, 2010). The role of the Cvt pathway is to deliver hydrolases, including aminopeptidase 1 (Ape1) and α-mannosidase (Ams1), to the vacuole. In yeast, the vacuole serves a similar purpose to the lysosome in mammalian cells. The stages of the Cvt pathway delivery are very similar to autophagy, where there is a PAS, which sequesters the cargo in a double membrane vesicle ready for fusion with the vacuole. However, the selective Cvt vesicle is much smaller (≈150 nm) than the bulk degradation autophagosome under starved conditions (≈500 nm) (Lynch-Day and Klionsky, 2010). This Cvt vesicle is then able to fuse with the vacuole and release its contents where it is degraded and transported back out of the vacuole. Hydrolases that are transported into the vacuole through this pathway become activated once inside the vacuole and can then carry out their degradation functions. The selective nature of this pathway comes from the specific hydrolases (precursors of Ape1 and Ams1) being selected as cargo. Cargo is usually selected for sequestration through cargo receptors. Ape1 is more well studied, and it was found that ATG19 (originally called Cv19) was the receptor which recognises Ape1 (Leber *et al.*, 2001; Scott *et al.*, 2001). In the Cvt pathway, there is also a specificity factor that connects the receptor on cargo to the autophagic machinery. In the case of Ape1 the specificity receptor is Atg11 and its main job, through its interaction with ATG19, is to transport the cargo to the PAS (Yorimitsu and Klionsky, 2005). Once there, a particular motif on the ATG19 called an LIR motif (LC3-interacting region) allows it to bind to ATG8 (Yamasaki and Noda, 2017). The LIR motif and its binding pocket in ATG8/LC3 is a highly conserved

motif throughout eukaryotic organisms and this is discussed in detail in the next section (Birgisdottir, Lamark and Johansen, 2013). There are many examples of selective autophagy in yeast including the selective degradation of mitochondria (mitophagy) and the selective removal of peroxisomes (pexophagy) (Kraft, Reggiori and Peter, 2009). As mentioned previously in selective autophagy it is the cargo and cargo complex with its receptors/adapters that comes first followed by its sequestering into vesicles.

### 1.5.2 ATG8/LC3 and the LIR Motif

The majority of selective autophagy interactions discovered so far occur through the LC3-interacting region motif (LIR motif) (Birgisdottir, Lamark and Johansen, 2013). This motif is found on a select number of proteins and binds the LIR docking site (LDS) found on the ATG8/LC3 protein found on the surface of the growing phagophore membrane. LIR motif containing proteins are usually proteins that are selectively degraded through basal levels of autophagy. However, they also include receptors and adapters that can act as a specific bridge between ATG8 and cargo.

The first targets for selective autophagy to be discovered were the p62 receptor and the Cvt cargo protein ATG19. As alluded to previously, the role of autophagy receptors is to bind both cargo and the ATG8 on the phagophore membrane, which sequester cargo for degradation. Once it was identified that p62 contained a motif which specifically binds ATG8 (Pankiv *et al.*, 2007), two groups, Noda et al and Ichimura et al, were able to provide structural evidence for this interaction (Ichimura *et al.*, 2008; Noda *et al.*, 2008). This was done through structural techniques such as NMR and x-ray crystallography. Similar experiments were conducted for the interaction between ATG19 and ATG8. The general LIR motif has the consensus sequence of [W/F/Y]-x-x-[L/I/V] where x represents any amino acid (Birgisdottir, Lamark and Johansen, 2013). The W/F/Y and the L/I/V are the most conserved positions amongst eukaryotes and are the most important. This is because these two hydrophobic amino acids bind the two hydrophobic binding pockets found on the LIR

docking site (LDS) of ATG8/LC3 protein. The most common amino acids in these two positions are W and L and so sometimes the motif is simply referred to as WxxL. It was also determined that the amino acids flanking the LIR motif are also important. Upstream of the tryptophan (W) and/or downstream of leucine (L) are usually acidic residues typically aspartic acid (D) and glutamic acid (E) but could also be serine/threonine (S/T). Pankiv et al showed that three aspartic acid residues upstream of tryptophan (W) was important for the interaction of p62 with LC3B (Pankiv *et al.*, 2007). This is likely due to the many basic residues which surround the first and second hydrophobic binding pocket on ATG8 (HP1 and HP2). The fact that serine/threonine is also present flanking the LIR motif is indicative of a potential control mechanism through post-translational modification (phosphorylation). The two x amino acids in the centre (now referred to as x1 and x2) usually have hydrophobic or acidic residues. The second amino acid, x2, is the most flexible and can sometimes contain basic residues (Johansen and Lamark, 2020). LIR motifs which contain an F in the first position tend not to have as high of an affinity for the hydrophobic binding pocked on ATG8a as motifs with W. However, for F containing LIR motifs, x1 seems to be a lot more important.

It is worth noting that not every protein which contains a LIR motif is able to interact with ATG8. Popelka and Klionsky helped narrow down the number of potential functional LIR motifs in a protein of interest (Popelka and Klionsky, 2015). They did this by using modelling to determine disorder propensity of different LIR motifs and discovered that many LIR motifs tend to occur in intrinsically disordered protein regions (IDPR). In many cases during interaction of a LIR motif protein with ATG8, the disordered region becomes ordered into a $\beta$-pleated sheet (occasionally $\alpha$ helices), to allow binding to the LIR docking site. Intrinsically disordered regions also tend to be phosphorylated more easily which could play a role in binding. The Nezis lab has used the in-silico analysis of functional LIR motif to create a new consensus sequence which extends the WxxL motif on either side. This motif, called xLIR, was (ADEFGLPRSK)(DEGMSTV)(**WFY**)(DEILQTV)(ADEFHIKLMPSTV)(**ILV**) where WFY and ILV are the two main hydrophobic residues. This information, along with the prediction of

intrinsically disordered regions, was then used to create a webtool which helps identify likely functional LIR motifs (Jacomin *et al.*, 2016; Kalvari *et al.*, 2014).

As mammalian cells have different forms of ATG8, including LC3 and the GABARAP family of proteins, different LIR motifs show preference to certain forms of ATG8. There are many LIR motif containing proteins that have a higher affinity for GABARAP than LC3, some that bind exclusively to GABARAP and a few that are specific to LC3 (Johansen and Lamark, 2020). LIR motifs which bind specifically to GABARAP family of proteins was given the name GABRAP interaction motif (GIM), which has the consensus sequence [W/F]-[V/I]-x-V (Rogov *et al.*, 2017). There are of course some exceptions to this motif, where some motifs do not contain a valine (V) or isoleucine (I) at position 2 or a valine (V) at position 4. The C-terminal end of the LIR motif up to position x10 in GIMs are very important as many seem to contain a lot of hydrogen and hydrophobic interactions (Johansen and Lamark, 2011). However, not every LIR motif which bind GABARAP specifically have a GIM.

There are also some LIR motifs which do not follow typical consensus sequence. For example, one of the two main amino acids (W/F/Y and L/I/V) could be missing, yet the interaction with ATG8/LC3 is maintained. An example of this is NDP52/CALCOCO2 which does not have the first aromatic residue in its LIR motif (von Muhlinen *et al.*, 2012). The interaction with LC3 is maintained as other hydrophobic residues can interact with the LDS. Examples of LIR motif proteins that have the second hydrophobic amino acid missing are Bcl-2 and TRIM5$\alpha$ (Ma *et al.*, 2013; Mandell *et al.*, 2014). Similarly, a protein called UBA5 (ubiquitin like modifier activating enzyme 5) has a modified LIR motif W-G-I-E-L-V, which not only bind the first and second hydrophobic binding pocket on GABARAP with Isoleucine (I) and valine (V), but also a new third hydrophobic binding pocket with its tryptophan (W) residue. This new binding pocket is only exposed during binding to LC3 as big changes to the proteins 3D structure allows this to be possible (Habisov *et al.*, 2016).

### 1.5.3 ATG8/LC3 and the UIM Motif

There has been identification of proteins that interact with ATG8 but not through the characterised LIR motif LDS interaction. For example, the Vierstra group identified RPN10 as cargo receptor for the autophagic degradation of the proteasome in Arabidopsis in a LIR motif independent manner (Johansen and Lamark, 2020; Marshall *et al.*, 2019; Lei and Klionsky, 2019). This group recently identified and characterised a novel motif which interacts with a different region on the ATG8 protein. They called this the ubiquitin interacting motif (UIM) which interacts with the UIM-docking site (UDS) on ATG8. By using alanine substitution on plant ATG8 and the 3D structure of yeast ATG8, they located this UDS site. This UDS is located on the opposite side to the LDS and so the simultaneous binding of a LIR motif containing protein and UIM containing proteins is possible. The group showed the binding of UIM containing RPN10 and LIR motif containing DSK2 (dominant suppressor of KAR 2) was possible (Marshall *et al.*, 2019).

The UIM, being only recently discovered, is broadly characterised as a 20 amino acid long sequence which takes the form of an amphipathic $\alpha$-helix. The UDS domain is described as having a conserved phenylalanine surrounded by many hydrophobic residues. However, exact points of interactions are not yet known as no structural biology experiments with a protein bound to ATG8 via the UDS have been done. In Arabidopsis there is a family of proteins called the plant ubiquitin regulatory X domain proteins (PUX) which interact with ATG8. Of these, PUX7_ARATH, PUX8_ARATH, PUX9_ARATH and PUX13_ARATH seem to bind ATG8 through the UIM-UDS interaction (Marshall *et al.*, 2019; Lei and Klionsky, 2019). As well as existing in Arabidopsis, the UIM-UDS interaction is conserved in humans and yeast. In yeast proteins Ent1 and Ent2, as well as Ubx5 bind ATG8 through the UDS. In humans, Epsin1/2/3, Rabenosyn, Ataxin-3 and Ataxin-3L bind either LC3 or GRABARAP through their UIM motifs. UIM/UDS interactions have yet to be identified in *Drosophila*.

A recent unpublished paper also described the UIM-UDS interaction in mammalian ATG9 proteins (Ting Zhang, 2020). This includes both ATG9a and ATG9b. It was shown that the ATG9s not only co-localise with the autophagosome, but also directly interact with LC3 through the UDS domain. ATG9a has one predicted UIM and ATG9b has two. The interaction of ATG8 with proteins through the UIM-UDS domain

seems to be very important at recruiting autophagy receptors and adapters to the autophagosome site. Over the next few years, more functional UIM containing proteins are likely to be discovered.

## 1.6 Autophagy adapters and substrates

Below is a table summarising key autophagy adapters and substrates discussed in the next two section.

Table 1 – Key Autophagy receptors, adapters, and substrates

| Adapter/ substrate name (Human) | Adapter/ substrate name (Drosophila) | Role | Reference |
|---|---|---|---|
| P62/SQSTM1 | Ref(2)P | Adapter involved in degradation of ubiquitinated proteins | (Zaffagnini and Martens, 2016) |
| NBR1 | | Adapter involved in degradation of ubiquitinated proteins and pexophagy | Johansen and Lamark, 2011 |
| NDP52 | | Xenophagy | Zaffagnini and Martens, 2016 |
| Optineurin | | Xenophagy, aggrephagy, mitophagy | Sharma *et al.*, 2018 |
| Alfy | Blue cheese | Adapter involved in degradation of ubiquitinated proteins | Filimonenko *et al.*, 2010 |
| SNX18 | SH3PX1 | Regulation of autophagy | Knaevelsrud *et al.*, 2013 |
| | CKA | Movement of autophagosomes | Neisch, Neufeld and Hays, 2017 |
| ULK1 | ATG1 | Regulator of autophagy | Alemu *et al.*, 2012 |

The interaction between ATG8/LC3 and proteins to be selectively degraded usually happens through receptors or adapters. The recognition of cargo by autophagy adapters is largely controlled through the post-translational modification of target proteins, specifically ubiquitination. The majority of adapters bind ubiquitinated proteins through one of three ubiquitin binding domains: UBA domain, UBAN domain and UBZ domains (Behrends and Fulda, 2012). The most well-known adapter is the P62/SQSTM1 found in mammals which is an autophagy adapter which can bind ubiquitinated proteins through its UBA domain. P62 also has a LIR motif through which it can tether selective cargo to LC3 on the autophagosome membrane. The UBA domain on P62 specifically recognises K48 and K49 polyubiquitin chains. Different ubiquitin binding domains have different preferences. Other adapters include the neighbour of BRCA1 (NBR1), optineurin (OPT) and nuclear dot protein 52 (NDP52). These proteins are discussed in detail in the following section (Abert, Kontaxis and Martens, 2016).

Selective autophagy can also happen through autophagy receptors. NIP3-like protein X (Nix) (also known as BNIP3L), is a mitophagy (selective degradation of the mitochondria) receptor which anchors its transmembrane domain to the outer mitochondrial membrane (Ding *et al.*, 2010). It is through this receptor that the selective clearance of mitochondria takes place. Nix also seems to play a role in the ubiquitination of damaged mitochondria for its targeted degradation. BNIP3 is another mitophagy receptor which seems to be important in the selective degradation of mitochondria in hypoxic conditions (as does Nix) (Zhang and Ney, 2009).

Post-translational modification is not only important for cargo selection, but also important for activation of functional LIR motifs. As mentioned previously, there are sometimes serine and threonine residues upstream of a LIR motif that can be the target of phosphorylation. Approximately 25% of LIR motifs contain this serine/threonine upstream of the motif, which can be used as a method of activating or inactivating the functionality of the LIR motif (Birgisdottir, Lamark and Johansen, 2013). Optineurin, an autophagy adapter, recruits TBK1 which phosphorylates optineurin at position S117 (the amino acid just before the LIR motif) which improves its binding to LC3B (Wild *et al.*, 2011). The negatively charged modification interacts

with Lys51 and Arg11 on LC3. S17 and S24 residues on BNIP3 which flank the LIR motif when phosphorylated show improved binding to ATG8. Whether or not this LIR motif is phosphorylated determines if BNIP3 induces apoptosis or pro-survival (mitophagy) (Zhu *et al.*, 2013). An example of phosphorylation negatively affecting LIR motif-LDS binding is with FUNDC1 (Liu *et al.*, 2012). This protein is inactivated upon phosphorylation, and unable to carry out its function as a selective mitophagy receptor. Under hypoxic conditions, the protein is dephosphorylated and mitophagy can continue as usual. There is also some evidence to suggest that the ATG8 protein itself may be phosphorylated to control which LIR motifs it may or may not bind, but more work is needed to verify this phenomenon (Cherra *et al.*, 2010). A more detailed description of different autophagy receptors and adapters are discussed in the following section.

## 1.7 Examples of selective autophagy substrates

### 1.7.1 P62/SQSTM1

The mammalian/yeast p62/SQSTM1 gene produces the ubiquitin binding p62 protein also known as sequestosome 1. As mentioned previously, this is an autophagy adapter that aids in the degradation of ubiquitinated cargo, such as aggregated proteins and pathogens (Zaffagnini and Martens, 2016). p62 is part of a group of autophagy adapters/receptors called the sequestosome-1-like receptors which also include: NBR1 (neighbour of BRCA1), NDP52 (nuclear dot protein 52), TAX1BP1 (tax1 binding protein 1) and OPTN (Optineurin) (Birgisdottir, Lamark and Johansen, 2013). The p62 protein is well studied in humans and mammals. The human p62 protein contain 440 amino acids which contains a PB1 (Phox and Bem1p domain) domain, ZZ-type zinc finger domain, nuclear localisation signal, LC3 interaction motif (LIR), KEAP1 interacting region motif, and a UBA (ubiquitin associated) domain (Johansen and Lamark, 2011). The most important of these for selective autophagy are the LIR motif,

the UBA domain and the PB1 domain. The UBA domain allows p62 to bind ubiquitinated proteins, and the LIR motif allows it to bind to the LDS on LC3. This allows it to act as a bridge holding the ubiquitinated cargo to the autophagosome membrane. The p62 protein as well as the Cvt cargo receptor in yeast (ATG19) was among the first selective autophagy adapter discovered. More recently, structural biology experiments have determined the exact points of interaction between the LIR motif on p62 and the LIR docking site (LDS) on ATG8a/LC3 (Kim, Kwon and Song, 2016). The PB1 domain of p62 is its polymerisation domain that means p62 along with any bound cargo can aggregate and strengthen its interaction to the autophagosome. This can counteract the fact that individually the UBA domain does not have a very high affinity for ubiquitin. The UBA domain of p62 also shows additional specificity to the type of ubiquitination. Once polymerised, p62 has a higher affinity for K63-linked and linear ubiquitin chains (both mono and poly-ubiquitin chains) (Johansen and Lamark, 2011). p62 is most well-known for its role in the selective degradation of proteins and aggrephagy, but it is also involved in pexophagy, xenophagy and mitophagy. Pexophagy and mitophagy through p62 is dependent on the E3 ligase PARKIN which is discussed in chapter 6 (Sharma *et al.*, 2018). p62, along with other members of the sequestosome-like receptor family of protein, was initially found as a selective autophagy adapter to *Salmonella* (xenophagy receptor). As bacteria are ubiquitinated upon entry to the cytosol, they can be recognised by the ubiquitin binding domains of such proteins and targeted to the LC3 protein on the autophagosome through the LIR motif. There is evidence of p62 being the selective autophagy adapter in the degradation of *S. typhimurium*, *S. flexneri* and *M. tuberculosis*. Similar to other adapters, the phosphorylation of p62 by TANK-binding kinase 1 (TBK1) enhances its xenophagy activity (Sharma *et al.*, 2018).

Ref(2)P (Refractory to sigma P) is the *Drosophila* homologue of the p62 protein with similar domains and functions. This protein is regularly used in this study as a marker of autophagic impairment and is discussed in more detail in chapter 3.

### 1.7.2 NBR1

NBR1 is another member of the sequestosome-like receptors. Although, this protein is much bigger, at 966 amino acids, it shares many of its domains with p62 (Johansen and Lamark, 2011). These include the ZZ-type zinc finger domain, the PB1 domain, the LIR motif, the UBA domain as well as domains unique to NBR1. As supported by its domain structure, NBR1 has a very similar role to p62 as an autophagy adapter. It tethers ubiquitin labelled cargo to the ATG8/LC3 on the autophagosome through its UBA domain/LIR motif. The UBA domain of NBR1 seems to prefer K63 polyubiquitin chains. Therefore, there is some redundancy in the roles of NBR1 and p62. However, there is a lot of evidence to suggest a more co-operative nature in the function of p62 and NBR1. The PB1 domain found in p62 not only allows for homo-polymerisation, but also hetero-polymerisation with the PB1 domain of NBR1 (Lamark *et al.*, 2009). Because this interaction happens in a slightly different region of the PB1 domain on p62, clusters of p62 as well as NBR1 at the phagophore membrane is seen. Both NBR1 and p62 also seem to have a role in pexophagy, the autophagic degradation of peroxisomes. The binding of NBR1 to peroxisomes involve the UBA domain and the upstream amphipathic α-helical J domain, the LIR motif, and an additional coiled coil domain (Deosaran *et al.*, 2013). Once NBR1 is on the peroxisome it recruits p62. Although both proteins are necessary for pexophagy under basal conditions, p62 is no longer required when NBR1 is overexpressed. It is worth noting that in the presence of p62, this process is more efficient, reinforcing the co-operative nature of NBR1 and p62.

### 1.7.3 NDP52

NDP52, also known as calcium-binding and coiled-coil domain-containing protein 2 (CALCOCO2), is a selective autophagy receptor involved in the selective degradation of bacteria (xenophagy) and damaged mitochondria (mitophagy) (Zaffagnini and Martens, 2016). NDP52 contains a coiled- coiled domain, two zinc

finger domains, galectin-8 binding region (Galbi), and a LIR motif. The coiled-coil region allows for dimerization and the two zinc finger domains are what make up the ubiquitin binding ability of this protein (UBZ type). The LIR motif of NDP52 is a non-canonical LIR motif and specifically binds LC3C (Birgisdottir, Lamark and Johansen, 2013). When bacteria invade the cytosol of mammalian cells, they are usually ubiquitinated as a signal to be degraded through autophagy (Behrends and Fulda, 2012). Similarly, bacteria can also be decorated with galectin-8, a protein which binds β-galactoside-containing glycans. another marker that can be recognised by NDP52. Therefore, NDP52 acts as an autophagy adapter by binding bacteria covered in ubiquitin and/or galectin-8 and attaching it to the autophagosome membrane through its interaction with LC3 (Viret, Rozieres and Faure, 2018). In terms of specificity with ubiquitin, it was shown that NDP52 can bind both individual and polyubiquitin chains (regardless of whether it is K48 or K63 linked). Much work has been done on NDP52 as an autophagy adapter specifically for the degradation of *Salmonella* bacteria (von Muhlinen *et al.*, 2010). The autophagy adapter p62 has also been shown to be involved in this degradation. Once NDP52 binds ubiquitinated bacteria, it recruits TANK-binding kinase 1 (TBK1), an IKK family member also found on the surface of cytosolic bacteria. NDP52 and TBK1 has been shown to degrade bacteria other than *Salmonella* such as *Streptococcus pyogenes*. NDP52 also has a paralogue called TAX1BP1/CALCOCO3 which has functional redundancy with NDP52 (Kirkin and Rogov, 2019). TAX1BP1 was shown to be important in the selective degradation of *S. typhimurium*. It performs this selective degradation by binding to the myosin motor VI and promoting autophagosome fusion with the lysosome.

### 1.7.4 OPTN

Optineurin (OPTN) is an autophagy adapter involved in xenophagy, aggrephagy and mitophagy (Sharma *et al.*, 2018). The human Optineurin protein is a 577 amino acid protein of which there are 4 isoforms generated through alternative splicing. Optineurin contains two ubiquitin binding domains which are of the UBAN type, a zinc

finger domain, a leucine zipper domain, multiple coiled-coil domains, a NEMO-like domain and a LIR motif (Ryan and Tumbarello, 2018). Again, the protein acts like other adaptors in the sense that it recognises mostly polyubiquitin chains on autophagy cargo and directs them to LC3 on the growing autophagosome membrane through its LIR motif. In terms of xenophagy, optineurin was recognised to be involved in the selective degradation of *Salmonella*, specifically *S. enterica (Wild et al., 2011)*. Many of these bacteria become covered in ubiquitin and thus were recognised through the ubiquitin binding domains on optineurin. Optineurin is required along with NDP52 and P62 for this process. Similar to NDP5, optineurin requires TBK1 to enhance its activity (Sharma *et al.*, 2018). Optineurin is needed as one of the final players in mitophagy to provide bind the targeted mitochondria to the autophagosome membrane via its LIR motif. Similarly, p62 is also recruited to the surface of the mitochondria but on a distinct part of the mitochondria. However, it was shown that while optineurin is mandatory for efficient mitophagy, p62 was not (Wong and Holzbaur, 2014). Optineurin is also a part of the degradation of aggregated proteins (aggrephagy) and is a key player in the degradation of ubiquitinated mutant Huntington-containing aggregates (Shen *et al.*, 2015). Overexpression of the p62 protein has been implicated in the progression of many cancers. Optineurin, along with the tumour suppressor protein HACE1, have a joint effect of supressing tumours through the increasing the autophagic degradation of damaged proteins and p62 (Liu *et al.*, 2014).

### 1.7.5 Alfy

Alfy is a mammalian autophagy receptor involved in the selective degradation of ubiquitinated proteins (Filimonenko *et al.*, 2010). It binds to and works alongside p62, while also being PI(3)P and ATG5 interactors. Therefore, Alfy acts as a scaffold protein that recruits other proteins to the autophagosome. It is a very large 3527 amino acid protein with a C-terminal ZZ-type zinc finger domain, BEACH domain, WD40 repeats and an FYVE domain. Alfy has also been shown to interact with LC3C and GABARAPs through a LIR motif dependent interaction (Lystad *et al.*, 2014).

Blue cheese is the *Drosophila* homologue of the mammalian Alfy protein. It is a highly conserved protein and has similar C-terminal domains to its human counterpart (Finley *et al.*, 2003). Blue cheese mutant flies have ubiquitinated protein aggregates in the brain which are Ref(2)P/p62 positive. This suggests that the degradation of ubiquitinated proteins via Ref(2)P is blue cheese dependent. These flies also have a reduced lifespan and age-related phenotypes like neurodegeneration.

### 1.7.6 SNX18/SH3PX1

SNX18 (SH3PX1 in *Drosophila*) is a mammalian sorting nexin protein involved in membrane deformation/remodelling and endocytic trafficking. It also has a role as a positive regulator of autophagy (Knaevelsrud *et al.*, 2013). When SNX18 is knocked down, no LC3 positive autophagosomes could form, however an overexpression of SNX18 increased the numbers of LC3 positive autophagosomes. Therefore, SNX18 likely has an important role in the formation of autophagosomes. SNX18 has also been shown to interreact with all members of the LC3 family of proteins apart from GABARAP2, however this interaction is not LIR motif dependent. Instead, SNX18 interreacts with LC3 family through a WDDEW motif. The *Drosophila* homologue of SNX18, SH3PX1 has similar functions and has been shown to interact with ATG8a.

### 1.7.7 CKA

CKA (connector of kinase to AP1) in *Drosophila* is a scaffolding protein that also has a role in autophagy in specific cells (Neisch, Neufeld and Hays, 2017). CKA in *Drosophila* is a 730 amino acid protein, which contains a striatin domain, a coiled coil domain and several WD40 domains. In *Drosophila* larval motoneurones CKA has been shown to facilitate the movement of autophagosomes to the assembly site for lysosomal fusion. CKA can interact with dynein (a motor protein) as well as ATG8a through a LIR motif dependent manner.

### 1.7.8 ULK1/ATG1

ATG1 is the *Drosophila* homologue of mammalian ULK1. ATG1 is an 855 amino acid serine/threonine kinase. Both the *Drosophila* and mammalian form of this protein has been shown to interact with ATG8a and the LC3 family of proteins respectively in a LIR motif dependent manner (Alemu *et al.*, 2012). ATG1/ULK1 is described earlier and is a regulatory protein found upstream of autophagosome formation. It acts as a scaffold that recruits other ATG proteins required for the formation of autophagosomes. ATG1/ULK1 is also found on the surface of autophagosomes, recruited through the LIR motif interactions. This means ULK1 likely has roles in early-stage autophagy initiation as well as downstream of autophagosome formation (Nakatogawa *et al.*, 2012). LIR motif mutations in yeast ATG1 only affects its role in late autophagy events.

### 1.7.8 Organellophagy

There are also many autophagy receptors involved in the selective degradation of organelles such as the mitochondria, nucleus, and ER. This is discussed in more detail in chapter 6.

## 1.8 Studying Autophagy in *Drosophila Melanogaster*

### 1.8.1 *Drosophila Melanogaster* as a model organism

*Drosophila melanogaster* make an excellent model organism due to being small, cost effective, easy to maintain and able to produce large numbers of progeny. They also have a very short lifecycle where; at 25°C, it takes 10-12 days to reach adulthood from an egg. This includes the 5 days of 3 larval stages and 3-5 days of pupae metamorphosis. Adults typically live for approximately 2 months.

Once the *Drosophila* genome was fully sequenced, it was found that it shares 60% homology with humans, making *Drosophila* useful for studying human diseases. In fact, 75% of genes in humans that are linked to diseases have a counterpart in *Drosophila*. The genes in *Drosophila* also have far less redundancy compared to humans, which makes studying the function of individual genes through overexpression or RNAi much easier. The genetics of *Drosophila* is also much simpler, the total 13,900 fly protein coding genes are spread across only 4 chromosomes (Kaufman, 2017). Mutant lines in *Drosophila* are usually maintained through balancer chromosomes, which are homologous chromosomes that contain many inversions and so prevent recovery of chromatids after recombination. Balancers usually also contain a marker gene, such as the CyO balancer of the second chromosome which gives flies curly wings, for easy identification. This helps maintain a mutation in a population and help identify flies that are heterozygotes and homozygotes for the mutant gene. The balancer itself contains recessive lethal mutations to ensure all flies contain at least one copy of the mutant gene (Yamaguchi M., 2018).

### 1.8.2 Genetic tools available in *Drosophila*

*Drosophila* are very easy to genetically manipulate with mobile transposable elements being the most common method used. Transposable elements can be used to introduce mutations as well as introduce new genetic material into the genome (Venken and Bellen, 2014). There are also systems that allow tissue and cell specific expression of genes such as the GAL4-UAS system and the FRT-FLP system.

The GAL4-UAS system is a targeted gene expression system (Brand and Perrimon, 1993). GAL4 is a transcription factor that binds to an upstream activating

sequence (UAS) to allow expression of any downstream genes. This system requires the use of two fly strains. One that contains a tissue specific expression of the GAL4 transcription factor (known as a driver line) and another strain which contains a transgene with an upstream UAS signal. When these two lines are crossed, GAL4 will drive the tissue specific expression of a transgene. This can also effectively be used for gene knockdown by replacing a transgene for an RNAi sequence.

The FRT-FLP, known as the FLP-out system, is commonly used in conjunction with the GAL4-UAS system for mosaic expression of genes in tissues (Golic and Lindquist, 1989). The FLP-out system requires a site-specific recombinase called flipase, the expression of which can be induced through heat-shock (Hs-FLP) and a FLP-out cassette. FLP recombinase recognises the FLP recognition site (FRT) which allows recombination at these sites. The FLP-out cassette contains a marker gene and a transcriptional termination signal flanked by the FRT sequences. Flies would usually have a transgene downstream of a UAS sequence as well as the GAL4 transcription factor which is downstream of a ubiquitous promotor. This would normally mean the transgene is expressed in every cell. However, the GAL4 gene and its promoter would contain the FLP-out cassette in between preventing its transcription. When these flies are grown at 25°C, there will be some leaky expression of the Hs-FLP recombinase. This recombinase would “Flip out” the cassette and allow normal GAL4 expression and subsequent UAS-transgene expression. This will only happen in the subset of cells which express the FLP recombinase, creating a mosaic pattern of expression where cells expressing the transgene will be next to cells that don’t.

Both the GAL4-UAS system and the FLP-out system allow the expression of genes in specific tissues/cells without altering the normal function of every tissue.

## 1.9 Project Outline

This project can be divided into two main sections. The main objective of this project is to further develop our understanding of selective autophagy specifically the

LIR motif and ATG8a-LDS interactions. This will involve a screening process that will identify new LIR motif containing proteins. This will be carried out using CRISPR-Cas9 and ATG8a-LDS mutants that should accumulate many LIR motif-containing proteins. Quantitative proteomics can then be used to identify novel ATG8a interactor proteins. Once identified, an interesting protein from the proteomics will be selected and studied further. The physiological significance of the LIR motif LDS interaction will be investigated as well as the broader functions of the protein.

# Chapter 2 Materials and Methods

## 2.1 Fly stocks

Table 2 List of fly stocks

| Name | Genotype | Source/ID |
|---|---|---|
| Wild Type (WT) | *w[1118]* | Well Genetics |
| da::Gal4 | *w[*];Ptw[`mW.hs]"GAL4-da.G32uUH1, Sb[1]/TM6B, Tb[1]* | Bloomington Stock Centre (55851) |
| $Atg8a^{KG}$ | *y P{hsFLP} Atg8a [KG07569]* | Gifted from Gábor Juhász, University of Budapest. |
| GMAP RNAi – 108063-KK | *P{KK107249}VIE-260B* | *Vienna Drosophila Resource Center* (*VDRC*) (108063) |
| Control RNAi – KK library | *y,w[1118];P{attP,y[+],w[3`]}* | *Vienna Drosophila Resource Center* (*VDRC*) (60,100) |
| FLP-out mCherry-Atg8a | *yw, hsflp; UAS- mCherryAtg8a; Ac>CD2>GAL4/SM66* | Lab Stock |
| ATG8a LDS mutant | *w[1118], Atg8a K48A Y49A CRISPR/ FM7a* | Well Genetics |
| GMAP LIR mutant | *w[1118], Gmap F322A V325A CRISPR/ FM7a* | Well Genetics |

ATG8a-LDS mutant and GMAP-LIR mutant flies were generated by Well Genetics (Taipei City, Taiwan (R.O.C)). Point mutations were introduced using PBacDsRed system, where excision of the selectable marker was done using *PiggyBac* (PBac) Transposition. Excision was validated by genomic PCR and sequencing. For experimental uses, homozygous flies (white eyes) were selected and used. Wild type flies provided by well genetics were used as controls throughout.

For GMAP RNAi fly experiments, GMAP RNAi or the associated control RNAi fly lines were crossed with the full body driver line (da::GAL4). This created offspring that expressed RNAi in the whole fly. These flies were aged 1-2 weeks before used experimentally. To produce mCherry-ATG8a/GMAP RNAi expressing mosaic flies, GMAP RNAi was crossed with FLP-out mCherry-ATG8a. Offspring from this cross had tissues where some cells were expressing both mCherry-ATG8a and the relevant RNAi and some cells expressing neither. The same cross was also done with the control RNAi. These flies were used to visualise the morphology of the autophagosome with or without GMAP knockdown. Method for crossing is described in the next section.

## 2.2 Fly Husbandry

### 2.2.1 Fly maintenance and fly food

Fly stocks were kept at 18°C at 70% relative humidity, while flies for experimental uses were kept at 25°C at 70% relative humidity, both in plastic tubes. Stocks were transferred to new food every 3-4 weeks and experimental flies were transferred every 2-3 days. To manipulate flies and view under a light microscope a gas pad with continuous carbon dioxide supply was used. Fly food recipe is as follows: 42g inactive dry yeast (Dutscher Ltd. Ref. 789126), 60g yellow cornmeal, 130g sucrose (Sigma-Aldrich), 5.5g agar, 6ml propionic acid, Nipagin 15ml, to 1 litre of water.

### 2.2.2 *Drosophila* crosses

For all genetic crosses males were added to female virgins (identified by the presence of a meconium and unexpanded wings) at a ratio of 3:1. Virgins were collected and left for 2 days to confirm their virginity.

### 2.2.3 Starvation

Starvation of flies and larvae was done through transferring flies into plastic tubes with 20% sucrose solution in distilled water. These flies were left for 4 or 24 hours for all starvation experiments.

## 2.3 Lifespan assays/ageing

1-2 days old flies were collected over a 24-36 hr period. One hundred flies per genotype were collected and split into 20 flies per tube. Flies were transferred to new food every 2-3 days and the number of deaths recorded. Similarly, when 1-3 weeks old flies were needed, flies are collected over 36 hours and transferred to new food every 2-3 days. This was repeated twice for three biological repeats and so 300 flies from each genotype were collected all together per experiment. All *Drosophila* lines used were isogenic.

## 2.4 Molecular Biology/Cloning

Molecular biology enzymes and buffers were acquired from New England Biolabs unless states otherwise.

### 2.4.1 DNA extraction from *Drosophila*

To verifying CRISPR mutant flies, genomic DNA from flies was extracted. Extraction was done using a slightly modified protocol of the QIAGEN DNeasy Blood and Tissue Kit. To create fly lysate 20 flies were frozen in dry ice and lysed in the lysis buffer provided in the kit, the rest of the steps were identical to the protocol provided

with the QIAGEN kit. The concentration of the DNA sample was determined using a NanoDrop ND-1000 spectrophotometer (Thermo Scientific, DE, USA). Mutations (of ATG8-LDS mutant flies) were confirmed by the LightRun Tube sequencing services of Eurofins genomics (Germany). Primers used for this is in Table 5.

### 2.4.2 Plasmids

pET28a[+] – main plasmid used for cloning and protein expression purposes. Contains 6x His tag for detection and purification, T7 promotor, and Kanamycin resistance gene.

pGEX – used for GST pull down experiments, contains only the GST tag alone, GST with Drosophila ATG8a (GST-ATG8a), or GST with Drosophila ATG8a-LDS mutant (GST-ATG8a-LDS mutant).

Both plasmids were created and verified in the lab.

### 2.4.3 Plasmid amplification and PCR clean up

Both amplification of plasmids and clean-up of PCR products was done using the respective QIAGEN kit. QIAprep® Spin Miniprep Kit was used to amplify/clone plasmids. QIAquick® PCR Purification kit was used to clean up PCR product.

### 2.4.4 Polymerase chain reaction (PCR)

PCR was used to amplify gene of interest (insert) as well as to PCR verify the successful insertion of insert into plasmid and selection of these clones. PCR was done using the Dream Taq PCR master mix (ThermoFisher Scientific, MA, USA). Table 3 shows a typical PCR reaction mix.

Table 3 Standard PCR reaction contents

| Component | Amount |
|---|---|
| Master mix | 1x |
| Forward Primer | 0.5 µM |
| Reverse Primer | 0.5 µM |
| Template | 100 ng |
| Nuclease free water | Make up to 50 µl |

Table 4 shows the PCR cycle conditions.

Table 4 PCR cycle conditions

| | Temperature °C | Time (mins) | Cycles |
|---|---|---|---|
| Initial Step | 95 | 1 | 1 |
| Denature | 95 | 0.5 | 25 |
| Anneal | Tm-5 | 0.5 | |
| Extension | 72 | 2* | |
| Final Step | 72 | 15 | 1 |

* 1 min for 2 kb and 1 min for each additional kb, for example for full length GMAP this was increased to 4 mins 15 secs.

Table 5 contains the list of primers used for generating GMAP inserts. These include primers for full length GMAP as well as a truncated form of GMAP. The truncated form was the first 490 amino acids of GMAP, which contained the DEFIVV LIR motif. Complementary restriction site overhangs were also added to each end. The restriction enzymes and their sequences were EcoRI: GAATTC and HindIII: AAGCTT.

Table 5 Primers used for creating GMAP inserts and ATG8a sequencing

| Primer | Sequence |
|---|---|
| Full length GMAP forward | CGGAATTCATGTCGTGGCTGAACAGC |
| Full length GMAP reverse | CCCAAGCTTTTACTACAACAATCAGGAGTC |
| Truncated GMAP (aa 1-490) forward | CGGAATTCATGTCGTGGCTGAACAGC |
| Truncated GMAP (aa 1-490) reverse | CCCAAGCTTTTATTAGTCCGCATCGTCCA |
| ATG8a sequencing primer | GGTCAGTTCTACTTCCTCATTCG |

For PCR validation of successful ligation of GMAP constructs, standard pET28a T7 promotor forward primer was used and the truncated GMAP reverse primer.

### 2.4.5 Digestion with restriction endonuclease

Plasmids used contained many restriction sites, two of which were used to cut open the plasmid to allow insertion of the gene of interest (GMAP). 1 µg of plasmid was digested with both restriction endonucleases and rSAP phosphatase, with the appropriate CutSmart© buffer at 37°C for 30 mins. The enzymes are then heat inactivated by heating to 65°C for 20 mins.

### 2.4.6. Ligation of plasmid and insert

Reaction involves 100 ng of total DNA (with an insert to plasmid ratio of 3:1), 1 µg of T4 DNA ligase, and the appropriate buffer in accordance with New England Biolabs instructions. Ligation conditions were 16°C overnight, after which the ligase enzyme was inactivated through heating to 65°C for 10 mins.

## 2.4.7 Transformation

1 µl of ligation mix was used to transform 50 µl of either NEB10-β or Rosetta™ 2(DE3)pLacI Competent Cells, which was left on ice for 30 mins. Sample was then heat shocked at 42°C for 20 secs, before being put back in ice for a further 2 mins. 1 ml of growth media (SOC media for Rosetta cells and LB for NEB10-β) was then added and incubated at 37°C with shaking for one hour. Cells were then streaked onto LB (Lennox broth) agar plates with the appropriate antibiotic (Table 6) and incubated at 37°C overnight. Plates were stored at 4°C and colonies selected when needed.

Table 6 Antibiotics used for selection

| Antibiotic | Working concentrations (µg/ml) |
|---|---|
| Ampicillin | 100 |
| Kanamycin | 50 |
| Chloramphenicol | 35 |

## 2.4.8 Agarose gel electrophoresis

100 ml of 2 % agarose in 1X TAE buffer (20 mM acetic acid, 40 mM Tris, 1 mM EDTA) was heated to boiling in a microwave and cooled before casting. 1X TAE buffer was used and gels were run at 100 V for 60 mins. Gels was the visualised in a UV transilluminator.

## 2.4.9 Mutagenesis

Mutagenesis was used introduce point mutations in pET28a plasmids containing GMAP. The identified LIR motif, DEFIVV, was mutated into DEAIVA using the appropriate primers (Table 9) and the Pfu high-fidelity (HF) DNA polymerase. Table 7 shows a typical PCR reaction mix.

Table 7 Mutagenesis PCR reaction mix

| Component | Amount |
|---|---|
| Reaction Buffer | 1x |
| DNA template | 5-50 ng |
| Primer 1 | 125 ng |
| Primer 2 | 125 ng |
| dNTPS | 200 µM |
| Nuclease free water | Make up to 50 µl |
| Pfu HF DNA polymerase | 2.5 Units |

Table 8 shows the PCR cycling set up.

Table 8 Mutagenesis PCR cycle conditions

| | Temperature °C | Time (mins) | Cycles |
|---|---|---|---|
| Initial Step | 95 | 0.5 | 1 |
| Denature | 95 | 0.5 | 18 |
| Anneal | 55 | 1 | |
| Extension | 68 | 1/Kb* | |
| Final Step | 68 | 10 | 1 |

*For pET28a containing full length GMAP this step was 10 mins, and for truncated GMAP it was 7 mins.

Once PCR was complete template DNA (methylated DNA) was digested through incubation with Dpn1 at 37°C for 1 hr.

Table 9 lists the primers used for mutagenesis, highlighted in red are the point mutations introduced. A sequencing primer upstream of GMAP was used to validate mutation.

Table 9 Mutagenesis Primers

| Primer | Sequence |
|---|---|
| GMAP LIR mutation forward | GCACAGCGAGGATGAGGCCATAGTTGCACGCCAAGC GGATGCC |
| GMAP LIR mutation Reverse | GGCATCCGCTTGGCGTGCAACTATGGCCTCATCCTCG CTGTGC |
| GMAP Sequencing Primer | CATCGAACGCGTACGCG |

# 2.5 Western blotting

## 2.5.1 Protein extraction

Flies or larvae were collected, and once appropriately aged they were frozen in dry ice. 10 whole flies or 20-30 fly heads were lysed in 200 µl RIPA lysis buffer using a mechanical pestle and mortar. RIPA buffer consists of: 50 mM Tris pH 7.4, 150 mM NaCl, 1 % Igepal, 0.5 % sodium deoxycholate, 0.1 % SDS, and a protease inhibitor tablet (Roche). Sample was then centrifuged 13,000 rcf 4°C 10 mins, and stored at -20°C.

### 2.5.2 Sample preparation

Protein concentration was determined using a protein assay (BSA assay). A standard curve was created using known concentrations of BSA (0 – 20 µg/ml). Bradford Reagent (BIO-RAD. Ref. 5000006) was added and absorbance measured at 595 nm. The standard curve was used to calculate the concentration of protein samples. Protein sample at a concentration of 1 µg/10 µl was added to 1x laemmli buffer. Sample was then boiled at 95°C for 5 mins. Stock solution of 6x laemmli buffer consists of: 12 % SDS, 60 % glycerol, 0.12 % bromophenol blue, 0.375 M tris pH 6.8 in water.

### 2.5.3 Sodium dodecyl sulphate - polyacrylamide gel electrophoresis (SDS-PAGE) and transfer

Either 8 % or 12 % polyacrylamide resolving gels were made using stocks of: 1.5 M Tris pH 8.5, 30 % acrylamide/0.8 % bis-acrylamide, 10% SDS, 10% APS, TMED in water. Stacking gel was made using stocks of 0.5 M Tris pH 6.8, 30 % acrylamide/0.8 % bis-acrylamide, 10 % SDS, 10 % APS, TMED in water.

Wells were loaded with 5-20 µl sample depending on well size, alongside 3 µl of Precision Plus Protein Dual Colour Standards (BioRad, UK). Electrophoresis was run at 50 V for 15 mins to allow sample to enter gel and then a further 60 mins at 150 V. Running buffer consisted of: 25 mM Tris-HCl pH 6.8, 200 mM glycine, 0.1 % SDS. Proteins on the gel was then transferred into PVDF membrane, which was soaked in ethanol for 5 mins. Transfer was done over 60 mins at 100 V, the transfer buffer consisted of: 25 mM Tris-HCl, 2 mM glycine, and 20 % ethanol.

## 2.5.4 Immunoblotting

PVDF membranes were blocked in 5 % milk made up in Tris-buffered saline (TBS) supplemented with 0.1 % Tween (TBST) for 40-60 mins. Membranes were incubates with primary antibodies in TBST overnight on a roller at 4°C. Membranes were washed in TBST. Membranes were incubated with secondary antibodies at room temperature for 60 mins before washing in TBST and treated with ECL reagent for 2-5 mins (GE Life Sciences). X-ray films were then exposed to the membrane and developed (AGFA automated developer). Bands were quantified using ImageJ/FIJI 2.0. A histogram was generated for each band where the peaks were proportional to the intensity of the band, the area under the curve was used as the quantitative value. Where necessary these bands were normalised to control bands. Table 10 is a list of antibodies used.

Table 10 List of antibodies used for western blotting

| Antibody | Dilution | Source |
|---|---|---|
| Rabbit pAb to Ref(2)p | 1:2000 | Abcam |
| Kenny | 1:5000 | Gift from Dr N. Silverman |
| Mouse mAb to mono/poly-ubiquitinated proteins (FK2) | 1:1000 | Enzo |
| Rabbit pAb to GM130 | 1:10,000 | Abcam |
| Rabbit pAb to Syntaxin16 | 1:2000 | Abcam |
| Mouse mAb to 6x His tag | 1:1000 | Abcam |
| Rabbit pAb to dGMAP | 1:2000 | Gift from Dr Pascal Therond |
| Mouse Anti-Tubulin | 1:40,000 | Sigma-Aldrich |
| Rabbit Anti-Mouse IgG HRP | 1:5000 | Thermo Scientific |
| Goat Anti-Rabbit IgG HRP | 1:5000 | Thermo Scientific |

# 2.6 Tissue staining/Immunofluorescence

## 2.6.1 Dissection and fixing of tissue

Larvae (feeding L3) were washed in PBS and adult flies anaesthetised with $CO_2$. Tissues (fat body, brain, salivary gland, gut, etc.) are then dissected in a drop of PBS under a light microscope and placed in a collection basket in PBS. Tissues were fixed in 4 % PFA (paraformaldehyde) for 20-30 mins.

## 2.6.2 Staining

Tissues are blocked and permeabilised in permeabilization buffer (0.1 % Triton-X100, 0.3 % BSA, in PBS (phosphate buffered saline)). Tissues were incubated with primary antibody (Table 11) diluted in permeabilization buffer overnight at 4°C. Tissues were then incubated with secondary antibody (Table 11), diluted in permeabilization buffer, for 2 hrs at room temperature. Wash steps took place between fixation and antibody incubations with either PBS or PBST (PBS with 0.1 % Tween). Nuclei were stained with 1 µg/ml Hoechst (Cell Signalling Technology, MA, USA) in PBS for 15 mins before being left in PBS prior to mounting.

Table 11 Antibodies used for immunofluorescence

| Antibody | Dilution | Source |
|---|---|---|
| Rabbit pAb to Ref(2)p | 1:500 | Abcam |
| Mouse mAb to mono/poly-ubiquitinated proteins (FK2) | 1:500 | Enzo |
| Rabbit pAb to GM130 | 1:1000 | Abcam |
| Goat pAb anti-GMAP | 1:1000 | Developmental Studies Hybridoma Bank |

| | | |
|---|---|---|
| Rabbit Anti-Goat IgG CF488A | 1:1000 | Sigma |
| Goat Anti-Mouse IgG CF488A | 1:1000 | Sigma |
| Chicken Anti-Goat IgG CF488A | 1:1000 | Sigma |
| Goat Anti-Rabbit IgG CF568 | 1:1000 | Sigma |
| Goat Anti-Mouse IgG CF568 | 1:1000 | Sigma |
| Donkey Anti-Mouse IgG CF568 | 1:1000 | Sigma |
| Goat pAb to GMAP | 1:2000 | Developmental Studies Hybridoma Bank |

### 2.6.3 Mounting

Stained tissues were placed in mounting media (2 % n-propyl gallate, 70% glycerol in PBS) on a microscope slide and covered with a cover slip. The edges of the cover slips were sealed with nail varnish and allowed to dry in the dark. Samples were visualised on a laser scanning confocal microscope (Zeiss LSM 880) and analysed with Zen Software (Black edition, V.8.1). Fluorophores were excited with the following: 488 nm laser for CF488/GFP, 405 nm laser for Hoechst, 561 nm laser for mCherry/RFP. Brain samples were viewed with a 64x/100x objective lens, whereas other tissues were viewed at 10x/40x/63x/100x objective lens. When images were captured, they were scanned, and an image was formed from an average of 8 scans.

## 2.7 Proteomics and Mass spectrometry

### 2.7.1 Proteomics sample preparation -Methanol/Chloroform precipitation

After protein extraction using the method described earlier, 4x sample volume of methanol was added to 100 µg of protein per sample. This was mixed via vortex for

1 min at room temperature. 1x sample volume of chloroform was added vortexed for 1 min and left at room temperature for 1 min. 3x sample volume of water was added and vortexed for one min at room temperature and then left for 10 mins at -20 °C. this was then centrifuged at 10000 xG for 5 mins at room temperature and the top aqueous phase removed. The white interface layer was not disturbed, as this is where the proteins are. 4x sample volume of methanol was added at vortexed for 1 min at room temperature. This was then centrifuged a final time at 10000 xG for 5 mins at room temperature and the liquid (methanol) removed. The protein (pellet) was first air-dried at room temperature and then resuspended in 8 M urea buffer.

### 2.7.2 Proteomics sample preparation – FASP technique

The samples for mass spectrometry were prepared using the FASP method (Filter aided sample preparation method). All the steps involve centrifugation at 8000 xG after incubation period which is done at room temperature unless stated otherwise. After protein extraction from whole fly or fly heads as described previously, 300 µg of protein from each sample was diluted into 8 M urea buffer (8 M Urea, 50 mM Tris, 75 mM NaCl). Sample was then added to a Millipore® protein concentration filter tube 10 KDa (Merck, Kenilworth, USA), for 20 mins followed by centrifugation and washed with 8 M Urea buffer. Buffer was then exchanged with 50 mM ABC (ammonium bicarbonate) for 20 mins. This is followed by a reduction/alkylation step which involves the addition of 10 mM TCEP (Tris (2-carboxyethyl) phosphine hydrochloride), 40 mM CAA (chloroacetamide) in ABC incubated for 30 mins. Sample is then washed in 50 mM ABC and digested with trypsin overnight at 37°C (2 µg trypsin per 100 µg of protein in 200 µl of 50 mM ABC). The peptides are then eluted into a clean tube through a 20 min centrifugation and then further eluted by repeating the step with the addition of 400 µl water. The peptides were vacuum dried and stored at -20°C.

The samples were run on a LC-MS (Liquid chromatography-mass spectrometry) by the University of Warwick proteomics facility. 1µg of peptide was

inserted into mass spectroscopy instrument. MaxQuant/Andromeda was used for proteomics analysis, this is discussed in more detail in chapter 5. The statistical analysis and generation of PCA/Volcano plots was done on the Perseus software and Excel.

## 2.8 GST-Pulldown for protein-protein interaction analysis

GST pull down assays were used to test for the interaction between GMAP and ATG8a wild type as well as ATG8a-LDS mutant. It was also used to test the interaction between GMAP LIR mutated protein with ATG8a. Assay involves capturing Glutathione-S-Transferase/ATG8a fusion proteins (bait) onto Glutathione Sepharose beads (4 fast flow) and testing the interaction of ATG8a with recombinant GMAP and its mutated form (prey).

### 2.8.1 Protein expression

Bait proteins (GST alone and GST-ATG8a) as well as prey proteins (GMAP and GMAP LIR mutants) were expressed in Rosetta$^{TM}$ 2(DE3) competent cells (Novagen). This is a protein expression strain that has an additional plasmid which contains tRNA's allowing for more efficient production of eukaryotic proteins. This additional plasmid contains a chloramphenicol resistance marker. The creation of each plasmid is described earlier.

1µg of plasmid is transformed into the competent cells through the same heat shock technique described earlier. Once the cells are transformed, they were streaked into an LB agar plate with the appropriate antibiotic and incubated overnight at 37°C. A colony is then used to inoculate a starter culture of 5 ml LB media in a shaking incubator (200 rpm, 37°C) overnight. This starter culture is used to inoculate a larger culture (200 ml) with a 1:100 dilution, which is incubated in a shaking incubator (200

rpm, 37°C) until 0.6 $OD_{600}$ is reached. 0.5 mM IPTG (Isopropyl β- d-1-thiogalactopyranoside) was used to include expression of recombinant protein following which the culture was incubated in a shaking incubator (200 rpm, approximately 16°C).

### 2.8.2 Lysate production

Samples were centrifuged at approximately 25,000 xG for pelleting and stored at -20°C until ready for lysis. For lysis, the pellet was resuspended in lysis buffer (25 mM Tris pH 7.4, 100 mM NaCl, 2 mM EDTA, 0.01% β-mercaptoethanol, 1x protease inhibitor tablet, 1µg/ml lysozyme. Sample is the sonicated 10 seconds on then 5 seconds off for 3 minutes at 35 % amplitude (EpiShear, probe sonicator, A5). Supernatant containing protein was then collected after high-speed centrifugation (48,500 xG).

### 2.8.3 GST-Pulldown

Glutathione beads were pelleted and resuspended in equal volume of lysis buffer before use. For capturing of GST bait proteins, 100 µl of beads were added per 50 ml pelleted bacterial culture. This was incubated at 4°C on a microfuge tube spinner for 40 mins. The beads were then pelleted and washed 3 times in high salt buffer (25 mM Tris pH 7.4, 500 mM NaCl, 2 mM EDTA) and then washed further with lysis buffer 2-3 times.

For the pulldown the prey lysate (GMAP or GMAP LIR mutants) was added to the beads bound to bait protein (GST only, GST-ATG8a, and GST-ATG8a-LDS mutant). This was incubated at 4°C on a microfuge tube spinner for 2 hrs. The beads were then washed 3-4 times with lysis buffer followed by 3-4 washes with high salt buffer supplemented with 10 mM imidazole. Equal volume of 2x laemmli buffer is then added and sample heated to 95°C for 10 mins for western blot analysis.

## 2.9 Software tools

### 2.9.1 iLIR resource

The iLIR software web resource was used to identify potential functional LIR motifs in the novel ATG8a interacting protein GMAP.

The iLIR software is an *in-silico* tool for identifying potential LIR motifs from an amino acid sequence. This allows the identification of [W/F/Y]-x-x-[L/I/V] motifs as well as the extended xLIR (ADEFGLPRSK)(DEGMSTV)(**WFY**)(DEILQTV) (ADEFHIKLMPSTV)(**ILV**). The software output is a list of potential LIR motifs from the inputted FASTA amino acid sequence, a PSSM (Position Specific Score Matrix) score, as well as whether the LIR motif is in an anchor region or not. PSSM is a scoring matrix which assigns values to residues based on the aligned sequence, where a negative value is for residues observed less frequently than expected and positive values for residues which occur more frequently. Thus, the higher the PSSM score the more confident we can be about the motif matching the xLIR sequence. Anchor regions are regions in a protein sequence that are likely to be an intrinsically disordered region. These are regions are more flexible as they lack secondary and tertiary structures, making them promising locations for protein-protein interactions. Therefore, a high PSSM score and the motif being found in an anchor region is a good candidate for a potential functional LIR motif.

### 2.9.2 Statistical Analysis

Blots and confocal images were processed using Fiji/Image J 2.0. For western blots this was used for quantification based on intensity of the bands as described earlier. For confocal images Fiji was used to add scale bars and measure sizes of

subcellular structures like Golgi and protein aggregates. Statistical analysis was done using Perseus, Excel and GraphPad Prism software. In all experiments, including western blotting, aging, and immunofluorescence, a minimum of three biological experiments were done for statistical analysis unless stated otherwise. For quantitative proteomics four biological repeats were done for statistical analysis.

## 2.10 Chemicals and reagents

All chemicals and reagents used for experiments are listed below (Table 12). For any chemicals not mentioned in the list their sources will be mentioned in the text.

Table 12 List of chemicals and reagents and their sources

| Chemical | Source |
|---|---|
| Absolute ethanol | SLS Stores |
| Acrylamide | AccuGel - SLS Stores |
| Agar | SLS Stores |
| Agarose | SLS Stores |
| Ammonium persulfate (APS) | SLS Stores |
| Bovine Serum Albumin (BSA) | Sigma A7906 |
| Bromophenol blue sodium | Sigma B8026 |
| ECL reagent | Amersham RPN2209 |
| EDTA | SLS Preparation room |
| Glutathione Sepharose | Sigma GE17-0756-01 |
| Glycerol | Sigma G6279 |
| Igepal CA-630 | MP 198596 |
| Imidazole | Sigma 12399 |
| IPTG | SLS Stores |
| NaCL | SLS Preparation room |

| | |
|---|---|
| Lysozyme | Fisher Scientific 10249843 |
| Ponceau S | Sigma P3504 |
| Protease inhibitor cocktail (EDTA free) | Roche 5892791001 |
| SDS | SLS Preparation room |
| Sucrose | Sigma 16104 |
| TEMED | Sigma T9281 |
| Tris-HCL | SLS Preparation room |
| Triton X-100 | Sigma T8787 |
| Tween-20 | SigmaP9416 |
| 16 % Formaldehyde | ThermoFisher 28908 |
| 2-Mercaptoethanol | Sigma M3148 |

# Chapter 3 Characterisation of ATG8a K48A/Y49A Mutant *Drosophila Melanogaster*

## 3.1 ATG8a and Cargo Selection

### 3.1.1 Introduction

Bulk degradation of cytoplasmic material tends to be a direct response to starvation, however, there is also the selective degradation of cytosolic proteins. The selective degradation of these proteins usually has physiological consequences in addition to aiding nutrient depravation. This project focusses on selective autophagy, which involves the specific interaction between ATG8a (the *Drosophila* homologue of the mammalian LC3 protein), and cargo targeted for degradation through the autophagosome. ATG8a can interact with cargo selectively through the UIM docking site (UDS) and the LIR docking site (LDS). Herein, we will exclusively investigate the interaction between the LDS of ATG8a and LC3 interacting region (LIR) motif containing proteins.

The ATG8/LC3 LDS-LIR motif interaction is highly conserved and observed in both bacteria and viruses. Xenophagy is the selective degradation of intracellular pathogens, through their ubiquitination and targeting of autophagosomes. Thus, many pathogens have evolved methods of avoiding degradation through autophagy. For example, the influenza A viral Matrix 2 (M2) protein contains a LIR motif which interacts with LC3. The interaction of M2 with LC3 inhibits autophagy by redistributing LC3 to the plasma membrane while also providing a method of enhancing viral budding and virion stability (Beale *et al.*, 2014). *Legionella pneumophila* is a bacterium which produces the cysteine protease RavZ which can inhibit autophagy through the irreversible de-lipidation of mammalian ATG8-PE. RavZ contains three LIR motif which

localise it to the autophagosome, and mutations of these LIR motifs prevent de-lipidation of ATG8-PE (Park *et al.*, 2019).

The *Drosophila* ATG8a LDS is a site contains two hydrophobic binding pockets and allows the binding of proteins which contain a LIR motif (Noda, Ohsumi and Inagaki, 2010) (Figure 3-1). The conserved LIR motif is broadly defined as [W/F/Y]-x-x-[L/I/V], although the motif has since been extended to become more relaxed.

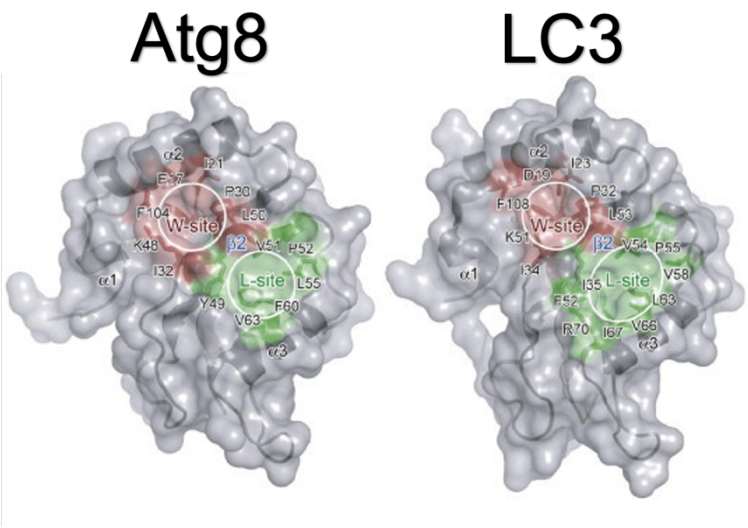


Figure 3-1 **The LIR motif-LDS interaction.** Diagram showing the 3D structure of yeast ATG8 (Left) and rodent LC3 proteins. Two hydrophobic binding pockets can be seen, the W and L sites where the hydrophobic residues of the LIR motif can bind. This interaction is highly conserved through evolution. Figure adapted from (Noda, Ohsumi and Inagaki, 2010).

The interaction between cargo and ATG8a can either happen directly or indirectly via adapters and receptors, as depicted in Figure 3-2 . An example of an adapter is Ref(2)P (refractory to sigma P) which is a LIR motif containing protein involved in the selective degradation of ubiquitinated proteins. It can do this by binding to ubiquitinated proteins through a ubiquitin binding domain (UBA domain) and targeting it to the autophagosome by interacting with ATG8a via its LIR motif. In *Drosophila*, Ref(2)P is the main adapter protein which is involved in the selective

degradation of many proteins, but other less characterised adapters and receptors also exist.

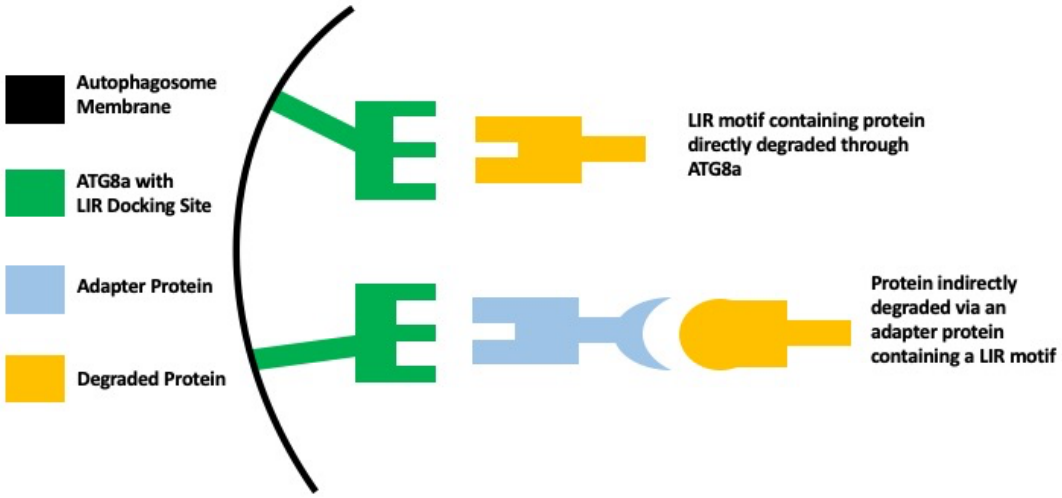


Figure 3-2 **Selective autophagy.** Cargo selectively targeted to the autophagosome for degradation can do so directly through interaction with ATG8a via its LIR motif or indirectly through adapter proteins such as Ref(2)P. Ref(2)P can bind to ATG8a through its LIR motif while also being able to bind to ubiquitinated proteins through its ubiquitin binding domain.

The initial goal of the project is to identify a panel of LIR motif containing proteins that are autophagy adapters, receptors, or substrates. To accomplish this, *Drosophila* with a full body ATG8a-LDS mutants were created.

### 3.1.2 *Drosophila* ATG8a K48A/Y49A

Two of the most important residues within the LDS is Lys-48 and Tyr-49. Alanine substitutions at both these positions (K48A/Y49A) have been shown to significantly reduce the LDS-LIR motif interaction. This has been extensively shown in *in-vitro* studies (Tusco *et al.*, 2017; Jain *et al.*, 2015). *Drosophila* containing the K48A/Y49A mutation have been created using Well Genetics (Taiwan, R.O.C) services. An overview of the process is described in Figure 3-3.

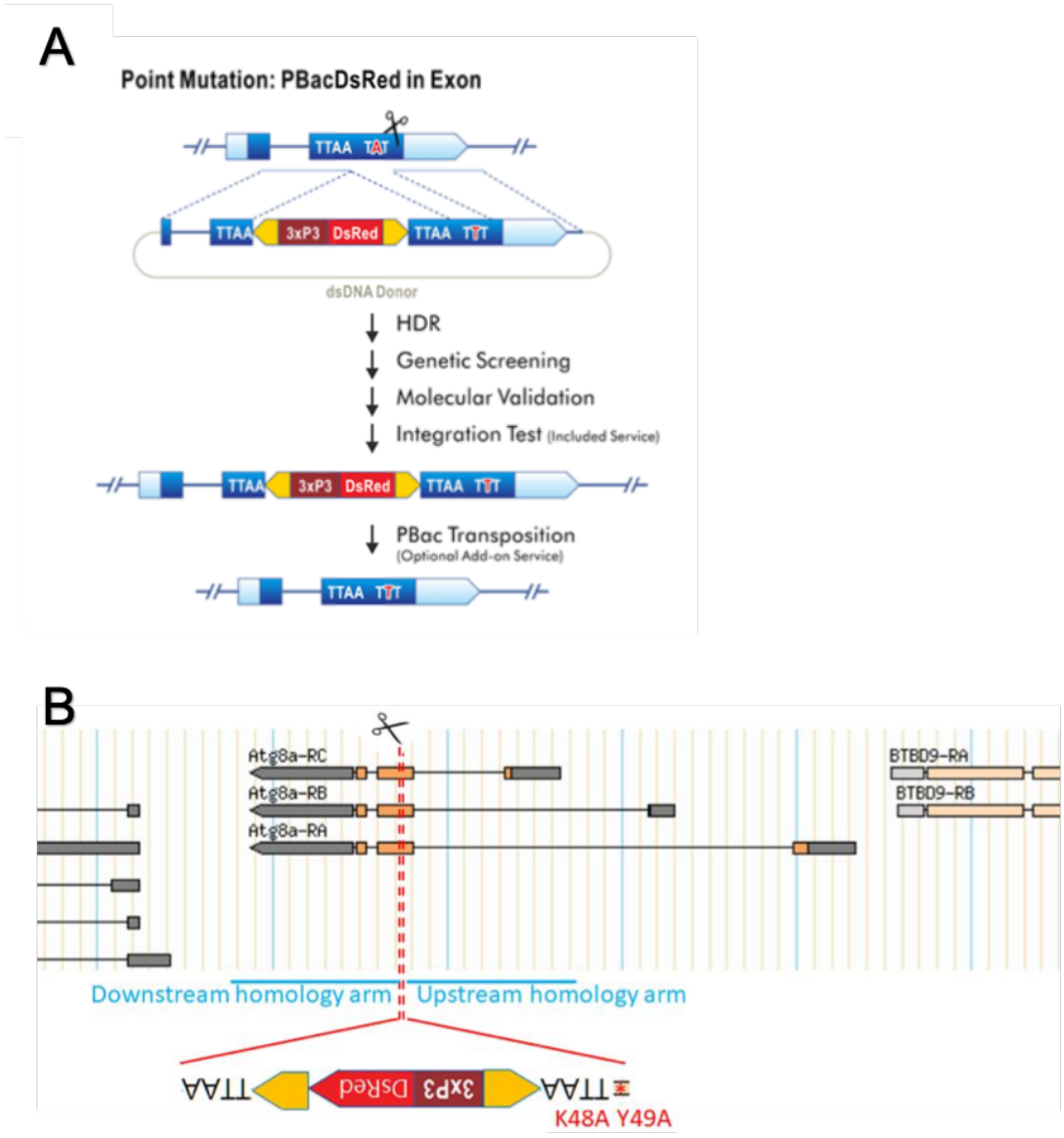


Figure 3-3 **Creation of ATG8a$^{K48A/Y49A}$ mutant flies.** A) Schematic showing the process of mutagenesis. B) Location of K48A/Y49A mutations within ATG8a. Well Genetics used CRISPR/Cas9 and the Piggybac™ transposition system for generation of ATG8a LDs mutant flies. CRISPR/Cas9 was used to create double strand breaks at the target gene and homologous recombination was used to insert the mutated DNA fragment along with the Piggybac™ vector. The vector contains DsRed a selectable marker that can be excised using the Piggybac™ transposase.

Well Genetics combines piggyBac™ transposition with CRISPR/Cas9 genome editing for the seamless editing of genomic DNA. The piggyBac™ transposase recognises inverted terminal repeat sequences (ITRs) which are on either end of the

transposon vector. It can then insert a DNA sequence from the transposon vector into the chromosomal TTAA sites found throughout the genome. The transposase also allows excision of the transposase is a seamless manner. To introduce the K48A and Y49A mutation into the ATG8a gene, a double strand DNA donor vector was created containing the mutation in the gene as well as the transposon. The vector also contained a selectable marker such as DsRed, which can be used in the selection of clones. CRISPR/Cas9 which is a site-specific nuclease is used to introduce double stand breaks in the point mutation site. This promotes the cell to use the piggyBac™ transposase vector in homology directed repair, that incorporates the K48A/Y49A mutations into the host genome. Once the selectable marker is used to find the successfully mutated clones, the transposase is used to seamlessly excise the piggyBac™ transposon from the genome. The result is a line of flies where every cell in the *Drosophila* body contains the ATG8a K48A/Y49A mutations.

Since these mutations reduce the interaction of ATG8a and LIR motif containing proteins, many LIR motif-containing proteins will accumulate in the cells of these flies. It was understood that the phenotype of these flies would be like the ATG8a null flies commonly used in the Nezis laboratory. In these flies, ubiquitinated proteins and other selective autophagy substrates form protein aggregates in the cells. If similar aggregates are seen in ATG8a K49A/Y49A mutant *Drosophila*, the aggregates are likely to be enriched for LIR motif containing proteins, which can then be identified through quantitative proteomics.

Therefore, the first experiments look to characterise the ATG8a K48A/Y49A mutant flies, validate the LDS mutation, check they display similar phenotypes to ATG8a null flies, and confirm their suitability for proteomics analysis.

## 3.2 Sequencing of ATG8a K48A/Y49A mutant flies

Multiple fly lines were sent by Well Genetics, including pre-excision lines. The ATG8a-LDS mutant flies were labelled Ex1, Ex2, and Ex4 with their associated pre-

excision line labelled C, F and G. All three excision lines were identical in the sense that they had the ATG8a K48A/Y49A mutation.

To confirm the successful mutation of the ATG8a protein, genomic DNA was extracted from each line and a small section of DNA containing the ATG8a gene was amplified with PCR. Standard primers used for ATG8a sequencing present in the laboratory were used for this. Figure 3-4 is the agarose gel of the PCR amplicon showing successful amplification of the ATG8a gene. The ATG8a gene is around 351 bp long, and the amplicon generated can be seen to be under the 500 bp marker.

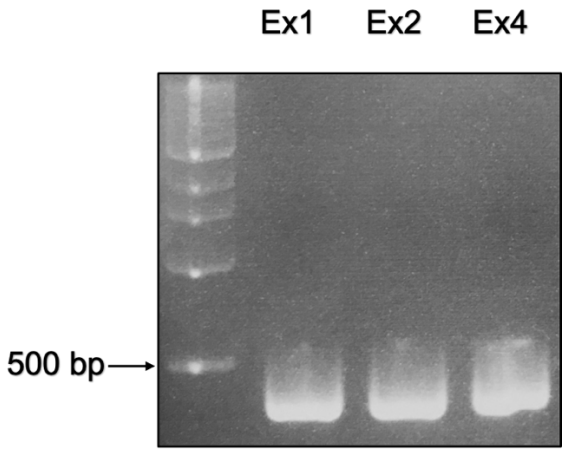


Figure 3-4 **Agarose gel showing PCR amplicon of ATG8a for sequencing.** Three fly lines (Ex1, Ex2, and Ex4) received from Well Genetics which all have the successful K48A/Y49A mutation had genomic DNA extracted and ATG8a gene amplified using PCR. The approximate size of ATG8a amplicon was 300 bp.

The PCR products were then quantified with a nanodrop and sequenced using the Eurofins genomics (Germany) sequencing services. Figure 3-5 is the sequencing chromatogram received from Eurofins confirming the K48A/Y49A mutation in all three excision lines.

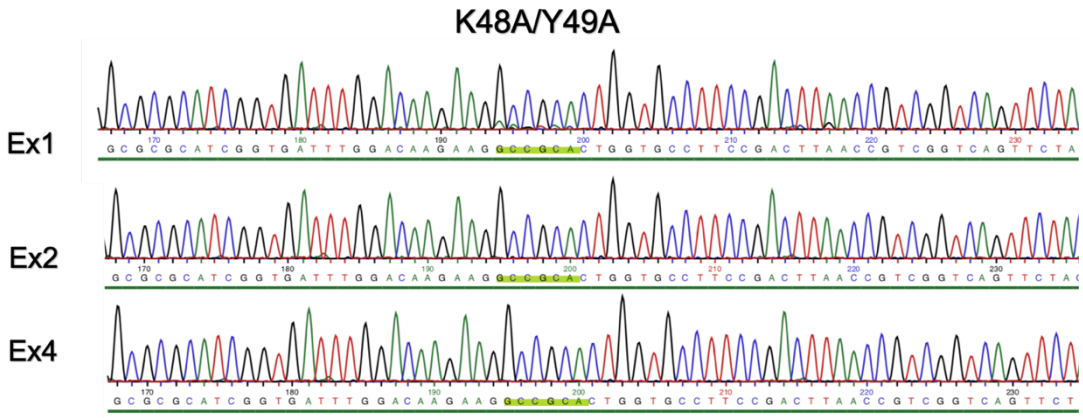


Figure 3-5 **Sequencing chromatogram of ATG8a from Ex1, Ex2 and Ex4.** Sequencing was done by Eurofins sequencing services. All three fly lines had successful incorporation of the K48A/Y49A point mutations. As all three were suitable, fly line Ex2 was used from this point onwards.

Since all three excision lines were confirmed to contain the correct ATG8a K48A/Y49A mutation, Ex2 was selected and used exclusively from here onwards. This Ex2 line will henceforth be referred to as ATG8a$^{K48A/Y49A}$ mutants.

## 3.4 ATG8a expression in ATG8a K48A/Y49A mutant flies

The expression of the ATG8a also needed to be confirmed. This is achieved through western blot analysis using the α-GABARAP antibody which recognises *Drosophila* ATG8a. ATG8a is a 15 kDa protein and its expression in mutant flies is shown in Figure 3-6. Expression of ATG8a can be seen in the wild type flies (WT) as well as the ATG8a$^{K48A/Y49A}$ mutants. This shows ATG8a is successfully being expressed in the CRISPR mutant flies. ATG8a null flies were used as a negative control as there was no expression of ATG8a. There is also no expression of ATG8a in the Ex2 line prior to excision. This is expected as the selectable marker must first be excised before proper expression can take place.

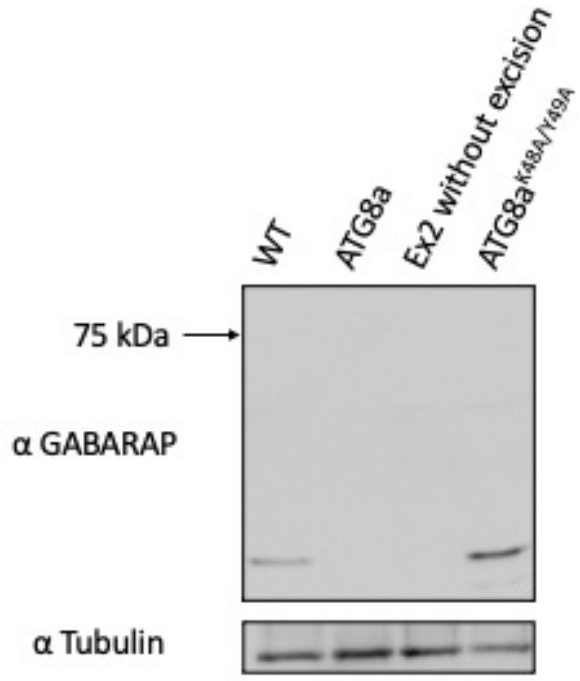


Figure 3-6 **Confirmation of ATG8a expression in ATG8a$^{K48A/Y49A}$.** ATG8a expression was confirmed with the GABARAP antibody which, can recognise *Drosophila* ATG8a. Both wild type (WT) and ATG8a$^{K48A/Y49A}$ expressed ATG8a. The ATG8a$^{K48A/Y49A}$ line prior to Piggybac$^{TM}$ excision as well as full ATG8a mutants did not express ATG8a. Tubulin was used as a loading control.

## 3.5 ATG8a K48A/Y49A mutant flies have a reduced lifespan

Wild type flies under laboratory conditions (25°C at 70% relative humidity), typically live for just over 2 months (65-70 days). In contrast to this, ATG8a null flies, which are commonly used in the Nezis lab would have a lifespan of approximately half this (30-40 days). Autophagy plays an important role in the ageing process since defects in autophagy tend to reduce lifespan. This is due to several reasons such as being unable to respond appropriately to starvation, the build-up of toxic aggregates, inefficient organelle turnover or mitochondria quality control (Rubinsztein, Marino and Kroemer, 2011). Yeast with autophagy defects were shown not to be sensitive to lifespan extension with limiting amino acids in growth media (Matecic *et al.*, 2010). In

*Drosophila,* sestrin1 is an activator of AMPK and a negative regulator of mTOR and therefore activates autophagy. Knock down of this sestrin1 protein decreased the lifespan and promoted age related phenotypes such as muscle degeneration, as well as cardiac and mitochondrial dysfunction (Lee *et al.*, 2010).

The lifespan of ATG8a$^{K48A/Y49A}$ compared to wild type and ATG8a null flies was assessed. 100 male flies of each genotype were collected and aged in an incubator (25°C at 70% relative humidity) while being transferred to new food every 2-3 days. This was repeated twice for 3 biological repeats making the total number of flies analysed 300 per genotype. The number of deaths were recorded and the percentage of flies that survived over time is shown in Figure 3-7.

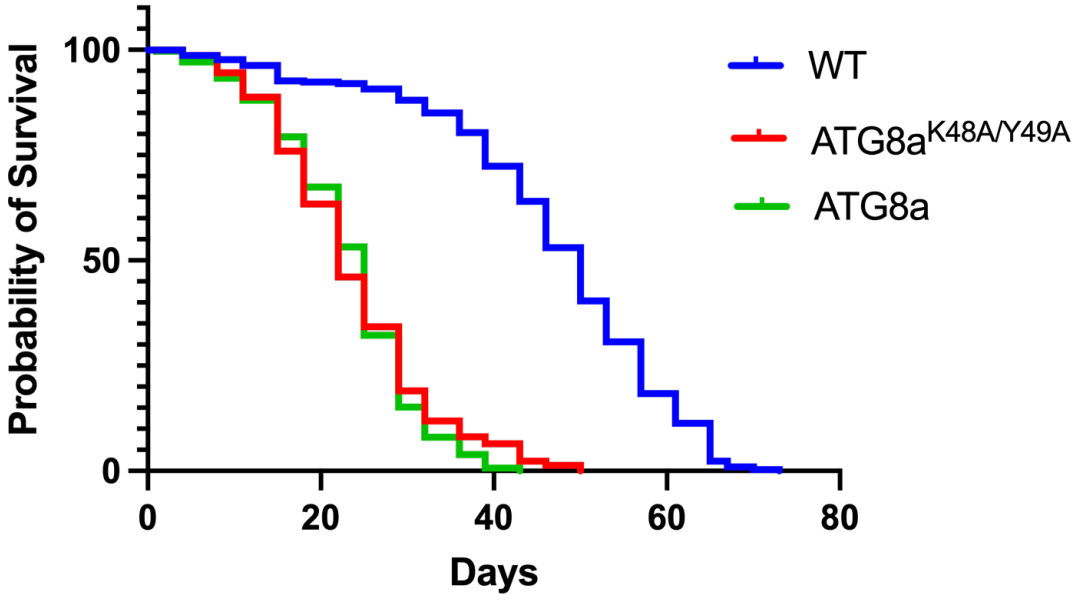


Figure 3-7 **Lifespan assay comparing WT control flies with ATG8a$^{K48A/Y49A}$ mutant flies and ATG8a mutant flies.** ATG8a$^{K48A/Y49A}$ had a significantly shorter lifespan than WT flies of approximately 1 month as opposed to two months (****p<0.0001). This reduction in lifespan is similar to that of ATG8a mutants (****p<0.0001). Graph shows % population survival (n=3 where curves were compared using Mantel-Cox longrank test)

As expected, the lifespan of ATG8a$^{K48A/Y49A}$ flies were like the ATG8a null flies. Both flies have a defect in autophagy, which significantly reduced their lifespan when

compared to wild type flies. Curve comparison was performed using the log-rank Mantel-Cox test (WT/ATG8a: chi square = 456.7 $p<0.0001$, WT/ATG8a$^{K48A/Y49A}$: chi square = 400.5 $p<0.0001$) Statistically the lifespan of the LDS mutant flies was the same as the full ATG8a knockout. This highlights the importance of the ATG8a-LDS-LIR motif interaction in the overall health of the flies. Selective autophagy is involved in many of the cells processes like pexophagy, mitophagy, aggrephagy and immunity. Therefore, it is unsurprising that an ATG8a-LDS mutant fly would experience similar shortening of lifespan compared to ATG8a null flies.

## 3.6 Accumulation of Ref(2)p, Kenny, and ubiquitinated proteins in ATG8a K48A/Y49A mutant flies

As mentioned previously, ATG8a$^{K48A/Y49A}$ flies cannot form ATG8a-LDS to LIR motif interactions and so these flies will naturally accumulate proteins containing LIR motifs. ATG8a null flies accumulate many proteins that are usually degraded by autophagy. These are typically found in the form of protein aggregates in fly cells. To assess the accumulation of proteins in the ATG8a-LDS mutant flies, Ref(2)p, Kenny and Ubiquitinated proteins were analysed though western blotting.

*Drosophila* Ref(2)p (Figure 3-8), the mammalian p62/SQSTM1 homologue, is a 599 amino acid protein which is an autophagy adapter. It contains a LIR motif which allows interaction with the ATG8a-LDS as well as a C-terminal UBA domain which further facilitates interaction with K63 linked polyubiquitin chains. Therefore, this adapter protein allows for the selective degradation of ubiquitinated proteins through the autophagosome. Other domains in Ref(2)p include the polymerisation domain PB1 (Phox and Bem1p domain) and the ZZ-type zinc finger domain (Nezis, 2012). Ref(2)P was shown to be a major component of protein aggregates in the brain of aged flies and autophagy impaired flies (Nezis *et al.*, 2008). As well as targeting ubiquitinated proteins to the autophagosome, Ref(2)P itself is an autophagy substrate. As the main

LIR motif containing selective autophagy cargo receptor in *Drosophila,* this protein should accumulate in ATG8a$^{K48A/Y49A}$ mutant flies.


Figure 3-8 **Ref(2)P domains.** Diagram showing the location of key domains in the 599 amino acid Ref(2)P protein which include: Phox and Bem1p domain (PB1), ZZ-type zinc finger domain (ZZ), Ubiquitin associated domain (UBA). The location of the LIR motif can also be seen

*Drosophila* Kenny, the homologue of the mammalian inhibitor of nuclear factor kappa-B kinase subunit gamma (IKKγ) also known as NF-kappa-B essential modulator (NEMO), is another selective autophagy receptor. Kenny is a 387 amino acid protein, which has two coiled coil domains, a UBAN (ubiquitin binding in ABIN and NEMO) domain and a ZnF (Zin finger motif) (Figure 3-9). Kenny along with IKKβ/ird5 is part of the IκB kinase (IKK) complex which is involved in the nuclear localisation of the transcription factor, Relish. Relish promotes the transcription of many innate immune genes such as the antimicrobial peptide gene, Diptericin (Rutschmann *et al.*, 2000). The immune deficiency (IMD) pathway is a conserved NF-kB immune signalling pathway in insects. IKKγ has been shown to be involved in selective degradation of the IKK complex, which prevents commensal bacteria from continuously activating the Immune Deficiency (IMD) pathway. Without this system in place, *Drosophila* would experience systemic inflammation leading to death. Kenny has a functional LIR motif which allows interaction with ATG8a (Tusco *et al.*, 2017). Surprisingly, this interaction is not conserved in mammals as mammalian IKKγ/NEMO does not interact with LC3 family of proteins. Kenny is also degraded by autophagy itself and so should accumulate in ATG8a$^{K48A/Y49A}$ mutant flies.

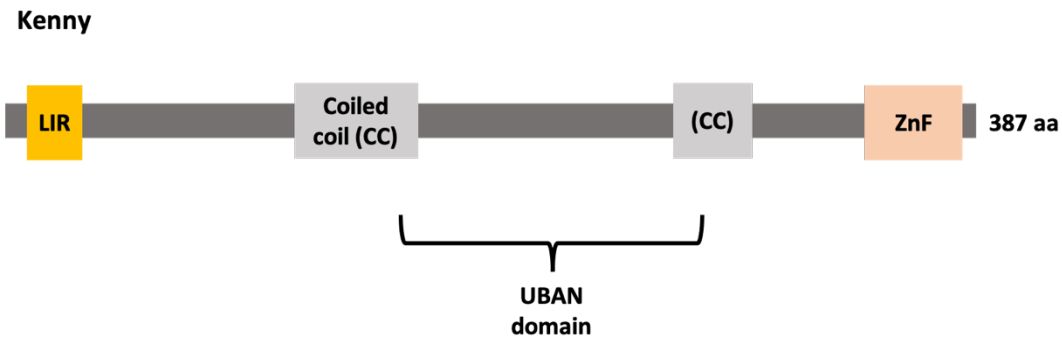


Figure 3-9 **Kenny domains.** Diagram showing location of key domains in the 387 amino acid Kenny protein. Domains include: two coiled-coil domains, ubiquitin binding in ABIN and NEMO domain (UBAN), and Zin finger motif (ZnF). The location of the LIR motif is also shown.

The accumulation of ubiquitinated proteins is a hallmark of autophagy disruption. Ubiquitination is a common post-translational modification which is used to tag proteins for degradation through either the proteosome or autophagy. It is adapter proteins like Ref(2)p which contain a ubiquitin binding domain that facilitate the selective degradation of such proteins. As alluded to previously, different adapters and ubiquitin binding domains have different preferences to the type of ubiquitin chains they interact with. For example, Ref(2)p and its UBA domain bind to both mono and poly-ubiquitinylated K63 linked linear chains (Johansen and Lamark, 2011). The FK2 antibody is often used to detect ubiquitinated proteins. Hybridoma clone FK2, is specific to K29, K48 and K63-linked mono and poly-ubiquitinylated proteins (Fujimuro, Sawada and Yokosawa, 1994). On a western blot, accumulation of ubiquitinated proteins appear as a high molecular smearing. As ATG8a null flies have an autophagy deficiency, we expect to see large amounts of ubiquitinated proteins and so a similar result in the ATG8a-LDS mutant flies is expected.

Flies were aged 1, 2 and 3 weeks before proteins were extracted and analysed using SDS-PAGE and western blotting (Ref(2)P, Kenny, Ubiquitinated proteins).

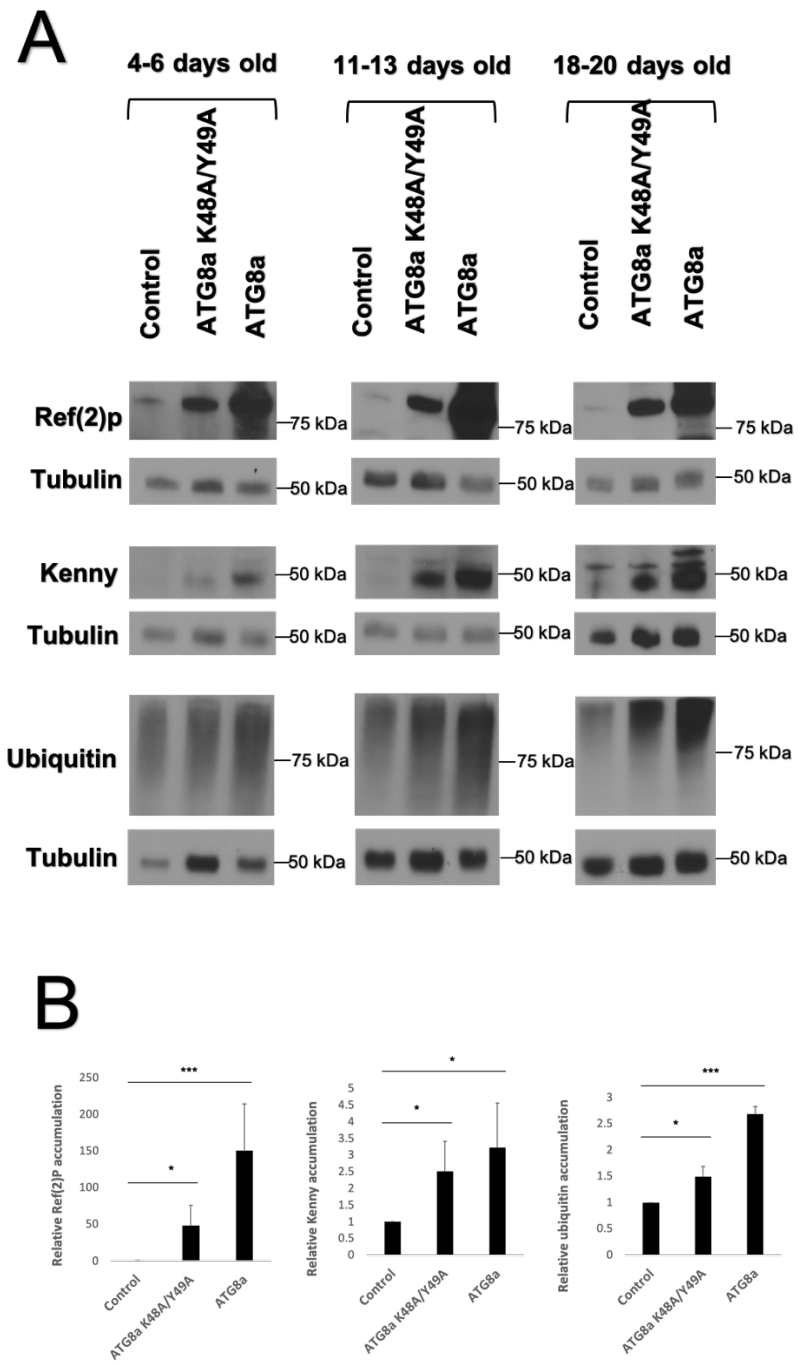


Figure 3-10 **Accumulation of Ref(2)P, Kenny and Ubiquitinated proteins in ATG8a$^{K48A/Y49A}$ and ATG8a mutant flies compared to WT controls.** A) Flies were aged approximately 1, 2 and 3 weeks and the protein lysate extracted and blotted for the relevant protein. There is an accumulation of Ref(2)P, Kenny and Ubiquitinated proteins in both autophagy mutant flies with the ATG8a mutant have the most amount of accumulation. The degree of accumulation was higher in older flies (2 and 3 weeks old). Tubulin was used as a loading control. B) Quantification of western blot for 2-week-old flies. Autophagy mutant samples are relative to control flies. Students t-test was used for statistical significance, n=3, error bars show + SDs. *p<0.05, ***p<0.001.

Figure 3-10 shows Ref(2)p accumulation in ATG8a and ATG8a$^{K48A/Y49A}$ mutant flies compared to wild type flies. There is a very small amount of Ref(2)p in wild type flies regardless of age, since it is degraded through basal autophagy. When autophagy is disrupted, either through loss of ATG8a or through the LDS mutant, Ref(2)P accumulates. There is a much higher degree of accumulation in ATG8a null flies compared to ATG8a-LDS mutant flies. The older the flies become, the more Ref(2)P accumulates in both autophagy disrupted flies, with 3 week old flies having the greatest amount of accumulation. ATG8a-LDS mutants seem to have an intermediate phenotype where there is accumulation of Ref(2)P compared to wild type but not as much as ATG8a mutants.

Figure 3-10 shows kenny and ubiquitinated proteins have a similar pattern of accumulation. Some kenny accumulation can be seen in 1-week-old flies but its only in 2- and 3-week-old flies where this is a lot more prominent. Again, ATG8a$^{K48A/Y49A}$ mutants have an intermediate phenotype between wild type and ATG8a null flies. For ubiquitinated proteins, there is much more high molecular weight smearing in the two mutants (ATG8a and ATG8a$^{K48A/Y49A}$) compared to wild type. This means these flies have more ubiquitinated protein aggregates. In 3-week-old flies, there are more ubiquitinated proteins in the ATG8a null flies compared to ATG8a$^{K48A/Y49A}$ mutant flies. Quantifications of 2-week-old fly blots can be seen in Figure 3-10B, showing that the accumulation of kenny and ubiquitinated proteins is significant compared to wild type flies..

Accumulation of protein aggregates increases linearly with fly age, and thus appear more abundant in a western blot. This is because there is more time for proteins to accumulate which are normally degraded through sequestration in the autophagosome. The fact that there are more LIR motif proteins (Ref(2)P and Kenny) and more ubiquitinated proteins in ATG8a null flies compared to ATG8a$^{K48A/Y49A}$ is promising. It suggests that proteins accumulating in the ATG8a$^{K48A/Y49A}$ are likely specifically due to the inhibition of the LDS-LIR motif interaction. Therefore, ATG8a$^{K48A/Y49A}$ mutant flies are likely to be enriched specifically with LIR motif containing proteins compared to ATG8a null flies.

The next goal is to confirm that the ATG8a$^{K48A/Y49A}$ mutants have protein aggregates similar to that of ATG8a null flies.

## 3.7 Visualisation of protein aggregates in ATG8a$^{K48A/Y49A}$ mutant flies

Confocal microscopy was used to visualise protein aggregates that contained ubiquitinated proteins and Ref(2)P. Flies aged 1-week did not have a large amount of protein accumulation (specifically Kenny and Ubiquitinated proteins (Figure 3-10). Therefore, 2-week-old flies were used for subsequent experiments. This would give enough time for potential LIR motif containing proteins to accumulate in ATG8a$^{K48A/Y49A}$ flies.

It is already known that ATG8a null flies have Ref(2)p aggregates in brain cells. These aggregates usually co-localise with ubiquitin staining as well. This is because Ref(2)P is required for the formation of ubiquitinated protein aggregates (DeVorkin and Gorski, 2014; Nezis *et al.*, 2008). Immunofluorescence with Ref(2)P and FK2 (mono- and polyubiquitin) antibodies were used to visualise these aggregates. Figure 3-11 are stained images of the mid brain of *Drosophila* which were aged 2-weeks.

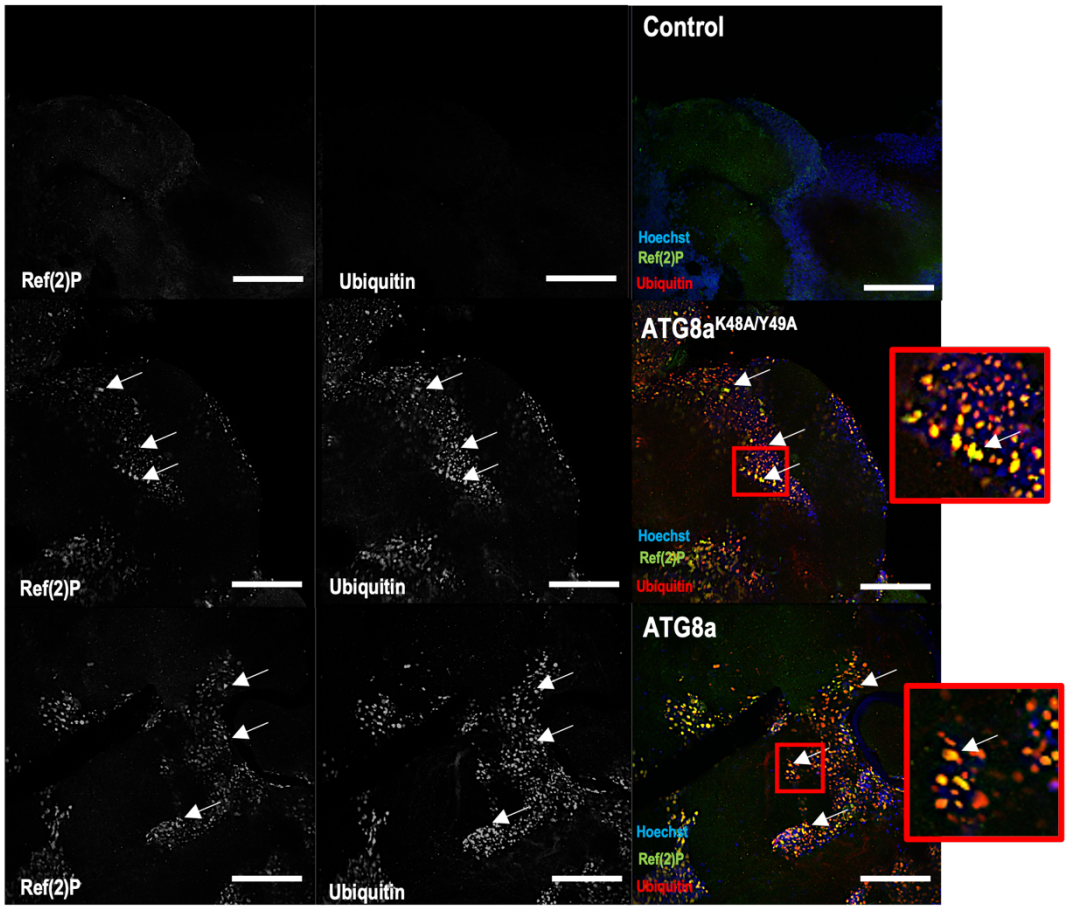


Figure 3-11 **Accumulation of Ref(2)P and ubiquitin positive aggregates in ATG8a$^{K48A/Y49A}$ and ATG8a mutant fly brains.** Flies were aged two weeks and the brain tissue was stained for Ref(2)P (green) and ubiquitin (Red). Co-localisation of Ref(2)P and ubiquitin staining (arrows) are protein aggregates which are found throughout the brain in both autophagy mutant flies. Arrows only indicate examples of the aggregates, but the aggregates are found throughout the sample. This is not seen in control flies. DNA was stained with Hoechst. Scale bars 60 µm.

Figure 3-11 shows Ref(2)P (green) and Ubiquitin (red) positive aggregates (white arrow) in the brains of both ATG8a$^{K48A/Y49A}$ as well as ATG8a null flies. These aggregates are similar in size to the nucleus (Hoechst stain – blue) and are usually found one per cell. These protein aggregates were not present in wild type brain samples. It was then tested whether these aggregates are also present in other tissues, specifically the mid-gut.

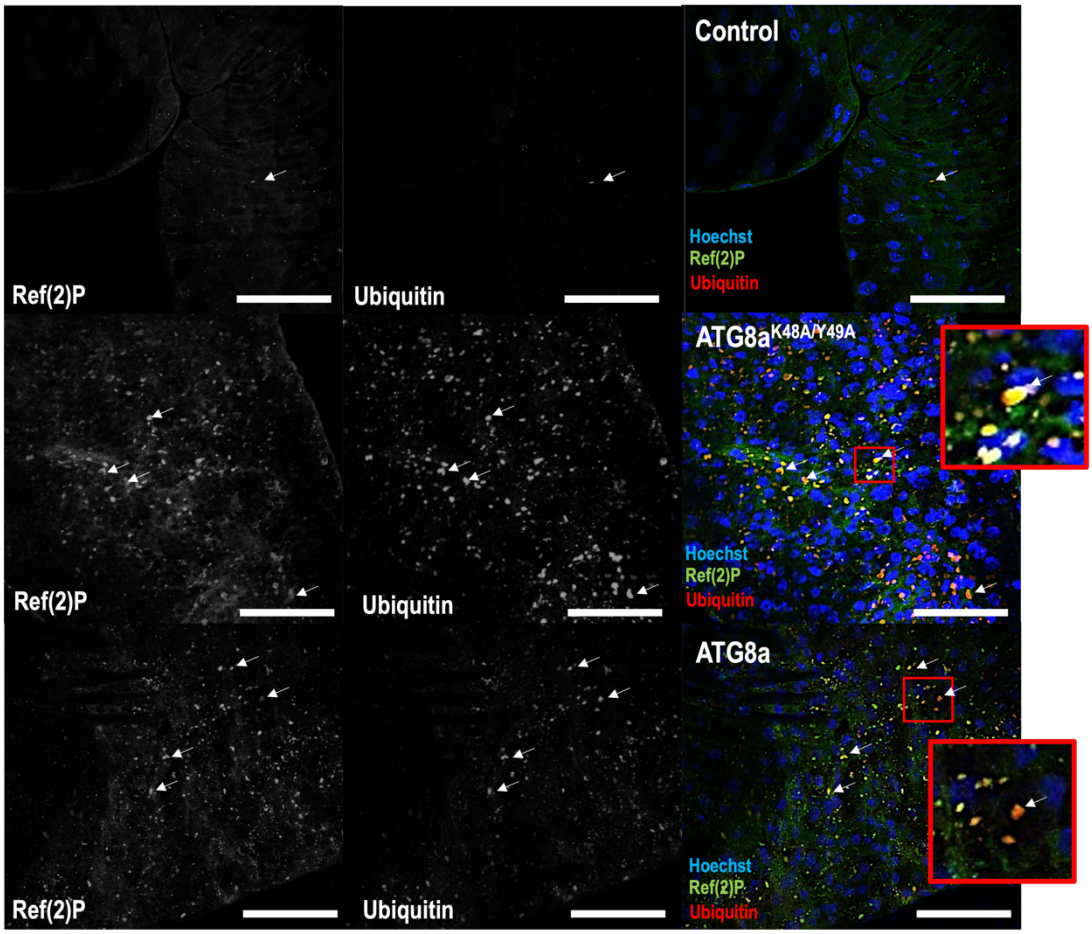


Figure 3-12 **Accumulation of Ref(2)P and ubiquitin positive aggregates in ATG8a$^{K48A/Y49A}$ and ATG8a mutant fly mid-gut.** Flies were aged two weeks and the gut tissue was stained for Ref(2)P (green) and ubiquitin (Red). Co-localisation of Ref(2)P and ubiquitin staining (arrows) are protein aggregates which are found throughout the gut in both autophagy mutant flies. Arrows only indicate examples of the aggregates, but the aggregates are found throughout the sample. Occasional aggregates were seen in control flies. DNA was stained with Hoechst. Scale bars 60 μm.

Figure 3-12 shows the same immunofluorescence experiment with 2-week-old *Drosophila* mid-gut. Some of the aggregates are highlighted with the white arrows. Just like in the brain ref(2)P (green) and ubiquitin (red) positive aggregates can be seen in ATG8a$^{K48A/Y49A}$ and ATG8a null flies. There were a few aggregates seen in wild type samples, but they were very sparse. Many more aggregates were present in the mutant lines and these aggregates were much bigger in size.

Since similar protein aggregates were found in ATG8a$^{K48A/Y49A}$ flies, it suggests that the point mutations were sufficient in disrupting autophagy. The aggregates

present in the ATG8a$^{K48A/Y49A}$ are likely to contain proteins that specifically interact with ATG8a through the LIR motif. It is important to note that not every protein in the aggregate will be a LIR motif containing protein. This is because many proteins interact with ATG8a for selective degradation indirectly. Ref(2)P and other adapter proteins may be responsible for the degradation of many other proteins and the disruption of the LDS-LIR motif interaction would also lead to accumulation of these proteins. Nonetheless, there should still be an enrichment of LIR motif containing proteins in the cells of ATG8a$^{K48A/Y49A}$ mutants compared to ATG8a null.

## 3.8 Summary

Characterisation of the ATG8a$^{K48A/Y49A}$ flies suggest that they can be used in quantitative proteomics to identify novel ATG8a interacting proteins. The K48A/Y49A mutation in ATG8a was confirmed through PCR and genomic DNA sequencing. It was shown that these flies have a similar phenotype to ATG8a null flies, such as reduced lifespan. The accumulation of LIR motif containing proteins such as Ref(2)P and Kenny as well as ubiquitinated protein aggregates was confirmed biochemically through western blotting and visually though confocal microscopy. Based on these data, flies can be aged 2-weeks to allow LIR motif proteins to accumulate, with subsequent analysis using quantitative proteomics.

# Chapter 4 Quantitative proteomics analysis of ATG8a and ATG8a K48A/Y49A mutant flies compared to wild type flies.

## 4.1 Introduction

### 4.1.1 Accumulation of aggregated proteins in autophagy deficient flies

Basal level of autophagy occurs all the time and is involved in the degradation and turnover of many proteins, which has physiological consequences. Many of these proteins are selectively chosen for degradation via the autophagosome which is the focus of this project. Proteins that are selectively degraded through the ATG8a-LDS and LIR motif interactions are of particular interest.

This project is focussed on identifying proteins that interact with ATG8a specifically through its LIR motif. Using ATG8a$^{K48a/Y49A}$ mutants, which have a mutated LDS, can further help identify such proteins. In chapter 2, it was shown that these flies have a similar phenotype to ATG8a mutant flies and show similar protein aggregates in their cells. However, these aggregates appear smaller as rather than removing the whole function of ATG8a only the LDS is mutated. Therefore, the proteins that aggregate in ATG8a$^{K48a/Y49A}$ mutant flies are likely to be enriched for LIR motif containing proteins. This makes using both ATG8a$^{K48a/Y49A}$ and ATG8a mutant flies advantageous over using ATG8a mutant flies alone. This is because ATG8a mutant flies alone will have too many proteins aggregating in the cells making it too difficult to detect specific proteins of interest. Quantitative proteomics of ATG8a$^{K48a/Y49A}$ mutant flies alongside ATG8a mutant flies will help narrow down the number of significantly abundant proteins. By utilising quantitative proteomics on aged flies, it is possible to identify proteins which are significantly overabundant in ATG8a mutant and

ATG8a$^{K48A/Y49A}$ mutant flies compared to wild type flies. Proteins that accumulate in both these flies are likely to good candidates for novel selective autophagy receptors and substrates.

### 4.1.2 Quantitative proteomics – LC/MS

Mass spectrometry-based proteomics is a commonly used technique in biology. A mass spectrometer allows analysis of ionised molecules by measuring their mass to charge ratio (m/z). The core components of a mass spectrometer include an ion source, mass analyser, and a detector. Molecules are transferred from a liquid or solid phase to a gaseous phase and ionised. The ionised molecules can then be separated in a mass analyser based on their m/z ratio. This ratio is then recorded by a detector. The output is a mass spectrum which shows the relative abundance of each signal based on their m/z ratio (Matthiesen, 2013).

For proteomics, proteins are usually digested with a protease such as trypsin before mass spectroscopy analysis ("bottom-up proteomics"). This is because unlike whole proteins, peptides produce less complex spectrums, rendering the analysis much easier. Once the protein is fragmented, it is usually separated using reverse phase liquid chromatography (LC) before being fed into the mass spectrometer. Reverse phase LC is a type of partition chromatography that uses a hydrophobic stationary phase and a hydrophilic mobile phase. By combining LC with mass spectrometry, you can obtain a series of mass spectrums as the peptides elute. Tandem mass spectrometry is employed often in proteomics studies where peptides are ionised (in this experiment using electrospray ionisation) and separated based on their m/z ratio using the first analyser. The molecules are then further fragmented (using collision-induced dissociation (CID)) into smaller ions and detected by a second mass analyser which again separates the fragments based on their m/z ratio (Matthiesen, 2013). The result is an MS/MS spectrum which can be used to query spectrums to known protein databases, such as the *Drosophila* protein database, using software (such as MaxQuant/Andromeda). Combining two mass analysers

allows for the unambiguous identification of peptides and proteins. In this study, shotgun proteomics was employed where mixtures of proteins are digested together and analysed using liquid chromatography – mass spectrometry (LC-MS). For quantitative analysis, labelled, and label free methods are available. For this study, label free quantification was used.

### 4.1.3 Label free quantification

Label free quantification analyses different protein samples and controls separately (Figure 4-1). This contrasts with labelled methods such as stable isotope labelling where different samples are labelled separately before being combined and analysed in one LC-MS. Quantification of peptides can based on two parameters, peak ion intensity and spectral count (Zhu, Smith and Huang, 2010). Quantification by peak intensity is much more difficult and requires specific programs that automatically align peak intensity values. Quantification of spectral count is much easier but requires additional normalisation and statistical analysis. Spectral counting relies on the quantification of the number of MS/MS spectra that belong to the same protein. The principle is that the more abundant a protein is, the more peptides which belong to that protein will be present in the sample. Proteins which are highly abundant have more peptides, more sequence coverage, and contain more unique peptides. However, larger proteins tend to have more peptides and thus more MS/MS spectra than smaller proteins which is why normalisation is required. Normalised spectral abundance factor (NSAF) is used to normalise label free quantification which considers protein length (Zhu, Smith and Huang, 2010). Label free quantification by spectral counting is the technique used in this study.

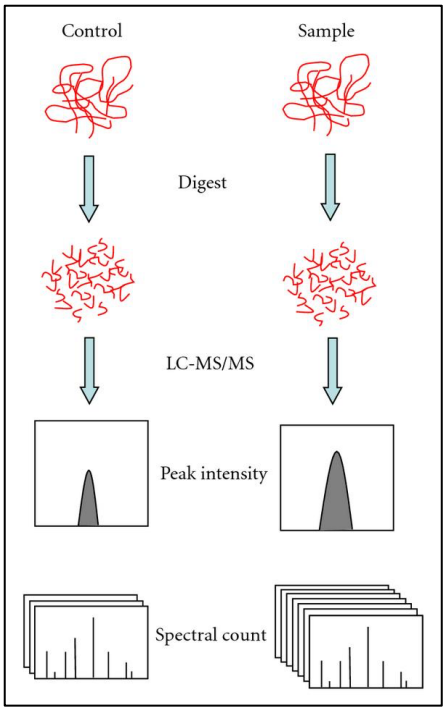


Figure 4-1 **Label free quantification technique.** Control and experimental samples are digested and analysed using LC-MS/MS separately. The proteins are then quantified using peak intensity or spectral counts and relative abundance compared between samples. Figure adapted from (Zhu, Smith and Huang, 2010).

### 4.1.4 MaxQuant and Andromeda

MaxQuant is the computational platform which was used in the proteomics study for data analysis (Tyanova, Temu and Cox, 2016). This platform is used in the identification of proteins and quantification of results from the raw MS/MS data. MaxQuant utilises andromeda, which is a peptide search engine that relies on probabilistic scoring. Andomreda generates theoretical fragment ions mass for comparisons with the experimental MS/MS spectra. The Andromeda score is -10 times the logarithm of matching at least *k* out of *n* theoretical masses by chance. Where *k* is the number of matching ions in the spectra and *n* is the total number of theoretical ions (Cox *et al.*, 2011). Andromeda was used for the identification of proteins based on the MS/MS spectra of peptides. MaxQuant also quantifies each protein based on the number of peptide MS/MS spectra for each protein. The resulting output is a label

free quantification (LFQ) value for each protein which represents its relative abundance in the biological sample (Cox *et al.*, 2011). For some of the data analysis, the software Perseus was used. This software allows pre-processing, such as normalisation and handling of missing values, as well as statistical and functional analysis (Tyanova and Cox, 2018).

## 4.2 Aims and objectives

The aim of the next sets of experiments is to use quantitative proteomics to identify novel LIR motif containing autophagy adapters, receptors, and substrates. Protein aggregates accumulate in ATG8a and ATG8a$^{k48A/Y49A}$ mutant flies compared to wild type. The proteomics experiment was used to identify proteins significantly overabundant in each of the mutant flies compared to wild type flies. This will generate two lists of significant proteins; ATG8a compared to wild type and ATG8a$^{k48A/Y49A}$ compared to wild type. Proteins which are significantly overabundant in both lists can be analysed further as a potential LIR motif containing ATG8a interactor.

## 4.3 Optimisation of proteomics protocol

The initial goal of the proteomics experiment is to use mass spectrometry to identify as many proteins as possible from the fly protein sample. The *Drosophila* proteome has approximately 14,000 proteins, so by identifying as many proteins as possible, we can be confident that most of the major accumulated proteins were identified. This required careful optimisation of sample preparation and use of the mass spectrometer.

### 4.3.1 Shotgun proteomics – methanol/chloroform precipitation

Figure 4-2 is a schematic showing the overview of the first attempt at the proteomics experiment. Ten flies, half male, and half female, from each genotype (wild type, ATG8a$^{K48A/Y49A}$, ATG8a) were collected over 2-3 days and aged 2-weeks. 2 weeks was selected as it allows sufficient time for LIR motif containing proteins, such as Ref(2)P and Kenny, to accumulate in these flies. Therefore, this would give ample time for other potential LIR motif containing proteins to accumulate as well. Proteins were extracted and digested in-solution (using trypsin), using the methanol/chloroform precipitation method. All three samples were then run on a mass spectrometer and processed using MaxQuant/Andromeda.

From this initial first experiment (n=1), only 1103 protein were identified. This was not a lot of proteins when compared to the total 14,000 that are in the fly proteome. Also, Ref(2)P, a protein which is known to accumulate in autophagy mutant flies was not identified in this experiment. It was thought that the process of methanol precipitation technique and in-solution digestion of proteins may be losing some proteins. Other techniques for digestion of proteins using trypsin before LC-MS was investigated.

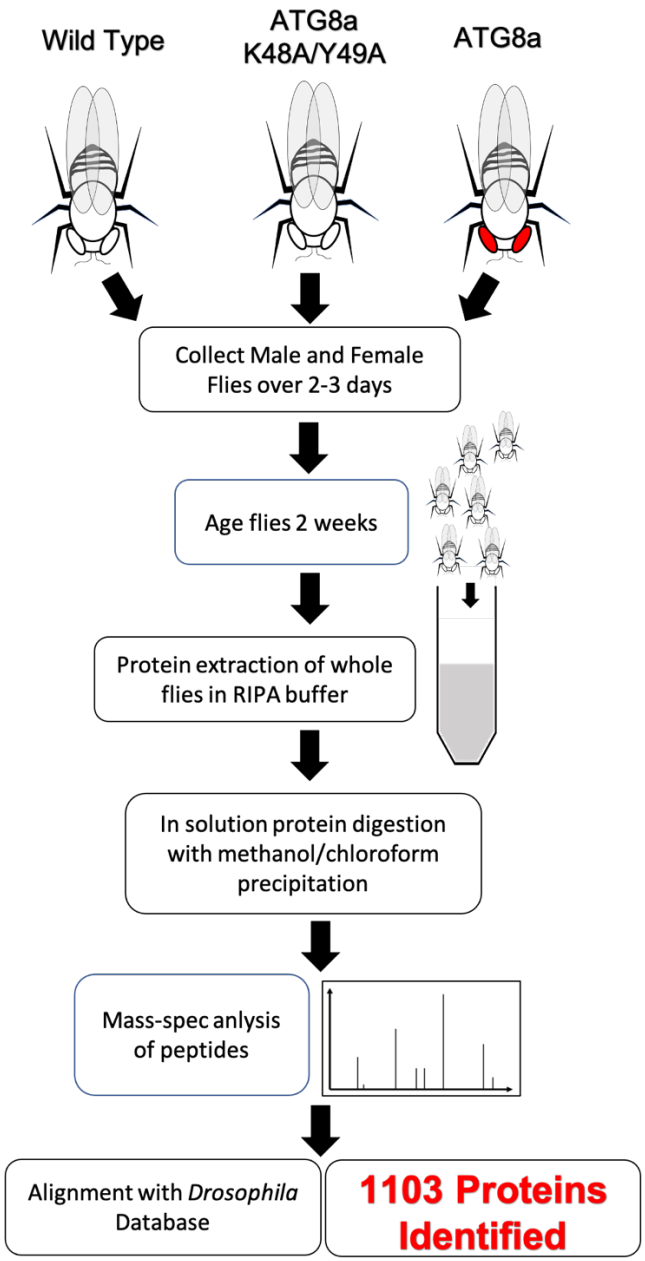


Figure 4-2 **Overview proteomics experiment using methanol/chloroform precipitation**. Using this technique, 1103 proteins were identified in the proteomics analysis. Experiment was one biological repeat (n=1).

### 4.3.2 Shotgun proteomics – Filter Aided Sample Preparation (FASP)

For the second attempt of the proteomics, a different protocol for sample preparation was used. Filter Aided Sample Preparation (FASP) is a technique where the detergent removal, buffer exchanges, digestion and elution of peptides is done in an ultra-filtration tube (Wisniewski *et al.*, 2009). For the experiment 10,000 molecular mass cut off filtration tube was used. This technique, over in-solution digestion, outputs pure peptides which covered much more of the proteome.

Figure 4-3 is the schematic for the second attempt (n=1) using the FASP technique, 1843 proteins were identified which is more than the first attempt. In this experiment Ref(2)P was among those proteins which were identified.

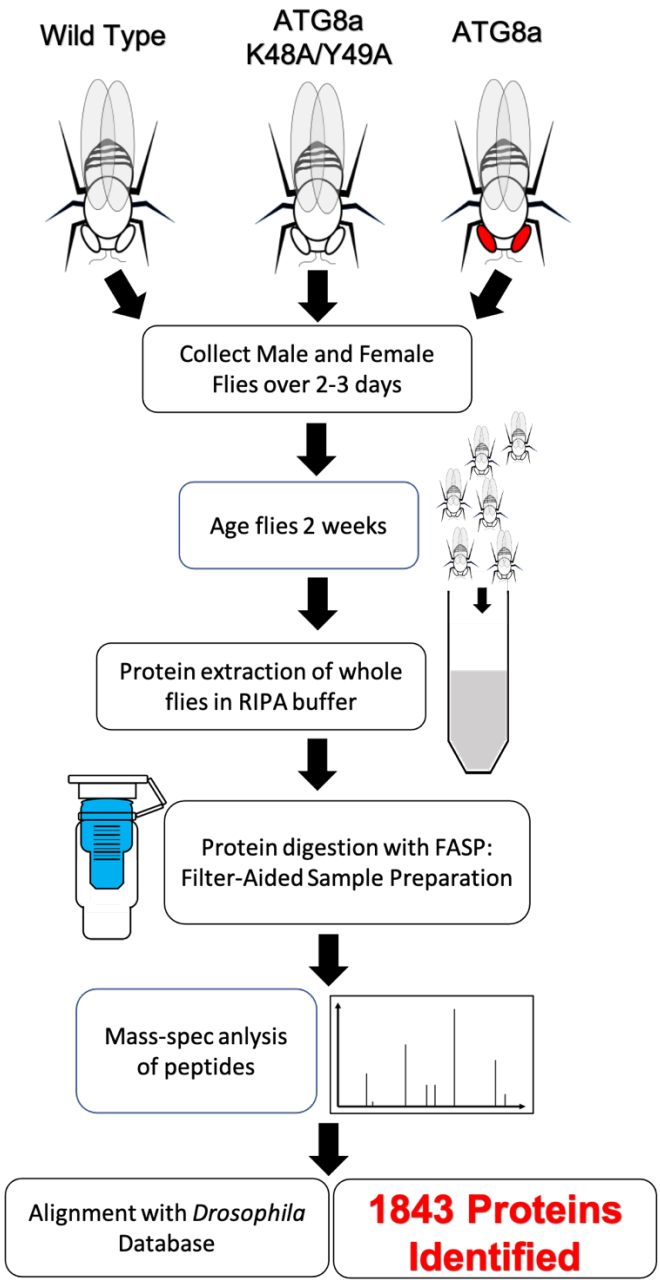


Figure 4-3 **Overview proteomics experiment using filter-aided sample preparation (FASP) technique**. Using this technique, 1843 proteins were identified in the proteomics analysis. Experiment was one biological repeat (n=1).

Although more proteins were identified than the first attempt, one more change was made to try to increase the protein number. This change was to use fly heads for the proteomics instead of the whole fly. Thirty fly heads (all male) were

lysed, and proteins extracted before trypsin digestion. The reason behind this is that very highly abundant proteins, for example Ref(2)P which was always one of the more abundant proteins in the mutant samples, can cause less abundant proteins to not be identified. Therefore, only using the fly heads can reduce the amount of these highly abundant proteins that are found throughout the fly body. Additionally, the whole fly contained many different organs and tissues. This means that quantitative analysis will be more difficult as some tissues may have an overabundance of a protein while in other tissues it is reduced. This can prevent proteins from appearing significantly increased in certain tissues. By using only fly heads, proteins specifically accumulating in the brain will be the focus.

Figure 4-4 is the schematic for the third attempt of the proteomics using fly heads 2528 proteins were identified which was higher than the 1843 proteins in whole flies. This experiment was conducted with three biological repeats (n=3) thus some statistical analysis could be undertaken.

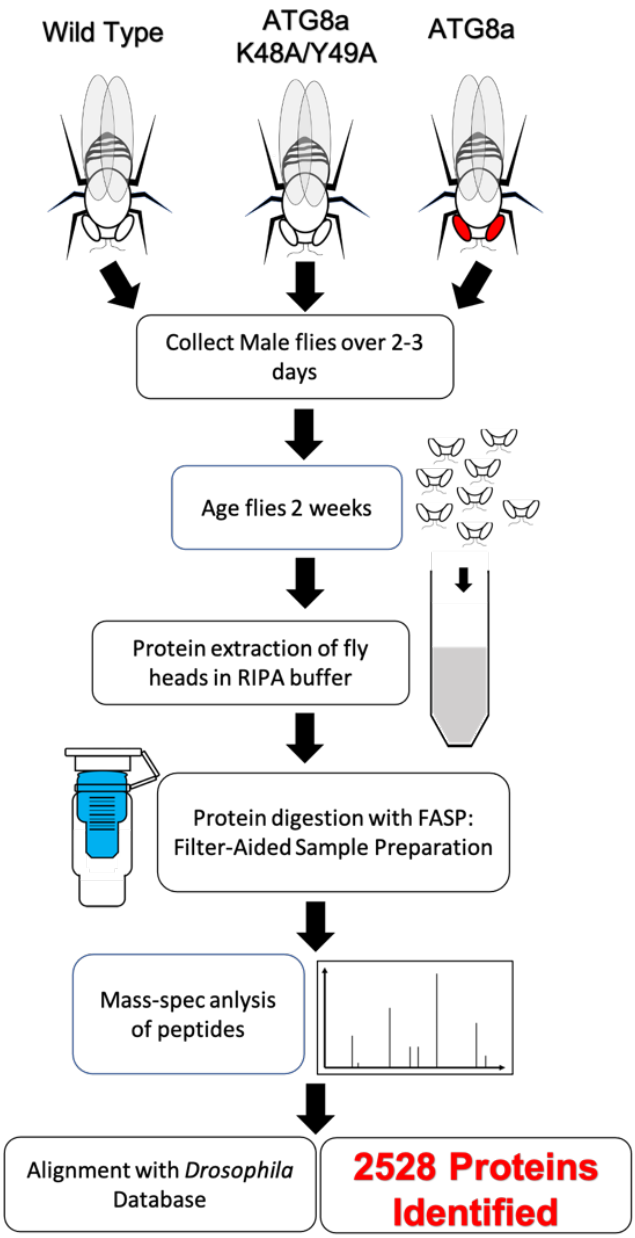


Figure 4-4 **Further optimisation of using the FASP technique to increase the number of proteins identified.** Only male flies were used for this experiment. Fly head were used as opposed to whole flies. 2528 proteins were identified in the proteomics analysis.

Figure 4-5 is the principal component analysis (PCA) for this experiment that shows that the different biological repeats for each genotype (wild type, ATG8a, ATG8a$^{K48A/Y49A}$) did not cluster very well together. This suggests that there was a lot of variability between the biological repeats.

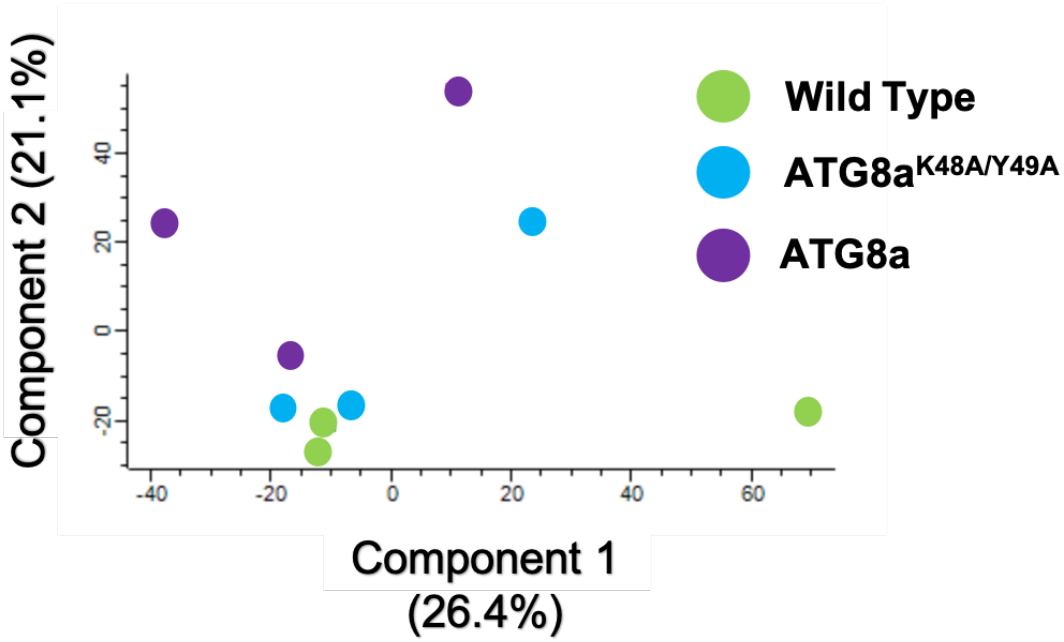


Figure 4-5 **PCA blot of wild type, ATG8a$^{K48A/Y49A}$ mutant, and ATG8a mutant flies.** The biological repeats of each sample to not cluster together denoting large variability between repeats. Three biological repeats are shown for each sample (n=3).

Two volcano plots (Figure 4-6) were produced with the three proteomics repeats. $Log_2$ fold change was plotted against -Log P. A two-tailed Students *t*-test was used, which compared wild type flies with each of the mutant flies (ATG8a and ATG8a$^{K48A/Y49A}$), with a significance level of p = 0.05. Anything above the black line represents proteins that were found to be significantly lower (left side) or higher (right side) in the mutants compared to wild type flies. In both comparisons, no proteins were found to be significant. This again would be because there was too much variability in the biological repeats (as can be seen in the PCA plot).

Although many more proteins were identified (2528 as opposed to 1843), the next issue to overcome was to improve the quality of the data.

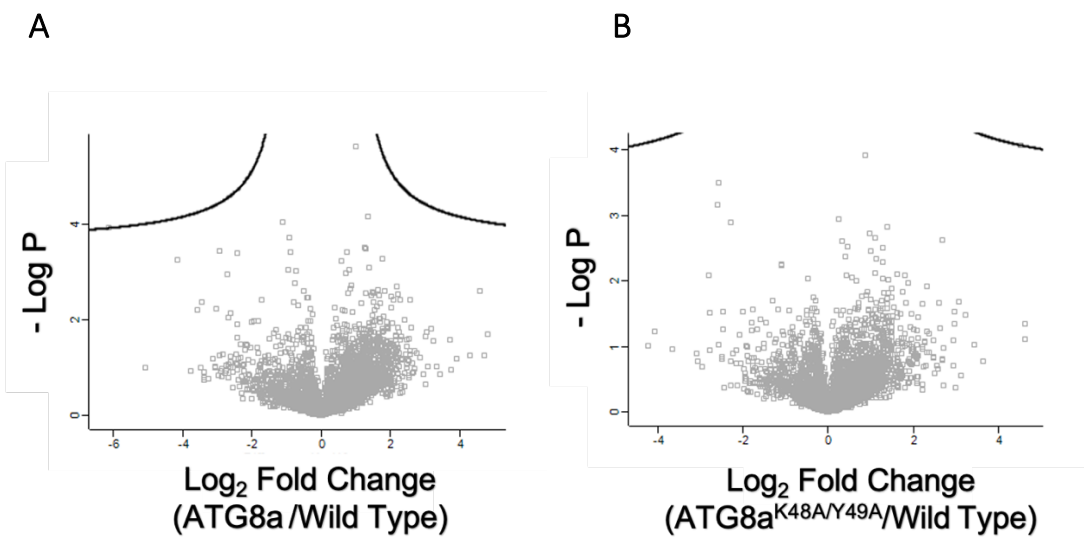


Figure 4-6 **Volcano plot of $Log_2$ fold change against -Log P-value for $ATG8a^{K48A/Y49A}$ (A) and ATG8a (B) mutant compared to wild type samples.** Black lines on the right indicate cut off for significant increased abundance of proteins in mutants compared to wild type ($p<0.05$). No proteins identified were significant in either group.

### 4.3.3 Optimised conditions

To minimise variation in biological repeats, changes were made to the collection of flies. The proteome of flies changes once the flies have started mating, therefore only virgin flies were collected. Like the previous experiment, these were all male flies to further reduce variation in the proteome between male and female flies. All flies were collected on the same day so that they were all aged to exactly 14 days as opposed to 13-16 days old. Since using *Drosophila* heads instead of whole flies lead to the identification of more proteins, thirty fly heads from each genotype were used to produce protein lysate.

In addition to fly collection, it was understood that running biological repeats on different days could impact results. This is because there may be slight variations to the mass spectrometry machinery on each day, which could also lead to inconsistent repeats. Therefore, to avoid this problem, protein lysates for biological repeats were collected and stored at -20°C until all repeats were ready. Mass

spectrometry data was collected for the samples on the same day. In addition to this, four biological repeats were conducted to ensure the results were representative.

3736 proteins were identified once the aforementioned modification was implemented. This is a substantial improvement over the previous attempts and similar statistical analysis was carried out with this new set of data. Figure 4-7 is an overview of the proteomics optimisation process.

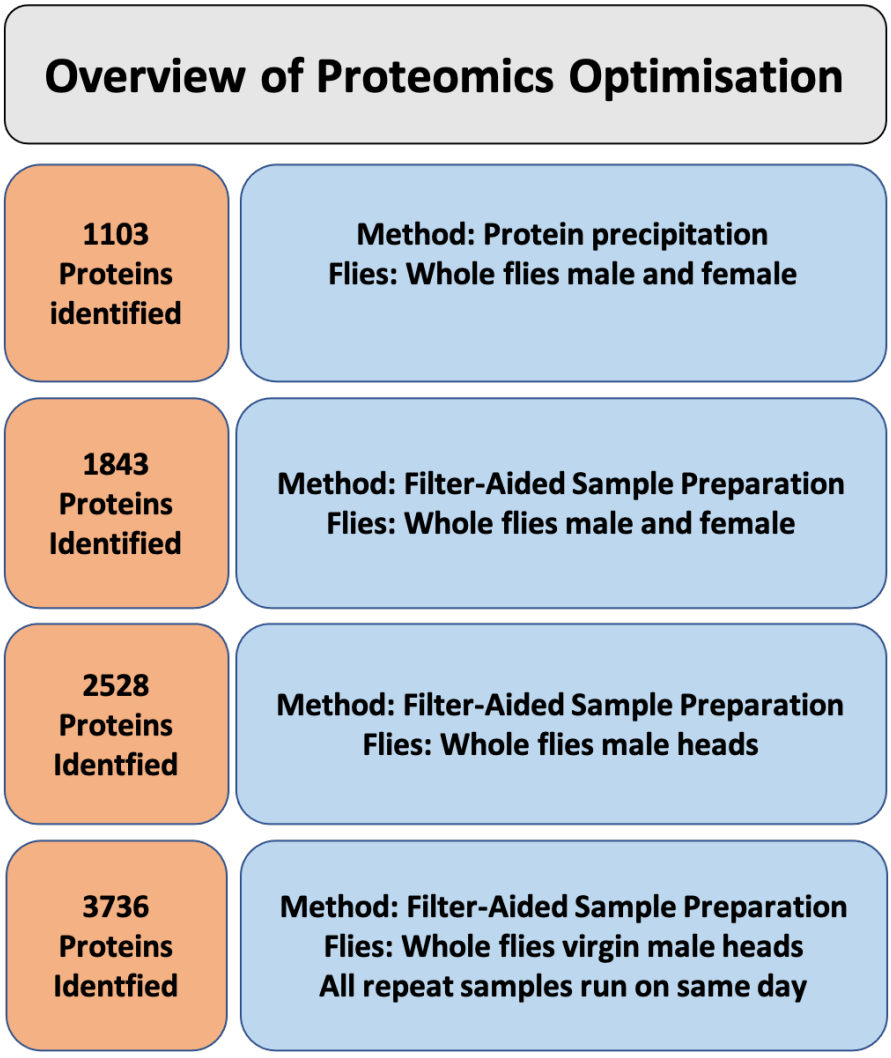


Figure 4-7 **Optimisation process of quantitative proteomics.** Filter-aided sample preparation was more effective than methanol/chloroform precipitation. The number of proteins identified was first increased through optimisation of fly collection and use of heads as opposed to whole flies. The quality of the data was improved through ensuring all variables were kept as identical as possible, such as fly age, and running all biological repeats for mass-spec analysis on the same day.

## 4.4 Optimised quantitative proteomics experiment

### 4.4.1 Principal component analysis and volcano plot

Figure 4-8 is the PCA plot of the optimised proteomics data from 4 biological repeats (n=4). All three genotypes (wild type, ATG8a, ATG8a$^{K48A/Y49A}$) of the four biological repeats were clustered together, indicating that the quality of the data was much better this time and far less variation between repeats was observed.

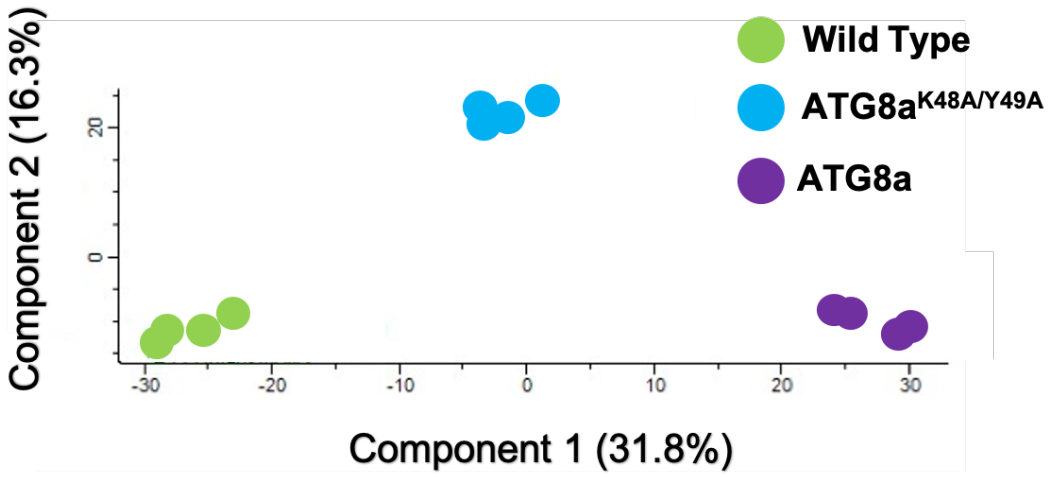


Figure 4-8 **PCA blot of optimised proteomics for wild type, ATG8a$^{K48A/Y49A}$ mutant, and ATG8a mutant flies.** The biological repeats of each sample cluster into obvious groups. Four biological repeats are shown for each sample (n=4).

Figure 4-9 is the volcano plot produced for this data. Similar to last time, Students *t*-test was done to find significant proteins when comparing each of the two mutants (ATG8a and ATG8a$^{K48A/Y49A}$) to wild type flies (P<0.05). Many proteins were seen to be significant (above the black line). Any protein on the top right-hand side of

the graph are proteins which are overabundant in the autophagy mutant flies and therefore these are the proteins of interest.

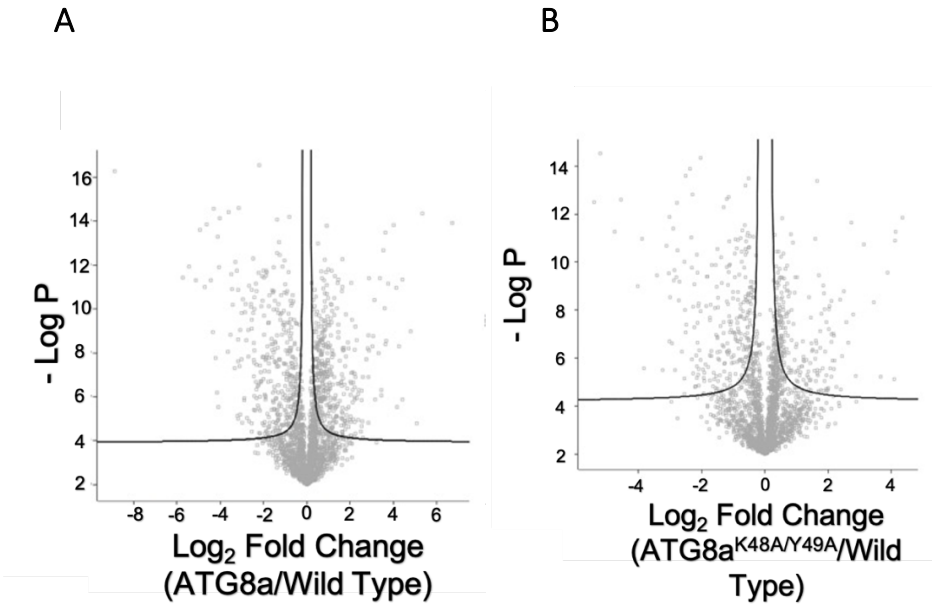


Figure 4-9 **Volcano plot of optimised proteomics showing $Log_2$ fold change against -Log P-value for ATG8a$^{K48A/Y49A}$ (A) and ATG8a (B) mutant compared to wild type samples.** Black lines on the right indicate cut off for significant increased abundance of proteins in mutants compared to wild type ($p<0.05$). Many proteins can be seen in this upper right region which are significantly overabundant in autophagy mutant flies compared to wild type.

## 4.4.2 Identification of significant proteins

Figure 4-10 is a Venn diagram highlighting the number of significant proteins identified when comparing wild type flies to ATG8a and ATG8a$^{K48A/Y49A}$ mutant flies. The numbers only include those which are significantly overabundant in the mutants as those are likely to be LIR motif containing proteins. 985 proteins were found significantly overabundant in the ATG8a mutants, and 876 proteins were found to be significantly overabundant in the ATG8a$^{K48A/Y49A}$ mutants compared to wild type flies. It was expected that LIR motif containing proteins would be significantly overabundant

in both these mutant flies and so proteins common to both lists (521 proteins) were investigated further.

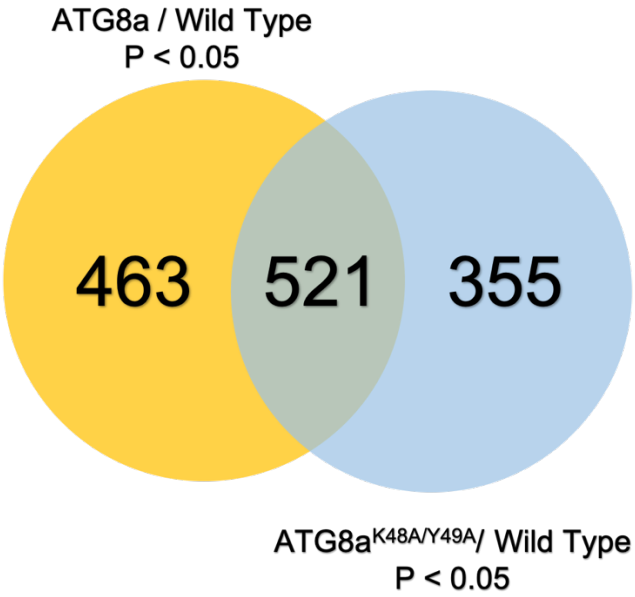


Figure 4-10 **Venn diagram showing proteins significantly overabundant in ATG8a$^{K48A/Y49A}$ and ATG8a mutant flies compared to wild type.** 984 proteins were significantly overabundant in ATG8a mutants compared to wild type and 876 proteins for ATG8a$^{K48A/Y49A}$ compared to wild type. 521 proteins were found to be significantly overabundant in both autophagy mutant flies.

Gene ontology analysis was carried out on the 521 proteins found significantly overabundant in both mutant flies (Figure 4-11). A range of GO terms that cover a variety of cellular processes were identified. This was expected due to autophagic degradation being involved in many physiological processes from protein turnover to immunity. Many proteins were involved with parts of the protein synthesis pathway, such as protein folding, translation, and amino acid/carbohydrate biosynthesis. Others were also involved in various other cell metabolic processes.

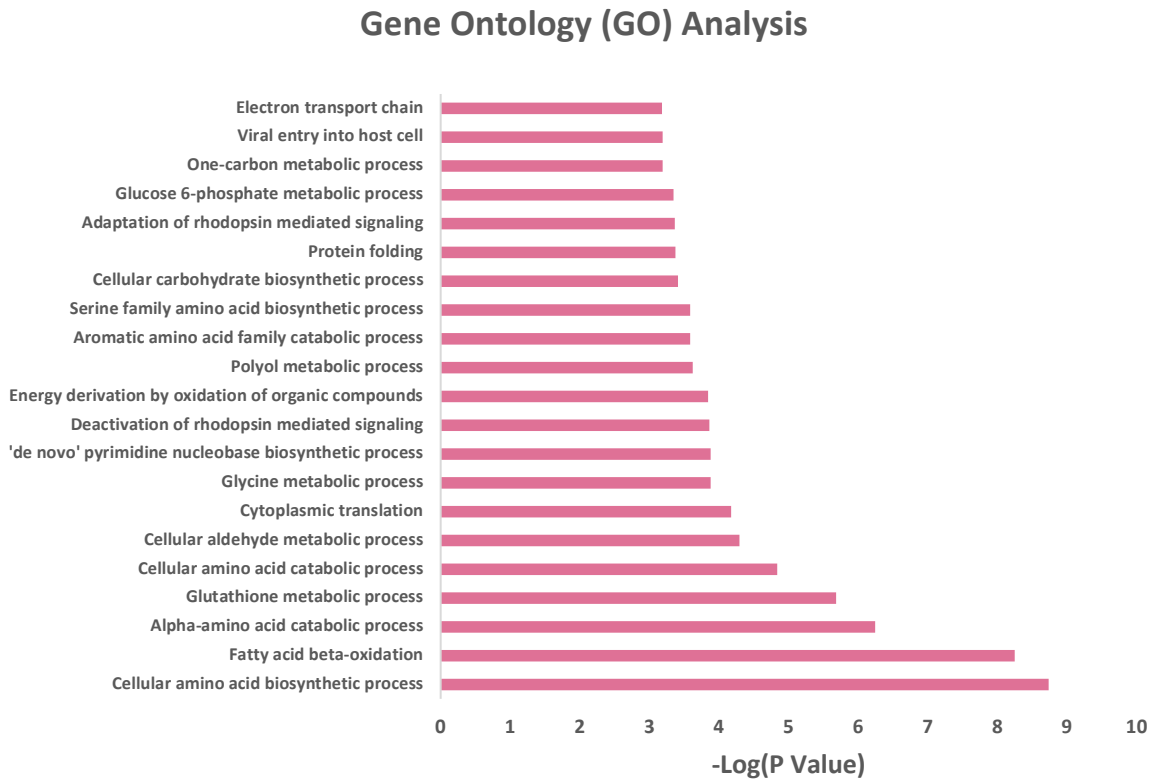


Figure 4-11 **Gene Ontology analysis of the 521 proteins significant in both autophagy mutant flies compared to wild type.** Broad range of biological processed are covered by these proteins.

Of the 521 proteins, only those that had at least a 2-fold increase in abundance were considered for further experimentation. 158 proteins were both significantly more abundant and had at least a 2-fold increase in ATG8a mutant flies compare to wild type flies. 102 proteins were both significantly more abundant and had at least a 2-fold increase in ATG8a$^{K48A/Y49A}$ mutant flies compared to wild type flies. 29 proteins were found to be common between both these lists (Figure 4-12).

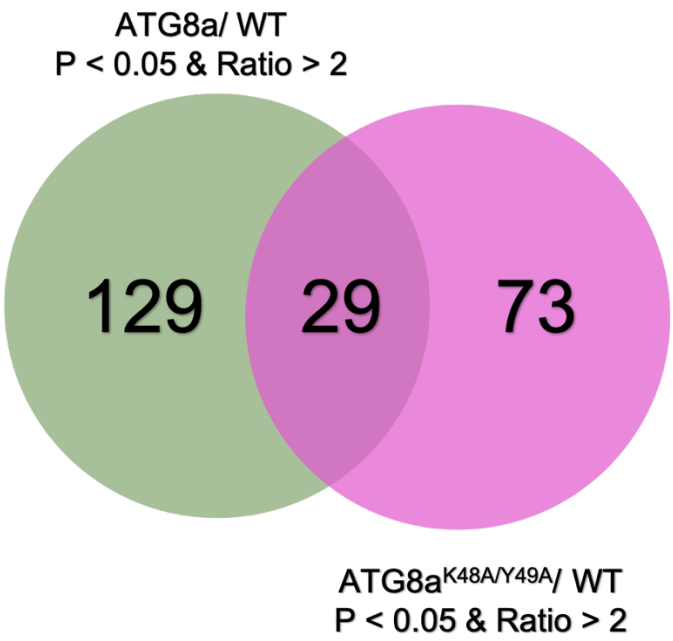


Figure 4-12 **Venn diagram of proteins which were significantly overabundant in autophagy mutant compared to wild type and had at least a 2-fold increase in quantification.** A total of 158 proteins met these criteria for ATG8a mutant flies and 102 proteins for $^{ATG8aK48A/Y49A}$. 29 proteins were common to both autophagy mutants.

## 4.5 Analysis of the 29 significant proteins

A list of the 29 significant proteins can be seen in Table 13. The label free quantification value of all proteins in each of the three fly genotypes (ATG8a, ATG8a$^{K48A/Y49A}$, wild type) is shown. Fold change was calculated as a ratio of one of the mutant flies LFQ compared to wild type flies. N/A in the ratio column is for calculations where no protein was detected in wild type flies (LFQ = 0). P values were calculated using an unpaired student's *t*-test, which compared the biological repeats of both mutant flies to wild type flies.

The amino acid sequence of each of the 29 proteins was obtained from the Uniprot website and analysed using the iLIR software. This software allowed for the detection of predicted LIR motifs in the sequence. As described in section 2.9.1 a predicted LIR motif with a high PSSM score is much more likely to be a functional LIR

motif. A PSSM score of greater than 13 was regarded as a high score. Although not always, the case most functional LIR motifs were found within an anchor region (intrinsically disordered regions). Therefore, proteins with a predicted LIR motif with a PSSM score of greater than 13 and found within an anchor region are good candidates for novel autophagy adapters/substrates.

4 proteins matched these criteria which are highlighted in Table 13. Amongst these is Ref(2)P, a well-studied LIR motif containing protein. This acts as a good positive control for the experiment, as one of the most important autophagy adapters was identified in this study. This is very promising for the other three proteins identified on the list, GMAP, Ras and Dally. A graph showing the label free quantification of Ref(2)P in ATG8a and ATG8a$^{K48A/Y49A}$ mutants compared to wild type control flies can be seen in Figure 4-13. The iLIR software output for Ref(2)P is also shown, which identified PEWQLI as the highest scoring LIR motif. This was already known as a functional LIR motif.

A

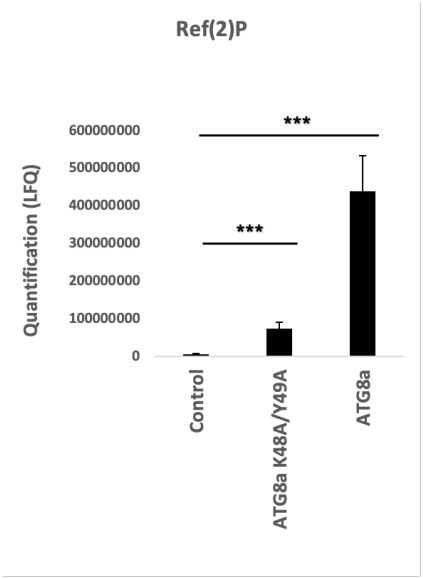


B

Query: >sp|P14199|REF2P_DROME Protein ref(2)P OS=Drosophila melanogaster OX=7227 GN=ref(2)P PE=1 SV=2

| Motif | Start | End | Pattern | PSSM Score | LIR in Anchor |
|---|---|---|---|---|---|
| xLIR | 452 | 457 | PEWQLI | 18 | Yes |
| WxxL | 28 | 33 | QNYTIL | 10 | No |
| WxxL | 138 | 143 | FRYKCV | 4 | No |
| WxxL | 342 | 347 | EMFSKI | 9 | Yes |
| WxxL | 485 | 490 | RDFGQL | 10 | Yes |

Figure 4-13 **Ref(2)P label free quantification and predicted LIR motif.** A) Label free quantification (LFQ) of Ref(2)P in wild type control, ATG8A$^{K48A/Y49A}$ mutants, and ATG8a mutants. There is a significantly increased quantity of Ref(2)P in both autophagy mutants compared to the control. B) Predicted LIR motifs from the iLIR software. The PEWQLI motif has the highest PSSM score and is found in an anchor region. This motif is known to be the functional LIR motif in Ref(2)P. Significance for quantification was calculated through one sample t-test, ***p<0.001, n=4.

| Protein name | Uniprot ID | Average LFQ intensity of ATG8a | Average LFQ intensity of ATG8a$^{K48A/Y49A}$ | Average LFQ intensity of Wild Type | Ratio ATG8a/Wild Type | Ratio ATG8a$^{K48A/Y49A}$ /Wildtype | p value ATG8a/Wild Type | p value ATG8a$^{K48A/Y49A}$ /Wildtype | LIR motif PSSM>13 | LIR motif in Anchor |
|---|---|---|---|---|---|---|---|---|---|---|
| CG5080 | Q7K3E2 | 66049000 | 49880000 | 24680750 | 2.68 | 2.02 | 0.011592959 | 0.03557181 | YES | NO |
| faf | A0A0B4K6W2 | 10005750 | 6905775 | 0 | N/A | N/A | 7.57817E-06 | 0.031221334 | YES | NO |
| CG34172 | Q6IHY5 | 78076250 | 65039750 | 0 | N/A | N/A | 0.000200425 | 0.028880452 | NO | NO |
| CG32638 | Q8IR72 | 71748250 | 47748500 | 0 | N/A | N/A | 0.030183763 | 0.024545484 | NO | NO |
| Naam | Q9VDU7 | 13968250 | 12606750 | 3127500 | 4.47 | 4.03 | 0.014600354 | 0.024337065 | NO | NO |
| Proc | Q9VLV9 | 9499525 | 5946700 | 2449725 | 3.88 | 2.43 | 0.001153117 | 0.023807031 | NO | NO |
| PI31 | A0A0B4KEK7 | 15120500 | 15557250 | 7441175 | 2.03 | 2.09 | 0.049797907 | 0.021273536 | YES | NO |
| CG17544 | Q9VIX4 | 64562500 | 29556500 | 7295675 | 8.85 | 4.05 | 0.002104985 | 0.018795974 | YES | NO |
| CG1309 | Q9VZF1 | 18514250 | 17333000 | 4914325 | 3.77 | 3.53 | 0.007762399 | 0.012796017 | NO | NO |
| Hsp22 | P02515 | 102654000 | 15283625 | 3565725 | 28.79 | 4.29 | 0.001372423 | 0.00707916 | YES | NO |
| RIC-3 | A0A0B4LH23 | 16832750 | 21163500 | 3699000 | 4.55 | 5.72 | 0.01354687 | 0.005457873 | NO | NO |
| Ect3 | Q9VGE7 | 17569000 | 22742000 | 7319475 | 2.40 | 3.11 | 0.013959163 | 0.004790721 | NO | NO |
| CG11208 | Q7K3B7 | 31894750 | 23780750 | 5412925 | 5.89 | 4.39 | 0.003005442 | 0.002326007 | YES | NO |
| Sip1 | Q7K5M6 | 13654500 | 12544500 | 1685325 | 8.10 | 7.44 | 0.001478584 | 0.001739584 | NO | NO |

| | | | | | | | | | | |
|---|---|---|---|---|---|---|---|---|---|---|
| GstD3 | Q9VG97 | 23691500 | 20629000 | 1531550 | 15.47 | 13.47 | 0.000945625 | 0.000784903 | YES | NO |
| dally | Q53XG2 | 6415900 | 6058650 | 0 | N/A | N/A | 4.06908E-06 | 0.000449452 | YES | YES |
| CG11857 | Q9VBU6 | 67521500 | 56856000 | 28036750 | 2.41 | 2.03 | 6.91077E-05 | 0.000258626 | YES | NO |
| ref(2)P | P14199 | 439115000 | 73883500 | 4403050 | 99.73 | 16.78 | 9.40137E-05 | 0.000198945 | YES | YES |
| CG10166 | Q9VIU7 | 16126750 | 14461625 | 0 | N/A | N/A | 1.29866E-08 | 0.000170861 | YES | NO |
| Pdp | Q9W3Q1 | 7285250 | 7405125 | 0 | N/A | N/A | 0.037598688 | 4.52877E-05 | YES | NO |
| Gmap | Q9VXU2 | 21619000 | 12620000 | 0 | N/A | N/A | 0.000306313 | 4.20151E-05 | YES | YES |
| numb | M9PCN6 | 9419675 | 7279075 | 0 | N/A | N/A | 9.77008E-05 | 2.04783E-05 | NO | NO |
| GstD8 | Q9VG92 | 7492950 | 9249725 | 0 | N/A | N/A | 4.91912E-06 | 1.72223E-05 | YES | NO |
| CG9775 | Q9VN39 | 4383875 | 6414125 | 0 | N/A | N/A | 0.031306116 | 9.1257E-06 | NO | NO |
| GstE4 | A1ZB69 | 100038250 | 141875000 | 45458750 | 2.200637941 | 3.120961311 | 0.000851777 | 8.33344E-06 | YES | NO |
| ras | A4V488 | 6900275 | 9904250 | 0 | N/A | N/A | 0.032566158 | 6.71249E-06 | YES | YES |
| CG10253 | A0A0B4JD21 | 17562750 | 12872500 | 0 | N/A | N/A | 1.54079E-07 | 5.61398E-06 | NO | NO |
| CG13284 | Q86BQ3 | 9120525 | 9271100 | 0 | N/A | N/A | 1.9801E-05 | 3.86807E-06 | YES | NO |
| Itp-r83A | A0A0B4LGN1 | 8355075 | 7834000 | 0 | N/A | N/A | 4.04003E-09 | 6.57104E-08 | YES | NO |

Table 13 List of significant proteins. Highlighted proteins (Dally, Ras, GMAP, and Ref(2)P) were selected as they had the following properties: 1) They were significantly overabundant in both ATG8a$^{K48A/y49A}$ and ATG8a mutant flies compared to WT, 2) a LIR motif found in an anchor region with a PSSM score of greater than 13, 3) They had at least a 2-fold increase in ATG8a$^{K48A/y49A}$ and ATG8a mutant flies compared to WT flies. An N/A in the fold change column was a high value as it means that no protein was detected in the WT sample.

## 4.6 Dally, Ras and GMAP

### 4.6.1 Dally

Division abnormally delayed (dally) is one of two *Drosophila* glypicans (the other being dally-like protein (Dlp)), which has a developmental role in the fruit fly. It is a glycosylphosphatidylinositol (GPI)-anchored heparan sulphate proteoglycan (HSPGs), which is a cell surface protein (Akiyama *et al.*, 2008). It is involved in the regulation of the morphogens such as Decapentaplegic (Dpp), Wingless (Wg) and Hedgehog (Hh). Morphogens form concentration gradients across the developing embryo/larvae and regulate the transcription of different genes and so determine the cell's fate (Han *et al.*, 2005). Morphogens are involved in many developmental processes such embryo segmentation, and limb pattering such as the wing.

Dpp has been shown to be specifically involved in the development of the wing and is distributed along the anterior to posterior axis (Akiyama *et al.*, 2008). When dally is knocked down, the Dpp pattering is not formed properly and when dally is overexpressed, Dpp signalling is increased. This suggests dally is an important regulator of Dpp during development. Similarly, daily has been shown to be involved in regulating the gradient of Wg gradients, which is also involved in the development of the wing. Morphogens such as Hh, need to signal over long distances such as patterning across the 300 µm of *Drosophila* neural tube. Therefore, the ability to spread over these distances is vital. Although dally is a membrane protein, there is evidence that it is cleaved by the enzyme Notum and take part in the long-range regulation of Hh gradients (Takeo *et al.*, 2005).

Dally also has specific roles for eye and nervous system development. Eye development is controlled through the regulation of the distribution of Unpaired (Upd) family. Upd is found upstream of the Janus kinase- signal transducer and activator of transcription (JAK-STAT) pathway (Zhang *et al.*, 2013). There is also

evidence that dally is involved in promoting cell division during post-embryonic development of the *Drosophila* nervous system (Nakato, Futch and Selleck, 1995).

In addition to the role in development and morphogens, dally seems to have a role in the maintenance of adult stem cells, such as the germline stem cells found in *Drosophila* ovaries (Su *et al.*, 2018). Dally has been shown to regulate and maintain follicle stem cells and facilitate stem cell replacement through competition for niche occupancy.

Unfortunately, as a potential LIR motif containing ATG8a interactor, dally is unlikely to be a good candidate. This is because dally is either found as a GPI anchored extracellular membrane protein or a secreted protein. This would mean dally does not have good access to the ATG8a protein LDS. Dally would be made in the ER and sent through the secretory pathway. Dally is likely an indirect accumulation of autophagy defect rather than direct ATG8a interactions.

The label free quantification of dally in ATG8a and ATG8a$^{K48A/Y49A}$ mutants compared to wild type control flies can be seen in Figure 4-14. The iLIR output for dally is also shown. The LIR motif GDYTQL has a PSSM score of 14 and was found to be in an anchor region and so a good potential LIR motif. However, as mentioned previously, dally is unlikely to be an ATG8a interactor.

A

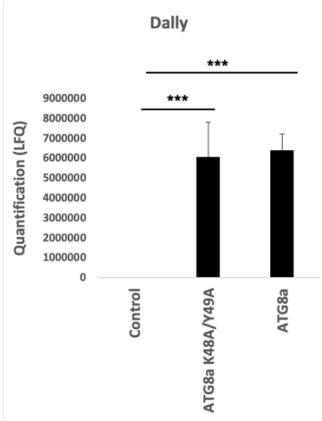


B

Query: >tr|Q53XG2|Q53XG2_DROME Division abnormally delayed, isoform B OS=Drosophila melanogaster OX=7227 GN=dally PE=1 SV=1

| Motif | Start | End | Pattern | PSSM Score | LIR in Anchor |
|---|---|---|---|---|---|
| WxxL | 12 | 17 | LLFTLL | 5 | No |
| WxxL | 18 | 23 | CGFVGL | 6 | No |
| WxxL | 74 | 79 | SYFESI | 8 | No |
| WxxL | 113 | 118 | GMFEQL | 10 | No |
| WxxL | 154 | 159 | SLFSKV | 4 | No |
| WxxL | 173 | 178 | QLYTEI | 7 | No |
| WxxL | 213 | 218 | HFFVQL | 3 | No |
| WxxL | 253 | 258 | HPFGDI | 1 | No |
| WxxL | 342 | 347 | AEYAGL | 7 | No |
| WxxL | 350 | 355 | SPWSGV | 10 | No |
| WxxL | 452 | 457 | EFYTTI | 8 | Yes |
| WxxL | 481 | 486 | GDYTQL | 14 | Yes |
| WxxL | 610 | 615 | ATWMLL | 15 | Yes |

Figure 4-14 **Dally label free quantification and predicted LIR motif**. A) Label free quantification (LFQ) of Dally in wild type control, ATG8A$^{K48A/Y49A}$ mutants, and ATG8a mutants. There is a significantly increased quantity of Dally in both autophagy mutants compared to the control. B) Predicted LIR motifs from the iLIR software. GDYTQL and ATWMLL are both predicted LIR motifs which have a PSSM score of >13 and found in an anchor region. Significance for quantification was calculated through one sample t-test, ***p<0.001, n=4.

### 4.6.2 Ras

Ras is a small G protein found upstream of the RAF-MEK-ERK signalling pathway, which is involved in development. It is involved in promoting cell division and growth as a response to epidermal growth factor (EGF) (Sriskanthadevan-Pirahas, Lee and Grewal, 2018). EGF would signal through the EGF receptor which is a receptor tyrosine kinase. Activation of this receptor leads to activation of guanine nucleotide exchange factors, replacing GDP for GTP on ras. Raf is a ras effector which is a serine/threonine protein kinase that phosphorylates MEK. MEK is also a serine/threonine kinase that phosphorylates ERK. ERK is part of the MAP-kinase family of proteins which can phosphorylate many targets such as proteins in the cytoplasm, cell membrane, nucleus and many transcription factors leading to downstream effects. These effects include growth, differentiation and cell division (Li *et al.*, 2016b).

Because of the ras protein effect on cell growth and proliferation, it is considered and oncogene and investigated extensively for it its ability to cause tumours and metastasis. Ras has been shown to promote tumorigenesis through accelerating G1/S cycle progression, causing DNA damage and inhibiting DNA damage repair (Murcia *et al.*, 2019). Ras has many other less characterised functions. For example, in *Drosophila* Ras-Ref inhibition of rho kinase (ROCK) is involved in inhibiting anaesthesia-resistant memory (ARM). This is a stable form of intermediate-term memory, which is essential for protein synthesis-dependent long-term memory (PSD-LTM) (Noyes, Walkinshaw and Davis, 2020).

Ras is a protein that is also discussed in detail in section 1.2, as it has a role in the regulation of autophagy. Both Raf/PKA and RAF/MAPK pathway have the ability to induce autophagy under nutrient depravation. This makes Ras a particularly interesting protein to study as an autophagy substrate. Upstream signalling molecules being part of the downstream degradation in the autophagosome may be indicative of self-regulated negative feedback of autophagy.

The label free quantification of Ras in ATG8a and ATG8a$^{K48A/Y49A}$ mutants compared to wild type control flies can be seen in Figure 4-15. The iLIR output for Ras

is also shown. The LIR motif NDFLIL has a PSSM score of 14 and it is found to be in an anchor region and so likely to be a functional LIR motif.

A

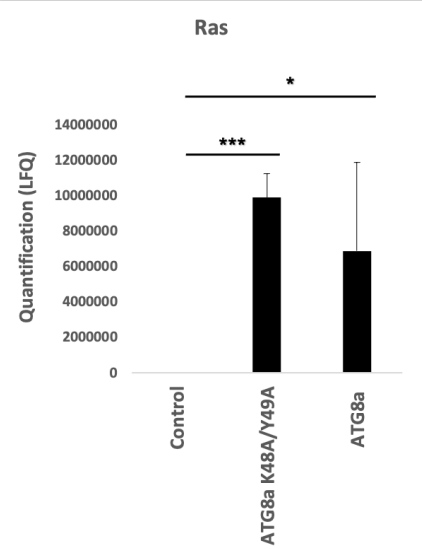


B

Query: >tr|A4V488|A4V488_DROME Inosine-5'-monophosphate dehydrogenase OS=Drosophila melanogaster OX=7227 GN=ras PE=1 SV=1

| Motif | Start | End | Pattern | PSSM Score | LIR in Anchor |
|---|---|---|---|---|---|
| xLIR | 119 | 124 | PEYQAL | 12 | No |
| WxxL | 55 | 60 | NDFLIL | 14 | Yes |
| WxxL | 311 | 316 | ETYPEL | 9 | No |

Figure 4-15 **Ras label free quantification and predicted LIR motif**. A) Label free quantification (LFQ) of Ras in wild type control, ATG8A$^{K48A/Y49A}$ mutants, and ATG8a mutants. There is a significantly increased quantity of Ras in both autophagy mutants compared to the control. B) Predicted LIR motifs from the iLIR software. NDFLIL is a predicted LIR motif which has a PSSM score of >13 and found in an anchor region. Significance for quantification was calculated through one sample t-test, *p<0.05, ***p<0.001, n=4.

### 4.6.3 GMAP

There is only one paper which describes the role of *Drosophila* GMAP titled "The cis-Golgi *Drosophila* GMAP has a role in anterograde transport and Golgi organization in vivo, similar to its mammalian ortholog in tissue culture cells" (Friggi-Grelin, Rabouille and Therond, 2006). Papers that describe the mammalian homologue of *Drosophila* GMAP called GMAP-210 exist and are discussed in the next chapter.

GMAP is a coiled-coil tethering protein found on the cis-Golgi. *Drosophila* GMAP has been shown to be involved in the anterograde transport pathway. As a tethering protein, its role is to capture vesicles coming from the ER or ERGIC to the Golgi apparatus. In *Drosophila,* the Golgi stacks are found scattered through the cytoplasm unlike mammalian Golgi where it is localised and connected through the Golgi ribbon. The *Drosophila* GMAP associates with the Golgi through a C-terminal GRAB (GRIP-related Arf-binding) domain, which interacts with Arf1 on the Golgi membrane (Sinka *et al.*, 2008). GMAP also has a role in the maintenance of Golgi morphology and stability, likely through its interaction with the cytoskeleton (Friggi-Grelin, Rabouille and Therond, 2006).

The label free quantification of GMAP in ATG8a and ATG8a$^{K48A/Y49A}$ mutants compared to wild type control flies can be seen in Figure 4-16. The iLIR output for GMAP is also shown. The LIR motif DEFIVV has a PSSM score of 14 and it is found to be in an anchor region and so it is likely to be a functional LIR motif. The LIR motif also has acidic residues upstream of the hydrophobic residues which is very promising.

A

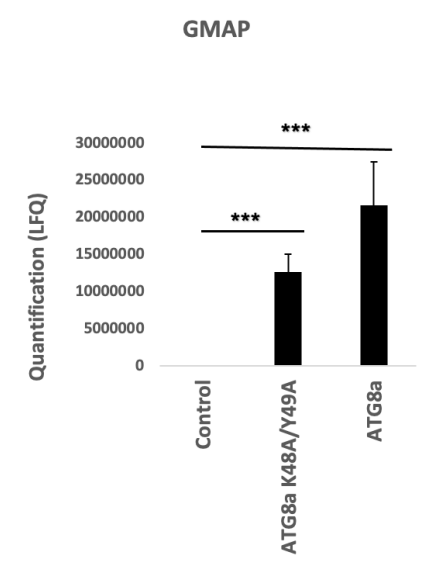


B

Query: >tr|Q9VXU2|Q9VXU2_DROME Golgi microtubule-associated protein, isoform A OS=Drosophila melanogaster OX=7227 GN=Gmap PE=1 SV=2

| Motif | Start | End | Pattern | PSSM Score | LIR in Anchor |
|---|---|---|---|---|---|
| xLIR | 320 | 325 | DEFIVV | 14 | Yes |
| WxxL | 524 | 529 | RAWNAL | 12 | No |
| WxxL | 531 | 536 | DRWHRL | 13 | No |
| WxxL | 655 | 660 | QEYLQL | 10 | Yes |
| WxxL | 948 | 953 | QYYAEI | 4 | No |

Figure 4-16 **GMAP label free quantification and predicted LIR motif**. A) Label free quantification (LFQ) of GMAP in wild type control, ATG8A$^{K48A/Y49A}$ mutants, and ATG8a mutants. There is a significantly increased quantity of GMAP in both autophagy mutants compared to the control. B) Predicted LIR motifs from the iLIR software. DEFIVV is a predicted LIR motif which has a PSSM score of >13 and found in an anchor region. Significance for quantification was calculated through one sample t-test, ***p<0.001, n=4.

## 4.7 Conclusions

Out of the 4 identified proteins from the proteomics study, GMAP was selected as the one to investigate further. GMAP has a very good predicted LIR motif, and it is a poorly studied protein. Despite this, there are many tools available for experimentation including *Drosophila* GMAP antibodies and GMAP RNAi flies which are both available commercially (listed in methods). GMAP is also of particular interest as it is part of the secretory system. There is a lot of cross play between the secretory system, the endosomal system and autophagy. GMAP is also a potential receptor for the less understood process of Golgiphagy, the selective degradation of the Golgi complex, as it is found on the surface of the Golgi. The confirmation of GMAP as a LIR motif containing substrate and determining the significance of the GMAP LIR motif-ATG8a LDS interaction is discussed in the next three chapters.

# Chapter 5 *Drosophila* GMAP is a LIR motif containing golgin.

## 5.1 Introduction

As described in the previous chapter, *Drosophila* GMAP (dGMAP) is a cis Golgi coiled coil Golgin involved in the anterograde transport in the secretory system. Before discussing the current understanding dGMAP as well as its homologues/orthologs in mammalian cells, a brief description of the role of the Golgi and the secretory system is discussed below.

## 5.2 The Golgi and the secretory system

### 5.2.1 The Golgi apparatus

The Golgi is a central player in the secretory and endosomal system. The Golgi organelle, in mammalian cells, appears as flattened sacks (cisternae) of membrane connected together to form a ribbon (Huang and Wang, 2017). This is usually around a microtubule organising centre and the structure is stabilised through tethering to microtubules. There are additional regions created either side of the Golgi called the cis/trans Golgi network (CGN/TGN) (Huang and Wang, 2017). The main function of the Golgi is to process the proteins which were synthesised in the rough endoplasmic reticulum (RER). Typically, proteins translated on the ribosome simultaneously enter the lumen of the RER. While secretory proteins enter the RER lumen, intermembrane proteins stay in the membrane of the RER through their start and stop transfer signals. These intermembrane proteins either stay in the RER or are later transferred to the plasma membrane of membranes of other organelles in the cell. Proteins made in

ribosomes which are intended to be a secreted protein must contain an N terminal ER signal sequence, which allows proteins to enter the RER (Lodish H, 2000).

In mammals, vesicles form on the RER and transport cargo to the ER to Golgi intermediary compartment (ERGIC) before being transported to the Golgi. The vesicles bud from a non-ribosome containing curved region of the RER called the ER exit sites (ERES). The ERGIC composed of a combination of vesicles and tubules but its function is not very well defined (Glick and Nakano, 2009). The Golgi itself has tubular connections which link Golgi stacks together to form a Golgi ribbon. Each region of the Golgi has a different purpose as they contain differing composition of modifying proteins. These enzymes can post-translationally modify proteins including glycosylation and phosphorylation. Many of these modifications are necessary for protein function as well as for directing them to the correct region of the cell. The cisternae themselves are held together by matrix proteins, which include a class of coiled-coil proteins called Golgins. Occasionally, there are additional regions created either side of the Golgi called the cis/trans Golgi network (CGN/TGN). The TGN is particular important as it has a role in cargo sorting, which allows proteins to move to the correct locations in the cell (Huang and Wang, 2017). The Golgi is a highly dynamic structure which has many variable features when looked at in different organisms and cells. The dynamic nature of the Golgi is most apparent during mitosis in cells, as the entire Golgi disassembles once mitosis starts and then reassembles towards the end of mitosis (Lucocq, Berger and Warren, 1989). In mammalian cells, Golgi disassembly involves the Golgi ribbon detaching, the cisternae separating and splitting into small vesicular and tubular structures which are seen throughout the cytoplasm. This is likely to make sure that the Golgi is separated equally into the two daughter cells. (Efimov *et al.*, 2007).

In *Drosophila*, as well as yeast, protozoa, plants, and *Caenorhabditis elagans*, Golgi organisation is different. Rather than a Golgi ribbon, stacks are found dispersed throughout the cytoplasm, next to different ERES. Interestingly, proteins necessary for the formation of the Golgi ribbon (GM130, Golgin 84, different GRASPS) are present in *Drosophila*. Golgi ribbons can be occasionally seen in some cells such as onion stage spermatids, but this is not the case for majority of cells. The Golgi stacks do often exist

in pairs which could be a primitive Golgi ribbon. However, unlike the mammalian Golgi ribbon, the stability of the pair is not reliant on microtubules but on actin instead. The cis-trans polarity of the *Drosophila* Golgi is still maintained and so is the presence of the trans Golgi network (TGN). There is also no ERGIC in *Drosophila*, although vesicles and tubules were identified between the two compartments. Similar to mammalian cells *Drosophila* Golgi disassembles and reassembles during mitosis (Stanley, Botas and Malhotra, 1997). The enzyme contents of the dispersed stacks are different and so likely process different proteins and may be important in the apical-basal polarity of cell membranes.

### 5.2.2 The secretory pathway

Movement through the secretory pathway is bi-directional, where there is the retrograde pathway and the anterograde pathway. The anterograde pathway is movement of proteins from the ER to Golgi, while the retrograde pathway is in reverse. Within the Golgi itself, newly synthesised proteins need to move through the Golgi whereas the Golgi proteins must remain within the Golgi (Rothman and Wieland, 1996). Coat proteins are the molecular machinery required for vesicle formation and selection of cargo and are very important in protein/lipid movement throughout the secretory and endosomal systems. Anterograde transport of cargo from the ER to Golgi is mediated by COPII (Coat protein complex 2) coated vesicles. The post-translational modification enzymes that must remain in the Golgi are transported back to the previous stack through COPI (coat protein complex 1) vesicles. However, COPI vesicles are not the only possible method of retrograde transport in the Golgi. There is evidence for tubular connections between Golgi stacks and if this is the case, it would provide a pathway for bi-directional movement between Golgi cisternae (Glick and Nakano, 2009). Any ER resident proteins in the Golgi are also transported back to the ER from the Golgi via COPI vesicles. Capturing of vesicles require various proteins like tethering proteins (TRAPP, golgins), Rab-GTPases (membrane identity markers), and SNARES. The homologue of COPI, COPII and all the aforementioned vesicle

capturing proteins are present in *Drosophila* and thus the mechanism of protein trafficking is likely conserved. Many of these proteins also have much more limited redundancy in *Drosophila* making it an excellent model to study the secretory system (Ke Yang, 2021).

When it comes to how proteins are moving through the Golgi stacks, there are two main models used to explain this movement (Connerly, 2010). The vesicular transport model, which is the lesser of the accepted models, states that the Golgi compartments are stable, and each contain distinct enzymes necessary for post-translational modification. Vesicles containing newly synthesised proteins arrive at the cis Golgi and once modified, move through each of the Golgi cisternae through budding and fusion of vesicles. The cisternal maturation model (Glick and Malhotra, 1998), which is more widely accepted amongst scientists, states that rather than the proteins moving through the cisternae, it is the enzymes which change over time. The Golgi cisternae forms on this cis side of the Golgi through the combining of vesicles, which then matures into the medial-Golgi followed by the trans-Golgi. Therefore, the individual stacks of the cisternae will contain the same newly synthesized protein, which progressively goes through series of changes and physically moves to the trans-Golgi location (Glick and Nakano, 2009). However, a problem when this model was first suggested, was the presence of many vesicles surrounding the Golgi stacks, presumably carrying the cargo forward through the stacks. It was suggested that these vesicles are actually moving backwards (retrograde transport) through the stacks carrying the Golgi enzymes to the previous cisternae (Glick and Malhotra, 1998).

From the Golgi, secreted proteins are packaged into vesicles and released by the cell through exocytosis. Budding of vesicles destined for the secretion through the plasma membrane usually happens at the trans Golgi network. These vesicles are made using a different class of carriers known as pleomorphic tubular-vesicular carriers. These vesicles tend to be varied in size and shape and lack any kind of coat protein. Different mechanisms of vesicle formation and transport have been suggested including, Arf1 positive carriers, LAMP1 positive carriers, Rab6 associated carriers, CtBP1-S/BARS (C-terminus binding protein 3/BFA adenosine diphosphate–

ribosylated substrate) positive carriers, sphingomyelin carriers, and CARTS (CARriers of the TGN to the cell Surface) (Stalder and Gershlick, 2020).

### 5.2.3 Golgins

Golgins are large coiled-coil vesicle tethering proteins found on the surface of the Golgi organelle. These proteins tend to form large rod like structures that extend far out of the Golgi in prime position to capture vesicles. Only 500 residues of coiled coil is 75 nm in length and so many golgins can reach much further out (Munro, 2011). These coiled coil regions are separated by non-coiled regions potentially to allow for flexibility. There are 11 golgins which are highly conserved and found in all eukaryotic organisms including *Drosophila*. Golgins can be found on the cis, medial and trans Golgi stacks, allowing the capture of vesicles to all Golgi compartments. These Golgins attach to the Golgi either through a transmembrane domain or through Arf/Rab family proteins (Muschalik and Munro, 2018). The vesicle tethering function of golgins were demonstrated originally through vesicle rerouting experiments. 10 conserved golgins were chosen (golgin-245, GCC185, Golgin-97, GCC88, TMF, Giantin, Golgin-84, CASP, GMAP-210 GM130), and attached to the mitochondria through fusion of the golgin with the transmembrane mitochondrial protein monoamine oxidase (MOA) (Wong and Munro, 2014). To identify which golgins capture vesicles from the endosome, the cargo cation-dependent mannose 6-phosphate receptor (CD-MPR), which traffics lysosomal hydrolases to endosomes and back to the Golgi were followed. It was found that trans-Golgi golgins, golgin-97, golgin-245 and GCC88 which all contain C-terminal GRIP domain, were involved in capturing vesicles from the endosome. For capturing newly synthesized proteins from the ER to golgi, a secreted protein was tagged with GFP and followed. The cis-Golgi golgins GM130, GMAP-210, was shown to capture vesicles from the ER. Golgin-84 and TMF were shown to be involved in the tethering of vesicles containing Golgi resident proteins, likely to be involved in recycling these proteins to earlier or later Golgi stacks. Giantin, CASP and GCC185 did not reroute any vesicles, and so either may be involved in anchoring to microtubules or may need

other golgins to carry out their tethering functions. In terms of the way in which golgins interact with vesicles it is largely unknown with a couple of exceptions. One of these is GMAP-210 which is discussed in more detail in the next section. The other is golgin-97 and golgin-245 which interacts with vesicles via an N-terminal motif which binds the vesicle adapter TBC1D23 (Shin *et al.*, 2017).

As alluded to previously, the Rab and Arf family of proteins play an important role in golgin recruitment and activity. Rab and Arf family of proteins are GTPases which along with phosphoinositide lipids are involved in membrane identity (Gillingham *et al.*, 2014). Specific Rabs are recruited to different membranes/organelles which in turn recruit other cytosolic proteins creating unique membrane protein structures. GTPases work by switching between an inactive state, where is it bound to guanosine diphosphate (GDP) and an active state, where it is bound to guanosine triphosphate (GTP). Activation is controlled by guanine nucleotide exchange factors (GEFs) and inactivation is controlled by GTPase activator proteins (GAPs). *Drosophila* contain many of the Rabs found in mammalian cells. Rab and Arf family GTPases facilitate the binding of some golgins to the golgi. Four GRIP domain containing golgins (golgin-97, golgin-245 and GCC88, GCC185) interact with the Golgi through Arl1 (Arf-like GTPase). TMF interacts with the Golgi through Rab6. Golgin-160 (no ortholog in *Drosophila*) and GMAP-210 interact with the Golgi through Arf1. There are also many Rab binding sites along the lengths of Golgi which no doubt has a role in golgin tethering function. Many of these Rab-golgin interactions have been identified.

The cis-Golgi golgin GMAP-210 is discussed in more detail in the next section. The other conserved cis-Golgi golgin is GM130 which interacts with Rab1, Rab30, and Rab33b. GM130 does not seem to be essential for protein trafficking and has redundant functions with other golgins. However, GM130 has been associated with a multitude of cellular functions such as: cell cycle progression, cell polarity and cell migration (Nakamura, 2010). Its binding partners include, the p115 tethering protein, GRASP65 (Golgi reassembly stacking protein) and giantin. Conserved medial Golgi golgins include: Giantin, Golgin-84 and CASP. These are all attached to the Golgi via their C-terminal transmembrane domain (Munro, 2011). The golgins are also found

on COPI vesicles and so involved in the retrograde transport in the golgi. Giantin is the largest golgin and not found in invertebrates like *Drosophila*, but the fruit fly does have another large, coiled coil protein called Lava Lamp. Giantin has been shown to interact with Rab1 and Rab6. Golgin-84 is a Rab1 GTPase binding golgin, which is found in *Drosophila* (Satoh *et al.*, 2003). CASP is another golgin not found in *Drosophila* and its function as well as Golgin-84 not very well understood. Knockdowns of these golgins suggest they have a role in Golgi structure and organisation but that is true for many golgins. Conserved trans-Golgi golgins include: golgin-245, GCC185, Golgin-97, and GCC88. As mentioned before, these are GRIP domain containing golgins that bind to the Golgi through Arf1. These interact with various Rabs such as Rab2, Rab6 and Rab30.

Investigating the function of individual golgins can be quite difficult. Many golgins interact with the same rabs and so potentially have many redundant functions. It is likely that the role of golgins is to create a network of tethering proteins around the golgi, which bring vesicles closer to the golgi, so more specific interactions can take place. Therefore, knocking down golgins tends to have very mild phenotypes and most of the time these phenotypes are tissue specific. For example, knocking down TMF in mice affects spermatogenesis, yet TMF is expressed in every cell (Muschalik and Munro, 2018). Most of the time when golgins are knocked down it causes Golgi fragmentation, since most golgins have some role in Golgi organisation and structure, and glycosylation defects. The exact mechanism of tethering and vesicle fusion is still under debate. Golgins are very long molecules so once captured, the distance between the vesicle and the Golgi needs to be reduced. The fact that golgins can bind multiple rabs could mean that golgins bend and interact with Golgi membrane rabs, bringing vesicles closer to the golgi. This is a possibility as many of the coiled-coil regions of golgins are spaced with more flexible regions. Another possibility is that vesicles may hop between different binding sites and potentially onto different golgins/tethering proteins bringing it closer to the golgi.

There are also other coiled-coil proteins found on the golgi, such as the vesicle tethering protein p115 and the dynein adapter Bicaudal-1/2. SCOCO (short coiled-coil protein) and golgin-45 also have short coiled-coil regions, but their functions are

unknown. SNAREs also all fall into this category of coiled-coil containing Golgi proteins (Munro, 2011). Other than golgins there are tethering proteins which are multi-unit complexes such as golgi-associated retrograde transport protein (GARP), conserved oligomeric Golgi (COG), and transport protein particle (TRAPP) (Muschalik and Munro, 2018). These are all also found in *Drosophila*. GARP is found on the trans-Golgi and captures vesicles from the endosome, COG is found in the cis-medial Golgi and involved in Golgi protein recycling, and TRAPP is found on the cis Golgi involved in ER to Golgi transport. However, these tethering proteins are much shorter than golgins and are likely involved in an intermediate step between golgin tethering and SNARE fusion.

### 5.2.4 GMAP-210 the mammalian ortholog of dGMAP

GMAP-210 is a GRAB domain containing protein which interacts with the Golgi through Arf1 GTPase. For most golgins the method of binding to vesicles is not well understood, but this is not the case for human GMAP-210. Human GMAP-210 has an N-terminal amphipathic lipid-packing sensor (ALPS) motif which can bind highly curved membranes. However, this motif is not well conserved and not seen in invertebrate GMAP such as *Drosophila* GMAP (Munro, 2011). This suggests that there are yet undiscovered methods of tethering vesicles.

In one study, knockdown of GMAP-210 seems to cause Golgi fragmentation, suggesting a structural role of GMAP-210 in Golgi organisation. Secretory protein trafficking seemed unaffected. However, overexpression of GMAP-210 caused inhibition of the secretory pathway. This is likely due to sequestering of important binding partners such as Rabs and Arf GTPases (Pernet-Gallay *et al.*, 2002). This was also shown to be true for dGMAP (Friggi-Grelin, Rabouille and Therond, 2006), which conflicts with previous studies that show GMAP-210 is required for membrane trafficking (Roboti, Sato and Lowe, 2015). Roboti et.al., showed that GMAP-210 is necessary for efficient anterograde and retrograde trafficking, acting on both the Golgi and the ERGIC. GMAP-210 also shares some redundancy in this function with

the golgin GM130, where the difference is that GM130 is only involved in anterograde trafficking.

GMAP-210 has been shown to interact with IFT20 which is part of the intra-flagellar transport particle. This protein is involved in the formation of the primary cilium, an organelle that has a role in monitoring the extracellular environment. GMAP-210 appears to localise IFT20 to the Golgi and potentially has a role in sorting proteins trafficked to the cilia. Knockdown and mutations in GMAP-210 is also implicated in some bone related diseases (Wehrle *et al.*, 2019). Mutations in GMAP-210 are implicated in impaired skeleton development (Smits *et al.*, 2010). Knockdowns in mice tend to specifically affect chondrocytes and their ability to secrete the extracellular matrix protein Perlecan. This indicates that in chondrocytes GMAP-210 does have some specificity towards certain cargo. Whether that is true for all golgins or all cells has not been ascertained. It is debateable why some golgins like GMAP-210, which are expressed in every cell, would only affect a specific subset of cells.

GMAP-210 is also able to bind to the minus end of microtubules through its C-terminus. Therefore, GMAP-210 likely forms a contact point between the cis-Golgi and microtubules extending from the centrosome, which is important for Golgi structure maintenance. GMAP-210 also recruits γ-tubulin complexes to the golgi, thus it is likely involved in localisation of Golgi near the centrosome as well as any mitotic events that the Golgi will take part in (Rios *et al.*, 2004).

There is only one published study of dGMAP which is discussed in the previous chapter, and so we aim to investigate further functions of this protein in *Drosophila*.

## 5.3 The dGMAP LIR motif

As described in Figure 4-16, dGMAP has a very good predicted LIR motif near its N-terminus. The predicted LIR motif is DEFIVV and located between amino acid 320 and 325 which is found in an anchor region. A schematic showing the major domains (coiled-coil domains and GRAB domain) and the location of the predicted LIR motif is

shown in Figure 5-1. There is also a region labelled “GMAP 1” which is a truncated form of dGMAP created for use in certain experiments. The next main objective is to prove that this LIR motif is functional. This means that the motif is responsible for its direct interaction with the *Drosophila* ATG8a protein. However, before this, the accumulation of GMAP in autophagy deficient flies must first be confirmed. Overabundance of dGMAP in ATG8a$^{K48A/Y49A}$ mutant flies would provide supporting evidence to the proteomics experiment.

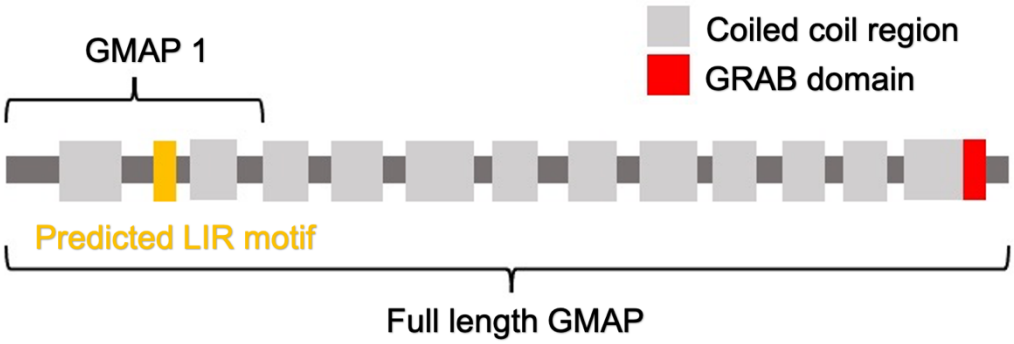


Figure 5-1 **Key domains in dGMAP.** Full length dGMAP is 1398 amino acids long with a N-terminal GRAB domain which interacts with Arf1, anchoring dGMAP to the cis-golgi. It contains 12 coiled-coil domains and a predicted LIR motif close to the N terminal (aa 320-325). GMAP1 is also labelled as this is the truncated for of dGMAP used for GST-pulldown experiments, this truncated form of dGMAP contains the predicted LIR motif (DEFIVV).

## 5.4 Accumulation of dGMAP in ATG8a and ATG8a$^{K48A/Y49A}$ mutant flies

The accumulation of dGMAP in ATG8a and ATG8a$^{K48A/Y49A}$ mutant flies compared to wild type controls was confirmed through both western blotting and immunofluorescence. There is a commercial dGMAP antibody available through hybridoma bank, however this antibody only seemed effective in immunofluorescence experiments. For western blotting, dGMAP antibody was given

as a gift from Dr Pasacal Therond an author from the paper "The cis-Golgi *Drosophila* GMAP has a role in anterograde transport and Golgi organization in vivo, similar to its mammalian ortholog in tissue culture cells.". Figure 5-2 is a western blot analysis which shows significantly increased levels of dGMAP in both autophagy mutant flies compared to wild type control flies.

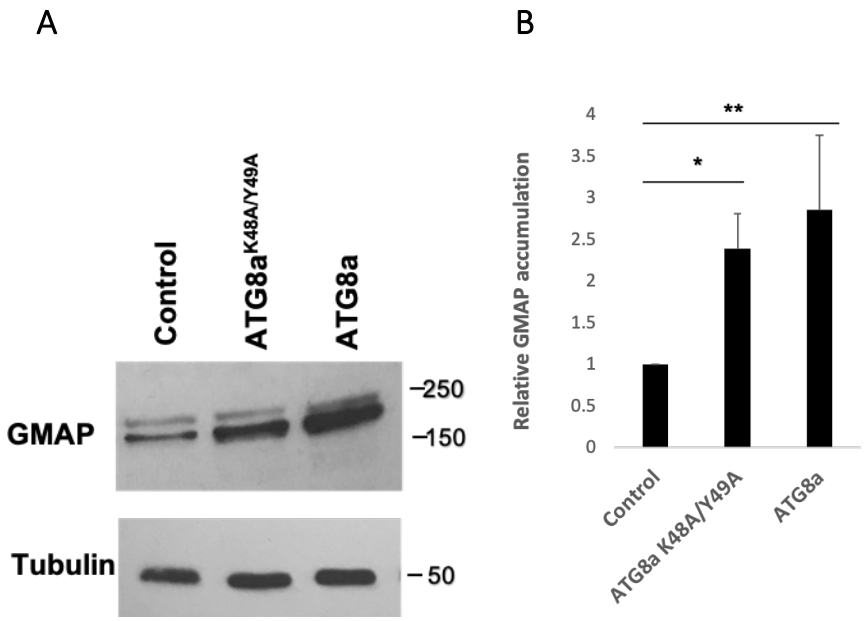


Figure 5-2 **GMAP accumulation in ATG8a$^{K48A/Y49A}$ and ATG8a mutant flies.** A) western blot showing increased levels of dGMAP in both autophagy mutant flies with a greater level of accumulation in ATG8a mutant flies. Tubulin was used as a loading control B) Quantification of western blot relative to control flies showing dGMAP accumulation in autophagy mutant flies are significant. Significance of quantification was done using a one sample t-test, error bars show + SDs. *p<0.05, **p<0.01, n=3.

Immunofluorescence was also used to see the accumulation of dGMAP in aged ATG8a and ATG8a$^{K48A/Y49A}$. Brain tissue for wild type, ATG8a and ATG8a$^{K48A/Y49A}$ mutant flies, as well as the larval fat body of wild type and ATG8a mutant flies, was stained for dGMAP and ubiquitinated proteins. ATG8a$^{K48A/Y49A}$ larval tissue could not be investigated as the homozygous marker can only be seen in adult flies.

Figure 5-3 shows brain tissue stained with dGMAP as well as ubiquitin. In wild type flies, dGMAP puncta can be seen which is likely staining the golgi. As described previously, the Golgi in *Drosophila* is fragmented and spread throughout the cell and dGMAP is a cis-Golgi marker. Multiple puncta can be seen around the nuclei in wild type cells. In ATG8a$^{K48A/Y49A}$ mutant flies, the dGMAP puncta staining is much brighter and larger in size. A similar phenotype is also seen in ATG8a mutant flies. Some of these dGMAP puncta co-localise with ubiquitin and so are likely part of the protein aggregates seen in these flies. The size of dGMAP puncta were also measured, and on average, the dGMAP puncta size was large in both autophagy mutant flies compared to the wild type flies.

A

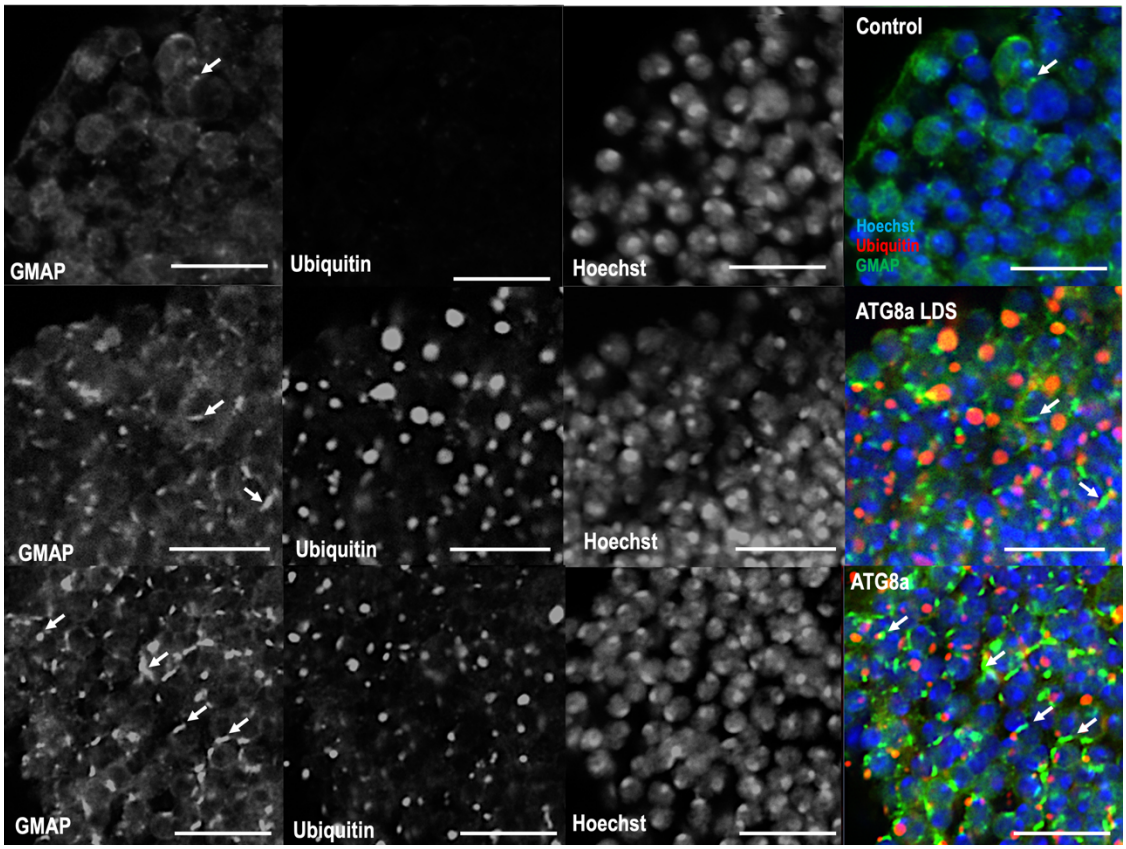


B

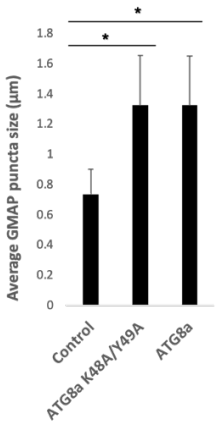


Figure 5-3 **Accumulation of dGMAP in 2-week-old ATG8a$^{K48A/Y49A}$ and ATG8a mutant fly brains.** A) dGMAP puncta (green) can be seen in control flies representing the golgi. In both autophagy mutant flies dGMAP puncta are much larger and brighter and sometimes elongated (white arrows). Some of these dGMAP puncta are part of the ubiquitin (red) positive aggregates but many are not. DNA is stained with Hoechst (blue), scale bars are 10 µm. B) Graph showing average dGMAP puncta size in wild type, ATG8a$^{K48A/Y49A}$ mutant and ATG8a mutant. Statistical significance of dGMAP size was calculated using one sample t-test. *p<0.05.

Figure 5-4 shows dGMAP and ubiquitinated protein staining in wild type and ATG8a mutant larval fat body. Again, dGMAP puncta can be seen in wild type larvae but these puncta appear brighter and more numerous in ATG8a mutant larvae. Some of these puncta also co-localise with the ubiquitin positive aggregates.

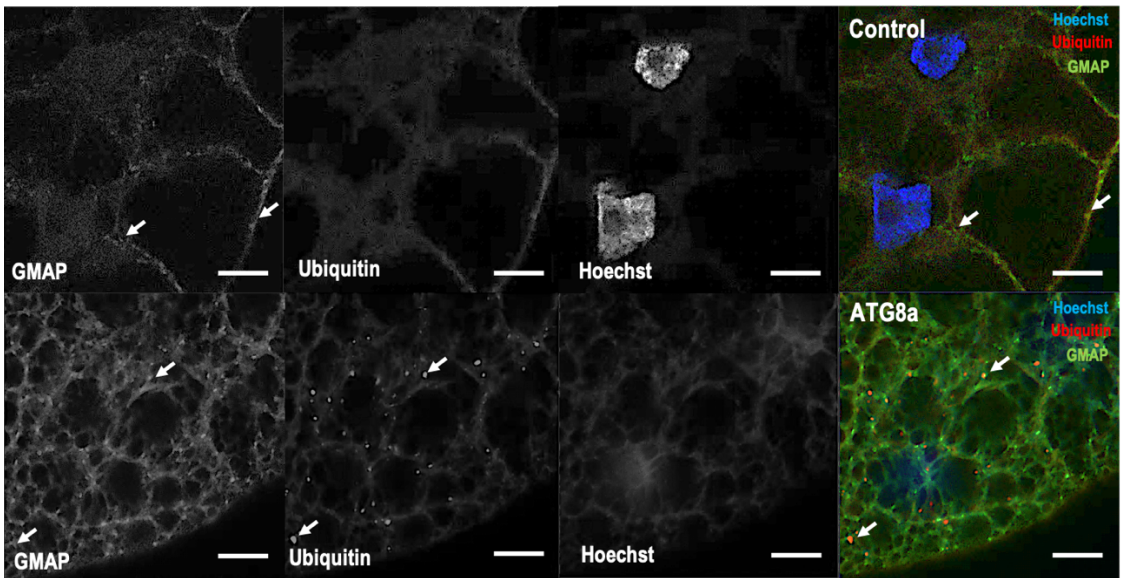


Figure 5-4 **Accumulation of dGMAP in ATG8a mutant larval fat body.** dGMAP puncta (green) are seen in both controls and ATG8a mutant fat body. However, the dGMAP puncta in ATG8a mutant larvae are larger and much brighter. Many of these puncta also co-localise with ubiquitin positive aggregates. Scale bars are 10 µm.

Together these results show that the dGMAP is overabundant in ATG8a$^{K48A/Y49A}$ and ATG8a mutants compared to wild type. This suggests that dGMAP may be degraded through autophagy, specifically through the LIR motif-LDS interaction. The next objective is to determine whether the predicted LIR motif in dGMAP is functional or not.

## 5.5 dGMAP has a functional LIR motif (DEFIVV)

The interaction between dGMAP and ATG8a was tested in-vitro using GST-pulldown experiments. A truncated form of dGMAP (referred to a GMAP 1) was cloned into a pET28 plasmid and expressed in Rosetta$^{TM}$ 2(DE3) cells. A truncated form of the protein was used as the full-length protein is too large (1398 aa) to effectively express in bacterial cells. This truncated form of dGMAP contained the first 490 amino acids and included the predicted LIR motif site DEFIVV. GMAP 1 was used as a prey protein and captured using GST-ATG8a bait proteins. GST-ATG8a with LDS mutations was also tested. This ATG8a had the same K48A/Y49A mutation in the hydrophobic binding pockets of the LIR motif binding site. Figure 5-5 shows the results of the GST pulldown experiment.

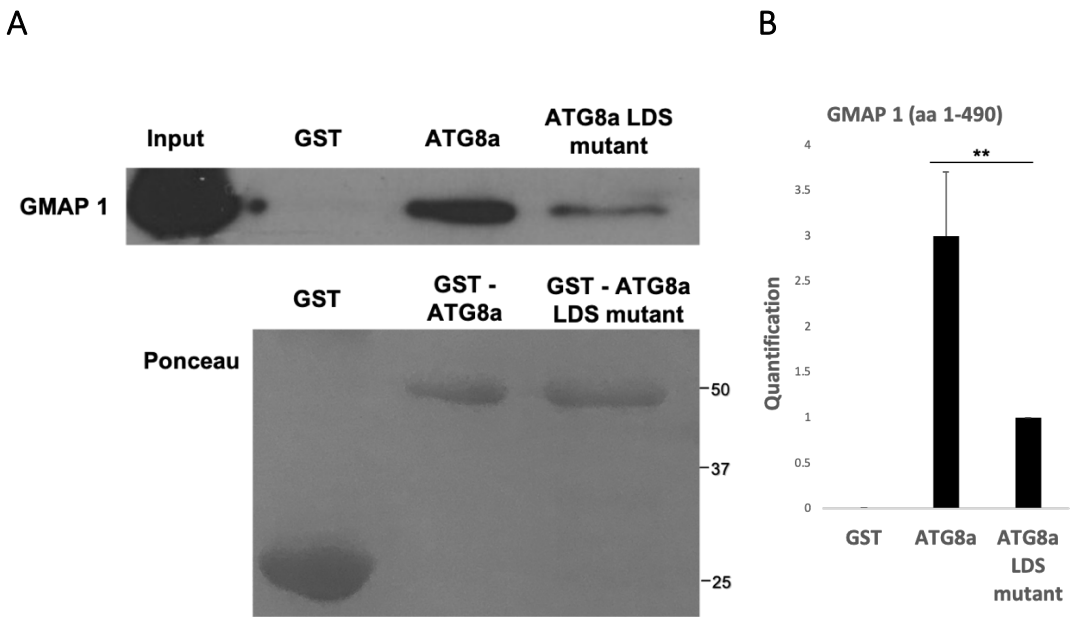


Figure 5-5 **dGMAP interacts with ATG8a through its LIR motif.** GST pulldown assay was done using the bait proteins GST tagged ATG8a and GST tagged ATG8a$^{K48A/Y49A}$ with GST alone used as control. A) GMAP1 (truncated dGMAP aa 1-490) which contains the predicted LIR motif (DEFIVV) was used as the prey protein. dGMAP can interact with ATG8a and this interaction is greatly reduced with the ATG8a LDS mutant bait protein. B) Quantification of the GMAP1 GST pulldown assay. Quantification of GMAP1 and ATG8a LDS mutant was relative to wild type ATG8a and normalised with the ponceau stain. There was a significant reduction in binding of GMAP1 to ATG8a-LDS mutant compared to wild type ATG8a. Statistical significance was determined using one sample t-test. **p<0.01, n=3.

There is a clear interaction with dGMAP1 and ATG8a. This interaction was significantly reduced for dGMAP1 in the ATG8a-LDS mutant pulldown suggesting an LDS dependent interaction. Since there was a reduction of interaction between dGMAP1 and ATG8a-LDS mutants, the predicted LIR motif was investigated next. The LIR motif of dGMAP 1 was mutated. The predicted LIR motif DEFIVV at position 320-325 was mutated to DEAIVA. The amino acid phenylalanine and valine are the two most important amino acids which position themselves in the hydrophobic binding pockets of the LDS. The mutated LIR motif should prevent the interaction between the LIR motif and ATG8a-LDS. The dGMAP$^{F322A/V325A}$ mutant was then tested for its interaction with ATG8a. This pull down is shown in Figure 5-6.

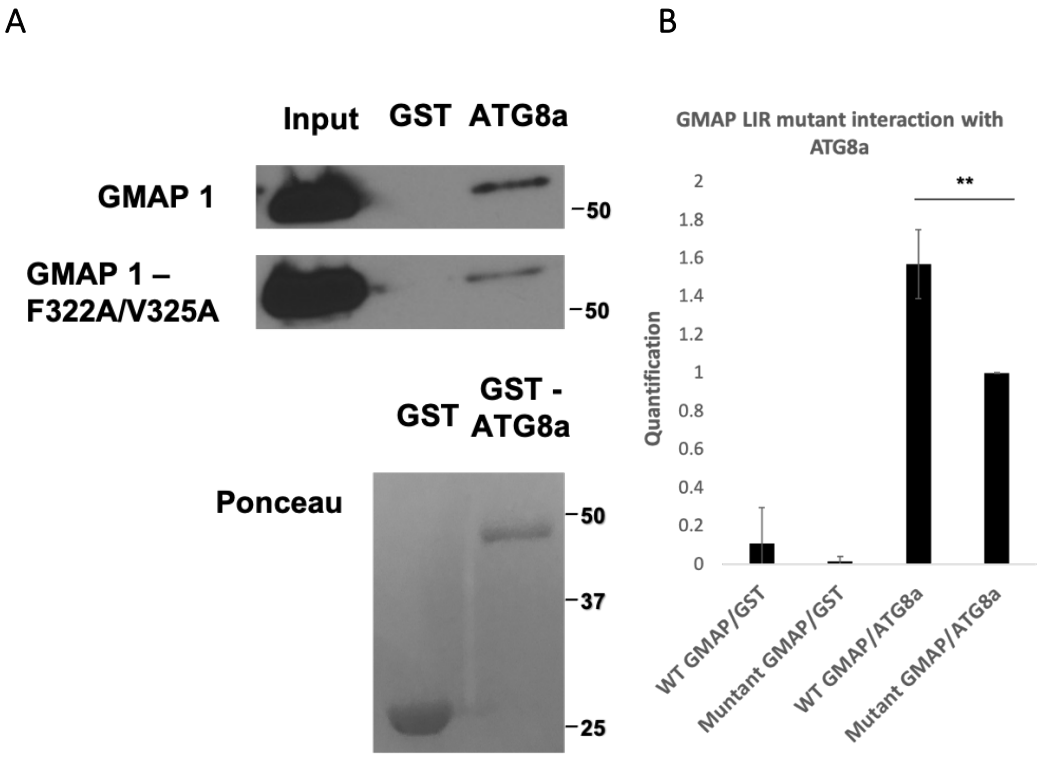


Figure 5-6 **DEFIVV at position 320-325 is a functional LIR motif of dGMAP.** A) GST pulldown assay was done using the bait proteins GST- ATG8a and GST (control). GMAP1 and GMAP1 LIR mutant (F322A/V325A) was used as a bait. As with before GMAP1 interacts with wild type ATG8a. This interaction is reduced when the LIR motif of dGMAP is mutated (dGMAP F322A/V325A). B) Quantification of GST pulldown with GMAP1$^{F322A/V325A}$ and ATG8a was relative to wild type dGMAP and normalised to the ponceau stain. Statistical significance was determined using one sample t-test. **p<0.01, n=3.

It is known that even if the LIR motif is mutated, the interaction between the LIR motif containing protein and ATG8a is not completely abolished (Tusco *et al.*, 2017). dGMAP$^{F322A/V325A}$ had a significantly reduced interaction with ATG8a compared to GMAP1. This indicates that dGMAP is an ATG8a interacting protein which specifically interacts through its LIR motif (DEFIVV).

## 5.5 Conclusions

Since we know dGMAP is a LIR motif containing protein, we next aim to further investigate the significance of the dGMAP LIR to ATG8a-LDS interaction. As dGMAP was identified as a novel ATG8a interacting protein, there are two main lines of investigation when trying to determine the functionality of this interaction. The first is to investigate dGMAP as an autophagy receptor/adapter. Since dGMAP is a cis-Golgi resident protein, it is natural to hypothesise that dGMAP may be involved with the selective degradation of the Golgi organelle (golgiphagy). The second is to investigate whether dGMAP may have a role in the autophagic process itself. It also cannot be disregarded that dGMAP turnover may simply be regulated through basal autophagy.

# Chapter 6 dGMAP is a golgiphagy receptor

## 6.1 Introduction

Selective autophagy receptors exist for many organelles such as mitochondria (mitophagy), peroxisomes (pexophagy), lysosomes (lysophagy), nucleus (nucleophagy), and endoplasmic reticulum (reticulophagy). However, the selective degradation of the Golgi apparatus (golgiphagy) is a field that is very understudied. An overview of our current knowledge on the selective degradation of organelles and the associated receptors/adapters are discussed below.

### 6.1.1 Mitophagy

Mitophagy is the selective degradation of mitochondria. There are several mitophagy receptors that are responsible for this including ATG32 in yeast, NIX3-like protein (NIX)/BNIP3 and FUNDC1 in mammals. Additionally, mitophagy in metazoan cells is partly controlled by Parkin and PTEN-induced putative kinase protein 1 (PINK1) which are known to be involved in Parkinson's disease (Youle and Narendra, 2011).

In yeast, the genes essential for mitophagy are AUP1, Uth1 and ATG32. AUP1 is a mitochondrial protein phosphatase and Uth1 is a SUN family protein. Although the function of AUP1 and Uth1 in relation to mitophagy are not yet known, ATG32 was identified as a specific mitophagy receptor (Kanki *et al.*, 2009). ATG32 is a 60kDa transmembrane protein found spanning the outer mitochondrial membrane. Its C-terminus is in the intermembrane space and majority of the protein is on the cytosolic side. Once mitophagy has been triggered, ATG32 binds to the adapter protein ATG11 and together they are able to recruit mitochondria to the autophagosome through interaction with ATG8 (Okamoto, Kondo-Okamoto and Ohsumi, 2009). Interestingly,

ATG32 also contains a LIR motif and so can interact with ATG8 both directly and through ATG11.

There is no homologue of ATG32 in mammalian cells, instead a mitophagy receptor called NIX/BINP3L in involved in the selective degradation of mitochondria. NIX is also an outer mitochondrial membrane protein, the cytosolic part of which contains a LIR motif. This provides a method of interacting with the LDS on the LC3/GABARAP protein, of the growing phagophore membrane. Mitophagy also requires the action of the proteins Parkin and PINK1 (Wei, Liu and Chen, 2015). Under normal conditions, PINK1 is transported into the mitochondria where it is subject to degradation. However, when mitochondria are damaged, indicated by a disruption in the mitochondrial membrane potential, PINK1 is stabilised on the surface of the mitochondria. In doing so, PINK1 acts as a marker for damaged mitochondria. Once stabilised, PINK1 is activated through post-translational modification, which in turn phosphorylates and activates Parkin. Parkin has E3-ubiquitin ligase activity and proceeds to ubiquitinate many outer mitochondrial membrane proteins (Jin and Youle, 2012). It is these ubiquitinated proteins that attract selective autophagy receptors such as those already mentioned (p62 and Optineurin). The exact interactions of p62 and Optineurin in the PINK1/Parkin pathway still needs to be studied further (Okatsu *et al.*, 2010; Wong and Holzbaur, 2014). PINK1/Parkin dependent mitophagy also takes place in *Drosophila* where Parkin null mutants had drastically reduced turnover of mitochondria compared to wild type flies (Vincow *et al.*, 2013).

In mammalian cells, the FUN14 domain containing protein 1 (FUNDC1) is another mitophagy receptor that is found on the outer mitochondrial membrane (Liu *et al.*, 2012). FUNDC1 is a transmembrane protein that has a LIR motif on its cytosolic side allowing it to interact with the LDS of LC3. FUNDC1 is a receptor that is specifically involved in hypoxia induced mitophagy and plays a much less significant role in starvation induced mitophagy (Wei, Liu and Chen, 2015). Meaning that under hypoxic conditions, there needs to be a control mechanism to activate FUNDC1. This is carried out through a kinase called SRC kinase. Under normal conditions, SRC kinase would phosphorylate the LIR motif of FUNDC1 which inhibits FUNDC1 interaction with LC3.

Under hypoxic conditions, SRC kinase is inactivated by dephosphorylation by an unknown phosphatase, and its inhibitory effects are reversed (J.Klionsky, 2014).

### 6.1.2 Pexophagy

Pexophagy is the autophagic degradation of peroxisomes. Peroxisomes are small organelles involved in the oxidation of fatty acids, synthesis of bile salts, and reduction of reactive oxygen species arising from hydrogen peroxide. Much of what is known about pexophagy was discovered in yeast, *Pichia pastoris*. Pexophagy is triggered upon change of nutrient conditions for example going from methanol to glucose. Two identified pexophagy receptors in yeast are ATG30 and ATG36. They interact with peroxin proteins found on the surface of peroxisomes such as pex3, pex5, and pex14. They can target peroxisomes to the autophagosome through interacting with ATG8 through its AIM and other ATG proteins (ATG11, ATG17). Peroxisome fission proteins have also been shown to be involved in pexophagy. It seems that damaged proteins are concentrated in certain parts of the peroxisome and pinched off before targeting to the autophagosome. Although there is no ATG30/36 in mammals, p62 and NBR1 has been shown to interact with ubiquitinated peroxisomes (through their UBA and JUBA domains respectively). These receptors contain LIR motifs which can interact with LC3 (Germain and Kim, 2020).

### 6.1.3 Lysophagy

As well as being part of the final stages of autophagy, the lysosomes themselves are turned over by autophagy. Lysosomes are acidic organelles that contain hydrolytic enzymes for digestion of cellular material. Thus far, lysophagy seems to be a galectin 3, p62, and ubiquitin dependent process. TAX1BP1 and other autophagy adapters were also found on damaged lysosomal membranes and may be involved. Different membrane damaging agents seem to recruit different autophagy

adapters. For example, salmonella induced damage leads to recruitment of the autophagy receptor NDP52 (Papadopoulos, Kravic and Meyer, 2020).

### 6.1.4 Nucleophagy

The nucleus contains all the genetic material of the cell and it would be detrimental to the cell if the nucleus is degraded through autophagy. Usually, there is only partial degradation through piecemeal micronucleophagy (PMN). However, in some fungal species like *Aspergillus oryzae,* macroautophagy of the whole nucleus does take place. It allows the release of nutrients which can be used for mycelial growth (Shoji *et al.*, 2010). In yeast, a nucleophagy receptor was identified, ATG39, although this protein is not present in higher eukaryotes (Mochida *et al.*, 2015). Here, nucleophagy is essential to rescue cells from nitrogen starvation. Plenty of evidence for nucleophagy taking place in mammalian cells have been described, however, as of yet, no selective autophagy receptor has been identified (Anding and Baehrecke, 2017). There is some evidence to suggest nucleophagy does occur such as the apparent degradation of the nuclei in fragmented nurse cells (Nezis *et al.*, 2010).

### 6.1.5 ER-Phagy (Reticulophagy)

When the endoplasmic reticulum (ER) is under stress, for example through a build-up of misfolded proteins, part of the response is the partial degradation of the ER through autophagy. This process is either described as ER-phagy or reticulophagy. In yeast, ATG39 (also involved in nucleophagy) and ATG40 are selective reticulophagy receptors which can interact with ATG8 through their AIM (Mochida *et al.*, 2015). Interestingly, these receptors are localised to different regions of the ER and are involved in the selective degradation of their respective region. ATG39 is localised to the perinuclear ER and ATG40 is found in the cortical ER.

The mammalian ATG40 protein is called FAM134B (family with sequence similarity 134 member B). FAM134B is an ER-phagy adapter protein containing a functional LIR motif. Since overexpression of this protein leads to fragmentation of the ER followed by degradation, it was proposed that this receptor could be involved in the pinching off the ER and then targeting to the autophagosome through its LIR motif (Khaminets *et al.*, 2015). It was shown that the GTPase family atlastins (ATL) may be involved in the FAM134B dependent fragmentation of the ER. Although ATL proteins may work downstream of FAM134B, recently ATL3 has been described as an autophagy receptor itself. ATL3 is a GTPase which contain two GABARAP-interacting motifs (GIMs) which specifically binds to the GABARAP subfamily of autophagy proteins (Chen, Teng and Chen, 2019). Other ER-phagy receptors include SEC62, RTN3, CCPG1, ATL3, EPR1, TEX264 and CALCOCO1 (described in golgiphagy section).

SEC62 is a LIR motif containing protein that is part of the translocon complex and is involved in ER-phagy after the unfolded protein response to clear excess ER (Fumagalli *et al.*, 2016).

Of all the isoforms of RTN3 (reticulon 3), the longest full-length isoform contains 6 LIR motifs which allows interaction with LC3/GABARAP. It is also able to oligomerise which enables ER fragmentation and is a response to starvation (Grumati *et al.*, 2017).

CCPG1 (cell cycle progression 1) is an ER-phagy receptor which responds to accumulation of misfolded and aggregated proteins in the ER. As it is a transmembrane receptor with its C-terminus in the ER lumen it could potentially directly recognise these aggregated proteins. It also contains a functional LIR motif and FIP200 interacting domain which together can target the ER to autophagosomes (Smith *et al.*, 2018).

TEX264 (testis expressed gene 264) is an ER resident transmembrane protein with a C-terminal cytosolic LIR motif (Chino *et al.*, 2019; An *et al.*, 2019). What is interesting about this receptor is that when multiple ER-phagy receptors were knocked down (FAM134B, CCPG1, RTN3 and Sec62), ER-phagy could still occur to a

significant level. However, when TEX264 was also knocked down, it significantly reduced ER-phagy, suggesting that TEX264 is a major player in ER-phagy.

EPR1 is a soluble ER-phagy receptor, identified in *Schizosaccharomyces pombe.* It can interact with ATG8 through its AIM and to the ER via the VAP (vesicle-associated membrane protein-associated protein) proteins Scs2 and Scs22. VAP proteins interact with proteins such as EPR1 which contain an FFAT (acid tract) motif. EPR1 appears to be dependent on the Ire1 UPR regulator and is upregulated in response to ER stress (Zhao and Du, 2020).

## 6.2 Golgiphagy

The selective degradation of the Golgi (golgiphagy) is something that is not very well understood. Currently, there are only two papers discussing golgiphagy and the receptors which could mediate this process are suggested.

### 6.2.1 The Golgi is degraded through autophagy and GOLPH3 is a potential autophagy receptor

For a long time, it was unclear whether the Golgi was degraded through autophagy. There is a need for the removal of damaged Golgi which can lead to many diseases such as neurodegeneration and cancer. The process of golgiphagy was confirmed by Lu et al., in 2020 in their paper titled: "Regulation of the Golgi apparatus via GOLPH3-mediated new selective autophagy" (Lu *et al.*, 2020). This study was done on mammalian cells (H9c2 cells, HUVECs, HA-VSMCs, and HEK293T cells). Lu et al., showed that under starvation conditions, there was co-localisation between the cis and trans Golgi markers, GM130/TGN46, and LC3B positive autophagosomes. The sequestration of Golgi in autophagosomes was confirmed using electron microscopy.

The study also proposes Golgi phosphoprotein 3 (GOLPH3) as a potential golgiphagy receptor.

GOLPH3 is a membrane protein found in the trans-Golgi and is involved in a variety of Golgi related processes. These processes include maintenance of Golgi structure, vesicle trafficking, and promoting Golgi budding. This protein is also considered oncogenic and investigated for many cancers such as gliomas (Wu *et al.*, 2018), lung adenocarcinoma (Zhao *et al.*, 2020) and nasopharyngeal carcinoma (Wang, Wang and Deng, 2020).

GOLPH3 can bind both LC3B and the Golgi membrane, making it a good candidate as a golgiphagy receptor. The study showed that knockdown of GOLPH3 decreased the co-localisation of cis and trans Golgi markers to LC3B positive autophagosomes. However, the specific interaction between GOLPH3 and LC3B and whether it was LIR motif dependent was not explored.

Nonetheless, this study did confirm that the Golgi is indeed degraded through autophagy and this process may be receptor mediated.

### 6.2.2 The reticulophagy receptor CALCOCO1 is also a golgiphagy receptor

A recent paper (June 2021), by Nthiga et al., showed that a previously discovered ER-phagy receptor also is a golgiphagy receptor (Nthiga *et al.*, 2020; Nthiga *et al.*, 2021). Previously, this group has showed that CALCOCO1 is able to degrade endoplasmic reticulum through interacting with ER localised VAP proteins. This interaction takes place through an FFAT (acid tract) motif on CALCOCO1. CALCOCO1 can interact with ATG8 through both its LIR motif and its UIM motif which occurs concomitantly. However, they also noticed that upon depletion of CALCOCO1, Golgi size as well as the quantity of Golgi associated proteins increased. This suggests that COLCOCO1 may be responsible for Golgi turnover and regulation of Golgi size.

Nthiga et al., showed that CALCOCO1 can interact with ZDHHC17/13 through its ZDHH-AR-binding motif (zDABM). ZDHHC17/13 is a Golgi transmembrane palmitoyl

transferase. CALCOCO1 dependent degradation of the Golgi seemed dependent on its interaction with ZDHHC17. Under normal conditions, CALCOCO1 would be anchored to the Golgi via ZDHHC17 and only when starvation in induced and the Golgi is fragmented, would it recruit ATG8 and start the autophagosome formation.

Under starvation conditions, CALCOCO1 would recruit and co-localise with some of the Golgi fragments to the autophagosome. This process was dependent on the LIR and UIM motif of CALCOCO1. This study also showed accumulation of Golgi resident protein under autophagy deficient conditions, indicating the degradation of these proteins via autophagy. This was supported by previous experiments showing that LIR motif and UIM motif double mutants interfered with Golgi protein (GM130/TMEM165) turnover.

Although it is clear that CALCOCO1 is involved in the degradation of the golgi, it does not account for all Golgi degradation in the cell. Therefore, there are potentially many more golgiphagy receptors yet to be identified.

## 6.3 dGMAP is involved in the turnover of the Golgi apparatus

Here experiments are highlighted which suggest that dGMAP is a novel golgiphagy receptor involved in the turnover of the Golgi organelle in *Drosophila*.

### 6.3.1 There is an accumulation of Golgi marker GM130 in autophagy deficient flies

To prove that dGMAP is indeed a golgiphagy receptor, the first objective is to show that there is more Golgi in autophagy deficient flies. To do this, two common Golgi markers were used. Antibodies for GM130 which is a cis-Golgi marker and

Syntaxin 16 which is a trans-Golgi marker were used. Syntaxin 16 is a commonly used trans-Golgi marker (Chen, Gan and Tang, 2010). It is a SNARE protein involved in membrane fusion activities, of which there is a homologue found in *Drosophila* (Xu, Boulianne and Trimble, 2002). GM130 is discussed earlier and is a cis Golgi golgin and a very useful marker of the cis golgi.

An accumulation of these Golgi markers will show that there is an increase in Golgi size and/or Golgi number. Figure 6-1 shows a western blot of GM130 and Syntaxin 16 in two-week-old wild type flies compared to ATG8a and ATG8a$^{K48A/Y49A}$ mutants. The cis-Golgi marker GM130 significantly accumulated in both mutant flies. This could suggest that there is an increased amount of Golgi in autophagy mutant flies. However, the trans Golgi marker Syntaxin 16 did not show any significant amount of accumulation. This means that it is specifically the cis Golgi which is increasing in size. If the hypothesis of dGMAP, a cis Golgi protein, being a golgiphagy receptor is true, then it makes sense that the cis-Golgi is disproportionately affected. This data does not tell us if there is simply more Golgi markers or if there a change in Golgi organelle size and morphology. Immunofluorescence experiments need to be done to elaborate on this.

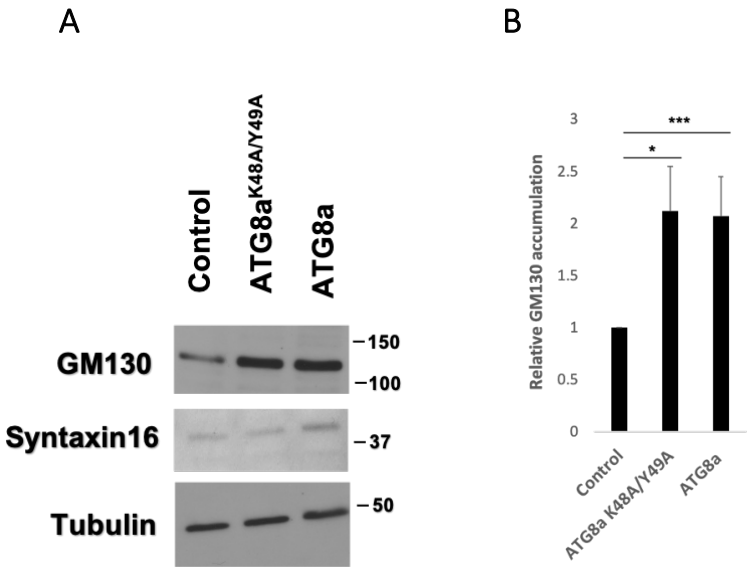


Figure 6-1 **Accumulation of cis Golgi markers in ATG8a$^{K48A/Y49A}$ and ATG8a mutant flies compared to wild type control.** A) Western blot showing accumulation of the cis Golgi marker GM130 in both autophagy mutant flies compared to wild type controls. No accumulation was seen in the trans Golgi marker Syntaxin 16. Tubulin was used as a loading control. B) Quantification of GM130 accumulation relative to control flies showing significant increase in GM130 in autophagy mutant flies compared to controls. Statistical significance was determined using one sample t-test, error bars show +SDs, *p<0.05, ***p<0.001.

## 6.4 There is no alteration of Golgi in the highly secretory organs of autophagy mutant flies

dGMAP is a tethering protein located on the cis Golgi and is responsible for capturing vesicles arriving from the ER. Therefore, it is logical that cells which are highly secretory will be most affected by a lack of dGMAP/Golgi degradation. In *Drosophila* the two main organelles that secrete many proteins are the malpighian tubules and the salivary gland. The malpighian tubule is the equivalent of the mammalian kidney, specifically the nephron tubules, in flies and so involved in the production of urine through movement of ions and organic substances (Gautam, Verma and Tapadia, 2017). The secretory system is important in mobilising membrane proteins, channels, and active transporters. The salivary gland contains secretory cells

which are involved in the secretion of many proteins. This gland is also very important in the secretion of salivary glue proteins that help the larvae get ready for pupariation (Andrew, Henderson and Seshaiah, 2000). If there is an issue with the Golgi size and Golgi trafficking in autophagy deficient conditions, it is likely that these tissues will be the most affected. Wild type, ATG8a and ATG8a$^{K48A/Y49A}$ mutant flies were aged two weeks and the malpighian tubules were stained for the cis Golgi marker GM130. This would allow identification of any accumulated and morphological changes to the Golgi apparatus. For the salivary gland, it is mostly degraded in adult flies and so the staining was only done in larvae, which is why only wild type and ATG8a mutant samples are shown. Figure 6-2 shows GM130 staining of malpighian tubules and salivary glands. For both these tissues, the Golgi apparatus in autophagy mutants appear to be normal is size and morphology.

The malpighian tubule is a hollow tube so the GM130 puncta representing the Golgi and the nuclei can be seen on the edges of the tube. In all three genotypes (wild type, ATG8a and ATG8a$^{K48A/Y49A}$), similar sized puncta can be seen and the Golgi does not appear to be malformed in any way.

For salivary gland staining, there is an even distribution of similar sized GM130 puncta throughout the salivary gland cells. There is also no obvious difference in Golgi morphology either. A similar experiment was done by Charroux and Royet, 2013, where the Golgi pH regulator protein (GPHR) mutants' effect on Golgi organisation was investigated. The Golgi puncta was uniformly distributed and when GPHR was mutated, it caused some of the puncta to become more diffuse and weaker (Charroux and Royet, 2014). Secretory organs did not show alterations in Golgi size or shape. To see if this is the case for most tissues in *Drosophila*, other organs which are likely less secretory in nature need to be checked for Golgi alterations.

A

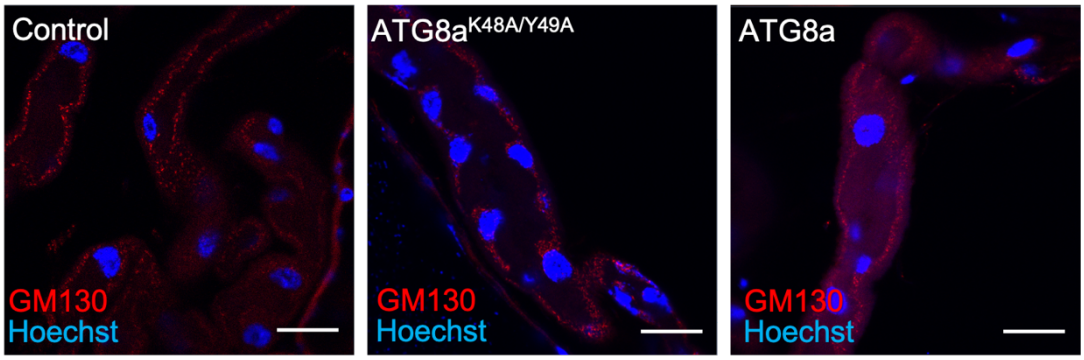


B

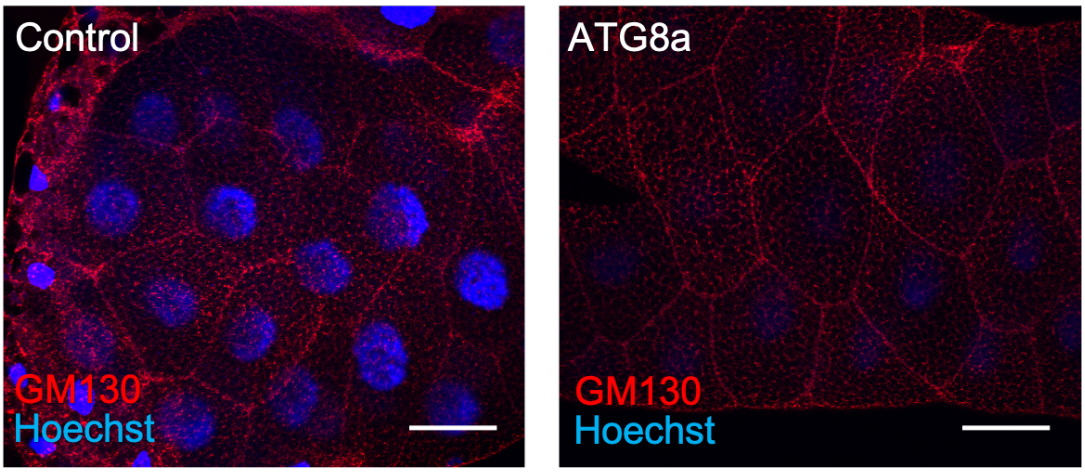


Figure 6-2 **There is no accumulation of Golgi in malpighian tubules and salivary glands in autophagy mutant flies.** A) GM130 staining (red) of 2-week-old fly malpighian tubules, showing Golgi size and morphology. GM130 puncta representing the Golgi can be seen in wild type, ATG8a$^{K48A/Y49A}$ mutant, and ATG8a mutant flies. As the malpighian tubules are a tube, cell contents such as the Golgi are seen on the edges of the tubules. No difference is seen between wild type and autophagy mutant samples. B) GM130 staining (red) of larval salivary gland. Many GM130 puncta (golgi) can be seen throughout the cytoplasm of both wild type and ATG8a mutant flies. No difference is seen between control and ATG8a mutant flies. DNA was stained with Hoechst (blue). Scale bars are 20 µm and 60 µm for A) and B) respectively.

## 6.5 There is a difference in Golgi size and morphology in autophagy mutant larval fat body and adult fly brains

Wild type and ATG8a mutant larval fat body was stained for GMAP and GM130 (Figure 6-3). Since these are both cis-Golgi localised proteins there should be some co-localisation of GM130 and GMAP puncta. Figure 6-3 shows that in wild type larval fat body there are small but numerous GMAP and GM130 puncta which do co-localise. In the ATG8a mutant larval fat body, the GMAP/GM130 puncta are much larger in size. There is a 2-3-fold increase in GM130 puncta size. Some GMAP/GM130 puncta were much larger than what the quantification suggests. The increase in size of the GMAP/GM130 puncta indicate that the Golgi organelle fragments in autophagy deficient flies are much larger. There also seems to be alterations in Golgi morphology. The Golgi puncta in ATG8a mutant larvae are more elongated and sometime appear to be hollow. This indicated that there is reduced degradation of the Golgi in autophagy mutants.

A

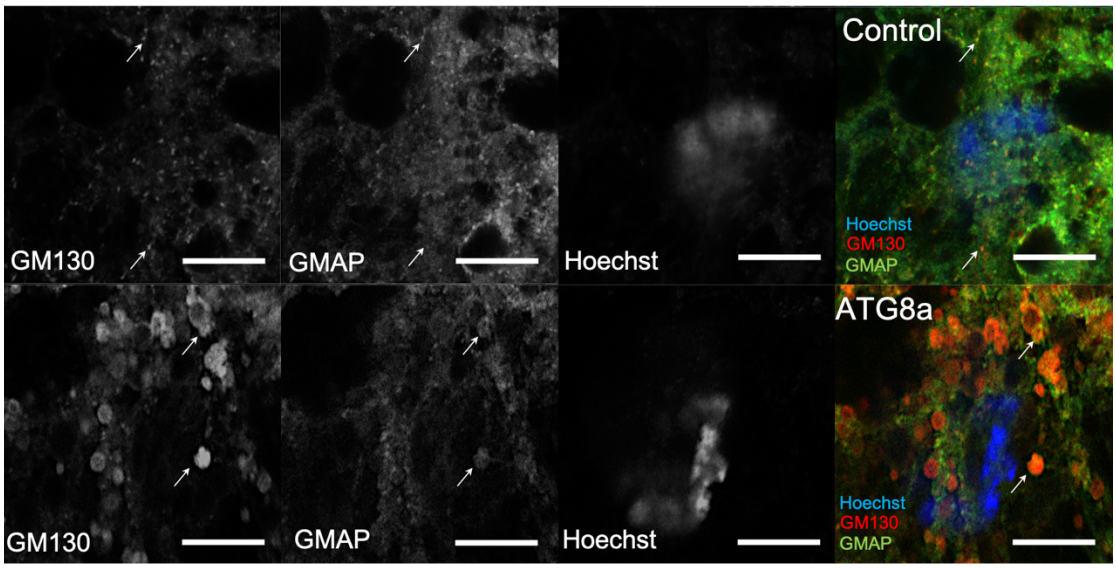


B

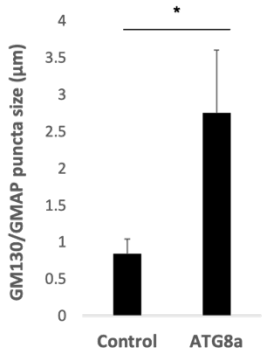


Figure 6-3 **There is an increase in Golgi size and change in Golgi morphology in ATG8a mutant larval fat body compared to wild type controls.** A) Co-localisation of GMAP (green) and GM130 (red) indicated Golgi apparatus. GM130 and GMAP positive puncta can be seen in both control and ATG8a mutant fat bodies (white arrows). The Golgi in ATG8a mutant fat bodies are much larger, elongated and occasionally hollow. DNA was stained with Hoechst (blue), scale bars are 10 µm. B) Quantification of average GMAP/GM130 positive puncta size shows that the Golgi is significantly larger in ATG8a mutant fat body compared to controls. Statistical significance was determined using t-test, error bars show +SDs, *p<0.05.

A similar experiment was also performed in adult *Drosophila* brain. This time, two-week-old wild type, ATG8a$^{K48A/Y49A}$ and ATG8a mutant adult brains were stained with

GM130 and GMAP. Figure 6-4 shows that in both autophagy mutant flies there is an increased amount of golgi. Both cis Golgi markers GM130 and GMAP accumulated in these flies and their colocalization suggests these puncta are golgi. The Golgi also appears much brighter and, in some places, longer in length suggesting changes to Golgi morphology as well.

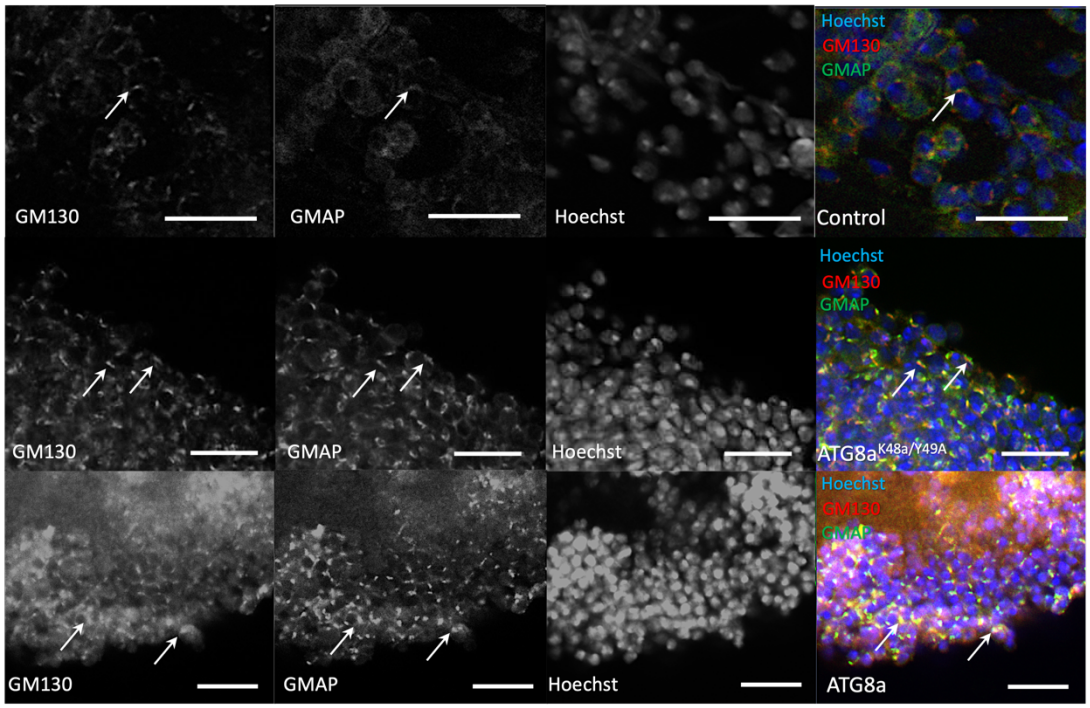


Figure 6-4 **There is an increase in Golgi size and change in Golgi morphology in ATG8a$^{K48A/Y49A}$ and ATG8a mutant fly brains compared to wild type controls**. Co-localisation of GMAP (green) and GM130 (red) represents the Golgi apparatus and is seen in controls and autophagy mutants. In both autophagy mutants GMAP and GM130 positive puncta are much brighter, larger, and sometimes elongated. This phenotype is most severe in ATG8a mutants. DNA was stained with Hoechst (blue), scale bars are 10 µm.

## 6.6 The *Drosophila* Golgi is degraded through autophagy

The Golgi is larger in autophagy mutant flies; however this does not confirm that the Golgi is degraded through autophagy. To confirm that the Golgi is degraded through autophagy like other organelles such as mitochondria and the ER, co-localisation between autophagosomes and the Golgi marker GM130 was investigated.

FLP-out mCherry-ATG8a flies were used for this experiment. They were created previously through crossing of: yw, hs::FLP; UAS-mCherry-Atg8a; AC>CD2>Gal4 (FLPout empty lines) with Bloomington's UAS-mCherry-Atg8a flies. These flies have a mosaic expression of mCherry-ATG8a, where in tissues some cells will express mCherry-ATG8a and cells around it will not. These flies were starved for 24 hours which induced autophagy. Autophagosomes can be visualised as there will be many small mCherry positive puncta in the cytoplasm. Fat body from these larvae were also stained for GM130 to see if there is any co-localisation between the cis Golgi marker and mCherry-ATG8a. Figure 6-5 shows that there were some co-localisations between mCherry-ATG8a and GM130 suggesting that the Golgi is degraded through autophagy. This result supports the data from Lu et al., the group who suggested GOLPH3 as a golgiphagy receptor. They also showed co-localisation of GM130 and LC3B positive puncta under starvation in mammalian cells. Figure 6-5 confirms that golgiphagy is also present in *Drosophila*.

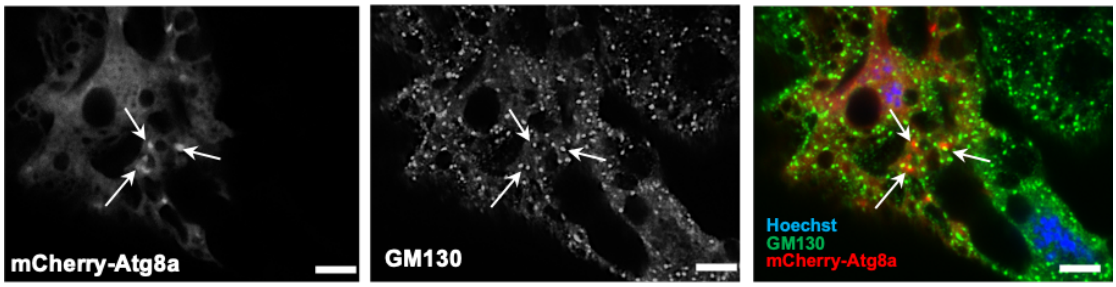


Figure 6-5 **The Golgi is degraded by autophagy (golgiphagy) in *Drosophila*.** Larvae from FLP-out mCherry-ATG8a were starved for 24 hours and stained for GM130 (green). Multiple mCherry puncta in each cell can be seen which represents autophagosomes in the cytoplasm. There is co-localisation of GM130 and mCherry (white arrows) suggesting that Golgi is present within the autophagosome. DNA was stained with Hoechst (blue), scale bars are 10 µm.

## 6.7 Knockdown of dGMAP causes accumulation of GM130

dGMAP RNAi lines were crossed with DaGAL4 driver lines. This created offspring which had dGMAP RNAi expressed in every cell of the body. These flies allowed the effect of dGMAP knockdown to be investigated. Figure 6-6 shows that dGMAP was successfully knocked down as there was a significant reduction in dGMAP expression in dGMAP RNAi lines compared to wild type. These RNAi lines also had a significantly increased level of GM130 which could suggest a lack of golgiphagy due to a reduction in dGMAP. However, it is worth noting that there are studies which suggest that a reduced expression in either GMAP or GM130 can cause the other gene to be overexpressed to compensate for it. This is due to the redundancy in some of their functions.

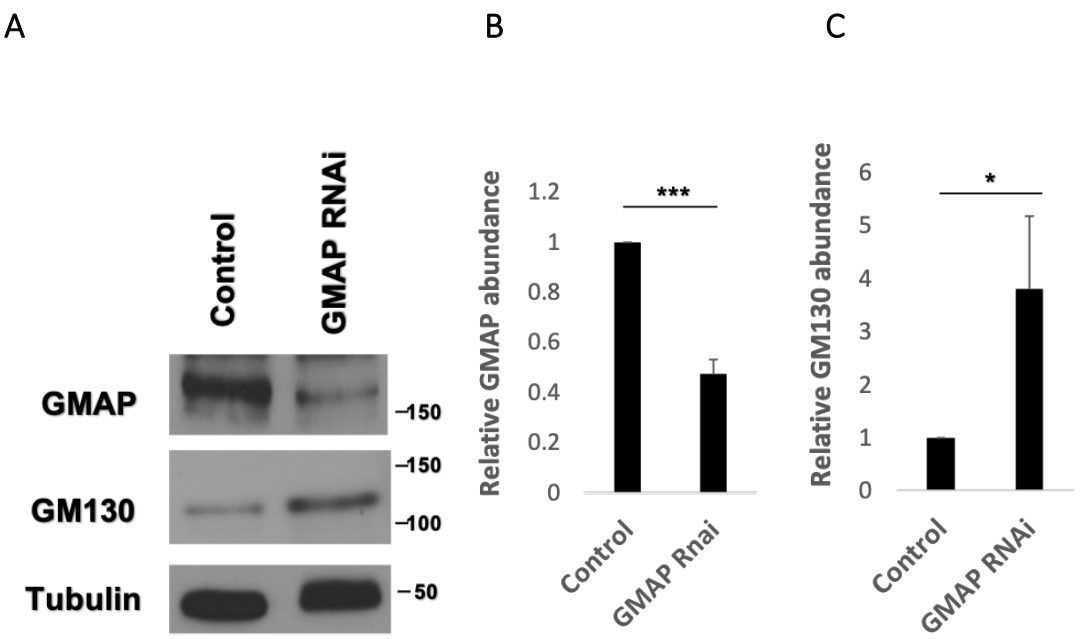


Figure 6-6 **dGMAP RNAi causes accumulation of cis Golgi marker GM130.** dGMAP RNAi flies were crossed with the full body driver line daGAL4 and aged 3-4 days. A) western blot confirming knockdown of dGMAP. GM130 accumulates in these flies. Tubulin was used as a loading control. B) and C) are quantifications of dGMAP and GM130 respectively. Statistical significance was determined using one sample two-tailed t-test, errors bars show +SDs, *p<0.05, ***p<0.001.

## 6.8 Generation of LIR mutant dGMAP

To investigate the importance of dGMAP LIR motif, dGMAP flies with a LIR motif mutation was created. This was done in the same was as creating the ATG8a$^{K48A/Y49A}$ mutants by Well Genetics. The LIR motif was mutated from DEFIVV to DEAIVA (F322A/V325A). A schematic of the CRISPR/Cas9 editing is shown in Figure 6-7.

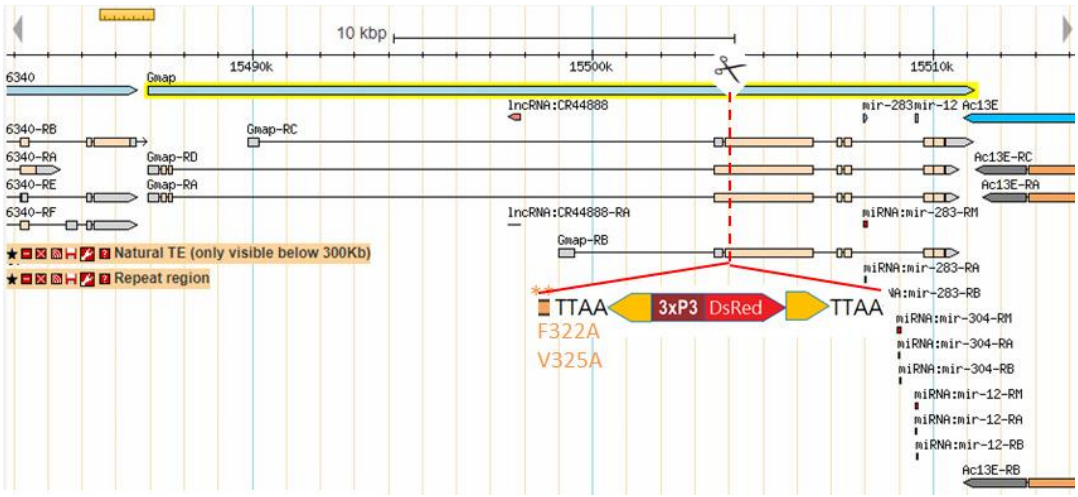


Figure 6-7 **Creation of dGMAP$^{F322A/V325A}$ mutant flies.** dGMAP LIR mutant (DEFIVV → DEAIVA) were created by Well Genetics using the same technique as when generating ATG8a$^{K48A/Y49A}$ mutant flies. CRISPR/Cas9 was used to create double strand breaks at the target gene and homologous recombination was used to insert the mutated DNA fragment along with the Piggybac™ vector. The vector contains DsRed a selectable marker which can be excised using the Piggybac™ transposase.

## 6.9 dGMAP LIR mutant flies have accumulation of golgi

dGMAP$^{F322A/V325A}$ mutants were aged two weeks and investigated for signs of Golgi accumulation. Figure 6-8 shows western blot analysis of GM130, in two-week-old wild type flies compared to dGMAP$^{F322A/V325A}$ and ATG8a mutant flies. There was a significant increase in the levels of GM130 in dGMAP$^{F322A/V325A}$ and ATG8a mutant flies. This suggests that there is reduced Golgi degradation in the dGMAP LIR mutant flies, therefore the LIR motif of dGMAP is crucial for golgiphagy to take place.

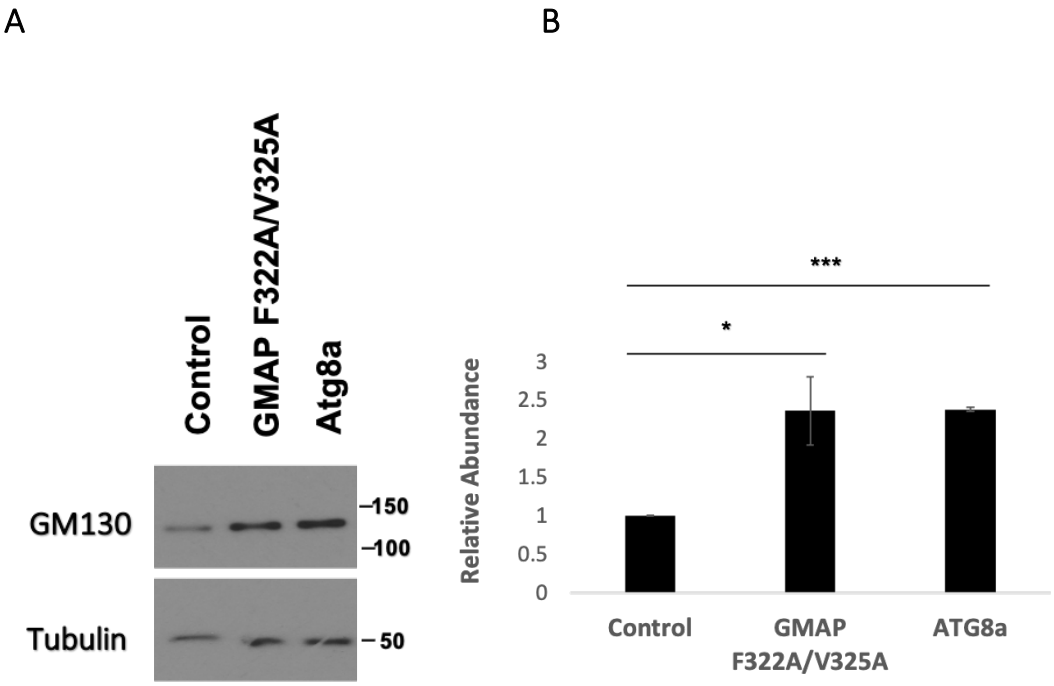


Figure 6-8 **There is an accumulation of cis-Golgi marker GM130 in dGMAP$^{F322A/V325A}$ mutant flies compared to wild type controls.** A) Western blot showing GM130 accumulation in dGMAP$^{F322A/V325A}$ mutant flies, ATG8a mutant flies are shown as a positive control. Tubulin is used as the loading control. B) Quantification of GM130 accumulation. Statistical significance was determined using one sample two-tailed t-test, error bars are +SDs, *p<0.05, ***p<0.001.

The accumulation of Golgi in the dGMAP$^{F322A/V325A}$ mutants was also verified using immunofluorescence. Figure 6-9 shows an increase in GM130 puncta (golgi) in dGMAP$^{F322A/V325A}$ and ATG8a mutant flies compared to wild type. The GM130 puncta appear to be much brighter and larger. There is also the presence of longer more elongated Golgi in the two mutant flies. The lengths of the puncta in each of the fly lines were measured and the relative size of the Golgi were compared. Quantification was calculated as a ratio of large puncta (>1 µm) to small puncta (<1 µm). The Golgi in dGMAP$^{F322A/V325A}$ and ATG8a mutant flies were significantly larger than wild type flies.

A

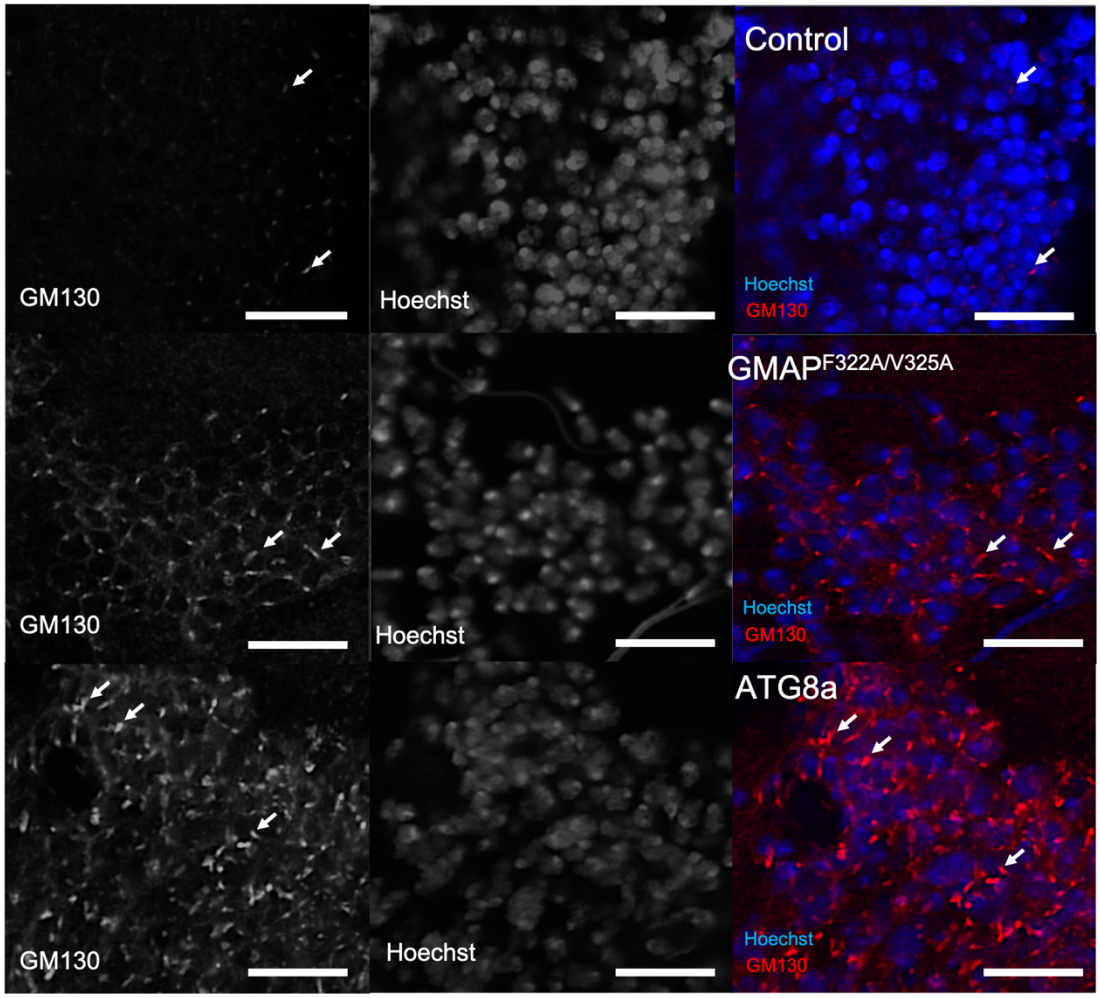


B

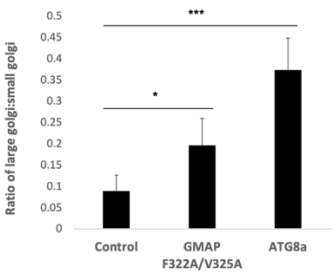


Figure 6-9 **Increase in Golgi size and change in Golgi morphology in dGMAP$^{F322A/V325A}$ fly brains compared to wild type control.** A) Flies were aged 2 weeks and stained for GM130 (red) which represents the golgi. GM130 puncta (golgi, white arrows) appear much larger and elongated suggesting a change in Golgi morphology. A similar phenotype is seen in the ATG8a mutant flies. DNA was stained using Hoechst (blue, scale bars are 10 µm. B) Quantification of relative size of GM130 puncta calculated as a ratio of large puncta (>1 µm) to small puncta (<1 µm). Statistical significance was determined using one sample two-tailed t-test, error bars are +SDs, *p<0.05, ***p<0.001.

The confocal data on the dGMAP$^{F322A/V325A}$ confirms that the identified LIR motif is necessary for dGMAP dependent turnover of the golgi.

## 6.10 Conclusion

Western blot analysis of ATG8a$^{K48A/Y49A}$ suggests that there is an accumulation of the cis-Golgi marker GM130 compared to wild type. It is unclear why the trans Golgi marker, Syntaxin 16, did not also accumulate. In the future it may be worth analysing the accumulation of other tans-Golgi markers. What is confirmed is the increase in Golgi size and change in Golgi morphology (through immunofluorescence) when autophagy is disrupted. A similar phenotype was seen when the LIR motif of dGMAP was mutated which confirms dGMAP as a novel LIR motif containing golgiphagy receptor. However, the Golgi in every cell was not affected in the same way. The fat body and brain had obvious alterations to Golgi structure and size yet the malpighian tubules and salivary glands seem unaffected. This is interesting as golgins when mutated cause tissue specific phenotypes which is described in the earlier section "Golgins". To summarise, even though some golgins are ubiquitously expressed, their knockdown affects some tissues more than others. There is obviously a more complex interaction between different golgins, redundant functions, and occasional niche roles of golgins in some tissues. Therefore, it is not surprising that dGMAP may be involved in golgiphagy in a subset of tissues/cells rather than ubiquitously. The fact that the quantitative proteomics analysis was done on fly heads mean that the aggregated proteins investigated were enriched for brain proteins. Therefore, it is not surprising that the golgin involved in golgiphagy in the brain was identified. The identification of dGMAP now makes the total golgiphagy receptor count three.

# Chapter 7 dGMAP is a potential regulator of autophagy

Although the evidence suggests that dGMAP is a golgiphagy receptor, this does not mean that dGMAP is not also a part of the autophagy process itself. By inhibiting LIR motif dependent autophagy through ATG8a$^{K48A/Y49A}$ mutant flies, it is likely that autophagy regulator proteins may also accumulate. To see if dGMAP and its interaction with ATG8a is involved in autophagy regulation, autophagy defects in dGMAP$^{F322A/V325A}$ mutant flies were investigated.

## 7.1 There is an accumulation of Ref(2)P in dGMAP F322A/V325A mutant flies

The easiest way to check for any defects in autophagy is to check for the accumulation of the LIR motif containing protein Ref(2)P in dGMAP LIR mutant flies. Figure 7-1 is the western blot showing that there is an increased amount of Ref(2)P present in the dGMAP LIR mutant flies.

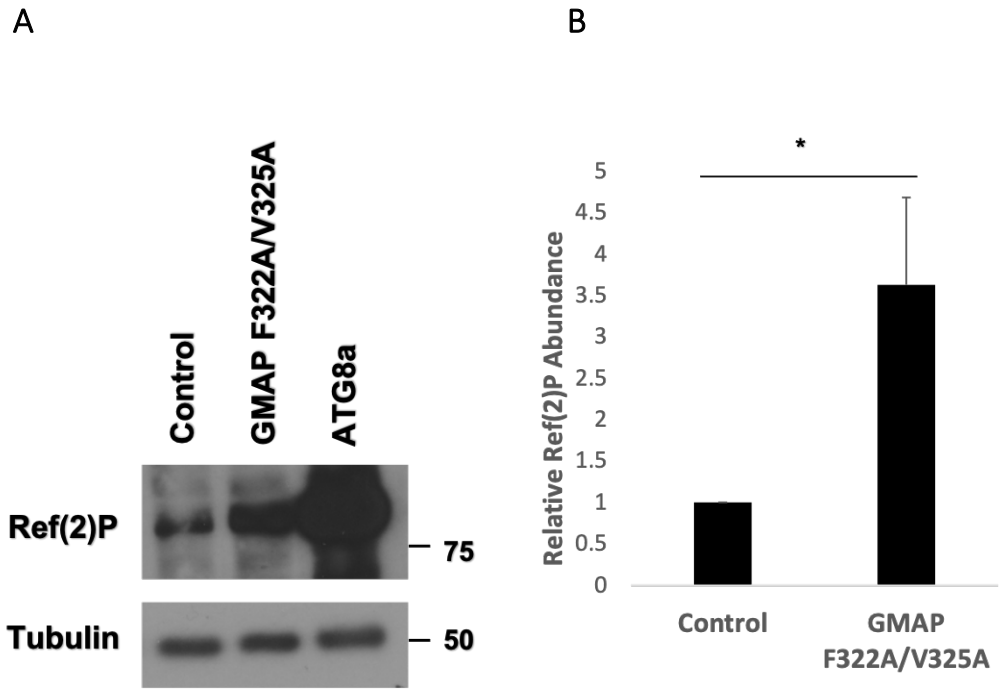


Figure 7-1 **Accumulation of Ref(2)P in dGMAP$^{F322A/V325A}$.** A) Flies were aged two weeks and blotted for Ref(2)P. Ref(2)P accumulation in ATG8a was used as a positive control. There was accumulation of Ref(2)P in the dGMAP LIR mutant flies but not as much as in the ATG8a mutants. Tubulin was used as a loading control. B) Quantification of Ref(2)P accumulation in dGMAP$^{F322A/V325A}$ mutant flies relative to wild type controls, shows the difference is significant. ATG8a mutant samples is now shown in the graph as the quantification value is much higher than both the control and dGMAP$^{F322A/V325A}$ mutant flies. Statistical significance was determined using one sample two-tailed t-test, error bars are +SDs, *p<0.05.

Accumulation of Ref(2)P was also tested using immunofluorescence, ubiquitin was stained for identification of protein aggregates. Figure 7-2 shows that There are Ref(2)P and ubiquitin positive aggregates present in two week old *Drosophila* brains in dGMAP$^{F322A/V325A}$ mutant flies compared to wild type. ATG8a mutant flies are also there as a positive control. However, it is worth noting that these protein aggregates were not seen across the whole brain but only in sub sections of different parts of the brain. This could mean that dGMAP is involved in regulating autophagy in only some cells and not ubiquitously. Although not done in this study, further experimentation investigating protein aggregates in different *Drosophila* tissue would provide more insight into this.

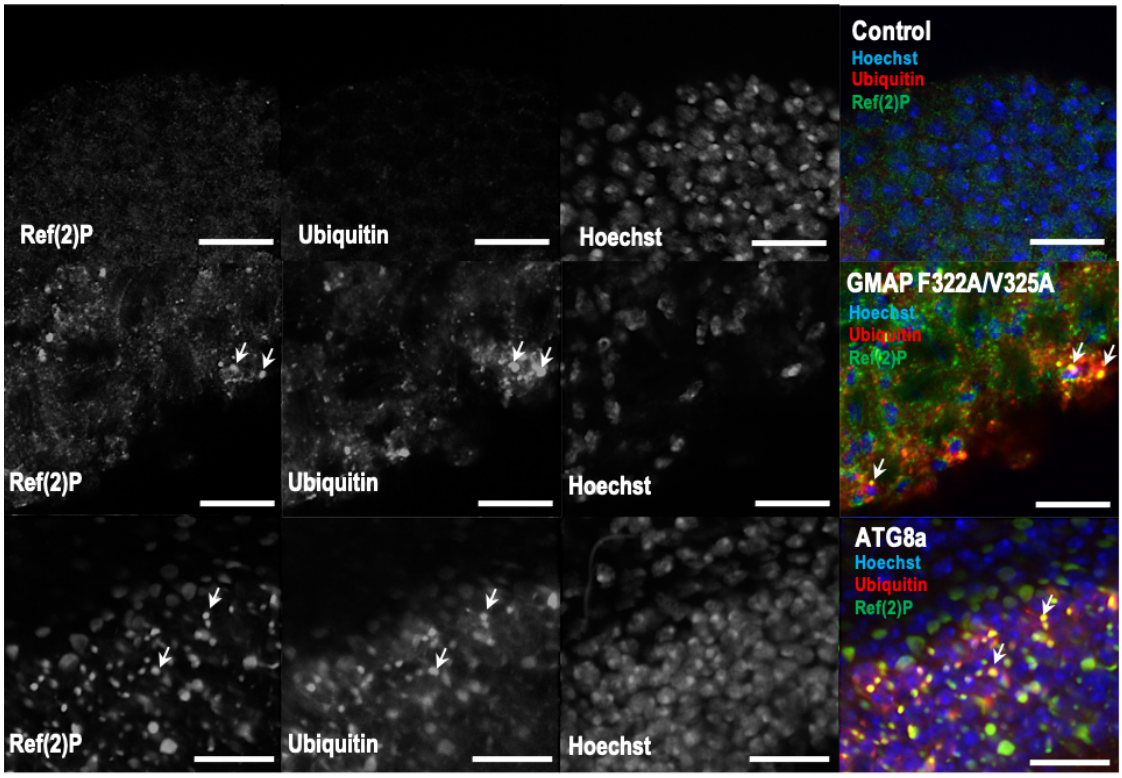


Figure 7-2 **Accumulation of Ref(2)P and ubiquitinated proteins in dGMAP$^{F322A/V325A}$ mutant fly brains.** Ref(2)P (green) and ubiquitin (red) positive puncta represent protein aggregates (white arrows) which, similar to ATG8a mutants, can be seen in some cells of dGMAP$^{F322A/V325A}$ mutant fly brains. These aggregates were not seen in wild type control fly brains. DNA was stained with Hoechst (blue), scale bars are 10 µm.

## 7.2 dGMAP LIR motif mutations cause defects in autophagosome formation

dGMAP RNAi flies were crossed with mCherry-ATG8a to see the effect of dGMAP knockdown on autophagosome formation. Control RNAi lines were also crossed with mCherry-ATG8a flies. Larvae of the offspring from this cross were starved for 4 hours to induce autophagy and the fat bodies stained for dGMAP (to verify

dGMAP knockdown). Larval fat bodies under fed conditions were used as controls. Like Figure 6-5, mCherry-ATG8a fly fat bodies will have a mosaic appearance where cells which express mCherry-ATG8a will be next to cells that don't. The mosaic staining of the tissue represents the fact that Gal4 is expressed in these cells, which means that the mCherry expressing cells will also be expressing the relevant RNAi. Figure 7-3 shows that under fed conditions, no distinct mCherry-ATG8a positive puncta can be seen in either cross. In starved conditions with the control RNAi cross, there were many mCherry-ATG8a puncta (autophagosomes) seen in the cytoplasm. This indicated normal autophagy taking place and autophagosomes forming as usual. Many of these mCherry-ATG8a puncta also co-localises with dGMAP further supporting the fact that dGMAP is facilitating the autophagic degradation of the golgi. In the dGMAP RNAi cross under starved conditions, there are some autophagosomes present but are far less common. In each mCherry-ATG8a positive cell there are much fewer or occasionally no mCherry puncta. When there are mCherry puncta they appear to be much larger. In cells which are positive for mCherry-ATG8a, the dGMAP staining is much more diffuse indicating successful knockdown of dGMAP in these cells. These data suggest there is a defect in autophagy in dGMAP LIR mutant flies.

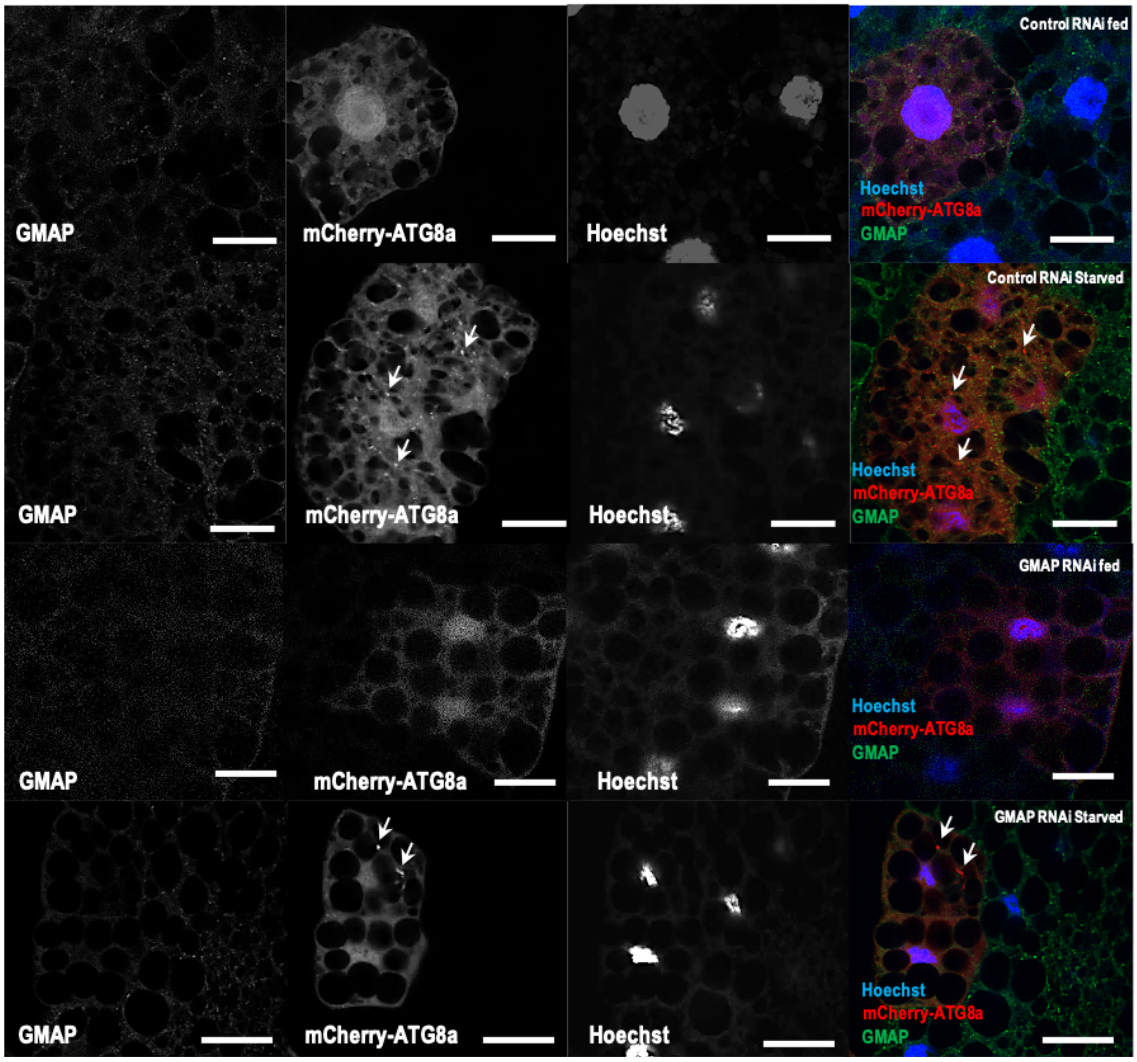


Figure 7-3 **dGMAP$^{F322A/V325A}$ has impaired autophagy.** FLP-out mChrry-ATG8a flies were crossed with either control RNAi flies or dGMAP RNAi flies. Larval fat bodies from larvae which were either fed or starved for 4 hours were then stained for GMAP (green). Cells which express mCherry-ATG8a will also express the associated RNAi. In control RNAi lines starved condition there are many mCherry puncta in the cytoplasm representing autophagosomes. These are not seen in fed conditions. In dGMAP RNAi flies starved conditions, there are much fewer mCherry puncta and the autophagosomes appear to be much larger. Again, these are not present in fed conditions. DNA was stained with Hoechst (blue), scale bars are 20 µm.

The fewer autophagosomes when dGMAP is knocked down could suggest a defect in autophagosome formation. For example, the initiation of the phagophore membrane may be affected by a lack of dGMAP. In addition, since the

autophagosomes appear much larger, defects in phagophore elongation and closure could also be present. Alternatively, dGMAP may be involved in the mobilisation of membrane which contributes to the growing phagophore. Many sources of membrane have been suggested for the autophagosome including mitochondria (Hailey *et al.*, 2010), plasma membrane (Ravikumar *et al.*, 2010), ER-mitochondria contact site (Hamasaki *et al.*, 2013), and ER-plasma membrane contact site (Nascimbeni *et al.*, 2017). The Golgi as a membrane source is probably the least understood and a potential role for dGMAP. Other tethering proteins like COG and TRAPP have been implicated in autophagosome biogenesis. ATG9 compartments and vesicles which contribute membrane to the growing phagophore has been shown to derive from many locations including the Golgi (Axe *et al.*, 2008). However, without further experimentation, a definitive role of dGMAP in the regulation of autophagy is difficult.

# Chapter 8 Summary and conclusions

The thesis can be split into two main sections; a screening process to identify a panel of potential LIR motif containing proteins and an in-depth analysis of one of these identified proteins. Chapter 3 and 4 describes the process of using quantitative proteomics to identify LIR motif containing proteins. The approach was to use flies which had a mutated ATG8a LDS binding pocket (K48A/Y49A) which are unable to interact with the LIR motif. Proteins which accumulate in these mutant flies are potential autophagy substrates/adapters which contain a LIR motif. This is much more effective that simply looking at accumulated proteins in ATG8a null mutant flies as ATG8a interacts with many proteins in a LIR motif independent manner. The Nezis lab has previously used different screening techniques to identify LIR motif containing proteins such as a yeast-2-hybrid (Y2H) screening. The Y2H screen allows in-vitro analysis of ATG8a interactors which helped identify many LIR motif containing proteins including Kenny. However, the main issue with the Y2H screen is that it identified all ATG8a interactors, which includes both LIR motif dependent and independent interactors. This means more downstream analysis of identified proteins is needed. By comparing both ATG8a and ATG8a$^{K48A/Y49A}$ mutants to wild type it is possible to quickly narrow down proteins which interact with ATG8a in a LIR motif dependent manner.

Chapter 3 describes the experiments used to characterise the ATG8a$^{K48A/Y49A}$ mutants, to see if they have a similar phenotype to ATG8a mutants. Once the mutations were verified with sequencing, experiments looking at Ref(2)P, Kenny and Ubiquitin accumulation showed that ATG8a$^{K48A/Y49A}$ had an intermediate phenotype between wild type and ATG8a mutants. Both western blotting (whole flies) and immunofluorescence (brain and gut) showed that LIR motif containing proteins and ubiquitinated proteins aggregate in ATG8a$^{K48A/Y49A}$ but to a slightly lesser degree than ATG8a mutants. Therefore, it can be speculated that the protein aggregates seen in ATG8a$^{K48A/Y49A}$ mutants are enriched for LIR motif containing proteins that are

selectively degraded. This makes ATG8a$^{K48A/Y49A}$ mutant flies useful for quantitative proteomics experiments.

Chapter 4 highlights the quantitative proteomics experiment used to identify proteins which accumulate in ATG8a$^{K48A/Y49A}$ mutant and ATG8a mutant flies compared to wild type flies. After optimisation it was found that the better technique for protein extraction and digestion was the FASP technique rather than the methanol/chloroform precipitation. Protein lysate of each genotype was collected from virgin male fly heads and four biological repeats were collected before all samples were run on the mass spectrometer on the same day. 3,736 proteins out of the total 14,000 in the *Drosophila* proteome were identified in the screening. Perseus software and excel were used to analyse the LFQ values and identify proteins which were significantly overabundant in both mutant lines compared to wild type. 29 proteins were identified which were significantly overabundant in both mutant lines compared to wild type and had at least a 2-fold increase in quantification.

Looking at the list of 29 proteins, there are a few proteins which we know cannot be selective autophagy substrates. Firstly, there are the proteins which are found within organelles which will not be able to interact with ATG8a. For example, CG11208 and CG10253 (AGPS) are enzymes found in peroxisomes, CG17544 is an enzyme found in mitochondria and CG10166 is an enzyme found in the ER lumen. These enzymes are all found within membrane bound compartments and so cannot physically interact with ATG8a. A likely explanation of this is that these proteins accumulate indirectly, as there is far less selective degradation of the associated organelle and their associated proteins. This could mean that receptors for mitophagy, ER-phagy and pexophagy accumulated in the autophagy mutant flies. It is likely that not every autophagy receptor was found as only 3736 proteins out of the total 14,000 proteins in the fly proteome was identified. Secondly, there are some extracellular proteins on the list, which again will not have access to ATG8a. This is not an issue for transmembrane proteins on the plasma membrane such as CG508, and Sip1 which likely have cytosolic domains for ATG8a interaction. This is likewise for organelle transmembrane proteins such as the ER membrane resident Itp-r83A. However, proteins such as dally, which are secreted or anchored to the outside of the cell, are

unlikely to be ATG8a interactors. The rest of the proteins could potentially be ATG8a interactors, as most of them are enzymes. Interestingly, there was also another Golgi protein found in the list (in addition to dGMAP) called RER1 which is involved in the retrieval of ER resident proteins from the early Golgi compartments. This protein may be worth investigating further as potential golgiphagy receptor. Three proteins RIC-3, PI3I and Prolactin are neuronal proteins, which is unsurprising considering the proteomics was done of fly heads.

After using the iLIR software to identify potential LIR motifs in the 29 proteins, only 4 proteins were found to contain a LIR motif which had a high PSSM score (>13) and was within an anchor region. These proteins were Ref(2)P, dGMAP, Dally and Ras. Ref(2)P being identified was a good positive control and shows that the proteomics was able to identify a known LIR motif containing protein which accumulates in ATG8a$^{K48A/Y49A}$ flies. As mentioned previously, daily is an extracellular protein and unlikely to be an ATG8a interactor. This leaves dGMAP and Ras as potential LIR motif containing ATG8a interactors. Although dGMAP was chosen for further investigation, Ras is worth looking into in the future. Ras is part of the MAPK pathway as well as autophagy and so its degradation through autophagy likely has important physiological consequences.

Chapters 5, 6, and 7 describe experiments used to confirm dGMAP as a functional LIR motif containing protein and investigates its physiological significance. Chapter 5 covered the experiments which confirmed dGMAP as a LIR motif containing protein. First the accumulation of dGMAP in autophagy mutants (ATG8a$^{K48A/Y49A}$ and ATG8a) was verified through western blotting and immunofluorescence (brain and larval fat body). Following this, the high PSSM score predicted LIR motif from iLIR (DEFIVV) was confirmed as a functional LIR motif. Truncated form of dGMAP which contained the predicted LIR motif was able to interact with ATG8a in GST pulldown experiments. This interaction was significantly reduced with the pull down was done with ATG8a LDS mutant. The same dGMAP with a mutated LIR motif (DEFIVV → DEAIVA) also had a reduced interaction with ATG8a. This suggests that dGMAP interacts with ATG8a through a functional LIR motif in position 320-325 (DEFIVV). Mutation of the LDS binding pocket of ATG8a and the dGMAP LIR motif did not

completely inhibit their interaction. It is likely that dGMAP can interact with ATG8a through both LIR motif dependent and LIR motif independent mechanisms which is not uncommon. However, the fact that dGMAP has significant accumulation in ATG8a$^{K48A/Y49A}$ means that the primary method of interaction would be through the LIR motif-ATG8a LDS.

Chapter 6 highlights experiments that identified dGMAP as a selective autophagy receptor, involved in the selective degradation of the Golgi complex (golgiphagy). Western blotting and immunofluorescence showed there was a lack of Golgi turnover in autophagy mutant flies. GM130 a cis Golgi marker was used for these experiments. However, the accumulation of Golgi affected some organs but not others. The salivary gland and malpighian tubules, two highly secretory organs did not show any difference in Golgi size or morphology. Whereas the brain and fat body had an increase in Golgi size and change in Golgi morphology in autophagy mutants. This indicates that golgiphagy may be tissue specific and regulated differently in different cells. This means there are likely many more golgiphagy receptors yet to be identified. The importance of the dGMAP LIR motif in Golgi turnover was demonstrated using dGMAP$^{F322A/V325A}$ mutant flies (LIR mutants). Western blotting and immunofluorescence (brain) in these flies showed that there is an increase in Golgi size and change in Golgi morphology compared to wild type. Therefore, dGMAP is a golgiphagy receptor which regulates the turnover of the Golgi through its interaction with ATG8a via its LIR motif. Figure 8-1 is a diagram showing the proposed way in which dGMAP may target the Golgi to the autophagosome. The C-terminal GRAB domain is what anchors dGMAP to the cis Golgi via Arf1 GTPase and the functional LIR motif which interacts with ATG8a is located near the N-terminus.

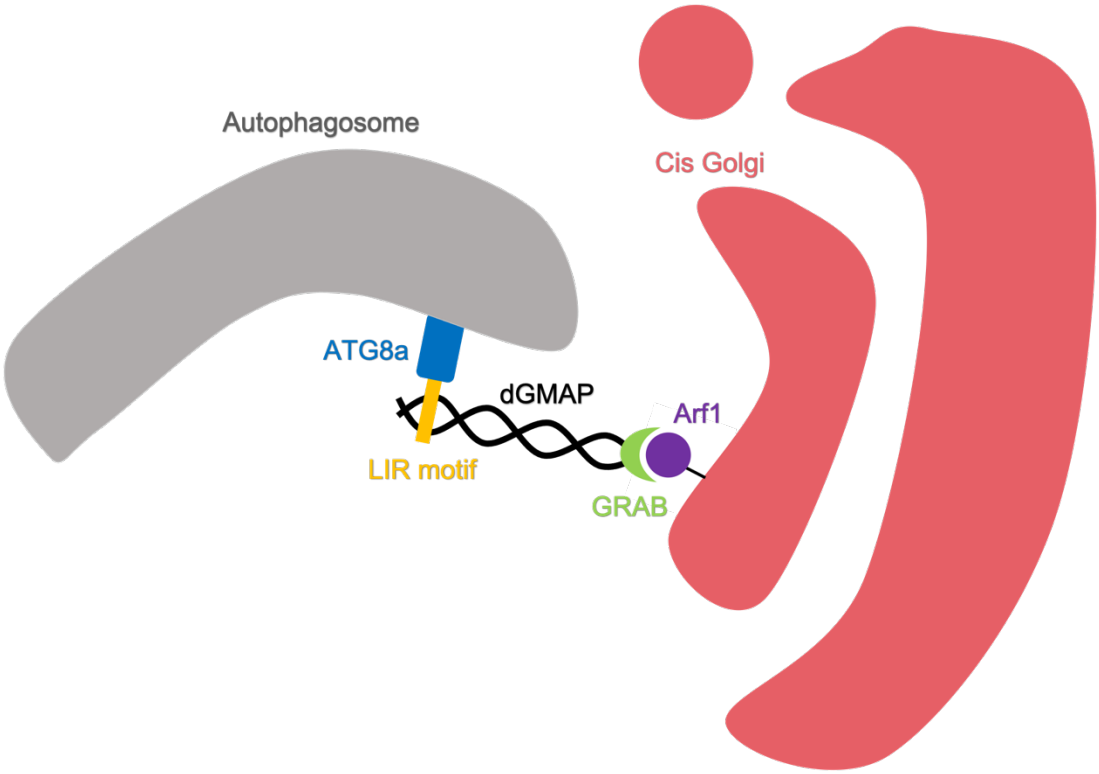


Figure 8-1 **Schematic showing the proposed model for dGMAP dependent golgiphagy.** dGMAP is a cis-Golgi resident protein which is anchored to the Golgi through interaction with Arf1 via its C-terminal GRAB domain. dGMAP has a functional LIR motif (DEFIVV) near its N-terminal which allows interaction with ATG8a-LDS. This targets the Golgi to the autophagosome for autophagic degradation.

Chapter 7 provides preliminary data to show dGMAP may have additional functions in autophagy. This was because it was found that ref(2)P accumulates in flies which have a mutated dGMAP LIR motif (F322A/V325A), suggesting some kind of defect in autophagy. This was verified in western blot and immunofluorescence of brain tissue although the phenotype in the brain was not as extreme. Not every cell in the brain had ref(2)P and ubiquitin positive aggregates. This could mean that dGMAP is not essential for autophagy to happen but may have a niche role in subsets of cells. In addition, when dGMAP was knocked down with RNAi, there were much fewer autophagosomes forming in starved larval fat body. The autophagosomes that did form were much larger, suggesting dGMAP may have a role in the regulation of autophagy and autophagosome formation.

Further study into the role of dGMAP as a golgiphagy receptor and its additional role as a regulator of autophagy is needed. To confirm whether the morphology of Golgi in dGMAP LIR mutant flies is different, transmission electron microscopy could be done for a more detailed image of Golgi structure. It is clear that dGMAP has tissue specific roles and so staining of other tissues for example, testis, ovaries, accessory glands, and different regions of the gut would be interesting. Lifespan assays on dGMAP$^{F322A/V325A}$ flies would also give an indication of the general health of flies which have reduced Golgi turnover. When it comes to the role of dGMAP in autophagy regulation, the downstream effect of dGMAP knockdown can be investigated. For example, are there any issues with lysosomes and autolysosome formation? Staining with LysoTracker labels acidic compartments which could identify defects in lysosome number and size. To check for defects in autophagosome-lysosome fusion, there are already systems which exist such as the mCherry-GFP-ATG8a fly lines. In these flies, after autophagy induction, mCherry-Atg8a puncta denotes autophagosome-lysosome fusion. This is because the GFP signal is quenched by the acidic hydrolases of the lysosome whereas the mCherry signal is unaffected. Co-localisation of GFP and mCherry is an indication that there is a defect in lysosomal fusion. Furthermore, checking the levels of dGMAP RNA under autophagy deficient conditions could rule out the possibility of dGMAP upregulation in autophagy deficient flies rather than the lack of Golgi degradation.

There are other questions which remain unanswered. Future work would look to investigate why only the cis Golgi marker accumulates in flies but not the trans golgi. From the immunofluorescence data, the Golgi is larger, so it may just be the case that other trans Golgi markers need to be tested. Additionally, elucidating the role of GM130 in golgiphagy and autophagy regulation would be another area of focus. Since GM130 is another cis Golgi coiled-coil tethering protein which has redundant functions with dGMAP and accumulates in autophagy deficient flies, it would not be surprising if GM130 is involved in golgiphagy or autophagy in general, within the same or different subsets of cells. It is quite possible that dGMAP has three functions: anterograde transport, autophagy regulation, and golgiphagy. The types of signalling molecules involved in switching the role of dGMAP whether this is facilitated through

protein-protein interaction or post-translational modification is worth exploring. Finally, it would be valuable to confirm if the LIR motif in dGMAP is conserved in higher organisms too. Whether the mammalian homologue GMAP-210 is a selective autophagy substrate or a LIR motif containing golgiphagy receptor has clinical implications.

In conclusion, this study has established dGMAP as a novel LIR motif containing ATG8a interacting protein. It is a selective autophagy receptor which is involved in the selective degradation of the Golgi (golgiphagy) and may also be involved in the regulation of autophagy. Golgiphagy is the least studied form of organelle degradation through autophagy, so the identification of a new golgiphagy receptor is a step closer to understanding this process. Another output of this study is the generation of candidate LIR-motif containing proteins which may be involved in selective autophagy. Further study into these proteins will unveil more mechanisms of selective autophagy.

# Chapter 9 Bibliography


Abert, C., Kontaxis, G. and Martens, S. (2016) 'Accessory Interaction Motifs in the Atg19 Cargo Receptor Enable Strong Binding to the Clustered Ubiquitin-related Atg8 Protein', *J Biol Chem,* 291(36), pp. 18799-808.

Abounit, K., Scarabelli, T. M. and McCauley, R. B. (2012) 'Autophagy in mammalian cells', *World J Biol Chem,* 3(1), pp. 1-6.

Agarraberes, F. A. and Dice, J. F. (2001) 'A molecular chaperone complex at the lysosomal membrane is required for protein translocation', *J Cell Sci,* 114(Pt 13), pp. 2491-9.

Akiyama, T., Kamimura, K., Firkus, C., Takeo, S., Shimmi, O. and Nakato, H. (2008) 'Dally regulates Dpp morphogen gradient formation by stabilizing Dpp on the cell surface', *Dev Biol,* 313(1), pp. 408-19.

Alemu, E. A., Lamark, T., Torgersen, K. M., Birgisdottir, A. B., Larsen, K. B., Jain, A., Olsvik, H., Øvervatn, A., Kirkin, V. and Johansen, T. (2012) 'ATG8 family proteins act as scaffolds for assembly of the ULK complex: sequence requirements for LC3-interacting region (LIR) motifs', *J Biol Chem,* 287(47), pp. 39275-90.

An, H., Ordureau, A., Paulo, J. A., Shoemaker, C. J., Denic, V. and Harper, J. W. (2019) 'TEX264 Is an Endoplasmic Reticulum-Resident ATG8-Interacting Protein Critical for ER Remodeling during Nutrient Stress', *Mol Cell,* 74(5), pp. 891-908 e10.

Anding, A. L. and Baehrecke, E. H. (2017) 'Cleaning House: Selective Autophagy of Organelles', *Dev Cell,* 41(1), pp. 10-22.

Andrew, D. J., Henderson, K. D. and Seshaiah, P. (2000) 'Salivary gland development in Drosophila melanogaster', *Mech Dev,* 92(1), pp. 5-17.

Arias, E. and Cuervo, A. M. (2011) 'Chaperone-mediated autophagy in protein quality control', *Curr Opin Cell Biol,* 23(2), pp. 184-9.

Axe, E. L., Walker, S. A., Manifava, M., Chandra, P., Roderick, H. L., Habermann, A., Griffiths, G. and Ktistakis, N. T. (2008) 'Autophagosome formation from membrane compartments enriched in phosphatidylinositol 3-phosphate and dynamically connected to the endoplasmic reticulum', *J Cell Biol,* 182(4), pp. 685-701.

Bandyopadhyay, U., Kaushik, S., Varticovski, L. and Cuervo, A. M. (2008) 'The chaperone-mediated autophagy receptor organizes in dynamic protein complexes at the lysosomal membrane', *Mol Cell Biol,* 28(18), pp. 5747-63.

Barth, S., Glick, D. and Macleod, K. F. (2010) 'Autophagy: assays and artifacts', *J Pathol,* 221(2), pp. 117-24.

Beale, R., Wise, H., Stuart, A., Ravenhill, B. J., Digard, P. and Randow, F. (2014) 'A LC3-interacting motif in the influenza A virus M2 protein is required to subvert autophagy and maintain virion stability', *Cell Host Microbe,* 15(2), pp. 239-47.

Behrends, C. and Fulda, S. (2012) 'Receptor proteins in selective autophagy', *Int J Cell Biol,* 2012, pp. 673290.

Bellot, G., Garcia-Medina, R., Gounon, P., Chiche, J., Roux, D., Pouyssegur, J. and Mazure, N. M. (2009) 'Hypoxia-induced autophagy is mediated through hypoxia-inducible factor induction of BNIP3 and BNIP3L via their BH3 domains', *Mol Cell Biol,* 29(10), pp. 2570-81.

Bellu, A. R., Kram, A. M., Kiel, J. A., Veenhuis, M. and van der Klei, I. J. (2001) 'Glucose-induced and nitrogen-starvation-induced peroxisome degradation are distinct processes in Hansenula polymorpha that involve both common and unique genes', *FEMS Yeast Res,* 1(1), pp. 23-31.
Birgisdottir, A. B., Lamark, T. and Johansen, T. (2013) 'The LIR motif - crucial for selective autophagy', *J Cell Sci,* 126(Pt 15), pp. 3237-47.
Birmingham, C. L., Smith, A. C., Bakowski, M. A., Yoshimori, T. and Brumell, J. H. (2006) 'Autophagy controls Salmonella infection in response to damage to the Salmonella-containing vacuole', *J Biol Chem,* 281(16), pp. 11374-83.
Bochtler, M., Ditzel, L., Groll, M., Hartmann, C. and Huber, R. (1999) 'The proteasome', *Annu Rev Biophys Biomol Struct,* 28, pp. 295-317.
Brand, A. H. and Perrimon, N. (1993) 'Targeted gene expression as a means of altering cell fates and generating dominant phenotypes', *Development,* 118(2), pp. 401-15.
Budovskaya, Y. V., Stephan, J. S., Reggiori, F., Klionsky, D. J. and Herman, P. K. (2004) 'The Ras/cAMP-dependent protein kinase signaling pathway regulates an early step of the autophagy process in Saccharomyces cerevisiae', *J Biol Chem,* 279(20), pp. 20663-71.
Burman, C. and Ktistakis, N. T. (2010) 'Regulation of autophagy by phosphatidylinositol 3-phosphate', *FEBS Lett,* 584(7), pp. 1302-12.
Caza, M. and Kronstad, J. W. (2019) 'The cAMP/Protein Kinase a Pathway Regulates Virulence and Adaptation to Host Conditions in Cryptococcus neoformans', *Front Cell Infect Microbiol,* 9, pp. 212.
Chakrabarti, A., Chen, A. W. and Varner, J. D. (2011) 'A review of the mammalian unfolded protein response', *Biotechnol Bioeng,* 108(12), pp. 2777-93.
Charroux, B. and Royet, J. (2014) 'Mutations in the Drosophila ortholog of the vertebrate Golgi pH regulator (GPHR) protein disturb endoplasmic reticulum and Golgi organization and affect systemic growth', *Biol Open,* 3(1), pp. 72-80.
Chen, D., Fan, W., Lu, Y., Ding, X., Chen, S. and Zhong, Q. (2012) 'A mammalian autophagosome maturation mechanism mediated by TECPR1 and the Atg12-Atg5 conjugate', *Mol Cell,* 45(5), pp. 629-41.
Chen, Q., Teng, J. and Chen, J. (2019) 'ATL3, a cargo receptor for reticulophagy', *Autophagy,* 15(8), pp. 1465-1466.
Chen, Y., Gan, B. Q. and Tang, B. L. (2010) 'Syntaxin 16: unraveling cellular physiology through a ubiquitous SNARE molecule', *J Cell Physiol,* 225(2), pp. 326-32.
Cheong, H. and Klionsky, D. J. (2008) 'Biochemical methods to monitor autophagy-related processes in yeast', *Methods Enzymol,* 451, pp. 1-26.
Cherra, S. J., 3rd, Kulich, S. M., Uechi, G., Balasubramani, M., Mountzouris, J., Day, B. W. and Chu, C. T. (2010) 'Regulation of the autophagy protein LC3 by phosphorylation', *J Cell Biol,* 190(4), pp. 533-9.
Chino, H., Hatta, T., Natsume, T. and Mizushima, N. (2019) 'Intrinsically Disordered Protein TEX264 Mediates ER-phagy', *Mol Cell,* 74(5), pp. 909-921 e6.
Colombo, M. I. (2007) 'Autophagy: a pathogen driven process', *IUBMB Life,* 59(4-5), pp. 238-42.
Connerly, P. L. (2010) *How Do Proteins Move Through the Golgi Apparatus?*: Nature Education. Available at: https://www.nature.com/scitable/topicpage/how-do-proteins-move-through-the-golgi-14397318/ (Accessed: 5/08/21.

Cox, J., Neuhauser, N., Michalski, A., Scheltema, R. A., Olsen, J. V. and Mann, M. (2011) 'Andromeda: a peptide search engine integrated into the MaxQuant environment', *J Proteome Res,* 10(4), pp. 1794-805.
Cuervo, A. M. and Dice, J. F. (1996) 'A receptor for the selective uptake and degradation of proteins by lysosomes', *Science,* 273(5274), pp. 501-3.
Cuervo, A. M., Knecht, E., Terlecky, S. R. and Dice, J. F. (1995) 'Activation of a selective pathway of lysosomal proteolysis in rat liver by prolonged starvation', *Am J Physiol,* 269(5 Pt 1), pp. C1200-8.
Cuervo, A. M., Stefanis, L., Fredenburg, R., Lansbury, P. T. and Sulzer, D. (2004) 'Impaired degradation of mutant alpha-synuclein by chaperone-mediated autophagy', *Science,* 305(5688), pp. 1292-5.
Cullinane, M., Gong, L., Li, X., Lazar-Adler, N., Tra, T., Wolvetang, E., Prescott, M., Boyce, J. D., Devenish, R. J. and Adler, B. (2008) 'Stimulation of autophagy suppresses the intracellular survival of Burkholderia pseudomallei in mammalian cell lines', *Autophagy,* 4(6), pp. 744-53.
Dawaliby, R. and Mayer, A. (2010) 'Microautophagy of the nucleus coincides with a vacuolar diffusion barrier at nuclear-vacuolar junctions', *Mol Biol Cell,* 21(23), pp. 4173-83.
Delgado, M. A., Elmaoued, R. A., Davis, A. S., Kyei, G. and Deretic, V. (2008) 'Toll-like receptors control autophagy', *EMBO J,* 27(7), pp. 1110-21.
Deosaran, E., Larsen, K. B., Hua, R., Sargent, G., Wang, Y., Kim, S., Lamark, T., Jauregui, M., Law, K., Lippincott-Schwartz, J., Brech, A., Johansen, T. and Kim, P. K. (2013) 'NBR1 acts as an autophagy receptor for peroxisomes', *J Cell Sci,* 126(Pt 4), pp. 939-52.
DeVorkin, L. and Gorski, S. M. (2014) 'Monitoring autophagic flux using Ref(2)P, the Drosophila p62 ortholog', *Cold Spring Harb Protoc,* 2014(9), pp. 959-66.
Di Malta, C., Cinque, L. and Settembre, C. (2019) 'Transcriptional Regulation of Autophagy: Mechanisms and Diseases', *Front Cell Dev Biol,* 7, pp. 114.
Diao, J., Liu, R., Rong, Y., Zhao, M., Zhang, J., Lai, Y., Zhou, Q., Wilz, L. M., Li, J., Vivona, S., Pfuetzner, R. A., Brunger, A. T. and Zhong, Q. (2015) 'ATG14 promotes membrane tethering and fusion of autophagosomes to endolysosomes', *Nature,* 520(7548), pp. 563-6.
Dice, J. F., Chiang, H. L., Spencer, E. P. and Backer, J. M. (1986) 'Regulation of catabolism of microinjected ribonuclease A. Identification of residues 7-11 as the essential pentapeptide', *J Biol Chem,* 261(15), pp. 6853-9.
Dikic, I. and Elazar, Z. (2018) 'Mechanism and medical implications of mammalian autophagy', *Nat Rev Mol Cell Biol,* 19(6), pp. 349-364.
Ding, W. X., Ni, H. M., Li, M., Liao, Y., Chen, X., Stolz, D. B., Dorn, G. W., 2nd and Yin, X. M. (2010) 'Nix is critical to two distinct phases of mitophagy, reactive oxygen species-mediated autophagy induction and Parkin-ubiquitin-p62-mediated mitochondrial priming', *J Biol Chem,* 285(36), pp. 27879-90.
Dohi, E., Tanaka, S., Seki, T., Miyagi, T., Hide, I., Takahashi, T., Matsumoto, M. and Sakai, N. (2012) 'Hypoxic stress activates chaperone-mediated autophagy and modulates neuronal cell survival', *Neurochem Int,* 60(4), pp. 431-42.
Efimov, A., Kharitonov, A., Efimova, N., Loncarek, J., Miller, P. M., Andreyeva, N., Gleeson, P., Galjart, N., Maia, A. R., McLeod, I. X., Yates, J. R., 3rd, Maiato, H., Khodjakov, A., Akhmanova, A. and Kaverina, I. (2007) 'Asymmetric CLASP-dependent

nucleation of noncentrosomal microtubules at the trans-Golgi network', *Dev Cell,* 12(6), pp. 917-30.
Eliopoulos, A. G., Havaki, S. and Gorgoulis, V. G. (2016) 'DNA Damage Response and Autophagy: A Meaningful Partnership', *Front Genet,* 7, pp. 204.
Epple, U. D., Suriapranata, I., Eskelinen, E. L. and Thumm, M. (2001) 'Aut5/Cvt17p, a putative lipase essential for disintegration of autophagic bodies inside the vacuole', *J Bacteriol,* 183(20), pp. 5942-55.
Filimonenko, M., Isakson, P., Finley, K. D., Anderson, M., Jeong, H., Melia, T. J., Bartlett, B. J., Myers, K. M., Birkeland, H. C., Lamark, T., Krainc, D., Brech, A., Stenmark, H., Simonsen, A. and Yamamoto, A. (2010) 'The selective macroautophagic degradation of aggregated proteins requires the PI3P-binding protein Alfy', *Mol Cell,* 38(2), pp. 265-79.
Finley, K. D., Edeen, P. T., Cumming, R. C., Mardahl-Dumesnil, M. D., Taylor, B. J., Rodriguez, M. H., Hwang, C. E., Benedetti, M. and McKeown, M. (2003) 'blue cheese mutations define a novel, conserved gene involved in progressive neural degeneration', *J Neurosci,* 23(4), pp. 1254-64.
Friggi-Grelin, F., Rabouille, C. and Therond, P. (2006) 'The cis-Golgi Drosophila GMAP has a role in anterograde transport and Golgi organization in vivo, similar to its mammalian ortholog in tissue culture cells', *Eur J Cell Biol,* 85(11), pp. 1155-66.
Fujimuro, M., Sawada, H. and Yokosawa, H. (1994) 'Production and characterization of monoclonal antibodies specific to multi-ubiquitin chains of polyubiquitinated proteins', *FEBS Lett,* 349(2), pp. 173-80.
Fumagalli, F., Noack, J., Bergmann, T. J., Cebollero, E., Pisoni, G. B., Fasana, E., Fregno, I., Galli, C., Loi, M., Solda, T., D'Antuono, R., Raimondi, A., Jung, M., Melnyk, A., Schorr, S., Schreiber, A., Simonelli, L., Varani, L., Wilson-Zbinden, C., Zerbe, O., Hofmann, K., Peter, M., Quadroni, M., Zimmermann, R. and Molinari, M. (2016) 'Translocon component Sec62 acts in endoplasmic reticulum turnover during stress recovery', *Nat Cell Biol,* 18(11), pp. 1173-1184.
Furuta, S., Hidaka, E., Ogata, A., Yokota, S. and Kamata, T. (2004) 'Ras is involved in the negative control of autophagy through the class I PI3-kinase', *Oncogene,* 23(22), pp. 3898-904.
Gautam, N. K., Verma, P. and Tapadia, M. G. (2017) 'Drosophila Malpighian Tubules: A Model for Understanding Kidney Development, Function, and Disease', *Results Probl Cell Differ,* 60, pp. 3-25.
Geng, J. and Klionsky, D. J. (2008) 'The Atg8 and Atg12 ubiquitin-like conjugation systems in macroautophagy. 'Protein modifications: beyond the usual suspects' review series', *EMBO Rep,* 9(9), pp. 859-64.
Germain, K. and Kim, P. K. (2020) 'Pexophagy: A Model for Selective Autophagy', *Int J Mol Sci,* 21(2).
Gillingham, A. K., Sinka, R., Torres, I. L., Lilley, K. S. and Munro, S. (2014) 'Toward a comprehensive map of the effectors of rab GTPases', *Dev Cell,* 31(3), pp. 358-373.
Glick, B. S. and Malhotra, V. (1998) 'The curious status of the Golgi apparatus', *Cell,* 95(7), pp. 883-9.
Glick, B. S. and Nakano, A. (2009) 'Membrane traffic within the Golgi apparatus', *Annu Rev Cell Dev Biol,* 25, pp. 113-32.
Glick, D., Barth, S. and Macleod, K. F. (2010) 'Autophagy: cellular and molecular mechanisms', *J Pathol,* 221(1), pp. 3-12.

Golic, K. G. and Lindquist, S. (1989) 'The FLP recombinase of yeast catalyzes site-specific recombination in the Drosophila genome', *Cell,* 59(3), pp. 499-509.
Gozuacik, D., Bialik, S., Raveh, T., Mitou, G., Shohat, G., Sabanay, H., Mizushima, N., Yoshimori, T. and Kimchi, A. (2008) 'DAP-kinase is a mediator of endoplasmic reticulum stress-induced caspase activation and autophagic cell death', *Cell Death Differ,* 15(12), pp. 1875-86.
Grumati, P., Morozzi, G., Holper, S., Mari, M., Harwardt, M. I., Yan, R., Muller, S., Reggiori, F., Heilemann, M. and Dikic, I. (2017) 'Full length RTN3 regulates turnover of tubular endoplasmic reticulum via selective autophagy', *Elife,* 6.
Gutierrez, M. G., Master, S. S., Singh, S. B., Taylor, G. A., Colombo, M. I. and Deretic, V. (2004) 'Autophagy is a defense mechanism inhibiting BCG and Mycobacterium tuberculosis survival in infected macrophages', *Cell,* 119(6), pp. 753-66.
Gutierrez, M. G., Saka, H. A., Chinen, I., Zoppino, F. C., Yoshimori, T., Bocco, J. L. and Colombo, M. I. (2007) 'Protective role of autophagy against Vibrio cholerae cytolysin, a pore-forming toxin from V. cholerae', *Proc Natl Acad Sci U S A,* 104(6), pp. 1829-34.
Habisov, S., Huber, J., Ichimura, Y., Akutsu, M., Rogova, N., Loehr, F., McEwan, D. G., Johansen, T., Dikic, I., Doetsch, V., Komatsu, M., Rogov, V. V. and Kirkin, V. (2016) 'Structural and Functional Analysis of a Novel Interaction Motif within UFM1-activating Enzyme 5 (UBA5) Required for Binding to Ubiquitin-like Proteins and Ufmylation', *J Biol Chem,* 291(17), pp. 9025-41.
Hailey, D. W., Rambold, A. S., Satpute-Krishnan, P., Mitra, K., Sougrat, R., Kim, P. K. and Lippincott-Schwartz, J. (2010) 'Mitochondria supply membranes for autophagosome biogenesis during starvation', *Cell,* 141(4), pp. 656-67.
Hamasaki, M., Furuta, N., Matsuda, A., Nezu, A., Yamamoto, A., Fujita, N., Oomori, H., Noda, T., Haraguchi, T., Hiraoka, Y., Amano, A. and Yoshimori, T. (2013) 'Autophagosomes form at ER-mitochondria contact sites', *Nature,* 495(7441), pp. 389-93.
Han, C., Yan, D., Belenkaya, T. Y. and Lin, X. (2005) 'Drosophila glypicans Dally and Dally-like shape the extracellular Wingless morphogen gradient in the wing disc', *Development,* 132(4), pp. 667-79.
Hara, K., Yonezawa, K., Weng, Q. P., Kozlowski, M. T., Belham, C. and Avruch, J. (1998) 'Amino acid sufficiency and mTOR regulate p70 S6 kinase and eIF-4E BP1 through a common effector mechanism', *J Biol Chem,* 273(23), pp. 14484-94.
Hargarten, J. C. and Williamson, P. R. (2018) 'Epigenetic Regulation of Autophagy: A Path to the Control of Autoimmunity', *Front Immunol,* 9, pp. 1864.
He, C. and Klionsky, D. J. (2009) 'Regulation mechanisms and signaling pathways of autophagy', *Annu Rev Genet,* 43, pp. 67-93.
Hegedus, K., Takats, S., Boda, A., Jipa, A., Nagy, P., Varga, K., Kovacs, A. L. and Juhasz, G. (2016) 'The Ccz1-Mon1-Rab7 module and Rab5 control distinct steps of autophagy', *Mol Biol Cell,* 27(20), pp. 3132-3142.
Hu, L. F. (2019) 'Epigenetic Regulation of Autophagy', *Adv Exp Med Biol,* 1206, pp. 221-236.
Huang, S. and Wang, Y. (2017) 'Golgi structure formation, function, and post-translational modifications in mammalian cells', *F1000Res,* 6, pp. 2050.
Hurley, J. H. and Young, L. N. (2017) 'Mechanisms of Autophagy Initiation', *Annu Rev Biochem,* 86, pp. 225-244.

Ichimura, Y., Kumanomidou, T., Sou, Y. S., Mizushima, T., Ezaki, J., Ueno, T., Kominami, E., Yamane, T., Tanaka, K. and Komatsu, M. (2008) 'Structural basis for sorting mechanism of p62 in selective autophagy', *J Biol Chem,* 283(33), pp. 22847-57.
Inoki, K., Ouyang, H., Zhu, T., Lindvall, C., Wang, Y., Zhang, X., Yang, Q., Bennett, C., Harada, Y., Stankunas, K., Wang, C. Y., He, X., MacDougald, O. A., You, M., Williams, B. O. and Guan, K. L. (2006) 'TSC2 integrates Wnt and energy signals via a coordinated phosphorylation by AMPK and GSK3 to regulate cell growth', *Cell,* 126(5), pp. 955-68.
Itakura, E., Kishi, C., Inoue, K. and Mizushima, N. (2008) 'Beclin 1 forms two distinct phosphatidylinositol 3-kinase complexes with mammalian Atg14 and UVRAG', *Mol Biol Cell,* 19(12), pp. 5360-72.
Itakura, E., Kishi-Itakura, C. and Mizushima, N. (2012) 'The hairpin-type tail-anchored SNARE syntaxin 17 targets to autophagosomes for fusion with endosomes/lysosomes', *Cell,* 151(6), pp. 1256-69.
J.Klionsky, K. (2014) *Autophagy: Cancer, Other Pathologies, Inflammation, Immunity, Infection, and Aging. Molecular Process and Physiological Significance of Mitophagy*. Available at: https://www.sciencedirect.com/science/article/pii/B978012405528500002X?via%3Dihub (Accessed: 05/08/21).
Jacomin, A. C., Samavedam, S., Promponas, V. and Nezis, I. P. (2016) 'iLIR database: A web resource for LIR motif-containing proteins in eukaryotes', *Autophagy,* 12(10), pp. 1945-1953.
Jain, A., Rusten, T. E., Katheder, N., Elvenes, J., Bruun, J. A., Sjottem, E., Lamark, T. and Johansen, T. (2015) 'p62/Sequestosome-1, Autophagy-related Gene 8, and Autophagy in Drosophila Are Regulated by Nuclear Factor Erythroid 2-related Factor 2 (NRF2), Independent of Transcription Factor TFEB', *J Biol Chem,* 290(24), pp. 14945-62.
Jin, S. M. and Youle, R. J. (2012) 'PINK1- and Parkin-mediated mitophagy at a glance', *J Cell Sci,* 125(Pt 4), pp. 795-9.
Johansen, T. and Lamark, T. (2011) 'Selective autophagy mediated by autophagic adapter proteins', *Autophagy,* 7(3), pp. 279-96.
Johansen, T. and Lamark, T. (2020) 'Selective Autophagy: ATG8 Family Proteins, LIR Motifs and Cargo Receptors', *J Mol Biol,* 432(1), pp. 80-103.
Juhasz, G., Hill, J. H., Yan, Y., Sass, M., Baehrecke, E. H., Backer, J. M. and Neufeld, T. P. (2008) 'The class III PI(3)K Vps34 promotes autophagy and endocytosis but not TOR signaling in Drosophila', *J Cell Biol,* 181(4), pp. 655-66.
Jung, C. H., Ro, S. H., Cao, J., Otto, N. M. and Kim, D. H. (2010) 'mTOR regulation of autophagy', *FEBS Lett,* 584(7), pp. 1287-95.
Kalvari, I., Tsompanis, S., Mulakkal, N. C., Osgood, R., Johansen, T., Nezis, I. P. and Promponas, V. J. (2014) 'iLIR: A web resource for prediction of Atg8-family interacting proteins', *Autophagy,* 10(5), pp. 913-25.
Kanki, T., Wang, K., Cao, Y., Baba, M. and Klionsky, D. J. (2009) 'Atg32 is a mitochondrial protein that confers selectivity during mitophagy', *Dev Cell,* 17(1), pp. 98-109.
Kaufman, T. C. (2017) 'A Short History and Description of Drosophila melanogaster Classical Genetics: Chromosome Aberrations, Forward Genetic Screens, and the Nature of Mutations', *Genetics,* 206(2), pp. 665-689.
Kawamata, T., Kamada, Y., Kabeya, Y., Sekito, T. and Ohsumi, Y. (2008) 'Organization of the pre-autophagosomal structure responsible for autophagosome formation', *Mol Biol Cell,* 19(5), pp. 2039-50.

Ke Yang, M. L., Zhi Feng, Marta Rojas, Lingjian Zhou, Hongmei Ke, View ORCID ProfileJosé Carlos Pastor-Pareja 2021. ER exit sites in Drosophila display abundant ER-Golgi vesicles and pearled tubes but no megacarriers. bioRxiv.
Khaminets, A., Heinrich, T., Mari, M., Grumati, P., Huebner, A. K., Akutsu, M., Liebmann, L., Stolz, A., Nietzsche, S., Koch, N., Mauthe, M., Katona, I., Qualmann, B., Weis, J., Reggiori, F., Kurth, I., Hubner, C. A. and Dikic, I. (2015) 'Regulation of endoplasmic reticulum turnover by selective autophagy', *Nature,* 522(7556), pp. 354-8.
Kihara, A., Noda, T., Ishihara, N. and Ohsumi, Y. (2001) 'Two distinct Vps34 phosphatidylinositol 3-kinase complexes function in autophagy and carboxypeptidase Y sorting in Saccharomyces cerevisiae', *J Cell Biol,* 152(3), pp. 519-30.
Kim, B. W., Kwon, D. H. and Song, H. K. (2016) 'Structure biology of selective autophagy receptors', *BMB Rep,* 49(2), pp. 73-80.
Kim, E., Goraksha-Hicks, P., Li, L., Neufeld, T. P. and Guan, K. L. (2008) 'Regulation of TORC1 by Rag GTPases in nutrient response', *Nat Cell Biol,* 10(8), pp. 935-45.
Kim, Y. M., Jung, C. H., Seo, M., Kim, E. K., Park, J. M., Bae, S. S. and Kim, D. H. (2015) 'mTORC1 phosphorylates UVRAG to negatively regulate autophagosome and endosome maturation', *Mol Cell,* 57(2), pp. 207-18.
Kirkin, V., McEwan, D. G., Novak, I. and Dikic, I. (2009) 'A role for ubiquitin in selective autophagy', *Mol Cell,* 34(3), pp. 259-69.
Kirkin, V. and Rogov, V. V. (2019) 'A Diversity of Selective Autophagy Receptors Determines the Specificity of the Autophagy Pathway', *Mol Cell,* 76(2), pp. 268-285.
Kissova, I., Salin, B., Schaeffer, J., Bhatia, S., Manon, S. and Camougrand, N. (2007) 'Selective and non-selective autophagic degradation of mitochondria in yeast', *Autophagy,* 3(4), pp. 329-36.
Knaevelsrud, H., Soreng, K., Raiborg, C., Haberg, K., Rasmuson, F., Brech, A., Liestol, K., Rusten, T. E., Stenmark, H., Neufeld, T. P., Carlsson, S. R. and Simonsen, A. (2013) 'Membrane remodeling by the PX-BAR protein SNX18 promotes autophagosome formation', *J Cell Biol,* 202(2), pp. 331-49.
Kouroku, Y., Fujita, E., Tanida, I., Ueno, T., Isoai, A., Kumagai, H., Ogawa, S., Kaufman, R. J., Kominami, E. and Momoi, T. (2007) 'ER stress (PERK/eIF2alpha phosphorylation) mediates the polyglutamine-induced LC3 conversion, an essential step for autophagy formation', *Cell Death Differ,* 14(2), pp. 230-9.
Kraft, C., Reggiori, F. and Peter, M. (2009) 'Selective types of autophagy in yeast', *Biochim Biophys Acta,* 1793(9), pp. 1404-12.
Lamark, T., Kirkin, V., Dikic, I. and Johansen, T. (2009) 'NBR1 and p62 as cargo receptors for selective autophagy of ubiquitinated targets', *Cell Cycle,* 8(13), pp. 1986-90.
Lapierre, L. R., Kumsta, C., Sandri, M., Ballabio, A. and Hansen, M. (2015) 'Transcriptional and epigenetic regulation of autophagy in aging', *Autophagy,* 11(6), pp. 867-80.
Laplante, M. and Sabatini, D. M. (2009) 'mTOR signaling at a glance', *J Cell Sci,* 122(Pt 20), pp. 3589-94.
Lazarou, M., Sliter, D. A., Kane, L. A., Sarraf, S. A., Wang, C., Burman, J. L., Sideris, D. P., Fogel, A. I. and Youle, R. J. (2015) 'The ubiquitin kinase PINK1 recruits autophagy receptors to induce mitophagy', *Nature,* 524(7565), pp. 309-314.

Leber, R., Silles, E., Sandoval, I. V. and Mazon, M. J. (2001) 'Yol082p, a novel CVT protein involved in the selective targeting of aminopeptidase I to the yeast vacuole', *J Biol Chem,* 276(31), pp. 29210-7.
Lee, J. H., Budanov, A. V., Park, E. J., Birse, R., Kim, T. E., Perkins, G. A., Ocorr, K., Ellisman, M. H., Bodmer, R., Bier, E. and Karin, M. (2010) 'Sestrin as a feedback inhibitor of TOR that prevents age-related pathologies', *Science,* 327(5970), pp. 1223-8.
Lee, M. N., Ha, S. H., Kim, J., Koh, A., Lee, C. S., Kim, J. H., Jeon, H., Kim, D. H., Suh, P. G. and Ryu, S. H. (2009) 'Glycolytic flux signals to mTOR through glyceraldehyde-3-phosphate dehydrogenase-mediated regulation of Rheb', *Mol Cell Biol,* 29(14), pp. 3991-4001.
Lei, Y. and Klionsky, D. J. (2019) 'UIM-UDS: a new interface between ATG8 and its interactors', *Cell Res,* 29(7), pp. 507-508.
Li, J., Ni, M., Lee, B., Barron, E., Hinton, D. R. and Lee, A. S. (2008) 'The unfolded protein response regulator GRP78/BiP is required for endoplasmic reticulum integrity and stress-induced autophagy in mammalian cells', *Cell Death Differ,* 15(9), pp. 1460-71.
Li, L., Fang, R., Liu, B., Shi, H., Wang, Y., Zhang, W., Zhang, X. and Ye, L. (2016a) 'Deacetylation of tumor-suppressor MST1 in Hippo pathway induces its degradation through HBXIP-elevated HDAC6 in promotion of breast cancer growth', *Oncogene,* 35(31), pp. 4048-57.
Li, L., Zhao, G. D., Shi, Z., Qi, L. L., Zhou, L. Y. and Fu, Z. X. (2016b) 'The Ras/Raf/MEK/ERK signaling pathway and its role in the occurrence and development of HCC', *Oncol Lett,* 12(5), pp. 3045-3050.
Li, W. and Zhang, L. (2019) 'Regulation of ATG and Autophagy Initiation', *Adv Exp Med Biol,* 1206, pp. 41-65.
Li, Y., Wang, Y., Kim, E., Beemiller, P., Wang, C. Y., Swanson, J., You, M. and Guan, K. L. (2007) 'Bnip3 mediates the hypoxia-induced inhibition on mammalian target of rapamycin by interacting with Rheb', *J Biol Chem,* 282(49), pp. 35803-13.
Lin, S. Y., Li, T. Y., Liu, Q., Zhang, C., Li, X., Chen, Y., Zhang, S. M., Lian, G., Liu, Q., Ruan, K., Wang, Z., Zhang, C. S., Chien, K. Y., Wu, J., Li, Q., Han, J. and Lin, S. C. (2012) 'GSK3-TIP60-ULK1 signaling pathway links growth factor deprivation to autophagy', *Science,* 336(6080), pp. 477-81.
Liu, C. C., Lin, Y. C., Chen, Y. H., Chen, C. M., Pang, L. Y., Chen, H. A., Wu, P. R., Lin, M. Y., Jiang, S. T., Tsai, T. F. and Chen, R. H. (2016) 'Cul3-KLHL20 Ubiquitin Ligase Governs the Turnover of ULK1 and VPS34 Complexes to Control Autophagy Termination', *Mol Cell,* 61(1), pp. 84-97.
Liu, L., Feng, D., Chen, G., Chen, M., Zheng, Q., Song, P., Ma, Q., Zhu, C., Wang, R., Qi, W., Huang, L., Xue, P., Li, B., Wang, X., Jin, H., Wang, J., Yang, F., Liu, P., Zhu, Y., Sui, S. and Chen, Q. (2012) 'Mitochondrial outer-membrane protein FUNDC1 mediates hypoxia-induced mitophagy in mammalian cells', *Nat Cell Biol,* 14(2), pp. 177-85.
Liu, Z., Chen, P., Gao, H., Gu, Y., Yang, J., Peng, H., Xu, X., Wang, H., Yang, M., Liu, X., Fan, L., Chen, S., Zhou, J., Sun, Y., Ruan, K., Cheng, S., Komatsu, M., White, E., Li, L., Ji, H., Finley, D. and Hu, R. (2014) 'Ubiquitylation of autophagy receptor Optineurin by HACE1 activates selective autophagy for tumor suppression', *Cancer Cell,* 26(1), pp. 106-20.

Lodish H, B. A., Zipursky SL (2000) *Molecular Cell Biology. Overview of the Secretory Pathway.*: New York: W. H. Freeman. Available at: https://www.ncbi.nlm.nih.gov/books/NBK21471/.
Long, X., Lin, Y., Ortiz-Vega, S., Yonezawa, K. and Avruch, J. (2005a) 'Rheb binds and regulates the mTOR kinase', *Curr Biol,* 15(8), pp. 702-13.
Long, X., Ortiz-Vega, S., Lin, Y. and Avruch, J. (2005b) 'Rheb binding to mammalian target of rapamycin (mTOR) is regulated by amino acid sufficiency', *J Biol Chem,* 280(25), pp. 23433-6.
Lu, L. Q., Tang, M. Z., Qi, Z. H., Huang, S. F., He, Y. Q., Li, D. K., Li, L. F. and Chen, L. X. (2020) 'Regulation of the Golgi apparatus via GOLPH3-mediated new selective autophagy', *Life Sci,* 253, pp. 117700.
Lucocq, J. M., Berger, E. G. and Warren, G. (1989) 'Mitotic Golgi fragments in HeLa cells and their role in the reassembly pathway', *J Cell Biol,* 109(2), pp. 463-74.
Lum, J. J., Bauer, D. E., Kong, M., Harris, M. H., Li, C., Lindsten, T. and Thompson, C. B. (2005) 'Growth factor regulation of autophagy and cell survival in the absence of apoptosis', *Cell,* 120(2), pp. 237-48.
Lynch-Day, M. A. and Klionsky, D. J. (2010) 'The Cvt pathway as a model for selective autophagy', *FEBS Lett,* 584(7), pp. 1359-66.
Lystad, A. H., Ichimura, Y., Takagi, K., Yang, Y., Pankiv, S., Kanegae, Y., Kageyama, S., Suzuki, M., Saito, I., Mizushima, T., Komatsu, M. and Simonsen, A. (2014) 'Structural determinants in GABARAP required for the selective binding and recruitment of ALFY to LC3B-positive structures', *EMBO Rep,* 15(5), pp. 557-65.
Ma, P., Schwarten, M., Schneider, L., Boeske, A., Henke, N., Lisak, D., Weber, S., Mohrluder, J., Stoldt, M., Strodel, B., Methner, A., Hoffmann, S., Weiergraber, O. H. and Willbold, D. (2013) 'Interaction of Bcl-2 with the autophagy-related GABAA receptor-associated protein (GABARAP): biophysical characterization and functional implications', *J Biol Chem,* 288(52), pp. 37204-15.
Mandell, M. A., Kimura, T., Jain, A., Johansen, T. and Deretic, V. (2014) 'TRIM proteins regulate autophagy: TRIM5 is a selective autophagy receptor mediating HIV-1 restriction', *Autophagy,* 10(12), pp. 2387-8.
Marshall, R. S., Hua, Z., Mali, S., McLoughlin, F. and Vierstra, R. D. (2019) 'ATG8-Binding UIM Proteins Define a New Class of Autophagy Adaptors and Receptors', *Cell,* 177(3), pp. 766-781 e24.
Martina, J. A., Chen, Y., Gucek, M. and Puertollano, R. (2012) 'MTORC1 functions as a transcriptional regulator of autophagy by preventing nuclear transport of TFEB', *Autophagy,* 8(6), pp. 903-14.
Matecic, M., Smith, D. L., Pan, X., Maqani, N., Bekiranov, S., Boeke, J. D. and Smith, J. S. (2010) 'A microarray-based genetic screen for yeast chronological aging factors', *PLoS Genet,* 6(4), pp. e1000921.
Matthiesen, R. (2013) *Mass spectrometry data analysis in proteomics. Methods in molecular biology,* Second edition. edn. New York: Humana Press.
McEwan, D. G., Popovic, D., Gubas, A., Terawaki, S., Suzuki, H., Stadel, D., Coxon, F. P., Miranda de Stegmann, D., Bhogaraju, S., Maddi, K., Kirchof, A., Gatti, E., Helfrich, M. H., Wakatsuki, S., Behrends, C., Pierre, P. and Dikic, I. (2015) 'PLEKHM1 regulates autophagosome-lysosome fusion through HOPS complex and LC3/GABARAP proteins', *Mol Cell,* 57(1), pp. 39-54.

Mizushima, N. (2007) 'Autophagy: process and function', *Genes Dev,* 21(22), pp. 2861-73.
Mizushima, N., Noda, T. and Ohsumi, Y. (1999) 'Apg16p is required for the function of the Apg12p-Apg5p conjugate in the yeast autophagy pathway', *EMBO J,* 18(14), pp. 3888-96.
Mochida, K., Oikawa, Y., Kimura, Y., Kirisako, H., Hirano, H., Ohsumi, Y. and Nakatogawa, H. (2015) 'Receptor-mediated selective autophagy degrades the endoplasmic reticulum and the nucleus', *Nature,* 522(7556), pp. 359-62.
Muller, O., Sattler, T., Flotenmeyer, M., Schwarz, H., Plattner, H. and Mayer, A. (2000) 'Autophagic tubes: vacuolar invaginations involved in lateral membrane sorting and inverse vesicle budding', *J Cell Biol,* 151(3), pp. 519-28.
Munoz-Gamez, J. A., Rodriguez-Vargas, J. M., Quiles-Perez, R., Aguilar-Quesada, R., Martin-Oliva, D., de Murcia, G., Menissier de Murcia, J., Almendros, A., Ruiz de Almodovar, M. and Oliver, F. J. (2009) 'PARP-1 is involved in autophagy induced by DNA damage', *Autophagy,* 5(1), pp. 61-74.
Munro, S. (2011) 'The golgin coiled-coil proteins of the Golgi apparatus', *Cold Spring Harb Perspect Biol,* 3(6).
Murcia, L., Clemente-Ruiz, M., Pierre-Elies, P., Royou, A. and Milan, M. (2019) 'Selective Killing of RAS-Malignant Tissues by Exploiting Oncogene-Induced DNA Damage', *Cell Rep,* 28(1), pp. 119-131 e4.
Murphy, M. P. (2009) 'How mitochondria produce reactive oxygen species', *Biochem J,* 417(1), pp. 1-13.
Muschalik, N. and Munro, S. (2018) 'Golgins', *Curr Biol,* 28(8), pp. R374-R376.
Nakamura, N. (2010) 'Emerging new roles of GM130, a cis-Golgi matrix protein, in higher order cell functions', *J Pharmacol Sci,* 112(3), pp. 255-64.
Nakamura, S. and Yoshimori, T. (2017) 'New insights into autophagosome-lysosome fusion', *J Cell Sci,* 130(7), pp. 1209-1216.
Nakato, H., Futch, T. A. and Selleck, S. B. (1995) 'The division abnormally delayed (dally) gene: a putative integral membrane proteoglycan required for cell division patterning during postembryonic development of the nervous system in Drosophila', *Development,* 121(11), pp. 3687-702.
Nakatogawa, H., Ohbayashi, S., Sakoh-Nakatogawa, M., Kakuta, S., Suzuki, S. W., Kirisako, H., Kondo-Kakuta, C., Noda, N. N., Yamamoto, H. and Ohsumi, Y. (2012) 'The autophagy-related protein kinase Atg1 interacts with the ubiquitin-like protein Atg8 via the Atg8 family interacting motif to facilitate autophagosome formation', *J Biol Chem,* 287(34), pp. 28503-7.
Nascimbeni, A. C., Giordano, F., Dupont, N., Grasso, D., Vaccaro, M. I., Codogno, P. and Morel, E. (2017) 'ER-plasma membrane contact sites contribute to autophagosome biogenesis by regulation of local PI3P synthesis', *EMBO J,* 36(14), pp. 2018-2033.
Neisch, A. L., Neufeld, T. P. and Hays, T. S. (2017) 'A STRIPAK complex mediates axonal transport of autophagosomes and dense core vesicles through PP2A regulation', *J Cell Biol,* 216(2), pp. 441-461.
Nezis, I. P. (2012) 'Selective autophagy in Drosophila', *Int J Cell Biol,* 2012, pp. 146767.
Nezis, I. P., Shravage, B. V., Sagona, A. P., Lamark, T., Bjorkoy, G., Johansen, T., Rusten, T. E., Brech, A., Baehrecke, E. H. and Stenmark, H. (2010) 'Autophagic degradation of dBruce controls DNA fragmentation in nurse cells during late Drosophila melanogaster oogenesis', *J Cell Biol,* 190(4), pp. 523-31.

Nezis, I. P., Simonsen, A., Sagona, A. P., Finley, K., Gaumer, S., Contamine, D., Rusten, T. E., Stenmark, H. and Brech, A. (2008) 'Ref(2)P, the Drosophila melanogaster homologue of mammalian p62, is required for the formation of protein aggregates in adult brain', *J Cell Biol,* 180(6), pp. 1065-71.
Nobukuni, T., Joaquin, M., Roccio, M., Dann, S. G., Kim, S. Y., Gulati, P., Byfield, M. P., Backer, J. M., Natt, F., Bos, J. L., Zwartkruis, F. J. and Thomas, G. (2005) 'Amino acids mediate mTOR/raptor signaling through activation of class 3 phosphatidylinositol 3OH-kinase', *Proc Natl Acad Sci U S A,* 102(40), pp. 14238-43.
Noda, N. N., Kumeta, H., Nakatogawa, H., Satoo, K., Adachi, W., Ishii, J., Fujioka, Y., Ohsumi, Y. and Inagaki, F. (2008) 'Structural basis of target recognition by Atg8/LC3 during selective autophagy', *Genes Cells,* 13(12), pp. 1211-8.
Noda, N. N., Ohsumi, Y. and Inagaki, F. (2010) 'Atg8-family interacting motif crucial for selective autophagy', *FEBS Lett,* 584(7), pp. 1379-85.
Nordmann, M., Cabrera, M., Perz, A., Brocker, C., Ostrowicz, C., Engelbrecht-Vandre, S. and Ungermann, C. (2010) 'The Mon1-Ccz1 complex is the GEF of the late endosomal Rab7 homolog Ypt7', *Curr Biol,* 20(18), pp. 1654-9.
Noyes, N. C., Walkinshaw, E. and Davis, R. L. (2020) 'Ras acts as a molecular switch between two forms of consolidated memory in Drosophila', *Proc Natl Acad Sci U S A,* 117(4), pp. 2133-2139.
Nthiga, T. M., Kumar Shrestha, B., Lamark, T. and Johansen, T. (2021) 'The soluble reticulophagy receptor CALCOCO1 is also a Golgiphagy receptor', *Autophagy*, pp. 1-2.
Nthiga, T. M., Shrestha, B. K., Lamark, T. and Johansen, T. (2020) 'CALCOCO1 is a soluble reticulophagy receptor', *Autophagy,* 16(9), pp. 1729-1731.
Okamoto, K., Kondo-Okamoto, N. and Ohsumi, Y. (2009) 'Mitochondria-anchored receptor Atg32 mediates degradation of mitochondria via selective autophagy', *Dev Cell,* 17(1), pp. 87-97.
Okatsu, K., Saisho, K., Shimanuki, M., Nakada, K., Shitara, H., Sou, Y. S., Kimura, M., Sato, S., Hattori, N., Komatsu, M., Tanaka, K. and Matsuda, N. (2010) 'p62/SQSTM1 cooperates with Parkin for perinuclear clustering of depolarized mitochondria', *Genes Cells,* 15(8), pp. 887-900.
Pankiv, S., Clausen, T. H., Lamark, T., Brech, A., Bruun, J. A., Outzen, H., Overvatn, A., Bjorkoy, G. and Johansen, T. (2007) 'p62/SQSTM1 binds directly to Atg8/LC3 to facilitate degradation of ubiquitinated protein aggregates by autophagy', *J Biol Chem,* 282(33), pp. 24131-45.
Papadopoulos, C., Kravic, B. and Meyer, H. (2020) 'Repair or Lysophagy: Dealing with Damaged Lysosomes', *J Mol Biol,* 432(1), pp. 231-239.
Papandreou, I., Lim, A. L., Laderoute, K. and Denko, N. C. (2008) 'Hypoxia signals autophagy in tumor cells via AMPK activity, independent of HIF-1, BNIP3, and BNIP3L', *Cell Death Differ,* 15(10), pp. 1572-81.
Papinski, D. and Kraft, C. (2016) 'Regulation of Autophagy By Signaling Through the Atg1/ULK1 Complex', *J Mol Biol,* 428(9 Pt A), pp. 1725-41.
Park, C., Suh, Y. and Cuervo, A. M. (2015) 'Regulated degradation of Chk1 by chaperone-mediated autophagy in response to DNA damage', *Nat Commun,* 6, pp. 6823.
Park, S. W., Jun, Y. W., Jeon, P., Lee, Y. K., Park, J. H., Lee, S. H., Lee, J. A. and Jang, D. J. (2019) 'LIR motifs and the membrane-targeting domain are complementary in the function of RavZ', *BMB Rep,* 52(12), pp. 700-705.

Parrish, W. R., Stefan, C. J. and Emr, S. D. (2004) 'Essential role for the myotubularin-related phosphatase Ymr1p and the synaptojanin-like phosphatases Sjl2p and Sjl3p in regulation of phosphatidylinositol 3-phosphate in yeast', *Mol Biol Cell,* 15(8), pp. 3567-79.
Parzych, K. R. and Klionsky, D. J. (2014) 'An overview of autophagy: morphology, mechanism, and regulation', *Antioxid Redox Signal,* 20(3), pp. 460-73.
Pernet-Gallay, K., Antony, C., Johannes, L., Bornens, M., Goud, B. and Rios, R. M. (2002) 'The overexpression of GMAP-210 blocks anterograde and retrograde transport between the ER and the Golgi apparatus', *Traffic,* 3(11), pp. 822-32.
Popelka, H. and Klionsky, D. J. (2015) 'Analysis of the native conformation of the LIR/AIM motif in the Atg8/LC3/GABARAP-binding proteins', *Autophagy,* 11(12), pp. 2153-9.
Ravikumar, B., Moreau, K., Jahreiss, L., Puri, C. and Rubinsztein, D. C. (2010) 'Plasma membrane contributes to the formation of pre-autophagosomal structures', *Nat Cell Biol,* 12(8), pp. 747-57.
Reggiori, F. and Tooze, S. A. (2012) 'Autophagy regulation through Atg9 traffic', *J Cell Biol,* 198(2), pp. 151-3.
Reggiori, F., Tucker, K. A., Stromhaug, P. E. and Klionsky, D. J. (2004) 'The Atg1-Atg13 complex regulates Atg9 and Atg23 retrieval transport from the pre-autophagosomal structure', *Dev Cell,* 6(1), pp. 79-90.
Reggiori, F. and Ungermann, C. (2017) 'Autophagosome Maturation and Fusion', *J Mol Biol,* 429(4), pp. 486-496.
Rios, R. M., Sanchis, A., Tassin, A. M., Fedriani, C. and Bornens, M. (2004) 'GMAP-210 recruits gamma-tubulin complexes to cis-Golgi membranes and is required for Golgi ribbon formation', *Cell,* 118(3), pp. 323-35.
Roboti, P., Sato, K. and Lowe, M. (2015) 'The golgin GMAP-210 is required for efficient membrane trafficking in the early secretory pathway', *J Cell Sci,* 128(8), pp. 1595-606.
Rogov, V. V., Stolz, A., Ravichandran, A. C., Rios-Szwed, D. O., Suzuki, H., Kniss, A., Löhr, F., Wakatsuki, S., Dötsch, V., Dikic, I., Dobson, R. C. and McEwan, D. G. (2017) 'Structural and functional analysis of the GABARAP interaction motif (GIM)', *EMBO Rep,* 18(8), pp. 1382-1396.
Rothman, J. E. and Wieland, F. T. (1996) 'Protein sorting by transport vesicles', *Science,* 272(5259), pp. 227-34.
Rubinsztein, D. C., Marino, G. and Kroemer, G. (2011) 'Autophagy and aging', *Cell,* 146(5), pp. 682-95.
Rutschmann, S., Jung, A. C., Zhou, R., Silverman, N., Hoffmann, J. A. and Ferrandon, D. (2000) 'Role of Drosophila IKK gamma in a toll-independent antibacterial immune response', *Nat Immunol,* 1(4), pp. 342-7.
Ryan, T. A. and Tumbarello, D. A. (2018) 'Optineurin: A Coordinator of Membrane-Associated Cargo Trafficking and Autophagy', *Front Immunol,* 9, pp. 1024.
Sagne, C., Agulhon, C., Ravassard, P., Darmon, M., Hamon, M., El Mestikawy, S., Gasnier, B. and Giros, B. (2001) 'Identification and characterization of a lysosomal transporter for small neutral amino acids', *Proc Natl Acad Sci U S A,* 98(13), pp. 7206-11.
Sahu, R., Kaushik, S., Clement, C. C., Cannizzo, E. S., Scharf, B., Follenzi, A., Potolicchio, I., Nieves, E., Cuervo, A. M. and Santambrogio, L. (2011) 'Microautophagy of cytosolic proteins by late endosomes', *Dev Cell,* 20(1), pp. 131-9.

Sakaki, K., Wu, J. and Kaufman, R. J. (2008) 'Protein kinase Ctheta is required for autophagy in response to stress in the endoplasmic reticulum', *J Biol Chem,* 283(22), pp. 15370-80.
Sanjuan, M. A., Dillon, C. P., Tait, S. W., Moshiach, S., Dorsey, F., Connell, S., Komatsu, M., Tanaka, K., Cleveland, J. L., Withoff, S. and Green, D. R. (2007) 'Toll-like receptor signalling in macrophages links the autophagy pathway to phagocytosis', *Nature,* 450(7173), pp. 1253-7.
Sardiello, M., Palmieri, M., di Ronza, A., Medina, D. L., Valenza, M., Gennarino, V. A., Di Malta, C., Donaudy, F., Embrione, V., Polishchuk, R. S., Banfi, S., Parenti, G., Cattaneo, E. and Ballabio, A. (2009) 'A gene network regulating lysosomal biogenesis and function', *Science,* 325(5939), pp. 473-7.
Satoh, A., Wang, Y., Malsam, J., Beard, M. B. and Warren, G. (2003) 'Golgin-84 is a rab1 binding partner involved in Golgi structure', *Traffic,* 4(3), pp. 153-61.
Scherz-Shouval, R., Shvets, E., Fass, E., Shorer, H., Gil, L. and Elazar, Z. (2007) 'Reactive oxygen species are essential for autophagy and specifically regulate the activity of Atg4', *EMBO J,* 26(7), pp. 1749-60.
Schofield, C. J. and Ratcliffe, P. J. (2004) 'Oxygen sensing by HIF hydroxylases', *Nat Rev Mol Cell Biol,* 5(5), pp. 343-54.
Schwarten, M., Mohrluder, J., Ma, P., Stoldt, M., Thielmann, Y., Stangler, T., Hersch, N., Hoffmann, B., Merkel, R. and Willbold, D. (2009) 'Nix directly binds to GABARAP: a possible crosstalk between apoptosis and autophagy', *Autophagy,* 5(5), pp. 690-8.
Scott, S. V., Guan, J., Hutchins, M. U., Kim, J. and Klionsky, D. J. (2001) 'Cvt19 is a receptor for the cytoplasm-to-vacuole targeting pathway', *Mol Cell,* 7(6), pp. 1131-41.
Settembre, C., Di Malta, C., Polito, V. A., Garcia Arencibia, M., Vetrini, F., Erdin, S., Erdin, S. U., Huynh, T., Medina, D., Colella, P., Sardiello, M., Rubinsztein, D. C. and Ballabio, A. (2011) 'TFEB links autophagy to lysosomal biogenesis', *Science,* 332(6036), pp. 1429-33.
Sharma, V., Verma, S., Seranova, E., Sarkar, S. and Kumar, D. (2018) 'Selective Autophagy and Xenophagy in Infection and Disease', *Front Cell Dev Biol,* 6, pp. 147.
Shaw, J., Yurkova, N., Zhang, T., Gang, H., Aguilar, F., Weidman, D., Scramstad, C., Weisman, H. and Kirshenbaum, L. A. (2008) 'Antagonism of E2F-1 regulated Bnip3 transcription by NF-kappaB is essential for basal cell survival', *Proc Natl Acad Sci U S A,* 105(52), pp. 20734-9.
Shaw, R. J., Bardeesy, N., Manning, B. D., Lopez, L., Kosmatka, M., DePinho, R. A. and Cantley, L. C. (2004) 'The LKB1 tumor suppressor negatively regulates mTOR signaling', *Cancer Cell,* 6(1), pp. 91-9.
Shefa, U., Jeong, N. Y., Song, I. O., Chung, H. J., Kim, D., Jung, J. and Huh, Y. (2019) 'Mitophagy links oxidative stress conditions and neurodegenerative diseases', *Neural Regen Res,* 14(5), pp. 749-756.
Shen, W. C., Li, H. Y., Chen, G. C., Chern, Y. and Tu, P. H. (2015) 'Mutations in the ubiquitin-binding domain of OPTN/optineurin interfere with autophagy-mediated degradation of misfolded proteins by a dominant-negative mechanism', *Autophagy,* 11(4), pp. 685-700.
Shi, C. S. and Kehrl, J. H. (2008) 'MyD88 and Trif target Beclin 1 to trigger autophagy in macrophages', *J Biol Chem,* 283(48), pp. 33175-82.

Shin, J. J. H., Gillingham, A. K., Begum, F., Chadwick, J. and Munro, S. (2017) 'TBC1D23 is a bridging factor for endosomal vesicle capture by golgins at the trans-Golgi', *Nat Cell Biol,* 19(12), pp. 1424-1432.
Shintani, T. and Klionsky, D. J. (2004) 'Cargo proteins facilitate the formation of transport vesicles in the cytoplasm to vacuole targeting pathway', *J Biol Chem,* 279(29), pp. 29889-94.
Shoji, J. Y., Kikuma, T., Arioka, M. and Kitamoto, K. (2010) 'Macroautophagy-mediated degradation of whole nuclei in the filamentous fungus Aspergillus oryzae', *PLoS One,* 5(12), pp. e15650.
Sinka, R., Gillingham, A. K., Kondylis, V. and Munro, S. (2008) 'Golgi coiled-coil proteins contain multiple binding sites for Rab family G proteins', *J Cell Biol,* 183(4), pp. 607-15.
Smith, M. D., Harley, M. E., Kemp, A. J., Wills, J., Lee, M., Arends, M., von Kriegsheim, A., Behrends, C. and Wilkinson, S. (2018) 'CCPG1 Is a Non-canonical Autophagy Cargo Receptor Essential for ER-Phagy and Pancreatic ER Proteostasis', *Dev Cell,* 44(2), pp. 217-232 e11.
Smits, P., Bolton, A. D., Funari, V., Hong, M., Boyden, E. D., Lu, L., Manning, D. K., Dwyer, N. D., Moran, J. L., Prysak, M., Merriman, B., Nelson, S. F., Bonafe, L., Superti-Furga, A., Ikegawa, S., Krakow, D., Cohn, D. H., Kirchhausen, T., Warman, M. L. and Beier, D. R. (2010) 'Lethal skeletal dysplasia in mice and humans lacking the golgin GMAP-210', *N Engl J Med,* 362(3), pp. 206-16.
Soreng, K., Neufeld, T. P. and Simonsen, A. (2018) 'Membrane Trafficking in Autophagy', *Int Rev Cell Mol Biol,* 336, pp. 1-92.
Sriskanthadevan-Pirahas, S., Lee, J. and Grewal, S. S. (2018) 'The EGF/Ras pathway controls growth in Drosophila via ribosomal RNA synthesis', *Dev Biol,* 439(1), pp. 19-29.
Stalder, D. and Gershlick, D. C. (2020) 'Direct trafficking pathways from the Golgi apparatus to the plasma membrane', *Semin Cell Dev Biol,* 107, pp. 112-125.
Stanley, H., Botas, J. and Malhotra, V. (1997) 'The mechanism of Golgi segregation during mitosis is cell type-specific', *Proc Natl Acad Sci U S A,* 94(26), pp. 14467-70.
Stokoe, D., Stephens, L. R., Copeland, T., Gaffney, P. R., Reese, C. B., Painter, G. F., Holmes, A. B., McCormick, F. and Hawkins, P. T. (1997) 'Dual role of phosphatidylinositol-3,4,5-trisphosphate in the activation of protein kinase B', *Science,* 277(5325), pp. 567-70.
Stroupe, C., Collins, K. M., Fratti, R. A. and Wickner, W. (2006) 'Purification of active HOPS complex reveals its affinities for phosphoinositides and the SNARE Vam7p', *EMBO J,* 25(8), pp. 1579-89.
Su, T. Y., Nakato, E., Choi, P. Y. and Nakato, H. (2018) 'Drosophila Glypicans Regulate Follicle Stem Cell Maintenance and Niche Competition', *Genetics,* 209(2), pp. 537-549.
Suzuki, K., Kubota, Y., Sekito, T. and Ohsumi, Y. (2007) 'Hierarchy of Atg proteins in pre-autophagosomal structure organization', *Genes Cells,* 12(2), pp. 209-18.
Takeo, S., Akiyama, T., Firkus, C., Aigaki, T. and Nakato, H. (2005) 'Expression of a secreted form of Dally, a Drosophila glypican, induces overgrowth phenotype by affecting action range of Hedgehog', *Dev Biol,* 284(1), pp. 204-18.
Talloczy, Z., Virgin, H. W. t. and Levine, B. (2006) 'PKR-dependent autophagic degradation of herpes simplex virus type 1', *Autophagy,* 2(1), pp. 24-9.

Tekirdag, K. and Cuervo, A. M. (2018) 'Chaperone-mediated autophagy and endosomal microautophagy: Joint by a chaperone', *J Biol Chem,* 293(15), pp. 5414-5424.
Terawaki, S., Camosseto, V., Prete, F., Wenger, T., Papadopoulos, A., Rondeau, C., Combes, A., Rodriguez Rodrigues, C., Vu Manh, T. P., Fallet, M., English, L., Santamaria, R., Soares, A. R., Weil, T., Hammad, H., Desjardins, M., Gorvel, J. P., Santos, M. A., Gatti, E. and Pierre, P. (2015) 'RUN and FYVE domain-containing protein 4 enhances autophagy and lysosome tethering in response to Interleukin-4', *J Cell Biol,* 210(7), pp. 1133-52.
Ting Zhang, L. G., Yanan Yang (2020) 'Mammalian ATG9s drive the autophagosome formation by binding to LC3', *bioRxiv*.
Tripathi, D. N., Chowdhury, R., Trudel, L. J., Tee, A. R., Slack, R. S., Walker, C. L. and Wogan, G. N. (2013) 'Reactive nitrogen species regulate autophagy through ATM-AMPK-TSC2-mediated suppression of mTORC1', *Proc Natl Acad Sci U S A,* 110(32), pp. E2950-7.
Tusco, R., Jacomin, A. C., Jain, A., Penman, B. S., Larsen, K. B., Johansen, T. and Nezis, I. P. (2017) 'Kenny mediates selective autophagic degradation of the IKK complex to control innate immune responses', *Nat Commun,* 8(1), pp. 1264.
Tyanova, S. and Cox, J. (2018) 'Perseus: A Bioinformatics Platform for Integrative Analysis of Proteomics Data in Cancer Research', *Methods Mol Biol,* 1711, pp. 133-148.
Tyanova, S., Temu, T. and Cox, J. (2016) 'The MaxQuant computational platform for mass spectrometry-based shotgun proteomics', *Nat Protoc,* 11(12), pp. 2301-2319.
Vander Haar, E., Lee, S. I., Bandhakavi, S., Griffin, T. J. and Kim, D. H. (2007) 'Insulin signalling to mTOR mediated by the Akt/PKB substrate PRAS40', *Nat Cell Biol,* 9(3), pp. 316-23.
Venken, K. J. and Bellen, H. J. (2014) 'Chemical mutagens, transposons, and transgenes to interrogate gene function in Drosophila melanogaster', *Methods,* 68(1), pp. 15-28.
Vincow, E. S., Merrihew, G., Thomas, R. E., Shulman, N. J., Beyer, R. P., MacCoss, M. J. and Pallanck, L. J. (2013) 'The PINK1-Parkin pathway promotes both mitophagy and selective respiratory chain turnover in vivo', *Proc Natl Acad Sci U S A,* 110(16), pp. 6400-5.
Viret, C., Rozieres, A. and Faure, M. (2018) 'Novel Insights into NDP52 Autophagy Receptor Functioning', *Trends Cell Biol,* 28(4), pp. 255-257.
von Muhlinen, N., Akutsu, M., Ravenhill, B. J., Foeglein, A., Bloor, S., Rutherford, T. J., Freund, S. M., Komander, D. and Randow, F. (2012) 'LC3C, bound selectively by a noncanonical LIR motif in NDP52, is required for antibacterial autophagy', *Mol Cell,* 48(3), pp. 329-42.
von Muhlinen, N., Thurston, T., Ryzhakov, G., Bloor, S. and Randow, F. (2010) 'NDP52, a novel autophagy receptor for ubiquitin-decorated cytosolic bacteria', *Autophagy,* 6(2), pp. 288-9.
Walczak, M. and Martens, S. (2013) 'Dissecting the role of the Atg12-Atg5-Atg16 complex during autophagosome formation', *Autophagy,* 9(3), pp. 424-5.
Wang, D. Y., Wang, J. and Deng, D. (2020) 'Golgi phosphoprotein-3 (GOLPH3) promote metastasis of nasopharyngeal carcinoma through regulating E-cadherin', *Eur Rev Med Pharmacol Sci,* 24(17), pp. 8871-8879.

Wang, J., Davis, S., Zhu, M., Miller, E. A. and Ferro-Novick, S. (2017) 'Autophagosome formation: Where the secretory and autophagy pathways meet', *Autophagy,* 13(5), pp. 973-974.
Wehrle, A., Witkos, T. M., Unger, S., Schneider, J., Follit, J. A., Hermann, J., Welting, T., Fano, V., Hietala, M., Vatanavicharn, N., Schoner, K., Spranger, J., Schmidts, M., Zabel, B., Pazour, G. J., Bloch-Zupan, A., Nishimura, G., Superti-Furga, A., Lowe, M. and Lausch, E. (2019) 'Hypomorphic mutations of TRIP11 cause odontochondrodysplasia', *JCI Insight,* 4(3).
Wei, H., Liu, L. and Chen, Q. (2015) 'Selective removal of mitochondria via mitophagy: distinct pathways for different mitochondrial stresses', *Biochim Biophys Acta,* 1853(10 Pt B), pp. 2784-90.
Wei, Y., Pattingre, S., Sinha, S., Bassik, M. and Levine, B. (2008) 'JNK1-mediated phosphorylation of Bcl-2 regulates starvation-induced autophagy', *Mol Cell,* 30(6), pp. 678-88.
Weidberg, H., Shvets, E., Shpilka, T., Shimron, F., Shinder, V. and Elazar, Z. (2010) 'LC3 and GATE-16/GABARAP subfamilies are both essential yet act differently in autophagosome biogenesis', *EMBO J,* 29(11), pp. 1792-802.
Wild, P., Farhan, H., McEwan, D. G., Wagner, S., Rogov, V. V., Brady, N. R., Richter, B., Korac, J., Waidmann, O., Choudhary, C., Dotsch, V., Bumann, D. and Dikic, I. (2011) 'Phosphorylation of the autophagy receptor optineurin restricts Salmonella growth', *Science,* 333(6039), pp. 228-33.
Wisniewski, J. R., Zougman, A., Nagaraj, N. and Mann, M. (2009) 'Universal sample preparation method for proteome analysis', *Nat Methods,* 6(5), pp. 359-62.
Wong, M. and Munro, S. (2014) 'Membrane trafficking. The specificity of vesicle traffic to the Golgi is encoded in the golgin coiled-coil proteins', *Science,* 346(6209), pp. 1256898.
Wong, P. M., Puente, C., Ganley, I. G. and Jiang, X. (2013) 'The ULK1 complex: sensing nutrient signals for autophagy activation', *Autophagy,* 9(2), pp. 124-37.
Wong, Y. C. and Holzbaur, E. L. (2014) 'Optineurin is an autophagy receptor for damaged mitochondria in parkin-mediated mitophagy that is disrupted by an ALS-linked mutation', *Proc Natl Acad Sci U S A,* 111(42), pp. E4439-48.
Wu, S., Fu, J., Dong, Y., Yi, Q., Lu, D., Wang, W., Qi, Y., Yu, R. and Zhou, X. (2018) 'GOLPH3 promotes glioma progression via facilitating JAK2-STAT3 pathway activation', *J Neurooncol,* 139(2), pp. 269-279.
Xie, Y., Kang, R., Sun, X., Zhong, M., Huang, J., Klionsky, D. J. and Tang, D. (2015) 'Posttranslational modification of autophagy-related proteins in macroautophagy', *Autophagy,* 11(1), pp. 28-45.
Xu, H., Boulianne, G. L. and Trimble, W. S. (2002) 'Drosophila syntaxin 16 is a Q-SNARE implicated in Golgi dynamics', *J Cell Sci,* 115(Pt 23), pp. 4447-55.
Yamaguchi M., Y. H. (2018) *Drosophila Models for Human Diseases. . Advances in Experimental Medicine and Biology*: Springer, Singapore. . Available at: https://link.springer.com/chapter/10.1007%2F978-981-13-0529-0_1.
Yamamoto, H., Kakuta, S., Watanabe, T. M., Kitamura, A., Sekito, T., Kondo-Kakuta, C., Ichikawa, R., Kinjo, M. and Ohsumi, Y. (2012) 'Atg9 vesicles are an important membrane source during early steps of autophagosome formation', *J Cell Biol,* 198(2), pp. 219-33.

Yamasaki, A. and Noda, N. N. (2017) 'Structural Biology of the Cvt Pathway', *J Mol Biol,* 429(4), pp. 531-542.
Yan, C., Liu, J., Gao, J., Sun, Y., Zhang, L., Song, H., Xue, L., Zhan, L., Gao, G., Ke, Z., Liu, Y. and Liu, J. (2019) 'IRE1 promotes neurodegeneration through autophagy-dependent neuron death in the Drosophila model of Parkinson's disease', *Cell Death Dis,* 10(11), pp. 800.
Yang, Z. and Klionsky, D. J. (2007) 'Permeases recycle amino acids resulting from autophagy', *Autophagy,* 3(2), pp. 149-50.
Yorimitsu, T. and Klionsky, D. J. (2005) 'Atg11 links cargo to the vesicle-forming machinery in the cytoplasm to vacuole targeting pathway', *Mol Biol Cell,* 16(4), pp. 1593-605.
Youle, R. J. and Narendra, D. P. (2011) 'Mechanisms of mitophagy', *Nat Rev Mol Cell Biol,* 12(1), pp. 9-14.
Yu, Z. Q., Ni, T., Hong, B., Wang, H. Y., Jiang, F. J., Zou, S., Chen, Y., Zheng, X. L., Klionsky, D. J., Liang, Y. and Xie, Z. (2012) 'Dual roles of Atg8-PE deconjugation by Atg4 in autophagy', *Autophagy,* 8(6), pp. 883-92.
Yung, H. W., Charnock-Jones, D. S. and Burton, G. J. (2011) 'Regulation of AKT phosphorylation at Ser473 and Thr308 by endoplasmic reticulum stress modulates substrate specificity in a severity dependent manner', *PLoS One,* 6(3), pp. e17894.
Zachari, M. and Ganley, I. G. (2017) 'The mammalian ULK1 complex and autophagy initiation', *Essays Biochem,* 61(6), pp. 585-596.
Zaffagnini, G. and Martens, S. (2016) 'Mechanisms of Selective Autophagy', *J Mol Biol,* 428(9 Pt A), pp. 1714-24.
Zalckvar, E., Berissi, H., Mizrachy, L., Idelchuk, Y., Koren, I., Eisenstein, M., Sabanay, H., Pinkas-Kramarski, R. and Kimchi, A. (2009) 'DAP-kinase-mediated phosphorylation on the BH3 domain of beclin 1 promotes dissociation of beclin 1 from Bcl-XL and induction of autophagy', *EMBO Rep,* 10(3), pp. 285-92.
Zens, B., Sawa-Makarska, J. and Martens, S. (2015) 'In vitro systems for Atg8 lipidation', *Methods,* 75, pp. 37-43.
Zhang, J. and Ney, P. A. (2009) 'Role of BNIP3 and NIX in cell death, autophagy, and mitophagy', *Cell Death Differ,* 16(7), pp. 939-46.
Zhang, Y., You, J., Ren, W. and Lin, X. (2013) 'Drosophila glypicans Dally and Dally-like are essential regulators for JAK/STAT signaling and Unpaired distribution in eye development', *Dev Biol,* 375(1), pp. 23-32.
Zhao, C., Zhang, J., Ma, L., Wu, H., Zhang, H., Su, J., Geng, B., Yao, Q. and Zheng, J. (2020) 'GOLPH3 Promotes Angiogenesis of Lung Adenocarcinoma by Regulating the Wnt/beta-Catenin Signaling Pathway', *Onco Targets Ther,* 13, pp. 6265-6277.
Zhao, D. and Du, L. L. (2020) 'Epr1, a UPR-upregulated soluble autophagy receptor for reticulophagy', *Autophagy,* 16(11), pp. 2112-2113.
Zhou, J., Yang, J., Fan, X., Hu, S., Zhou, F., Dong, J., Zhang, S., Shang, Y., Jiang, X., Guo, H., Chen, N., Xiao, X., Sheng, J., Wu, K., Nie, Y. and Fan, D. (2016) 'Chaperone-mediated autophagy regulates proliferation by targeting RND3 in gastric cancer', *Autophagy,* 12(3), pp. 515-28.
Zhu, W., Smith, J. W. and Huang, C. M. (2010) 'Mass spectrometry-based label-free quantitative proteomics', *J Biomed Biotechnol,* 2010, pp. 840518.
Zhu, Y., Massen, S., Terenzio, M., Lang, V., Chen-Lindner, S., Eils, R., Novak, I., Dikic, I., Hamacher-Brady, A. and Brady, N. R. (2013) 'Modulation of serines 17 and 24 in the

LC3-interacting region of Bnip3 determines pro-survival mitophagy versus apoptosis', *J Biol Chem,* 288(2), pp. 1099-113.
Zoncu, R., Bar-Peled, L., Efeyan, A., Wang, S., Sancak, Y. and Sabatini, D. M. (2011) 'mTORC1 senses lysosomal amino acids through an inside-out mechanism that requires the vacuolar H(+)-ATPase', *Science,* 334(6056), pp. 678-83.

# Chapter 10 Appendix

**Title:**

# GMAP is an Atg8a-interacting protein that regulates Golgi turnover in *Drosophila*

Ashrafur Rahman[1], Peter Lőrincz[2,3], Gabor Juhász[2,4], Yan Zhang[1,5,6] and Ioannis P. Nezis[1,6]*

[1] School of Life Sciences, University of Warwick, CV4 7AL Coventry, UK.

[2]Department of Anatomy, Cell and Developmental Biology, Eötvös Loránd University, Budapest, Hungary.

[3]Premium Postdoctoral Research Program, Hungarian Academy of Sciences, Budapest, Hungary.

[4]Institute of Genetics, Biological Research Centre, Szeged, Hungary.

[5] State Key Laboratory of Silkworm Genome Biology, Biological Science Research Center, Southwest University, Chongqing 400715, China.

[6]senior authors

*Corresponding author (email: I.Nezis@warwick.ac.uk).

## Abstract

Selective autophagy receptors and adaptors contain short linear motifs called LIR motifs (LC3-interacting region) which are required for the interaction with the Atg8-family proteins. LIR motifs bind to the hydrophobic pockets of the LIR docking site (LDS) of the respective Atg8-family proteins. The physiological significance of LDS binding site has not been clarified. Here, we show that Atg8a-LDS mutant *Drosophila* flies accumulate autophagy substrates and have reduced lifespan. Using quantitative proteomics to identify the proteins that accumulate in Atg8a-LDS mutants, we identified the cis-Golgi protein GMAP (Golgi microtubule-associated protein) as a novel LIR-motif containing protein that interacts with Atg8a. GMAP LIR-mutant flies exhibit accumulation of Golgi markers and elongated Golgi morphology. Our data suggest that GMAP mediates the turnover of Golgi by selective autophagy to regulate its morphology and size via its LIR-motif dependent interaction with Atg8a.

## Introduction

Autophagy is an evolutionary conserved process where the cells degrade their own cellular material. It is involved in protein and organelle degradation and plays an essential role in both cellular and whole-animal homeostasis. Autophagy is a cellular response in nutrient starvation but also responsible for removing aggregated proteins, damaged organelles, invading bacteria & viruses (Lamb, Yoshimori and Tooze, 2013; Randow and Youle, 2014). There are various types of autophagy such as macroautophagy, microautophagy and chaperone-mediated autophagy (Lamb, Yoshimori and Tooze, 2013). During macroautophagy there is sequestration of cellular material into double-membrane vesicles called autophagosomes. The autophagosomes are subsequently fused with the lysosomes where the sequestered cargoes are degraded by lysosomal hydrolases. The products of degradation are transported back into the cytoplasm through lysosomal membrane permeases and can be reused by the cell (Lamb, Yoshimori and Tooze, 2013). Although it was initially believed that autophagy occurs randomly inside the cell, it is now established that sequestration and degradation of cytoplasmic material by autophagy can be selective through receptor and adaptor proteins (Randow and Youle, 2014; Johansen and Lamark, 2020).

Selective autophagy receptors and adaptors contain short linear motifs called LIR motifs (LC3- interacting region motifs), LC3 recognition sequences (LRS) or Atg8-interacting motifs (AIM), which are required for the interaction with Atg8-family proteins (Atg8/LC3/GABARAP) (Pankiv *et al.*, 2007; Ichimura *et al.*, 2008; Noda, Ohsumi and Inagaki, 2010). LIR-motif containing proteins (LIRCPs) bind via their LIR motif to the hydrophobic pocket 1 (HP1) and hydrophobic pocket HP2 of the LIR docking site (LDS) of the respective Atg8 protein (Johansen and Lamark, 2020). Another type of interaction with Atg8 proteins that is LIR motif/LDS-independent was also recently identified (Marshall *et al.*, 2019). Despite the growing identification of selective autophagy receptors and adaptors in mammals, the regulation and mechanisms of action of selective autophagy receptors and adaptors and the physiological significance of Atg8's LDS docking site are poorly described in the fruit fly *Drosophila melanogaster.*

Selective autophagy mediates the degradation of organelles (Anding and Baehrecke, 2017). However, autophagic degradation of Golgi apparatus is not well studied (Mijaljica, Prescott and Devenish, 2006; Lu *et al.*, 2020; De Tito *et al.*, 2020; Nthiga *et al.*, 2021). In this study, we created Atg8a LDS mutant flies using CRISPR. Atg8a LDS mutants exhibit a similar phenotype with Atg8a full mutant flies, like accumulation of ubiquitin positive aggregates and reduced lifespan. To identify the proteins that accumulate in these mutants we performed quantitative proteomics. We identified GMAP, a cis Golgi protein, as a novel Atg8a interacting protein that regulates Golgi turnover.

## Results and discussion

### Generation and characterization of Atg8a$^{K48A/Y49A}$ mutants

To elucidate the physiological significance of Atg8a-LIRCPs interactions in *Drosophila*, we used CRISPR to generate Atg8a$^{K48A/Y49A}$ mutants (Suppl. Fig. 1A, B). Atg8a$^{K48A/Y49A}$ flies have two point mutations (K48A & Y49A) within the hydrophobic LDS of Atg8a that abolish interactions with LIR motif containing proteins (Johansen and Lamark, 2020). The K48A/Y49A mutation was confirmed using genomic sequencing (Fig. 1A). Expression of Atg8a is observed in the wild type flies (WT) as well as the Atg8a$^{K48A/Y49A}$ mutants. This shows that ATG8a is successfully being expressed in Atg8a$^{K48A/Y49A}$ mutant flies. Atg8a mutant flies were used as a negative control as there was no expression of Atg8a (Suppl. Fig. 1A). Atg8a$^{K48A/Y49A}$ flies are homozygous viable. To examine whether Atg8a$^{K48A/Y49A}$ flies accumulate LIRCPs, we did western blotting for Ref(2)P and Kenny, two proteins that have been shown to interact with Atg8a via a LIR motif (Jain *et al*, 2015; Nezis *et al.*, 2008; Tusco *et al.*, 2017). Western blotting analysis showed that Ref(2)P, Kenny as well as ubiquitin accumulated in Atg8a$^{K48A/Y49A}$ mutant flies, (Figs. 1B and 1C), indicating that LIR motif is important for their degradation by autophagy. We further used immunofluorescence confocal microscopy to determine the expression of Ref(2)P in adult *Drosophila* brain and found that Atg8a$^{K48A/Y49A}$ mutant flies showed a significant number of Ref(2)P- and ubiquitin-positive structures (Fig. 1D). We also observed that

Atg8a$^{K48A/Y49A}$ mutant flies have a short lifespan which was similar to that of Atg8a full mutant flies (Fig. 1E). All together these data show that Atg8a's LDS docking site is physiologically important for the function of Atg8a protein to degrade LIRCPs.

**Quantitative proteomics analysis of Atg8a$^{K48A/Y49A}$ mutants**

To identify the proteins that accumulate in Atg8a$^{K48A/Y49A}$ mutants, we collected 2-week-old fly heads and performed quantitative proteomics analysis. Analysis by LC-MS/MS identified 3036, 2342, 2468 proteins from wild type, Atg8a and Atg8a$^{K48A/Y49A}$ mutant fly heads (Supplementary Table S1). Principal component analysis (PCA) divided the twelve protein samples into obvious three groups, wild type, Atg8a and Atg8a$^{K48A/Y49A}$ mutant (Fig 2A). To identify the up-regulated proteins in mutant flies, we set the cut-off p-value as less than 0.05 together with a difference of more than two-fold between mutant and wild-type flies (Supplementary Table S2). 29 proteins passed these two criteria and showed up-regulated expression in both of Atg8a and Atg8a$^{K48A/Y49A}$ mutant (Fig 2B and Supplementary Table S2). Among them, Ref(2)P (Fig 2C) has been already shown to have a functional LIR motif (Jain *et al.*, 2015). GMAP (Golgi microtubule associated protein) was also shown to be significantly upregulated in Atg8a$^{K48A/Y49A}$ flies (Fig 2C).

**GMAP is a novel Atg8a-interacting protein**

GMAP is a cis-Golgi protein that has a role in anterograde transport and Golgi organization in vivo (Friggi-Grelin, Rabouille and Therond, 2006; Sinka *et al.*, 2008). To verify the proteomics data, we tested if GMAP accumulates in Atg8a LDS mutants. Western blot analysis showed that GMAP is accumulated in Atg8a and ATG8a$^{K48A/Y49A}$ mutant flies compared to wild type flies (Figs. 3A and 3B). We further used immunofluorescence confocal microscopy to determine the expression pattern of GMAP in adult *Drosophila* brain. We observed that there is a significant increase in the number of GMAP and ubiquitin-positive structures in the adult brain of Atg8a and ATG8a$^{K48A/Y49A}$ mutant flies, compared to wild type files (Fig. 3C). Additionally, the size of GMAP puncta was significantly increased in Atg8a and ATG8a$^{K48A/Y49A}$ mutant

flies (Figs. 3C and 3D). These data suggest that selective autophagy regulate the size and morphology of the cis Golgi.

GMAP is a coiled-coil protein which has 12 coiled-coil domains and a GRAB domain (Friggi-Grelin, Rabouille and Therond, 2006; Sinka *et al.*, 2008) (Fig. 4A). We used iLIR software (Kalvari *et al.*, 2014; Jacomin *et al.*, 2016) to predict functional LIR motifs in the GMAP protein. GMAP has a predicted LIR motif at position 320–325 with the sequence DEFIVV (Fig. 4B). To examine whether GMAP interacts with Atg8a and has a functional LIR motif, we performed GST pulldowns and we confirmed the direct interaction between GMAP and Atg8a (Figs. 4C and 4D). Atg8a-LDS showed significantly less binding to GMAP (Figs. 4C and 4D). Additionally, point mutations of the GMAP LIR motif in positions 322 and 325 by alanine substitutions of the aromatic and hydrophobic residues (F322A and V325A) reduced its binding to Atg8a (Figs. 4E and F). These results together indicate that GMAP interacts with Atg8a in a LIR motif dependent manner.

**GMAP mediates Golgi turnover**

Since GMAP is a cis Golgi protein that interacts with Atg8a we examined if it regulates the autophagic degradation of the Golgi complex. We observed that GMAP colocalizes with mCherry-Atg8a during starvation (Fig. 5A). We also observed that the Golgi marker GM130 accumulates in Atg8a LDS and Atg8a full mutants suggesting that autophagy regulates Golgi turnover (Fig. 5B). Additionally, knockdown of GMAP also led to accumulation of GM130 (Fig 5C). To elucidate the role of GMAP in Golgiphagy we used CRISPR/Cas9 technology to generate GMAP LIR mutants (GMAP F322A V325A) (Suppl. Fig. 1C). $GMAP^{F322A/V325A}$ mutants are homozygous viable. To examine whether $GMAP^{F322A/V325A}$ mutant flies accumulate Golgi markers, we used western blotting. We observed that GM130 significantly accumulates in GMAP LIR mutant flies (Fig. 5D). We further used immunofluorescence confocal microscopy to examine the morphology of the Golgi using GM130, in adult *Drosophila* brain of $GMAP^{F322A/V325A}$ and Atg8a mutant flies. We observed that Golgi appeared to be deformed and elongated compared to wild type flies (Figs. 5E and 5F). To further examine Golgi morphology, we used transmission electron microscopy.

We observed that the area and length of cis Golgi compartments is significantly larger in GMAP LIR mutants compared to controls (Suppl. Figure 2). All together these results suggest that GMAP regulates Golgi complex turnover via selective autophagy.

Molecular mechanisms of selective autophagy are mostly characterized in mammals (Johansen and Lamark, 2020). To elucidate selective autophagy in the fruit fly Drosophila melanogaster, we created Atg8a LDS mutants that cannot bind LIRCPs. Atg8a LDS mutants have a similar phenotype with Atg8a full mutants: i) they are homozygous viable, ii) they accumulate experimentally verified LIRCPs and ubiquitinated proteins, iii) and they have reduced lifespan. These results show that LIR motif is important for the function of Atg8a in autophagy in vivo.

Selective of autophagy mitochondria, peroxisomes, lysosomes and ER has been described and their receptors have been identified (Johansen and Lamark, 2020). Golgi turnover by autophagy is poorly described. Very recently work by Johansen group identified CALCOCO1 as a selective autophagy receptor for Golgiphagy (Nthiga *et al.*, 2021). They showed that CALCOCO1 binds the Golgi palmitoyl-transferase ZDHHC17 to mediate Golgi degradation by autophagy during starvation. Depletion of CALCOCO1 causes expansion of the Golgi and accumulation of its proteins. Here, we show that in *Drosophila*, cis Golgi protein GMAP binds directly to Atg8a (without the involvement of an intermediate receptor) to mediate Golgi turnover and control the size and morphology of the Golgi complex. GMAP binding to Atg8a is mediated by a LIR motif and GMAP LIR motif mutants exhibit accumulation of Golgi markers and elongated Golgi morphology.

In summary, we have shown that LDS binding pocket in Atg8a plays an important role in the execution of autophagy. We identified the cis Golgi protein GMAP as a novel Atg8a-intarcting protein. We suggest that GMAP mediates Golgi turnover via its LIR motif dependent interaction with Atg8a. Our study highlights the physiological importance of Atg8a's LDS binding pocket and opens new avenues in the regulation of Golgi turnover by selective autophagy.

## Materials and Methods

### Fly Husbandry and generation of Transgenic Lines

Flies used in experiments were kept at 25C and 70% humidity raised on cornmeal-based feed. CRISPR-mediated mutagenesis was performed by WellGenetics Inc. For generation of Atg8a-LDS and GMAP-LIR mutants, selected gRNA sequences were cloned into U6 promoter plasmid(s). Cassettes K48A/Y49A-PBacDsRed and F322A/V325A-PBacDsRed containing two PiggyBac sites, 3xP3-DsRed, designed point mutation and two 1kb-homology arms were cloned into pUC57-Kan as donor template for repair. Atg8a- and GMAP targeting gRNAs and hs-Cas9 were supplied in DNA plasmids, together with donor plasmid for microinjection into embryos of control strain w[1118]. F1 flies carrying selection marker of 3xP3-RFP were further validated by genomic PCR and sequencing. CRISPR generates a break in Atg8a and GMAP and is replaced by cassettes K48A/Y49A-PBacDsRed and F322A/V325A-PBacDsRed respectively.

### Protein extraction and western blotting

Protein content was extracted from the head and the full fly body in RIAP lysis buffer (50 mM Tris pH 7.4, 150 mM NaCl, 1% Igepal, 0.5% sodium deoxycholate, 0.1% SDS supplemented with EDTA-free proteases inhibitors cocktail, Roche, 5892791001) using a motorized mortar and pestle. Protein concentrations were determined by the Bradford method. 100-200 µg proteins were loaded on polyacrylamide gels and were transferred onto PVDF membranes (cold wet transfer in 10% ethanol for 1h at 100V). Membranes were blocked in 5% non-fat milk in TBST (0.1% Tween-20 in TBS) for 1h. Primary antibodies diluted in TBST were incubated overnight at 4C with gentle agitation. HRP-coupled secondary antibodies binding was done at room temperature (RT) for 1 h in 1% non-fat milk dissolved in TBST and ECL mix incubation for 2 min. All washes were performed for 10 min in TBST at RT. The following primary antibodies were used:

*List of antibodies used for western blotting*

| Antibody | Dilution | Source |
|---|---|---|
| Rabbit pAb to Ref(2)p | 1:2000 | Abcam |
| Kenny | 1:5000 | Gift from Dr N. Silverman |
| Mouse mAb to mono/poly-ubiquitinated proteins (FK2) | 1:1000 | Cell Signalling Technology |
| Rabbit pAb to GM130 | 1:10,000 | Abcam |
| Mouse mAb to 6x His tag | 1:1000 | Abcam |
| Rabbit pAb to dGMAP | 1:2000 | Gift from Dr Pascal Therond |
| Mouse Anti-Tubulin | 1:40,000 | Sigma-Aldrich |
| Rabbit Anti-Mouse IgG HRP | 1:5000 | Thermo Scientific |
| Goat Anti-Rabbit IgG HRP | 1:5000 | Thermo Scientific |

Protein bands were quantified using ImageJ/FIJI 2.0. A histogram was generated for each band where the peaks were proportional to the intensity of the band. The area under the curve was used as the quantitative value. Where necessary these bands were normalised to control bands. At least three biological repeats were done and averaged. Statistical analysis was done using a one sample-two tailed t-test.

**Immunohistochemistry**

Fly tissues were dissected in PBS and fixed for 30 min in 4% formaldehyde in PBS. Blocking and antibody incubations were performed in PBT (0.3% BSA, 0.3% Triton X-100 in PBS). Primary antibodies were incubated overnight at 4 °C in PBST, secondary antibodies were incubated 2 h at room temperature in PBST. Samples were observed under a Zeiss 880 confocal microscope. The following primary antibodies were used:

| Antibody | Dilution | Source |
|---|---|---|
| Rabbit pAb to Ref(2)p | 1:500 | Abcam |
| Mouse mAb to mono/poly-ubiquitinated proteins (FK2) | 1:500 | Gift from Dr N. Silverman |
| Rabbit pAb to GM130 | 1:1000 | Abcam |

| | | |
|---|---|---|
| Goat pAb anti-GMAP | 1:1000 | Developmental Studies Hybridoma Bank |
| Rabbit Anti-Goat IgG CF488A | 1:1000 | Sigma |
| Goat Anti-Mouse IgG CF488A | 1:1000 | Sigma |
| Chicken Anti-Goat IgG CF488A | 1:1000 | Sigma |
| Goat Anti-Rabbit IgG CF568 | 1:1000 | Sigma |
| Goat Anti-Mouse IgG CF568 | 1:1000 | Sigma |
| Donkey Anti-Mouse IgG CF568 | 1:1000 | Sigma |

**Proteomics**

Proteins were extracted from the drosophila head by using RIAP buffer. Solubilized proteins were recovered by centrifugation (12,000 g, 10 min) and placed in an ultrafiltration tube (MWCO 3,000, Millipore, USA), and reduced with 15 mM dithiothreitol for 120 min, and alkylated with 50 mM iodoacetamide for 60 min in the dark. Protein samples were washed three times with 50 mM NH4HCO3 and then digested with trypsin at a weight ratio of 1:50 (trypsin:protein) for 20 hours at 37°C. Tryptic peptides were recovered by centrifugation, lyophilized, and resuspended in 40 μL 0.1% formic acid. Tryptic peptides (4 μL) were separated on a Thermo Fisher Scientific EASY-nLC 1000 system using a Thermo Fisher Scientific EASY-Spray column (C18, 2 μm, 100 Å, 50 μm × 15 cm), and were analyzed using a Thermo Scientific Q Exactive mass spectrometer. Four biological replicates were used for the LC-MS/MS analyses. Mass spectra raw data were analysed using MaxQuant software. Peptide searches were performed with Andromeda search algorithms. All common contaminants and reverse hits were removed. The label-free intensity quantification (LFQ) algorithm in MaxQuant was used to estimates the protein abundance. Identified proteins were listed in Supplementary Table S1. FactorMineR was used to perform PCA analysis on the basis of protein expression (log10-transformed LFQ values). To find the differential proteins between wild-type and mutant drosophila, unpaired t-tests were used with a significance level set at $p < 0.05$ and a cut-off difference of more than two-fold (Supplementary Table S2). LIR motifs were predicted using iLIR software at https://ilir.warwick.ac.uk/.

**Lifespan measurement**

All fly lines used were isogenic. We used the Kaplan-Meier method to measure lifespan of flies, which estimates survival probability of each risk group according to daily death events counted. Male and female flies were collected within 24 hours from hatching and cohorts of 20-25 flies were maintained on standard or autoclaved/antibiotics supplemented *Drosophila* food at 25ºC in a humidified incubator. Flies were transferred into new tubes every 2-3 days. Dead events were recorded daily. Survival curves were constructed in Prism (GraphPad, versions 8 and 9), which was also used to perform the statistical analysis for curve comparison using the Mantel-Cox test.

**Plasmid constructs**

GMAP plasmid were obtained from Drosophila Genomics Resource Centre. Sequences of the GMAP were amplified by PCR and inserted in desired plasmid using either Gateway recombination system or restriction enzyme cloning. PCR products were amplified from cDNA using Phusion high fidelity DNA polymerase with primers containing the Gateway recombination site or restriction enzyme sites for Gateway entry vector and cloned into pDONR221 or pENTR using Gateway recombination cloning. Point mutants were generated using the QuickChange site-directed mutagenesis (Stratagene, 200523). Plasmid constructs were verified by conventional restriction enzyme digestion and/or by DNA sequencing (Applied Biosystems, 4337455). Primers are as follow:

GMAP truncated protein: Forward Primer: CGGAATTCATGTCGTGGCTGAACAGC
Reverse Primer (R490):
CCGCTCGAGTTATTAGTCCGCATCGTCCA.

Primers for GMAP F322A/V325A mutagenesis: Forward Primer: GCACAGCGAGGATGAGGCCATAGTTGCACGCCAAGCGGATGCC
Reverse Primer:

GGCATCCGCTTGGCGTGCAACTATGGCCTCATCCTCGCTGTGC

**GST Pull-down assays**

GST-fusion proteins were expressed in *Escherichia coli* Rosetta2. GST pull-down assays were performed using recombinant proteins produced in bacteria. A volume of 10 mL of the in vitro translation reaction products (0.5 mg of plasmid in a 25 mL reaction volume) were incubated with 1–10 mg of GST-recombinant protein in 200 mL of NETN buffer (50 mM Tris, pH 8.0, 150 mM NaCl, 1 mM EDTA,
0.5% Nonidet P-40, 1 mM dithiothreitol supplemented with Complete Mini EDTA-free protease inhibitor cocktail (Roche Applied Science)) for 2 h at 4C, washed six times with 1 mL of NETN buffer, boiled with 2X SDS gel loading buffer, and subjected to SDS-PAGE. Gels were stained with Coomassie Blue and vacuum- dried.

**Transmission Electron Microscopy**

Brains of 20 days (after emerging from the pupal case) old adult control and mutant animals were dissected in ice cold PBS, then fixed with 3.2% paraformaldehyde, 1% glutaraldehyde, 1% sucrose, and 3mM $CaCl_2$ in 0.1 N sodium cacodylate (pH 7.4, overnight, 4 $^{o}$C). Next day samples were washed with sodium cacodylate then post-fixed in 0.5% osmium tetroxide (60 min, RT) then in half-saturated aqueous uranyl acetate (30 min, RT). Samples were then dehydrated in graded series of ethanol and embedded in araldite to the manufacturer's instructions. Ultrathin sections were stained with Reynold's lead citrate and viewed at 80kV operating voltage on a JEM-1011 transmission electron microscope (JEOL) equipped with a Morada digital camera (Olympus) using iTEM software (Olympus). All reagents and materials used for electron microscopy were obtained from Merck. The area and width of cis-Golgi cisterns were measured using iTEM software (Olympus). Cells with whole Golgi apparatus were quantified and only the cis-Golgi cisterns facing the nucleus (first cistern) were measured to avoid the possibility of misidentification of different cisterns. Cells in which the whole Golgi apparatus were not present and therefore it was not possible to identify the first cis-Golgi cistern were not evaluated. The quantified data were evaluated using SPSS21 (IBM) and independent samples t-test.

**Statistical analysis and reproducibility**

Statistical analyses were done with Prism6/7 software (GraphPad). For the comparison of two groups, two-tailed *t*-test was used.

## Figure legends

**Figure 1. Characterization of Atg8a$^{K48A/Y49A}$ (LDS) mutant flies. (A)** Genomic DNA from Atg8a $^{K48A/Y49A}$ mutant flies was extracted, and the sequenced results confirmed the successful incorporation of the K48A/Y49A mutations. **(B)** Wild type, Atg8a and Atg8a$^{K48A/Y49A}$ mutant flies were aged for 2 weeks. Western blot analysis of lysates from whole flies showed that Ref(2)P, Kenny and ubiquitin were accumulated in both Atg8a and Atg8a$^{K48A/Y49A}$ mutant flies. **(C)** Quantifications of the western blottings in B shows significant accumulations of the aforementioned proteins in both Atg8a and ATG8a$^{K48A/Y49A}$ mutant flies. **(D)** Confocal images from 2-week-old adult brains. Ref(2)P (green) and ubiquitin (red) aggregates (arrows) can be seen in Atg8a and ATG8a$^{K48A/Y49A}$ mutant flies and not in wild type flies. DNA was dyed with Hoechst (blue). Scale bars are 60 μm. **(E)** Survival test of wild type, Atg8a and ATG8a$^{K48A/Y49A}$ mutant flies. The results show that Atg8a and ATG8a$^{K48A/Y49A}$ mutant flies have a short lifespan.

Bar charts show means ± s.d. Statistical significance was determined using two-tailed Student's *t*-test. *$p < 0.05$, **$p < 0.01$, ***$p < 0.001$.

**Figure 2. Quantitative proteomic analysis of Atg8a$^{K48A/Y49A}$ mutant flies**. **(A)** PCA analysis of wild type, Atg8a and ATG8a$^{K48A/Y49A}$ mutant adult Drosophila heads. Two-week-old male flies were selected and collected the heads to perform the proteomics. Four biological replicates were performed for each sample. PCA analysis divided the twelve protein samples into obvious three groups. **(B)** Venn diagram representing up-regulated genes in Drosophila mutant flies. The cut-off p-value was set as less than 0.05 together with a difference of more than two-fold between mutant and wild type drosophila heads. 29 proteins passed these two criteria and showed up-regulated

expression in both of Atg8a and ATG8a$^{K48A/Y49A}$ mutants. **(C)** The iBAQ intensity is used to show upregulation of Ref(2)P and GMAP. Bar charts show means ± s.d. *$p < 0.05$, **$p < 0.01$, and ***$p < 0.001$.

**Figure 3. Accumulation of GMAP in Atg8a and ATG8a$^{K48A/Y49A}$ mutant flies. (A)** Western blot analysis shows that GMAP is accumulated in both Atg8a and ATG8a$^{K48A/Y49A}$ mutant flies. **(B)** Quantification of GMAP in Atg8a and ATG8a$^{K48A/Y49A}$ mutant flies. **(C)** Confocal images from 2-week-old adult brains, GMAP (green) and ubiquitin (red) aggregates (arrows) can be seen in Atg8a and ATG8a$^{K48A/Y49A}$ mutant flies and not in wild type flies. DNA was dyed with Hoechst (blue). Scale bars are 10 μm. **(D)** Average GMAP puncta size is larger in Atg8a and ATG8a$^{K48A/Y49A}$ mutant flies compared to wild type flies. Bar charts show means ± s.d. Statistical significance was determined using two-tailed Student's *t*-test. *$p < 0.05$.

**Figure 4. GMAP interacts with Atg8a via a LIR motif**. **(A)** Structure of GMAP. GMAP is a coiled-coil protein which has 12 coiled-coil domains (gray) and a GRAB domain (red). Yellow represent the predicted LIR motif. **(B)** GMAP has a predicted LIR motif as identified using iLIR at position 320-325. **(C-D)** GST-pull-down assay between GST-tagged Atg8a-WT or GST-tagged Atg8a-LDS mutant and GMAP. GMAP interacts with Atg8a-WT but significantly less with Atg8a-LDS. GST was used as negative control. **(E-F)** GST-pull-down assay between GST-tagged Atg8a-WT and GMAP or GMAP LIR mutant. GMAP interacts with Atg8a. Point mutations of the GMAP LIR motif in positions 322 and 325 by alanine substitutions of the aromatic and hydrophobic residues (F322A and V325A) significantly reduced its binding to Atg8a. GST was used as negative control. Truncated form of GMAP (1-490 aa) was used. Bar charts show means ± s.d. Statistical significance was determined using two-tailed Student's *t*-test. **$p < 0.01$.

**Figure 5. GMAP regulates Golgi turnover via autophagy**. **(A)** Confocal images showing co-localisation of mCherry-Atg8a and the Golgi marker GM130 under

starvation conditions in larval fat body. **(B)** Western blots showing accumulation of the Golgi marker GM130 in Atg8a and ATG8a$^{K48A/Y49A}$ mutant flies compared to wild type flies and its quantification below. **(C)** Western blots showing accumulation of GM130 in GMAP RNAi lines compared to control RNAi and its quantification shown below. **(D)** Western blots showing accumulation of GM130 in GMAP LIR mutant flies (GMAP $^{F322A/V325A}$) compared to wild type flies, and its quantification shown below. **(E)** Immunofluorescence confocal microscopy of *Drosophila* brain showing increased accumulation of the golgi marker (GM130) and the altered morphology of Golgi in GMAP $^{F322A/V325A}$ and ATG8a mutant flies. Scale bars are 10 μm. **(F)** Quantification of relative size of GM130 puncta shown as a ratio of large puncta (> 1 μm) to small puncta (< 1 μm). Significantly more large puncta were seen in GMAP $^{F322A/V325A}$ and ATG8a mutant flies compared to wild type flies. Bar charts show means ± s.d. Statistical significance was determined using two-tailed Student's *t*-test. *$p < 0.05$, **$p < 0.01$, ***$p < 0.001$.

## References:


Anding, A. L. and Baehrecke, E. H. (2017) 'Cleaning House: Selective Autophagy of Organelles', *Dev Cell,* 41(1), pp. 10-22.

De Tito S, Hervás JH, van Vliet AR, Tooze SA (2020) . The Golgi as an Assembly Line to the Autophagosome. Trends Biochem Sci. 2020 Jun;45(6):484-496.

Friggi-Grelin, F., Rabouille, C. and Therond, P. (2006) 'The cis-Golgi Drosophila GMAP has a role in anterograde transport and Golgi organization in vivo, similar to its mammalian ortholog in tissue culture cells', *Eur J Cell Biol,* 85(11), pp. 1155-66.

Ichimura, Y., Kumanomidou, T., Sou, Y. S., Mizushima, T., Ezaki, J., Ueno, T., Kominami, E., Yamane, T., Tanaka, K. and Komatsu, M. (2008) 'Structural basis for sorting mechanism of p62 in selective autophagy', *J Biol Chem,* 283(33), pp. 22847-57.

Jacomin, A. C., Samavedam, S., Promponas, V. and Nezis, I. P. (2016) 'iLIR database: A web resource for LIR motif-containing proteins in eukaryotes', *Autophagy,* 12(10), pp. 1945-1953.

Jain A, Rusten TE, Katheder N, Elvenes J, Bruun JA, Sjøttem E, Lamark T, Johansen T. (2015). p62/Sequestosome-1, Autophagy-related Gene 8, and Autophagy in Drosophila Are Regulated by Nuclear Factor Erythroid 2-related Factor 2 (NRF2), Independent of Transcription Factor TFEB. J Biol Chem. 2015 Jun 12;290(24):14945-62

Johansen, T. and Lamark, T. (2020) 'Selective Autophagy: ATG8 Family Proteins, LIR Motifs and Cargo Receptors', *J Mol Biol,* 432(1), pp. 80-103.

Kalvari, I., Tsompanis, S., Mulakkal, N. C., Osgood, R., Johansen, T., Nezis, I. P. and Promponas, V. J. (2014)

'iLIR: A web resource for prediction of Atg8-family interacting proteins', *Autophagy,* 10(5), pp. 913-25.
Lamb, C. A., Yoshimori, T. and Tooze, S. A. (2013) 'The autophagosome: origins unknown, biogenesis complex', *Nat Rev Mol Cell Biol,* 14(12), pp. 759-74.
Lu LQ, Tang MZ, Qi ZH, Huang SF, He YQ, Li DK, Li LF, Chen LX. (2020) Regulation of the Golgi apparatus via GOLPH3-mediated new selective autophagy. Life Sci. 2020 Jul 15;253:117700.
Marshall, R. S., Hua, Z., Mali, S., McLoughlin, F. and Vierstra, R. D. (2019) 'ATG8-Binding UIM Proteins Define a New Class of Autophagy Adaptors and Receptors', *Cell,* 177(3), pp. 766-781 e24.
Mijaljica, D., Prescott, M. and Devenish, R. J. (2006) 'Endoplasmic reticulum and Golgi complex: Contributions to, and turnover by, autophagy', *Traffic,* 7(12), pp. 1590-5.
Nezis, I. P., Simonsen, A., Sagona, A. P., Finley, K., Gaumer, S., Contamine, D., Rusten, T. E., Stenmark, H. and Brech, A. (2008) 'Ref(2)P, the Drosophila melanogaster homologue of mammalian p62, is required for the formation of protein aggregates in adult brain', *J Cell Biol,* 180(6), pp. 1065-71.
Noda, N. N., Ohsumi, Y. and Inagaki, F. (2010) 'Atg8-family interacting motif crucial for selective autophagy', *FEBS Lett,* 584(7), pp. 1379-85.
Nthiga, T. M., Shrestha, B. K., Bruun, J. A., Larsen, K. B., Lamark, T. and Johansen, T. (2021) 'Regulation of Golgi turnover by CALCOCO1-mediated selective autophagy', *J Cell Biol,* 220(6).
Pankiv, S., Clausen, T. H., Lamark, T., Brech, A., Bruun, J. A., Outzen, H., Overvatn, A., Bjorkoy, G. and Johansen, T. (2007) 'p62/SQSTM1 binds directly to Atg8/LC3 to facilitate degradation of ubiquitinated protein aggregates by autophagy', *J Biol Chem,* 282(33), pp. 24131-45.
Randow, F. and Youle, R. J. (2014) 'Self and nonself: how autophagy targets mitochondria and bacteria', *Cell Host Microbe,* 15(4), pp. 403-11.
Sinka, R., Gillingham, A. K., Kondylis, V. and Munro, S. (2008) 'Golgi coiled-coil proteins contain multiple binding sites for Rab family G proteins', *J Cell Biol,* 183(4), pp. 607-15.
Tusco, R., Jacomin, A. C., Jain, A., Penman, B. S., Larsen, K. B., Johansen, T. and Nezis, I. P. (2017) 'Kenny mediates selective autophagic degradation of the IKK complex to control innate immune responses', *Nat Commun,* 8(1), pp. 1264.

## Acknowledgements

We thank Prof. P. Therond for the anti-GMAP antibody and Prof N. Silverman for the anti-Kenny antibody. We acknowledge Wellgenetics for the construction of Atg8a-LDS and GMAP-LIR CRISPR mutants. We thank Warwick Proteomics research technology platform for help with the proteomics analysis and members of Nezis lab for helpful discussions. This work was supported by BBSRC grants BB/L006324/1 and BB/P007856/1 and Leverhulme Trust Project grant RPG-2017-023 awarded to I.P.N. A.R. holds a PhD studentship funded by the Midlands Integrative Biosciences Training Partnership funded by BBSRC. PL was funded by the Hungarian Academy of Sciences (PPD-2018-222) and the National Research Development and Innovation Office (FK 138851)

**Author contributions**

I.P.N. conceived the project. A.R. performed all the experiments. Y.Z. performed the mass spectrometry analysis. P.L. and G.J performed EM analysis. I.P.N and Y.Z. composed the manuscript. All authors reviewed the manuscript and discussed the work.

**Competing interests**

The authors declare no competing interests.

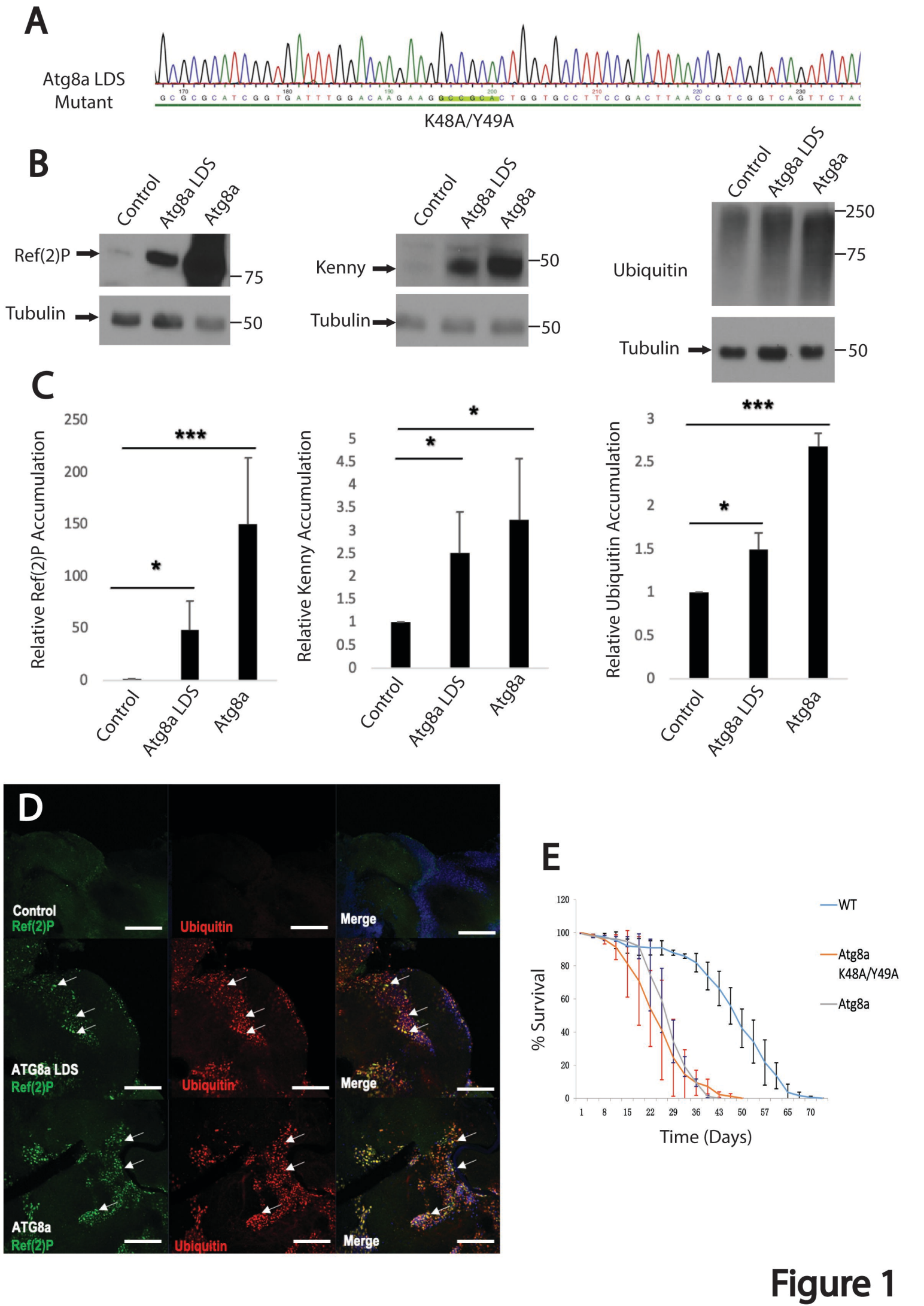
A
Atg8a LDS Mutant
K48A/Y49A
B
Control
Atg8a LDS
Atg8a
Ref(2)P
Tubulin
75
50
Kenny
Ubiquitin
250
C
Relative Ref(2)P Accumulation
Relative Kenny Accumulation
Relative Ubiquitin Accumulation
***
*
D
Control
Ref(2)P
Ubiquitin
Merge
ATG8a LDS
ATG8a
E
% Survival
Time (Days)
WT
Atg8a K48A/Y49A
Atg8a

Figure 1

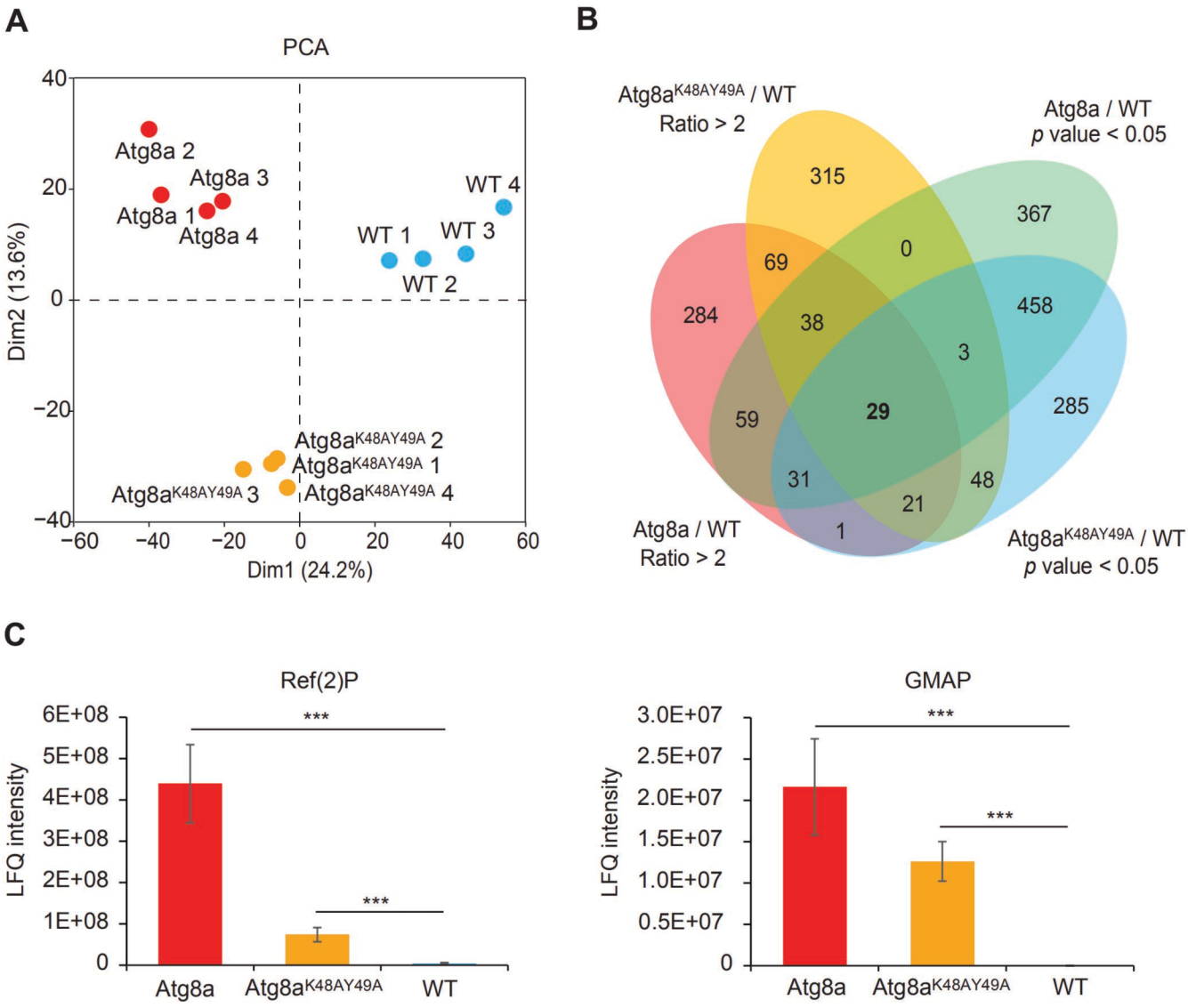
A
PCA
Atg8a 2
Atg8a 3
Atg8a 1
Atg8a 4
WT 4
WT 1
WT 3
WT 2
Atg8aK48AY49A 2
Atg8aK48AY49A 1
Atg8aK48AY49A 3
Atg8aK48AY49A 4
Dim2 (13.6%)
Dim1 (24.2%)
B
Atg8aK48AY49A / WT
Ratio > 2
Atg8a / WT
p value < 0.05
Atg8a / WT
Ratio > 2
Atg8aK48AY49A / WT
p value < 0.05
315
367
0
69
284
38
458
3
59
29
285
31
48
21
1
C
Ref(2)P
LFQ intensity
GMAP
LFQ intensity
Atg8a
Atg8aK48AY49A
WT

**Figure 2**

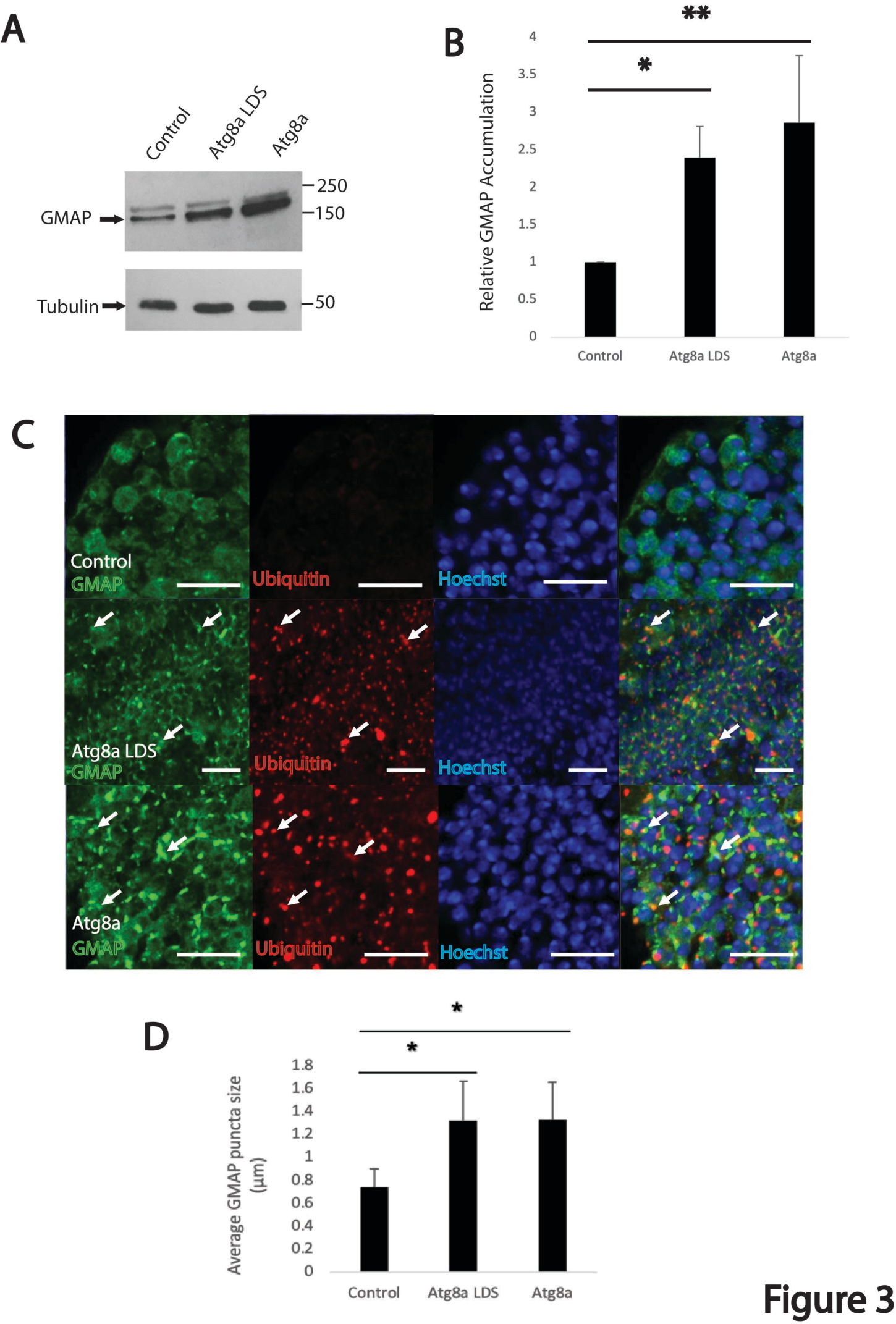
A
Control
Atg8a LDS
Atg8a
GMAP
250
150
Tubulin
50
B
**
*
Relative GMAP Accumulation
4
3.5
3
2.5
2
1.5
1
0.5
0
Control
Atg8a LDS
Atg8a
C
Control
GMAP
Ubiquitin
Hoechst
Atg8a LDS
GMAP
Ubiquitin
Hoechst
Atg8a
GMAP
Ubiquitin
Hoechst
D
*
*
Average GMAP puncta size (µm)
1.8
1.6
1.4
1.2
1
0.8
0.6
0.4
0.2
0
Control
Atg8a LDS
Atg8a

Figure 3

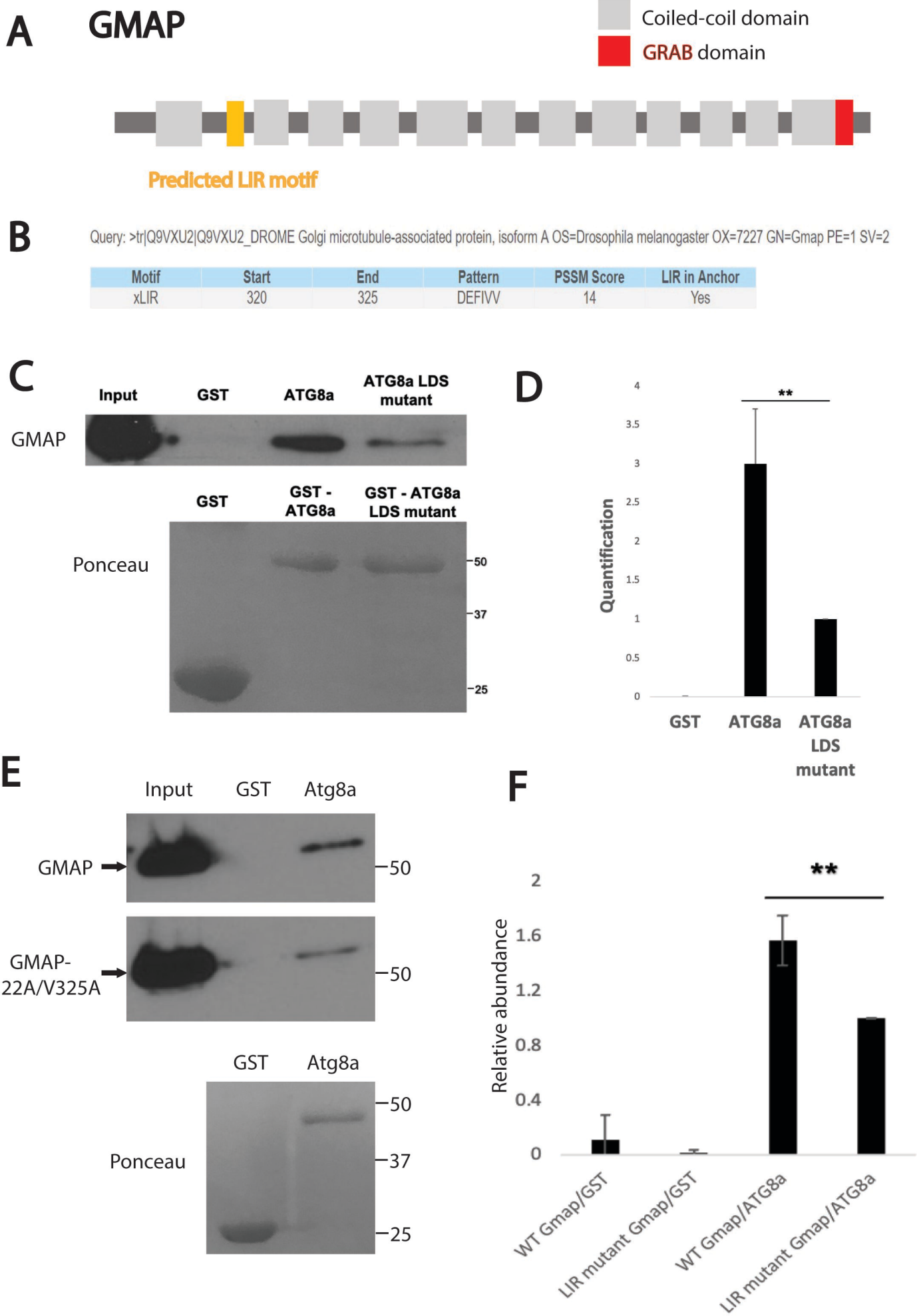
A
GMAP
Coiled-coil domain
GRAB domain
Predicted LIR motif
B
Query: >tr|Q9VXU2|Q9VXU2_DROME Golgi microtubule-associated protein, isoform A OS=Drosophila melanogaster OX=7227 GN=Gmap PE=1 SV=2
Motif Start End Pattern PSSM Score LIR in Anchor
xLIR 320 325 DEFIVV 14 Yes
C
Input
GST
ATG8a
ATG8a LDS mutant
GMAP
GST
GST - ATG8a
GST - ATG8a LDS mutant
Ponceau
50
37
25
D
Quantification
**
GST
ATG8a
ATG8a LDS mutant
E
Input
GST
Atg8a
GMAP
GMAP-F322A/V325A
50
50
GST
Atg8a
Ponceau
50
37
25
F
Relative abundance
**
WT Gmap/GST
LIR mutant Gmap/GST
WT Gmap/ATG8a
LIR mutant Gmap/ATG8a

Figure 4

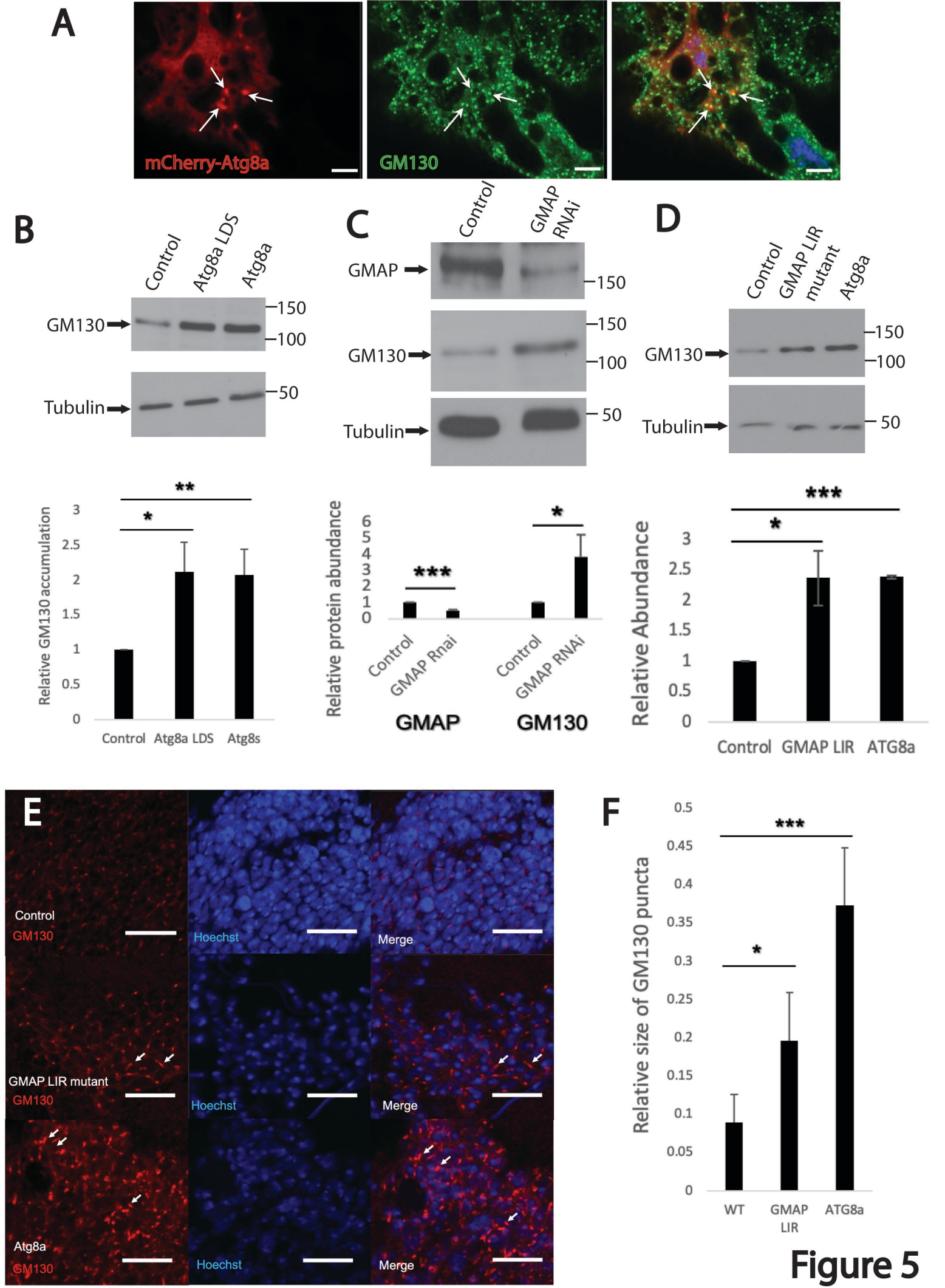
A
mCherry-Atg8a
GM130
B
Control
Atg8a LDS
Atg8a
GM130
Tubulin
150
100
50
Relative GM130 accumulation
Control
Atg8a LDS
Atg8s
C
Control
GMAP RNAi
GMAP
GM130
Tubulin
Relative protein abundance
GMAP
GM130
D
Control
GMAP LIR mutant
Atg8a
Relative Abundance
Control
GMAP LIR
ATG8a
E
Control
GM130
Hoechst
Merge
GMAP LIR mutant
Atg8a
F
Relative size of GM130 puncta
WT
GMAP LIR
ATG8a

Figure 5

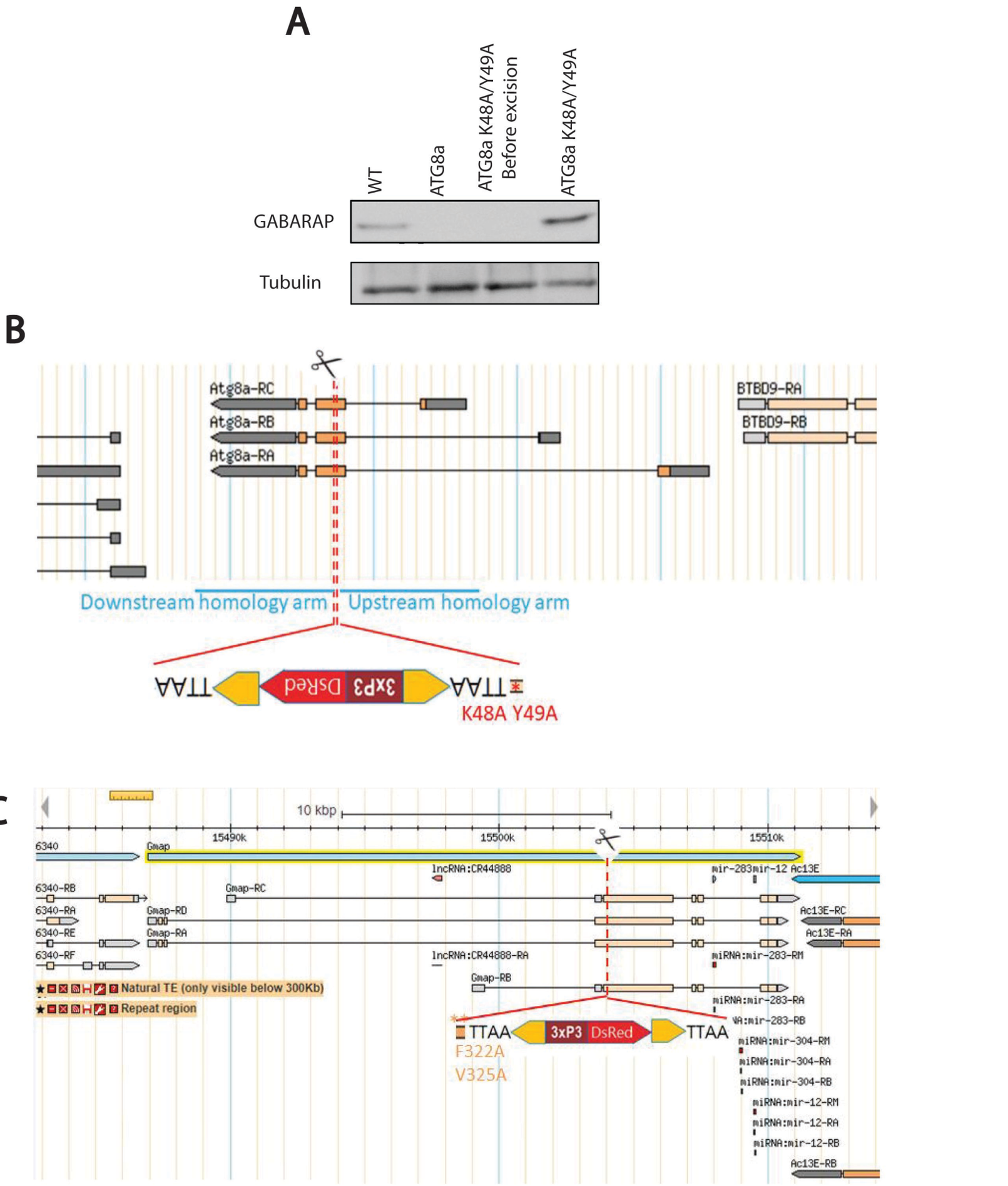


# Supplementary Figure 1

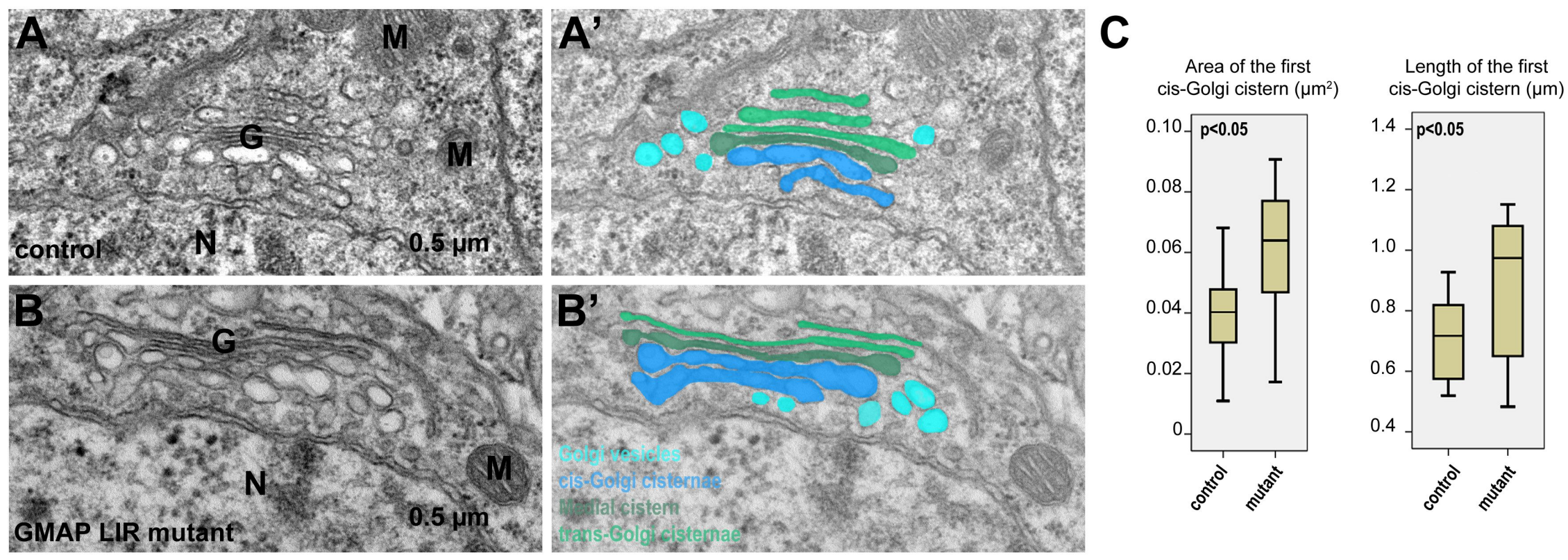
A
M
G
M
control
N
0.5 µm
A'
B
G
N
M
0.5 µm
GMAP LIR mutant
B'
Golgi vesicles
cis-Golgi cisternae
Medial cistern
trans-Golgi cisternae
C
Area of the first cis-Golgi cistern (µm²)
p<0.05
0.10
0.08
0.06
0.04
0.02
0
control
mutant
Length of the first cis-Golgi cistern (µm)
p<0.05
1.4
1.2
1.0
0.8
0.6
0.4
control
mutant

**Supplementary Figure Legends**

**Supplementary Figure 1. (A)** Western blots showing expression Atg8a. Expression of ATG8a can be seen in the wild type flies (WT) as well as the ATG8a$^{K48A/Y49A}$ mutants. This shows ATG8a is successfully being expressed in the ATG8a CRISPR mutant flies. ATG8a null flies were used as a negative control as there was no expression of ATG8a. There is also no expression of ATG8a in the Ex2 line prior to excision which is expected as the selectable marker must first be excised before proper expression can take place. **(B)** Schematics showing the generation of ATG8a$^{K48A/Y49A}$ mutant flies using CRISPR. **(C)** Schematics showing the generation of GMAP $^{F322A/V325A}$ mutant flies using CRISPR.

**Supplementary Figure 2.** Electron micrographs of adult neurons of control **(A)** and GMAP LIR mutants **(B)**. Enlarged cis-Golgi cisternae are readily apparent in mutants compared to control **(A-C)**. Abbreviations: Golgi (G), Nucleus (N), Mitochondria (M). Scale bars: 0.5 um.

**Supplementary Table 1**. Results of identified proteins from Atg8a mutant, Atg8aK48A/Y49A mutants, and wild-type (WT) flies using quantitative proteomics.

**Supplementary Table 2**. Results showing the expression level of 29 proteins that are upregulated in Atg8a and Atg8aK48A/Y49A mutants. The proteins are listed by accession number in Uniprot, number of protein and peptides, and LFQ (label-free quantification) intensity. These 29 proteins were screened using the following contitions: ratio > 2 and p value < 0.5.